THE
PHYSICAL REVIEW
A Journal of Experimental and Theoretical Physics Established by E. L. Nichols in 1893
VOL. 52, NO. 4 AUGUST 15, 1937 SECOND SERIES

Electron Scattering in Helium

MAX GOODRICH*
University of Minnesota, Minneapolis, Minnesota
(Received February 8, 1937)

An electron scattering apparatus has been used to investigate the scattering of 100 volt incident electrons in helium gas. The angular distribution curves for total scattering and for elastic scattering are compared with the theory as given by Morse and by Mott and Massey and are found to give greater relative scattering at angles near both 0° and 180° than is predicted by the theory. In absolute magnitude the experimental curves generally fall somewhat below the theoretical curves. The angular distributions of electrons scattered with various energy losses equal to or greater than the ionization loss were determined. The curves show that in general, the greater the energy loss the more uniform is the distribution in angle of the scattered electrons. There is a pronounced preference for forward scattering when the energy loss over that required for ionization is small. Integration over the entire solid angle gives the probability for scattering with different energy losses. Curves so obtained for this probability as a function of the energy loss are in qualitative agreement with Wetzel's theoretical calculations except for electrons which have lost nearly all their energy or just slightly more than the ionization energy.

INTRODUCTION

WHEN a gas atom is ionized by the impact of a colliding electron, the electron must give up kinetic energy equal to the ionization energy of the atom and may also transfer any amount of its remaining energy to the ejected electron. If V_c is the collision energy and V_i the ionization energy, then both the incident and the ejected electrons will have energies lying between 0 and $V_c - V_i$. Furthermore, since other processes in which the electron loses as much energy as V_i are relatively unlikely, it is possible to investigate the electrons involved in an ionization by studying those electrons scattered with energies between 0 and $V_c - V_i$.

Studies on the electrons scattered with energies in this region have been made by several experimenters.[1-3] Their results have indicated that, for such electrons, the smaller the loss in energy of the electron, the more likely it is to be scattered in the forward direction. It appears, further, that when an electron ionizes an atom, the remaining energy tends to be divided unequally between the incident and the ejected electron.

The theory has been investigated by Wetzel,[4] who calculated, with the Born approximation, the angular distribution of electrons deflected in ionizing collisions with the helium atom. From the results he was able to arrive at the probability that an electron of incident energy V_c shall retain, after ionizing a helium atom, an energy V,

* Now at Louisiana State University, Baton Rouge, Louisiana.

[1] C. B. O. Mohr and F. H. Nicoll, Proc. Roy. Soc. **A144**, 596 (1934).
[2] A. L. Hughes and J. H. McMillen, Phys. Rev. **39**, 585 (1932); **41**, 39 (1932).
[3] J. T. Tate and R. R. Palmer, Phys. Rev. **40**, 731 (1932).
[4] W. W. Wetzel, Phys. Rev. **44**, 25 (1933).

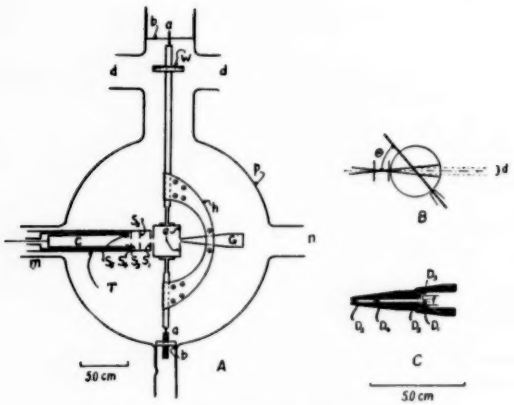

FIG. 1. Diagram of apparatus.

as a function of V. The curves show the general characteristics mentioned as appearing in the experimental results. Wetzel also found the probability for ionization as a function of the incident energy. This last calculation was compared with the efficiency of ionization as measured by Smith[5] and found to predict reasonably well both the absolute magnitude and the shape of the curve.

A more intimate test of the theory can be obtained by comparing with experiment, either the angular distributions of these electrons or the curve giving the probability for an electron to retain a given energy. The present experiment was therefore undertaken to determine, with 100 volt incident electrons in helium, the angular distributions of electrons scattered with various energy losses from 25 to 100 volts over as wide an angular range as possible.

APPARATUS

The apparatus, Fig. 1, was constructed of copper and housed in a 5-liter Pyrex flask sealed without ground glass or wax joints so that it could be thoroughly outgassed by baking. The inside of the flask was coated with a thin layer of evaporated platinum which both shielded the scattering region from stray electrostatic fields and collected the initial beam of electrons passed through the tube. A pair of Helmholtz coils around the tube neutralized the earth's magnetic field. The apparatus was baked out at bright red heat before, and at 300°C for 30 hours after, it was assembled in the tube.

[5] P. T. Smith, Phys. Rev. **36**, 1293 (1930).

The electron gun G, is shown in cross section in Fig. 1C. Preliminary tests with electron guns had shown that good focusing with good velocity distribution could be attained by dividing the accelerating potential into two parts with diaphragms quite close together. For 100 volt electrons, 20 volts were placed between D_1 and D_2 and 80 placed between D_2 and D_3. The spread in velocity was such that at 100 volts, about 90 percent were within 0.3 volt of the mean. The gun was mounted so that it could be rotated about the axis a–a by means of a cable of copper wires making one turn about the wheel W and extending into the sidearms d–d. This was actuated by an electromagnetic device such that all magnetic material could be removed after a setting was made. The angular setting was read on a scale at W with a vernier attachment. The cups e–e, separated by about 4 mm to permit the electron beam to pass between them, served further to shield the scattering region from both stray electrostatic fields and secondary electrons. All leads were shielded and carried out through the lower bearing.

The collector system T, consisted of a long rectangular box with collimating slits in the diaphragms as shown, a "guard ring" box with opening S_5 and the Faraday cage C. The slit dimensions were 0.5×2.6 mm, 0.65×3.8 mm, 0.5×4.2 mm, 0.8×6.0 mm, and 2.0×10.0 mm in the order of S_1 to S_5. The slits S_1 and S_3 determined the solid angle for collection of electrons as seen from a point in the scattering region. Since slits S_1 to S_4 were all at the same potential, that of the scattering region, potentials applied between S_4 and S_5 could penetrate S_3 very little. Consequently, the effective solid angle of collection was assumed to be equal to that calculated from the geometry of the slits. If a and b are, respectively, the widths of S_1 and S_3, A and B the respective distances of S_1 and S_3 from the scattering center and h the height of S_3, then

$$\Delta\Omega = abh/B(Ab+aB),$$

where $\Delta\Omega$ is the average solid angle for collection. This calculation is similar to one given by Brode[6] and assumes that in the vertical plane of the collector slits, most of the electron beam lies in the umbra of slits S_1 and S_3. In our

[6] R. B. Brode, Rev. Mod. Phys. **5**, 273 (1933).

apparatus A and B were respectively 18.0 and 38.0 mm and the beam was not more than 1 mm in cross section at the scattering center. A simple calculation with these values shows that the above condition was satisfied. The formula gives $\Delta\Omega = 0.98 \times 10^{-3}$. The length of electron beam path from which the scattered electrons were taken was $d/\sin\theta$ where $d = 1.4$ mm and θ is the angle of scattering. The scattered currents were measured with one of the d.c. amplifiers built by Distad and Williams[7] having a sensitivity of 125,000 mm/volt. A balancing-out arrangement was used such that in the region of small angles, the total current received by the Faraday cage would equal 15,000 divisions on the scale. It was then possible, when conditions were good, to measure differences of the order of 1 percent with an accuracy of a few percent.

Tests on the Apparatus

To determine the angular scale reading for electrons directed straight into the collector, that is, the zero angle, the scattering was measured over a considerable range on each side of the approximately known zero angle. In Fig. 2a we have shown such a measurement for 100 volt impacts in helium. The ordinates represent the total number of electrons, both elastic and inelastic, received by the collector.

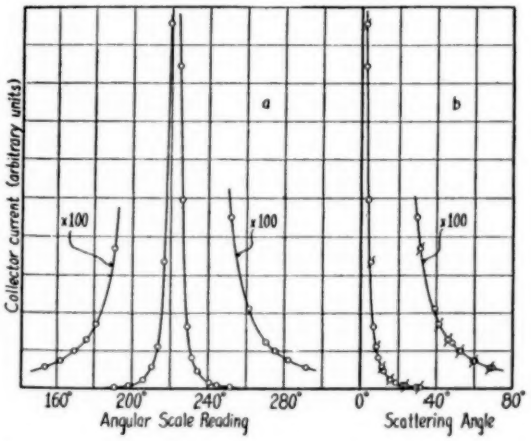

FIG. 2. a, Determination of zero angle. b, Test for symmetry about the zero angle. Circles are for one side of the beam and circles with lines through are for the other side. Curves are for 100 volt impacts and for total scattering uncorrected for change of scattering volume with angle.

[7] M. Distad and J. H. Williams, Rev. Sci. Inst. **5**, 289 (1934).

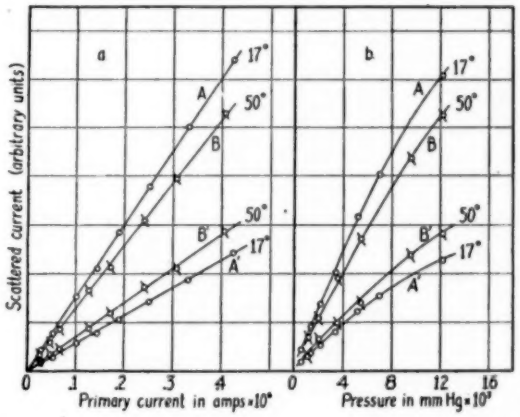

FIG. 3. Curves A and B for total scattered current with 100 volt primaries. Curves A' and B' for elastically scattered current with 100 volt primaries.

If the position of zero angle is taken as 222°, the data from the two sides of the zero angle can be plotted together as is done in Fig. 2b. The circles are for one side of the beam and the circles with lines through them are for the other side. The symmetry is seen to be excellent down to angles as small as about 3°. This indicates that the alignment of the apparatus is good and that the electron beam is itself quite symmetrical.

That the effect of secondary electrons in the apparatus was negligible was demonstrated by measuring the collector current when no gas was present in the tube. This current was too small to be measured at the large angles and at the small angles was never more than a few percent of that obtained with gas in the tube at the pressures ordinarily used.

Figure 3 shows the relation of the scattered current to the primary current and to the gas pressure. The first of these shows very good linearity as indeed it should but the second shows a slight bending. A number of factors may contribute to such a lack of linearity, most important of which is multiple scattering. This enters in two ways, (1) electrons may be scattered through angles whose sum is equal to the measured angle of deflection and thus be added to the proper scattered current and (2) electrons scattered through the measured angle may subsequently collide with another atom and thereby fail to reach the collector. An additional factor which, in our case, added to the apparent nonlinearity was an uncertainty in the measurement

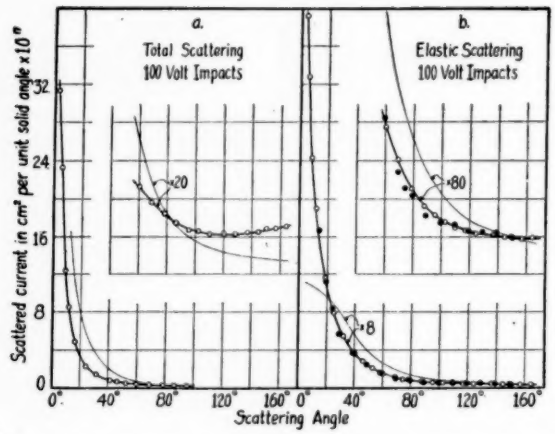

FIG. 4. Circles with heavy lines are experimental curves. Light lines are theoretical curves. Solid curves are from the data of Hughes, McMillen and Webb.

of the gas pressure. The pressure was measured with a McLeod gauge which was later found to be nonuniform. As the data which we shall report were all taken at the same pressure, the relative values of the scattering coefficients should not be greatly affected. However, since the curve in Fig. 3b bends over as it does, we should expect the absolute values to be too low.

In the region of 90° scattering, Arnot[8] observed a considerable number of positive ions entering the collector and came to the conclusion that they were due to a radial field about the electron beam caused by the slowly moving heavy ions. Although the same effect was observed in our apparatus with mercury vapor, it was not found with helium. This was attributed to two causes, (1) the number of ions formed was smaller because of the lower probability of ionization of helium and (2) as the mass of the helium ion is only 1/50 that of the mercury ion, the former has a temperature velocity $(50)^{\frac{1}{2}}$ times that of the latter and therefore the helium ions built up a smaller space charge. A very small positive current was attributed to ions formed in the collector slits and pulled into the collector by the retarding potential for electrons. This effect was observed by Tate and Palmer.[3]

TOTAL SCATTERING AND ELASTIC SCATTERING

The scattering coefficient $P_t(\theta)$ (the total current scattered through an angle θ per atom per unit primary current per unit solid angle) for 100 volt incidence in helium has been plotted as a function of θ in Fig. 4a. Morse[9] has given an expression calculated from the wave mechanics for such scattering. It is,

$$P_t(\mu)=(m^2e^4/4h^4)[(Z-F)^2+(Z^2-F^2)/Z]\mu^{-4},$$

where Z is the atomic number of the scattering atom, $F(\mu)$ its atom form factor and $\mu=(\sin\theta/2)/\lambda$. θ is the angle of scattering and λ is the de Broglie wave-length of the electron, given by $\lambda=h/mv$, where m and v are, respectively, the mass and velocity of the incident electron. With values of the atom form factor given by James and Brindley,[10] this expression was evaluated and is shown as the light solid line in the Fig. 4a. At the small angles the theoretical scattering curve is not steep enough and at the large angles it is too steep. This is in accord with the results of Hughes and Harris[11] who measured the total scattering in helium for impacts of from 200 volts upwards. They did not obtain absolute values but by "matching" the curves at one point, found agreement in shape of the curves for 700 volt incidence and higher. According to our results, the absolute magnitude predicted by the theory would appear to be correct at about 80°. However, it must be remembered that our values are undoubtedly too low.

Figure 4b shows the scattering coefficient $P_e(\theta)$ for elastically scattered electrons only. The heavy line with the circles represents our experimental values while the light line represents the theoretical curve. The latter, excepting for the small angle values, was calculated from Morse's expression,

$$P_e(\mu)=(m^2e^4/4h^4)(Z-F^2)\mu^{-4},$$

using James and Brindley's F values. Of these F values the one for $\mu=0.1\times10^8$ cm is apparently unreliable as it gives a maximum in $P_e(\theta)$ at about 20°. Mott and Massey[12] have given a table of values for $P_e(\theta)$ calculated by the use of

[8] F. L. Arnot, Proc. Roy. Soc. **A129**, 361 (1930).

[9] P. M. Morse, Rev. Mod. Phys. **4**, 609 (1932).

[10] R. W. James and G. W. Brindley, Phil. Mag. **12**, 81 (1931).

[11] A. L. Hughes and W. Harris, Phys. Rev. **48**, 408 (1935).

[12] N. F. Mott and H. S. W. Massey, *The Theory of Atomic Collisions*, p. 120.

the Hylleraas[13] ψ function for helium. These values decrease monotonically as θ increases and agree with the values from Morse's expression for angles of above 30°. For angles of less than 30° we have used Mott and Massey's table in making up the theoretical curve. As in the case of the total scattering the theoretical curve is too steep at the large angles and not steep enough at the small angles. Hughes, McMillen and Webb[14] have determined the relative values of the elastic scattering coefficients in helium

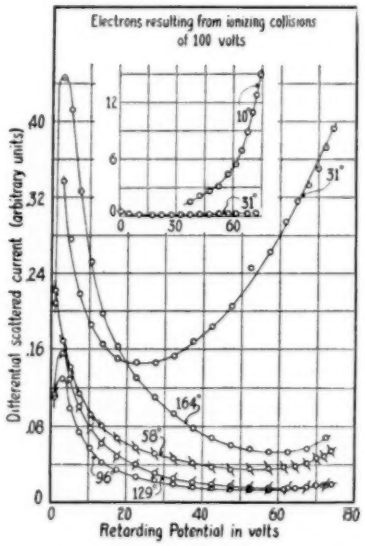

FIG. 5. Energy distribution of scattered electrons at the various indicated angles.

for a number of incident voltages and have found, for impacts of 500 volts and upwards, agreement with the theory in the shapes of the curves. That their results agree with ours can be seen in the figure where we have plotted their values as the solid circles. Their results have been adjusted to agree with ours at $\theta = 50°$.

SCATTERING FROM IONIZING COLLISIONS

The curves in Fig. 5 illustrate the method of taking the data for the electrons from ionizing collisions. At each angular setting, the distribution in energy of the electrons received by the collector was taken by recording the changes in the collector current when the retarding potential was changed by definite amounts. The data have all been reduced to correspond to uniform increments of one volt so that the ordinates are proportional to the number of electrons received by the collector with energies between $V_r - \frac{1}{2}$ and $V_r + \frac{1}{2}$ volts when the collector is set at the various indicated angles.

Since energy losses of less than 24.5 volts (the ionization energy) were not investigated, the curves do not extend to electron energies above $V_e - V_i$ or 75.5 volts. The curves show that the higher energy electrons, that is, those which have lost small amounts in addition to the ionization energy, predominate at the small angles whereas the low energy electrons or those which have lost most of their energy, predominate at the larger angles. It is interesting to note that for angles of above 90° there is a peak in the curves at about 3 volts, showing that the probability for an electron to come off at these angles with V volts energy approaches zero as V approaches zero, for V less than about 3 volts.

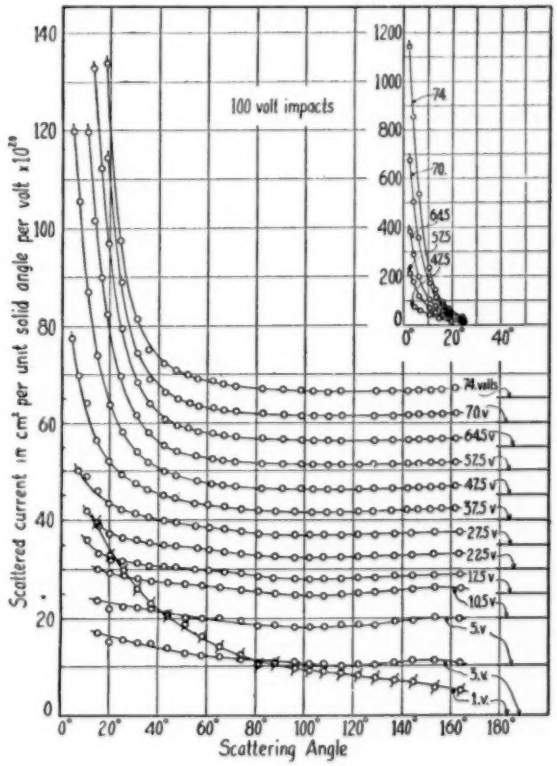

FIG. 6. Angular distribution curves for electrons scattered with the indicated energies when the incident electron energy is 100 volts. The zeros of the curves are shifted upwards as shown.

[13] E. Hylleraas, Zeits. f. Physik **54**, 347 (1929).
[14] A. L. Hughes, J. H. McMillen and G. M. Webb, Phys. Rev. **41**, 154 (1932).

On account of the inherent difficulties in measuring the number of such low velocity electrons, the exact shape of the curves in this region cannot carry much importance. However, the peak is quite definite at the large angles.

In order to compare the scattering of electrons of a given energy loss at the different angles it is necessary to divide the ordinates of Fig. 5 by the length of primary beam path from which the electrons are taken. This, as previously stated, is $0.14/\sin\theta$ cm where θ is the angle of scattering. When this is done one gets the curves shown in Fig. 6. Here we have also multiplied by a constant $K/(3.56\times10^{16}\times P\times\Delta\Omega)$ where P is the gas pressure ($=0.012$ mm Hg), $\Delta\Omega$ is the average solid angle of collection ($=0.98\times10^{-3}$) and K is a factor depending on the sensitivity of the amplifier and that of the galvanometer which measures the total gun current. The ordinates then represent the number of electrons scattered through the angle θ in the given energy range, per primary electron per unit solid angle when there is one atom per cubic centimeter at the scattering center.

The curves in Fig. 6 show that the electrons which have lost most of their energy, that is, those which have very little remaining energy, are scattered rather uniformly over all angles with a slight preference for the forward direction. Those which have retained a greater amount of their energy are scattered more in the forward direction. In fact, the greater the energy retained by the electrons, the steeper the angular distribution curve is. This is in accord with the observations of Tate and Palmer[3] in mercury vapor and with those of Mohr and Nicoll[1] in helium. The one volt electrons, that is, those which come away with energies between 0 and 2 volts, form an apparent exception. It is quite likely that this is a spurious effect. While our scattering region appeared to be quite free from electrostatic and magnetic fields, it is easily possible that there may have been fields present great enough to affect electrons of a few tenths of a volt velocity.

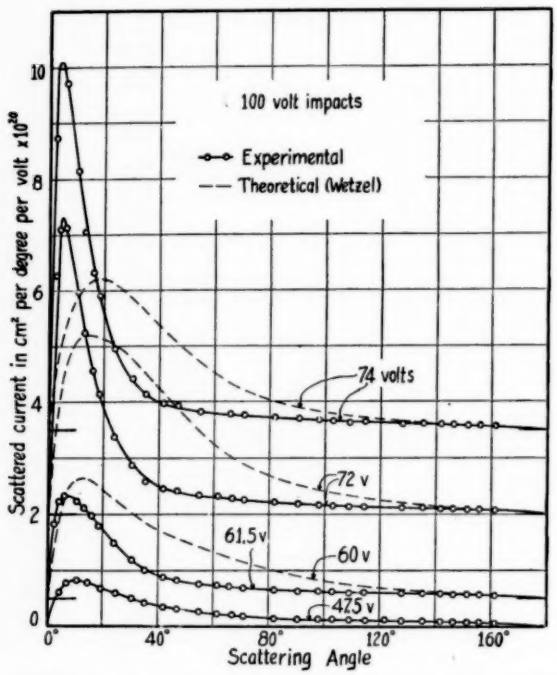

FIG. 7. Scattering per degree of electrons of the indicated energies when the incident electron energy is 100 volts. The zeros are shifted upwards as shown.

In Figs. 7 and 8, the experimentally determined scattering per unit angle curves are shown as the circles with the solid lines drawn through them. The zeros of the various curves are shifted upwards as indicated to avoid congestion of the lines. The ordinates here represent the effective cross section of a helium atom for scattering electrons of the indicated energy into the region between the cones θ and $\theta+\Delta\theta$ when the impinging electron has an energy of 100 volts. As before, each curve includes the electrons having energy within $\frac{1}{2}$ volt of that indicated. Since $\Delta\theta$ was made equal to one degree of arc, the ordinates are expressed in cm^2 per volt per degree. To obtain these curves, the scattering per unit solid angle must be integrated over the azimuthal angle which is accomplished by multiplying by $2\pi\sin\theta\cdot\Delta\theta$. The solid angle between the cones θ and $\theta+\Delta\theta$ obviously approaches zero as θ approaches both 0° and 180°. Therefore, if the scattering per unit solid angle is to remain finite, it is necessary that the scattering per unit angle approach zero at these two angles. This makes it possible to extrapolate the curves if they can be determined to a point where they appear to be past any maxima. In all cases it was possible to get at least one point far enough beyond the maximum so that the extrapolation could be be made. To do this it was necessary to measure the scattering for the higher energy electrons at

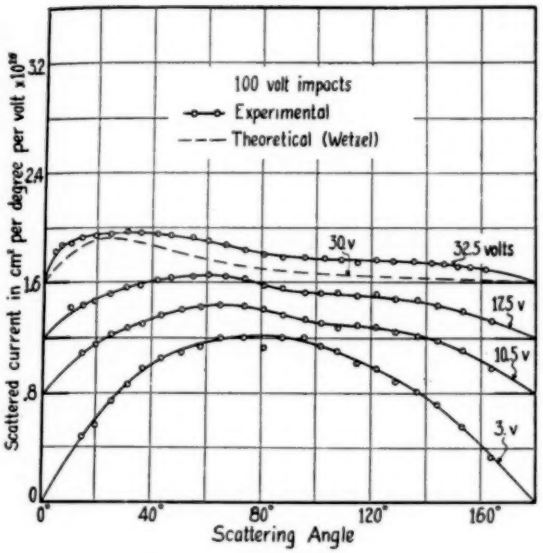

FIG. 8. Scattering per degree of electrons of the indicated energies when the incident electron energy is 100 volts. The zeros are shifted upwards as shown.

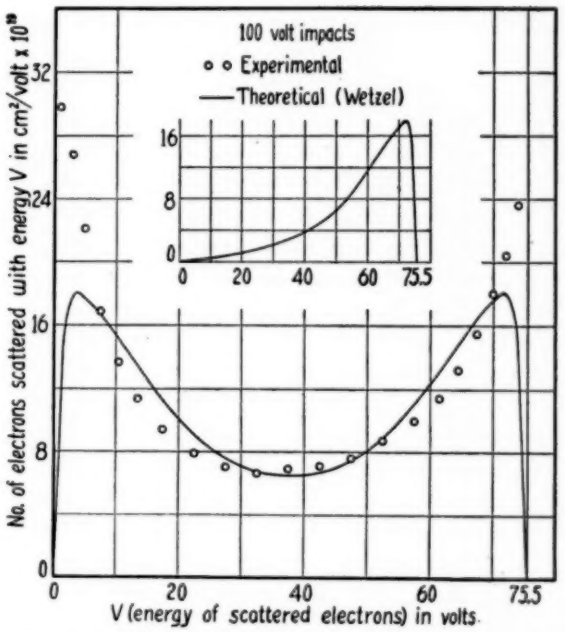
100 volt impacts
Experimental
Theoretical (Wetzel)
No. of electrons scattered with energy V in cm²/volt x 10¹⁸
V (energy of scattered electrons) in volts
75.5

FIG. 9. Distribution in energy of the sum of incident and ejected electrons scattered over the entire solid angle. Inset: theoretical distribution for incident electrons only.

very small angles. The curves obtained are reasonably regular in spite of the fact that any errors in the reading of the angle are extremely important here since the experimental data have to be multiplied by $\sin^2\theta$. The extrapolation of the lower energy curves is much less evident both because the maxima are flatter and because small angle data for these energies were harder to get. The latter is due to the fact that at small angles these currents are very small relative to the total scattered current.

Since the angular distribution curves calculated by Wetzel[4] are for the incident electrons only and the experiment curves include both incident and ejected electrons, the two are not strictly comparable. However, the higher energy electrons may be supposed to be made up largely of incident electrons so that here the theory might be expected to predict the experimental curves. In Fig. 7 we have shown Wetzel's results in the case of 100 volt impacts for 74, 72 and 60 volt scattered electrons along with our results for 74, 72 and 61.5 volt electrons. The theoretical curves are the dashed lines. In each of these cases the experimental data show a greater concentration of scattered electrons in the forward direction than is predicted by the theory. The maxima in the theoretical curves fall considerably below the experimental maxima in the cases of the 74 and 72 volt electrons whereas the maximum in the 60 volt theoretical is somewhat higher than that in the 61.5 volt experimental curve. The absolute magnitude predicted by the theory appears to become more accurate at the larger angles in all three of these cases. In Fig. 8, the theoretical curve for 30 volt electrons is compared to the experimental curve for 32.5 volt electrons. Since the number of ejected electrons of this energy is presumably greater than the number of incident electrons, we expect the theoretical curve to be low, which it is found to be. For the larger losses in helium and in hydrogen, Mohr and Nicoll[1] have compared the theoretical angular distribution of the incident electrons with that of the ejected electrons and found the two to be quite similar. Therefore, we might expect Wetzel's 30 volt curve to predict the shape of the experimental curve. This is seen to be only very roughly true, the relative scattering at the large angles being much larger than predicted.

By integrating numerically, theoretical curves of the type shown in Figs. 7 and 8, Wetzel obtained the number of incident electrons scattered with a given energy over the whole solid angle as a function of this energy. This curve

for 100 volt impacts is shown in the inset of Fig. 9. An accurate, though less detailed comparison with the theory can be made at this point. Since, for every electron scattered with a loss of V volts in addition to the ionization loss (V_i) there is an ejected electron coming away with V volts energy, we can find the theoretical curve for the sum of the incident and ejected electrons by adding to the curve in the inset of Fig. 9, its mirror image. The result, which obviously must be symmetrical about the energy $(V_e-V_i)/2$ or 37.75 volts, is given by the solid line in Fig. 9. We see that the theory predicts a minimum probability for an ionization which leaves the incident and the ejected electrons with equal energies. Furthermore, the most probable process is one in which one electron carries all but about 3.5 volts of the available energy. The experimental results which we have determined by numerical integration of the curves in Figs. 7 and 8 are given by the circles in Fig. 9. The absolute values have been multiplied by the factor 1.9 to effect a better comparison. They confirm the minimum at $(V_e-V_i)/2$ volts but show no evidence of maxima at 72 and 3.5 volts. In order to determine more accurately the shape of the curve in the regions of the predicted maxima, retarding potential increments smaller than the 2 volts used, are necessary. Intensity limitations prevented us from making the increments smaller excepting for the high energy electrons in the region of small angles. Fig. 7 shows that the small angles contribute most of the scattered electrons of high energy. Therefore one would expect to observe the higher energy maxima of Fig. 9 as a peak near 75 volts in the velocity distribution of electrons scattered at small angles. Although retarding potential increments as small as 0.2 volt were used, no such peak was found. It must be remembered that the accuracy of the theory should be better at higher incident electron energies. Consequently, it is necessary to get further experimental data before making any certain evaluation of the theory on this point.

In conclusion, the writer wishes to express his gratitude to Professor John T. Tate under whose direction the work was done. Thanks are due also to Professor E. L. Hill for helpful discussions on the theory of electron scattering.

AUGUST 15, 1937 PHYSICAL REVIEW VOLUME 52

Disintegration of Aluminum by Polonium Alpha-Particles

W. R. KANNE
Johns Hopkins University, Baltimore, Maryland
(Received June 12, 1937)

In order to investigate the discrepancies existing in the experiments of Pose and of Chadwick and Constable regarding the protons emitted by aluminum under alpha-particle bombardment, the thick target absorption curve for the protons has been repeated. The radioactive source was polonium, and an FP-54 vacuum tube electrometer was used to detect the protons. The structure of the groups observed in the present experiment agrees with the work of Chadwick and Constable, and confirms their interpretation of the results. The ranges of the principal groups are in better accord with those found by Pose. It is suggested that Pose's discrepancies were due to sources which predominantly emitted particles of shortened range, and to an insufficient number of accurate points. An increase in proton yield with the height of the resonance levels has been observed. The relative intensity of the short and long range groups is 4.0, and the difference in energy of any two corresponding groups is 2.4 Mev.

INTRODUCTION

IN many respects aluminum makes an ideal target for nuclear investigations. For this reason the reaction

$$_{13}Al^{27}+{}_{2}He^{4}={}_{15}P^{*31}={}_{14}Si^{30}+{}_{1}H^{1}+Q,$$

where Q represents the energy balance, is today the most thoroughly studied of its type. In aluminum only the $_{13}Al^{27}$ nucleus is stable, so there is no confusion as to which of several isotopes might be involved in the reaction. The

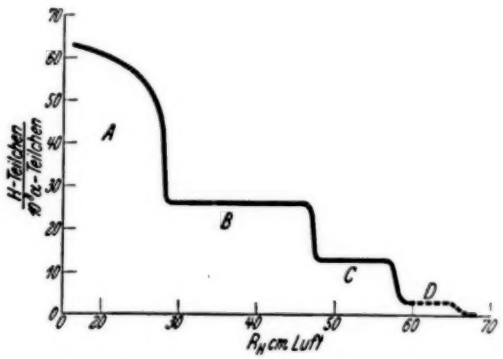

FIG. 1. Thick target absorption curve (after Diebner and Pose).

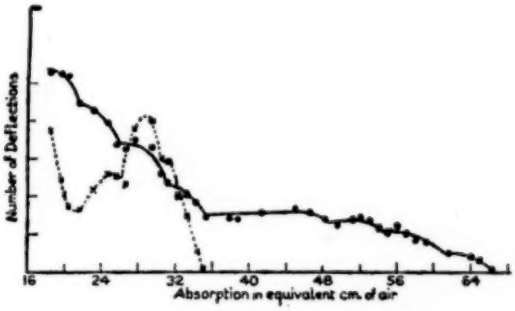

FIG. 2. Thick target absorption curve (after Chadwick and Constable).

metal is chemically stable, and thin foils are easily obtainable.

The first observation of resonance in nuclear processes was made by Pose[1] in his investigation of this reaction. Chadwick and Constable[2] have confirmed the existence of resonance, but disagree regarding the shape of the absorption curve and the interpretation of the process. Pose concluded that alpha-particles of the same energy can, (a) cause resonance excitation of a proton group of definite energy, or (b) penetrate without resonance and excite a group of different energy, while Chadwick and Constable have found only resonance excitation, and have interpreted their results in terms of a system of nuclear levels.

Figure 1 shows the thick target absorption curve obtained by Diebner and Pose.[3] The energy of group *A* is, within experimental error, equal to that of the alpha-particles producing it. Due to the fact that they found this group to be produced by slow as well as fast alpha-particles, but with greater efficiency by the latter, it was attributed to alpha-particles which penetrate the potential barrier without resonance. They assumed that when this group is produced the alpha-particle does not remain with the nucleus, but that it transfers its entire kinetic energy to the proton. Groups *B* and *C* were found to be due to a resonance of alpha-particles of 2.2 cm and 3.2 cm range, respectively, the energy of each group being 2.5 Mev greater than that of the alpha-particle producing it. The existence of group *D* was barely observed in Fig. 1, and this group did not enter the investigation of resonance. Pose[4] attributed it to the beginning of nonresonance disintegration at alpha-ranges just below 4 cm—the energy change being the same as that for the resonance groups.

Chadwick and Constable obtained the absorption curve shown in Fig. 2, where the dotted curve refers to a count of protons near the ends of their ranges. Altogether, eight groups are present. Pose's short range group is observed as four separate groups, and there are four groups, instead of two, having ranges greater than 40 cm. The analysis showed that corresponding high intensity (short range) and low intensity (long range) groups appear and disappear together as the energy of the alpha-particle is changed. For example, the first and fifth groups are produced together and are due to the same alpha-particle resonance.

These results led Chadwick and Constable to the conclusion that there are four resonance levels of the combined nucleus into which the alpha-particle and the aluminum nucleus may unite. Each of these states may then disintegrate so as to leave the final $_{14}Si^{30}$ nucleus in either its ground state or an excited state, giving rise to the four sets of corresponding groups. The transition from the excited state of silicon to the normal state takes place with the emission of a gamma-ray, whose energy is the difference between the energies of any corresponding long and short range groups.

EXPERIMENT

A repetition of the thick target absorption curve was chosen as the simplest test between

[1] Pose, Zeits. f. Physik **64**, 1 (1930).
[2] Chadwick and Constable, Proc. Roy. Soc. **A135**, 48 (1932).
[3] Diebner and Pose, Zeits. f. Physik **75**, 753 (1932).
[4] Pose, Zeits. f. Physik **95**, 84 (1935).

the two experiments. The procedure used in the present experiment was similar to that described by Hafstad.[5] The detecting apparatus was an FP-54 vacuum tube electrometer, which was operated at a sensitivity of 35,000 mm per volt in a circuit of the simple nonbalancing type described by Kanne and Bearden.[6] The alpha-particles from a polonium source were absorbed in an aluminum target 5 mm in diameter and of 4.2 cm air equivalent. The protons emitted in this foil passed through calibrated mica absorbing screens into an ionization chamber which was made of steel and contained air at atmospheric pressure. It was conical in shape, with a central electrode, and was 1.5 cm deep. The aperture admitting the protons to the chamber, like both the source and the target, was 5 mm in diameter, and the centers of all three were in line.

The distance from the source to the target was 7.5 mm, and that from the target to the detector was 16.7 mm. If ϵ is the half-angle subtended by the target at the source, α the half-angle subtended by the detector at the target, and θ the largest angle possible between the incident alpha-particle and an emitted proton which can reach the ionization chamber, then

$$\epsilon = \tan^{-1}(2.5/7.5) = 18^\circ\ 30',$$
$$\alpha = \tan^{-1}(2.5/16.7) = 8^\circ\ 30', \text{ and}$$
$$\theta = \tan^{-1}(5/7.5) + \tan^{-1}(5/16.7) = 51^\circ.$$

The straggling of the proton groups should cover 3 or 4 cm. The total intensity factor introduced by solid angle in this arrangement is 1.57×10^{-4}.

The experiment was performed with two different sources, both of which were prepared by chemical deposition on silver.[7, 8] The results of the experiment are based on the data obtained with the second source, but those obtained with the first source are included in the report because they lend weight to the results and suggest a possible origin of the conflict. At the end of the experiment the particles emitted by the second source were counted by a linear amplifier and it was found to have been 1.4 mc in strength originally. Particles of ranges from 3.0 cm to 3.9 cm were present, and the decrease in number between these two ranges was linear. On the basis of a comparison of the proton yields obtained with the two sources, the first source was calculated to have been 1.1 mc originally. Since this source was weaker, it is reasonable to assume that it emitted alpha-particles of more uniform range.

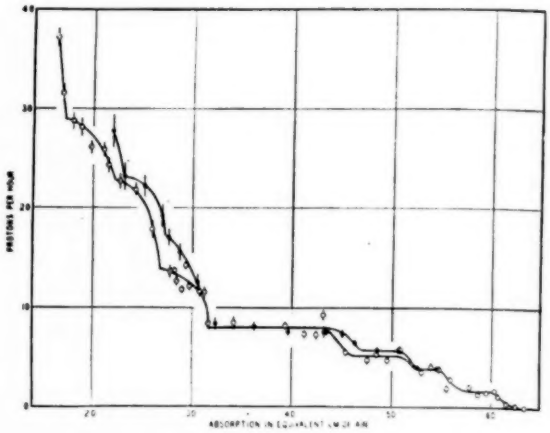

FIG. 3. Thick target absorption curve, using FP-54.

In the interpretation of an absorption curve the protons which come to the ends of their ranges are of interest. These ranges were obtained by determining the stopping power of the mica in the following manner. As a first approximation 1.43 mg per sq. cm of mica was taken as equivalent to one cm of air, and the air equivalent of the absorption at each experimental point calculated on this basis. The velocity of a proton having such a range was taken from Duncanson's data,[9] and an accurate value for the stopping power of the mica, considering the integrated velocity, was obtained from Mano's stopping power-velocity tables.[10]

DISCUSSION OF RESULTS

In Fig. 3 is shown the absorption curve for the protons emitted by a thick aluminum target, obtained with the FP-54 pliotron. The group structure described by Chadwick and Constable is present, and comparisons with Figs. 1 and 2 show the agreement with their work in preference to that of Pose. This agreement, and a partial explanation of Pose's results, support the interpretation given by Chadwick and Constable.

[5] Hafstad, Phys. Rev. **44**, 201 (1933).
[6] Kanne and Bearden, Phys. Rev. **50**, 935 (1936).
[7] I. Curie, J. Chem. Phys. **22**, 471 (1925).
[8] Hafstad, J. Frank. Inst. **221**, 191 (1936).
[9] Duncanson, Proc. Camb. Phil. Soc. **30**, 102 (1934).
[10] Mano, J. de phys. **5**, 628 (1934).

The experimental points indicated by solid circles were obtained from the first source and were multiplied by a constant factor for purposes of comparison with the data obtained from the second source, indicated by open circles. The yield scale refers to the latter data.

The only important discrepancy between this work and that of Chadwick and Constable is that the ranges found here are consistently several centimeters shorter. The group of shortest range, if present, was masked by the intense recoil protons from the source. But if the onset of the rise just above 17 cm is considered to be due to this group, rather than to the recoil protons, the difference between its energy and that of the related 45.5 cm group is found to agree with the energy differences of the other short and long range groups.

The origin of this discrepancy is not clear from the experiments, but a criticism of Chadwick and Constable's evidence for this group shows that it is not impossible that it may have been confused with the natural protons. The dotted curve in Fig. 2, which represents a count of the protons near the ends of their ranges, shows no tendency to form a maximum corresponding to this group. The same is true in the differential count obtained in the analysis of the groups, where only this group and its companion appear (Chadwick and Constable, Fig. 7). This would indicate that the absorption curve should have a large, rather than very small slope in the region between 17 and 20 cm. It is suggested as a possibility that Chadwick and Constable's entire curve may need to be shifted slightly toward smaller absorptions. The two curves obtained in the present experiment are entirely consistent with each other, their differences being traceable to the different range distributions of the two sources.

It is much to be regretted that experimenters who have used natural radioactive sources have not made statements regarding their range distributions. Chadwick and Constable have mentioned that the source with which they investigated resonance was only slightly tarnished, which from experiences in this laboratory would indicate a very nearly uniform range distribution. They make no statement, however, regarding the source with which they obtained the absorption curve.

Pose's sources were presumably prepared in Vienna, and he neither describes the method by which they were prepared nor gives their range distributions. Lacking the latter information, one can only surmise the reasons for his failure to observe the more complicated group structure. First, the fact that his group *D*, of longest range, was observed only with very small intensity would indicate that his source was almost lacking in high energy alpha-particles. A group of corresponding range has been observed with considerable intensity by both Chadwick and Constable and the author. The absence of a short range group due to alpha-particles of the same energy would account for the fact that he found the "range" of group *A* to be 27 cm, rather than 32 or 34 cm. A range of 27 cm is in good agreement with that of the next group observed in this work. His failure to observe the break in the absorption curve at 22 cm is probably due to an insufficiency of points, to an insufficiency of counts at each point, and to the failure of his apparatus to count all the protons. The latter is indicated by the fact that the rise at low absorptions is much greater than his curve shows. The groups at 52.5 and 57 cm are very close together, so that it is probable that Pose's "group" *C* corresponds to these two groups unresolved. And finally, his group *B* may be identified with the 45.5 cm group.

It should be mentioned that the appearance in the curves published by Diebner and Pose of only a small indication of a short range group

TABLE I. *Energies of proton groups from Al. Their differences (γ-rays) and intensity ratios are also given.*

RANGE cm	ENERGY Mev	RANGE cm	ENERGY Mev	γ-RAY Mev	RELATIVE INTENSITY
17.2	3.4	45.5 (47)	5.9 (6.1)	2.5	
22 (23)	3.9 (4.0)	52 (52.5)	6.4 (6.45)	2.5 (2.45)	4.0
27 (27.7)	4.4 (4.5)	57	6.75	2.35	4.1
32 (32)	4.8 (4.8)	62.5	7.2	2.4	4.0

TABLE II. *Proton yields for resonance levels. Average α-particle ranges and the ranges of the protons ejected are given.*

AVERAGE R_α	R_p	YIELD
2.95	22 cm and 52.5 cm	2.65×10^{-7}
3.3	27 cm and 57 cm	7.7×10^{-7}
3.75	32 cm and 62.5 cm	19×10^{-7}

when the 46 cm group is excited, supports the present findings that this first group, if present, is very close to the natural protons.

The data on corresponding proton groups are given in Table I, where the numbers in brackets refer to the data indicated by solid circles in Fig. 3. Since the relative intensities of the short and long range proton groups do not change, the silicon potential barrier has no effect on protons emitted with energies greater than 3.9 Mev.

Only a tentative determination of the proton yields may be made from the present experiment, since the range of the resonant alpha-particles is necessary in order to find the number of particles emitted by the source that can be effective in producing the particular mode of disintegration. Chadwick and Constable give as the values of the maximum ranges of the resonant alpha-particles: 2.7, 3.1, 3.45, and 3.9 cm. They have observed that the resonances are about 300,000 volts wide, so that the average ranges of the alpha-particles would be 2.55, 2.95, 3.3, and 3.75 cm. Then considering the number of effective alpha-particles emitted by the source, the total proton yields for each resonance level may be calculated. (Table II.)

If the 17.2 cm group had four times the intensity of the 45.5 cm group, the yield for this pair would be 3.8×10^{-7}. Chadwick and Constable give 3.5×10^{-7} as the yield for each resonance level.

A summary of work of this type up to 1935 on the several light elements has been given by Pollard.[11] Experiments on aluminum with the higher energy particles from Th C′ and Ra C′ have been performed by Haxel[12, 13] and by Duncanson and Miller.[14] The results of these experiments are in agreement with the interpretation that is accepted here. They have found that the high energy projectiles are able to give enough energy to the combined $_{15}P^{31}$ nucleus so that the $_{14}Si^{30}$ nucleus may be left in either its normal state or any of three excited states, with enough energy left to the proton for it to be observable. Duncanson and Miller have observed two additional resonance levels at 4.25 cm and 5.25 cm. In all, six resonance levels of the combined nucleus, and four states of the final nucleus have been observed.

Recent work by Waring and Chang,[15] in agreement with the Bohr concepts of nuclei and of nuclear reactions, has shown that resonance is closely associated with the emitted particle. Further work by Chang and Szalay[16] has led to similar results. They have suggested that the potential barrier of a nucleus does not exhibit resonance levels, as Chadwick and Constable had described, but that the maxima in the yield of protons are due to pronounced changes in the probability of the "transition" in which a proton is emitted.

The writer wishes to acknowledge his indebtedness to Professor J. A. Bearden, under whose direction this work was done, for his continued advice and encouragement. He also wishes to thank Dr. L. R. Hafstad for valuable discussions regarding the problem. The radioactive sources used in the present experiment were prepared from a Ra D +E+F solution extracted by L. R. Hafstad from old radon bulbs generously supplied by Drs. C. F. Burnham and F. West, of the Kelly Hospital, Baltimore, Maryland.

[11] Pollard, Phys. Rev. **47**, 611 (1935).
[12] Haxel, Zeits. f. Physik **88**, 346 (1934).
[13] Haxel, Zeits. f. Physik **90**, 373 (1934).
[14] Duncanson and Miller, Proc. Roy. Soc. **A146**, 396 (1934).
[15] Waring and Chang, Proc. Roy. Soc. **A157**, 652 (1936).
[16] Chang and Szalay, Proc. Roy. Soc. **A159**, 72 (1937).

The Photoelectric Effect of H^2

LLOYD MOTZ AND WILLIAM RARITA
Columbia University, New York, N. Y.

(Received June 19, 1937)

The total photoelectric cross section of H^2 for an exponential potential is computed with the best available nuclear constants. The value obtained for Th C' γ-rays is 13.1×10^{-28} cm^2.

SINCE recent work[1] has indicated that the exponential potential is well adapted for exact calculations in the study of the two-, three-, and four-body nuclear problems, the photoelectric cross section of H^2 is calculated in this paper with the above potential in anticipation of more accurate experimental data. It is to be hoped that these more precise data will cause the photoelectric effect to play an important role in the development of nuclear theory.

THEORETICAL FORMULAE

The method used in this paper follows the treatment given by Bethe and Bacher.[2]

Assuming the potential for the triplet state of H^2 to be $-Be^{-2r/b}$ (B is the depth and b is the range of the interaction), we first compute the cross section for an electric dipole transition, $\sigma_{E.D.}$:

$$\sigma_{E.D.}=\frac{\pi}{3}\times\frac{e^2}{\hbar c}\times\frac{2\pi\hbar\nu}{k}\times|M_{E.D.}|^2, \qquad (1)$$

$$M_{E.D.}=\int_0^\infty u_0 r u_E dr.$$

In the above equation we have used nuclear units,[3] to be retained throughout the entire paper.

$e^2/\hbar c$ is the fine structure constant; $2\pi\hbar\nu$ is the energy of the γ-ray; and $k=(E)^{\frac{1}{2}}$, where E is the energy of the neutron and proton in the final state relative to their center of mass.

u_0 is the normalized radial wave function of the ground state of H^2 and is given by the Bessel function:

$$u_0=NJ_p(\beta e^{-r/b}).$$

N is a constant of normalization; $\beta=b(B)^{\frac{1}{2}}$; and $p=b(\epsilon)^{\frac{1}{2}}$, where ϵ is the binding energy of H^2.

u_E is the radial wave function of the final state of H^2. In the zeroth order, i.e. for the neutron and proton considered as being free

$$u_E\equiv u_E{}^0=-\cos kr+\sin kr/kr.$$

The detailed evaluation of $M_{E.D.}$ is reserved for the appendix.

Assuming the potential for the singlet state of H^2 to be $-B'e^{-2r/b}$, we calculate the photoelectric cross section for a magnetic dipole transition, $\sigma_{M.D.}$:

$$\sigma_{M.D.}=\frac{m}{M}\times(\mu_P-\mu_N)^2\frac{|M_{M.D.}|^2}{|M_{E.D.}|^2}\sigma_{E.D.}, \qquad (2)$$

$$M_{M.D.}=\int_0^\infty u_0 v_E dr.$$

m and M are the electron and proton masses, respectively; and μ_p and μ_n are the proton and neutron nuclear magnetic moments, respectively, expressed in nuclear magnetons.

v_E is the radial wave function of the final state, normalized to unit amplitude at infinity:

$$v_E=\frac{|\Gamma(1+iq)|}{|J_{iq}(\beta')|}Im[J_{iq}(\beta')J_{-iq}(\beta'e^{-r/b})],$$
$$v_E\rightarrow\sin(kr+\delta_0) \quad \text{as} \quad r\rightarrow\infty,$$
$$q=bk, \quad \beta'=b(B')^{\frac{1}{2}}.$$

Im indicates the imaginary part.

The explicit expansion for $M_{M.D.}$ appears in the appendix. For completeness, we give the cross section for an electric quadrupole transition, $\sigma_{E.Q.}$:

$$\sigma_{E.Q.}=\frac{\pi^2}{5\lambda^2}\times\frac{|M_{E.Q.}|^2}{|M_{E.D.}|^2}\times\sigma_{E.D.}$$

$$M_{E.Q.}=\int_0^\infty u_0 r^2 w_E dr.$$

λ is the wave-length of the γ-ray; and w_E is the radial wave function of the final state. In zero order,

$$w_E\equiv w_E{}^0=\left(\frac{3}{k^2r^2}-1\right)\sin kr-\frac{3}{kr}\cos kr.$$

[1] Rarita and Present, Phys. Rev. **51**, 788 (1937).
[2] Bethe and Bacher, Rev. Mod. Phys. **8**, 82 (1936).
[3] mc^2 for energy $(\hbar^2/Mmc^2)^{\frac{1}{2}}$ for length, and $M/\hbar^2=1$.

Numerical Calculation

We have carried out the calculation for Th C′ γ-rays. Using the best available nuclear constants, $2\pi\hbar\nu=5.12$ (or 2.64 Mev), $E=0.77$, $\epsilon=4.35$, $b=0.193$, $B=242$, $B'=137.6$, $\beta=3.002$, $\beta'=2.264$, $p=0.4026$, $\mu_p-\mu_n=4.9$, we obtain[4]

$$\sigma_{\text{E.D.}}=9.5\times10^{-28}\text{ cm}^2,\quad \sigma_{\text{M.D.}}=0.38\sigma_{\text{E.D.}},$$
$$\sigma_{\text{E.Q.}}=0.00035\sigma_{\text{E.D.}}.$$

The total cross section is then

$$\sigma_{\text{total}}=13.1\times10^{-28}\text{ cm}^2.$$

Appendix

(1) Evaluation of N

We have $\int_0^\infty u_0^2dr=1$. Two rapidly converging series can be used to compute N.

$$\frac{1}{N^2}=\frac{b}{2}\sum_{m=0}^{\infty}\frac{(-1)^m(\beta/2)^{2p+2m}}{(p+m)m!}\frac{\Gamma(2p+2m+1)}{\Gamma(2p+m+1)\Gamma^2(p+m+1)};$$

or

$$\frac{1}{N^2}=\frac{b\beta}{2p}J_{p+1}(\beta)\left[\frac{\sigma(p+1)(\beta/2)^{p+2}}{1!(p+1)!}-\frac{\sigma(p+2)(\beta/2)^{p+4}}{2!(p+2)!}+\cdots\right],$$

where

$$\sigma(p+n)=\sigma(p+n-1)+\frac{1}{p+n}\quad\text{and}\quad\sigma(p+1)=\frac{1}{p+1}.$$

(2) Evaluation of $M_{\text{E.D.}}$

Let $M_{\text{E.D.}}\equiv M^0{}_{\text{E.D.}}$ for $u_E=u_E{}^0$. The expansion of $M^0{}_{\text{E.D.}}$ converges extremely rapidly:

$$M^0{}_{\text{E.D.}}=N\sum_{n=0}^{\infty}\frac{(-1)^n}{n!}\frac{(\beta/2)^{p+2n}}{\Gamma(n+p+1)}\frac{2k^2}{[((p+2n)/b)^2+k^2]^2}.$$

We now calculate $M_{\text{E.D.}}$ correct to the first order.

The differential equation for u_E is

$$\left(\frac{d^2}{dr^2}-\frac{2}{r^2}+E\right)u_E=Be^{-2r/b}u_E.$$

We set u_E on the right-hand side of this equation equal to $u_E{}^0$, and solve the resulting inhomogeneous differential equation for $u_E{}^1$.[5]

Define $M^1{}_{\text{E.D.}}=\int_0^\infty u_0ru_E{}^1dr$, then

$$M^1{}_{\text{E.D.}}=\cos\delta_1\,M^0{}_{\text{E.D.}}+\frac{NB}{4}\sum_{n=0}^{\infty}\sum_{m=0}^{\infty}\frac{(-1)^{n+m+1}}{n!}\frac{(\beta/2)^{p+2n}(k/2)^{2m-1}}{\Gamma(n+p+1)}$$
$$\times\left\{\frac{\pi\binom{2m+3}{m}(2m+4)!k^3}{8\Gamma^2(m+5/2)}\left[\left(\frac{b}{2}\right)^{2m+5}K(n)-\left(\frac{b}{2}\right)^{2m+7}\sum_{s=2}^{2m+6}K(n,s)\sin(n,s)\right]\right.$$
$$\left.+\frac{\pi\binom{2m}{m}(2m+1)!}{\Gamma(m+5/2)\Gamma(m-\frac{1}{2})}\left[\left(\frac{b}{2}\right)^{2m+4}\sum_{s=2}^{2m+3}K(n,s)\cos(n,s)\right]\right\}$$

with[6]

$$\sin\delta_1=\frac{B}{k^2}\cdot\left\{\frac{1}{2bk}\log[1+(bk)^2]-\frac{bk}{2}\frac{1+(bk)^2/2}{1+(bk)^2}\right\},$$

$$K(n)=\frac{((p+2n)/b)^3+((p+2n)/b)3k^2}{[((p+2n)/b)^2+k^2]^2},$$

$$K(n,s)=\frac{[((p+2n+2)/b)^2+s^2k^2]^{1/2}}{(b/2)^s[((p+2n+2)/b)^2+k^2]^{s/2}},$$

$$(n,s)=\arctan\frac{p+2n+2}{sbk}+s\arctan\frac{bk}{p+2n+2}.$$

[4] $\sigma^1{}_{\text{E.D.}}=0.96\sigma^0{}_{\text{E.D.}}$ for this energy. $\sigma^1{}_{\text{E.D.}}$ and $\sigma^0{}_{\text{E.D.}}$ are related to $M^1{}_{\text{E.D.}}$ and $M^0{}_{\text{E.D.}}$, respectively. See appendix.

[5] $u_E=u_E{}^1$ for this approximation.

[6] $\binom{x}{y}=\frac{x!}{(x-y)!\,y!}$.

(3) Evaluation of $M_{\text{M.D.}}$.

$$M_{\text{M.D.}}=-\frac{b(\beta/2)^p}{|J_{iq}(\beta')|\,|\Gamma(1+iq)|\,\Gamma(1+p)}\times\sum_{n=0}^{\infty}\sum_{m=0}^{\infty}\sum_{l=0}^{\infty}Im\left[\frac{A_lA_mA_n}{p+2n+2m+iq}\right],$$

$$A_l=\frac{(-1)^l(\beta'/2)^{2l}\Gamma(1-iq)}{l!\,\Gamma(l+1-iq)},\quad A_m=\frac{(-1)^m(\beta'/2)^{2m}\Gamma(1+iq)}{m!\,\Gamma(m+1+iq)},\quad A_n=\frac{(-1)^n(\beta/2)^{2n}\Gamma(1+p)}{n!\,\Gamma(n+1+p)}.$$

AUGUST 15, 1937 PHYSICAL REVIEW VOLUME 52

Note on Nuclear Photoeffect at High Energies

F. KALCKAR, J. R. OPPENHEIMER AND R. SERBER
University of California, Berkeley, California

(Received May 19, 1937)

In I we consider nuclear transmutations when the energy is so high that the levels of the compound nuclei formed have a spacing smaller than their breadth, and investigate the relations between the cross sections for the various possible reactions and the decay constants characteristic of the compound nuclei. When the collision may be treated as a resonance effect, these relations take a simple form. In II we apply these considerations to the photoelectric disintegration of nuclei of intermediate atomic weight by 17 Mev γ-rays, and suggest that the yields should show a marked increase for γ-rays of somewhat lower energy. In III we study the formal connection between the evaluation of transmutation probabilities here given and the resonance formulae appropriate for lower excitation energies, and show that both descriptions may be derived as limiting cases from the same formalism.

I

BOHR'S analysis[1] of nuclear phenomena has shown the great importance, for an understanding of the processes of nuclear disintegration, of the capture of the incident particle with the formation of an intermediate nucleus having a considerable excitation energy, and so long a lifetime that the subsequent transformation of this unstable structure by the emission of particles (or γ-rays) may be treated as an independent process. A formalism consistent with these ideas, and especially appropriate to the study of the behavior of slow neutrons, has been developed by Breit and Wigner,[2] who have considered the case that the energy levels of the compound nucleus lie far apart compared to their breadth, and have applied the familiar quantum mechanical dispersion formulae to this problem. For sufficiently heavy nuclei and sufficiently high excitation energies the intermediate nucleus will however no longer have well-defined energy levels; instead the states of the system, and even the states of a particular kind, e.g., of a given angular momentum, will form a continuum. One might hope that the disappearance of any characteristic level structure would lead to a simplification in the description of the probabilities of nuclear disintegration, and that the only quantities which then determine these probabilities would be the rates at which a wave packet representing the intermediate nucleus comes apart into the various possible residual nuclei and emitted particles.

This expectation is not however in agreement with the result given by a simple application of the principle of detailed balancing to the processes of formation and disintegration of the compound system. Thus we may divide the states of the compound nucleus into sets (i) each of which is characterized by decay constants which in the limit of close lying levels may be regarded as slowly varying functions of the energy, and by a density of levels $1/s^i$ per unit energy. Then we obtain a relation between the cross section σ_c for the capture of an incident particle and the decay constants $\Gamma_{a0}{}^i/\hbar$ for the reemission of this particle with its original energy:

$$\sigma_c=(\lambda^2/2w_A)\sum_i\Gamma_{a0}{}^i/s^i, \qquad (1)$$

[1] N. Bohr, Science, to be published.
[2] Breit and Wigner, Phys. Rev. **49**, 519 (1936).

where $\lambda=h/p$ is the wave-length of the incident particle, and w_A is the combined statistical weight of the initial states of incident particle and bombarded nucleus. If then $\Gamma_k{}^i/\hbar$ is the rate of emission of a particle of type k, $\Gamma^i/\hbar$ is the total decay constant of a state (i), then the cross sections for transmutation are just

$$\sigma_k=\frac{\lambda^2}{2w_A}\sum_i\frac{\Gamma_{a0}{}^i\Gamma_k{}^i}{s^i\Gamma^i}. \tag{2}$$

This formula can also be brought into connection with the results derived by Breit and Wigner for the case of well separated levels ($\Gamma^i\ll s^i$):

$$\sigma_k(E)=\frac{\lambda^2}{4\pi w_A}\sum_i\frac{\Gamma_{a0}{}^i\Gamma_k{}^i}{(E-E_\rho{}^i)^2+\frac{1}{4}(\Gamma^i)^2},\quad E\sim E_\rho{}^i. \tag{3}$$

Here E is the total energy of the system, and $E_\rho{}^i$ the energy of one of its quasi-stationary states. As Bethe and Placzek[3] have pointed out, from (3) we can obtain a cross section, averaged over a range of energy large compared to spacing of the levels, which agrees with (2). One might thus suppose that although for the derivation of (3) the condition $\Gamma^i\ll s^i$ is essential, no such restriction limited the validity of (2).

Nevertheless, if one formulates the problem for the case $\Gamma^i\gg s^i$ in terms of the same dispersion-theoretic formalism as leads in the other limiting case to (3), and assumes as before that the collision may be treated as a resonance effect, one is led, not to (2), but to the radically different

$$\sigma_k=\frac{\lambda^2}{\pi w_A}\sum_i\frac{\Gamma_{a0}{}^i\Gamma_k{}^i}{(\Gamma^i)^2}, \tag{4}$$

where the summation $\sum_i$ is to be taken over all sets of noncombining states of the compound nucleus, and where, as before, the Γ's for each set are supposed to vary slowly with energy. Since (4) differs from (2) by the substitution for $1/s^i$ of $2/(\pi\Gamma^i)$, and since $\Gamma^i\gg s^i$, the cross sections given by (4) are smaller than those given by (2). As we shall see in III, the formal reason for this, and the reason for the failure of the statistical argument leading to (2), is that the "combining" states of the compound nucleus lying within a line breadth of each other do not at all act independently, and that strong destructive interference is involved in the probability of their excitation [cf. (12)]. The coherence of phases implied by this interference is itself a consequence of the assumption that the processes involved in the collision may be adequately described in terms of resonance between states representing the incident particle (which may be elastically scattered at the surface of the nucleus), and other states of the compound system which have a very long life ($\sim\hbar/\Gamma^i$). This in turn implies that it is not necessary to include in the description those wave packets built up from the long lived states of the compound system, which represent short lived compound nuclei, and which correspond physically, on the one hand, to "surface effect" inelastic scattering and transmutation, and on the other to the possibility of forming the intermediate nucleus by a sequence of processes involving compound systems of increasingly long life and more complete energy degradation.

In the problem of the radiative capture of slow neutrons to which the Breit-Wigner formula was first applied, the characteristic energy dependence of the observed cross sections itself indicates the appropriateness of describing the collision as a resonance effect. But in the other limiting case, where $\Gamma^i\gg s^i$, neither (2) nor (4) may be applied without a careful examination of the physical problem. Since Γ^i increases, and s^i decreases, with the excitation energy, (2) and (4) differ more and more as the energy of the bombarding particle increases. It is in any case clear that the factor $\Gamma_{a0}{}^i/\Gamma^i$ which occurs in (4) will fall off rapidly with energy because of the increasing improbability of a complete concentration of the excitation energy, and for sufficiently high energies the description of the collision as a resonance effect must in general be completely inappropriate.

A striking illustration of this is afforded by the impacts of quite fast neutrons on nuclei. In this case, as one may see from the simple mechanical model discussed by Bohr,[1] it will be extremely unlikely that the energy of the incident neutron will at once be divided among all the nuclear particles; rather the normal course of events will involve an inelastic impact near the surface of the nucleus, in some cases leading merely to the

[3] Bethe and Placzek, Phys. Rev. **51**, 450 (1937).

ejection of a particle with reduced energy, but quite often followed by a series of further impacts which lead ultimately to the complete degradation of the energy and the formation of a compound system of very long life. Such a situation cannot be formally described in terms of a simple resonance effect, nor can the formation of the compound system be treated without considering the wave packets which represent the surface disturbances and short lived intermediate states. On the other hand just the complication of the mechanisms actually involved in the formation of the compound nucleus may offer some justification, in this case, for the assumption of random phases[4] involved in the derivation of (2).

A still more striking case of the inadequacy of (4) to describe transmutations we find in reactions initiated by bombardment with high energy deuterons, where, in spite of the fact that the emission of a deuteron of high energy from a compound nucleus must be extremely rare, the cross section for deuteron induced transmutations can be of the order of magnitude of the area of the nucleus. It is clear that here in the course of the formation of the compound nucleus, the original coupling between proton and neutron will be completely dissolved, and that the formation of the compound nucleus, whether it involves the capture of proton or neutron or both, may surely not be considered as a single process.

As an example of a problem to which we may make a tentative application of (4), we may consider the nuclear photoeffect in complex nuclei, for γ-ray energies high enough to make $\Gamma^2 \gg s^i$, and yet low enough so that the absorption of the radiation can be treated as a resonance effect. That such a treatment can remain valid for higher excitation energies for γ-rays than for neutrons depends upon the fact that the interaction between a γ-ray and a nuclear particle is smaller in order of magnitude than that between the particles themselves: whereas the waves representing incident neutrons of high energy will be very rapidly damped out at the surface of the nucleus, those representing γ-rays will be practically undamped, and therefore far more effective in exciting oscillations of the nucleus as a whole. Apart from a necessarily rough estimate of the contribution of the nonresonance effects, to which we shall refer again in II, and which shows that it may well be smaller than that given by (4), there is some experimental evidence in favor of the applicability of (4) to this problem, in that the smallness of the ratio of the effects observed for light nuclei (N^{14}, O^{16}) to those observed for nuclei of intermediate atomic weight is most easily interpreted in terms of the far shorter lifetime of the lighter compound nuclei.

[4] Compare the discussion of W. Pauli, Sommerfeld Festschrift, p. 30, 1928.

II

It is, of course, not possible at present to calculate the Γ's on the basis of any complete nuclear theory; and, particularly in those problems to which classical arguments cannot be simply applied, one must resort to the transmutation experiments themselves, and may hope to use (4) and (2) in some cases to correlate the values of the Γ's so obtained. It is from this point of view that we shall discuss the photodisintegration of nuclei by high energy γ-rays. For nuclei of intermediate weight we would expect that the compound nucleus formed by absorption of the γ-ray will ordinarily dissipate its energy by the emission of neutrons, since the emission of a charged particle would require a much greater concentration of energy in the escaping particle than is required by a neutron, because of the necessity of its clearing the Coulomb barrier. This argument may not however be applied to those nuclei, relatively common for atomic weight below 20 and above 150, for which the emission of a charged particle is energetically far more favorable than that of a neutron.

Experiments on the capture of thermal energy neutrons (nuclear excitation energy$\sim$8 Mev) give neutron widths $\Gamma_n \sim 10^{-4}$v. As the excitation energy is increased, the neutron width will at first be proportional to the velocity of the neutron; hence for an energy a million volts higher we would estimate $\Gamma_n \sim 1$v. For still larger excitation energy the neutron width will increase very rapidly, because of the rapidly increasing number of probable modes of disintegration. For several million volts additional excitation energy

we would therefore expect Γ_n of the order of some tens or hundreds of volts. The spacing between levels is between 10 and 100 v for 8 Mev excitation energy, decreases rapidly with increasing energy, and should become less than Γ_n for several million volts additional energy. Thus when a nucleus is raised by absorption of a γ-ray to an excitation energy greater than this, the level breadth will surely be wider than the spacing between levels, and we may try to use (4) to discuss the problem. Since in all probability $\Gamma \sim \Gamma_n \gg \Gamma_\gamma$, the cross section for neutron emission is

$$\sigma_n = (\lambda^2/w_A\pi)\sum_i \Gamma_{\gamma 0}{}^i/\Gamma_n{}^i.$$

We may expect that the number of noncombining sets (i) which contribute appreciably would be comparable with w_A, and shall thus write

$$\sigma_n \sim (\lambda^2/\pi)\Gamma_{\gamma 0}/\Gamma_n, \qquad (5)$$

where here the Γ's may be regarded as appropriate averages over the contributing noncombining sets (i).

The photoeffects produced in many nuclei by the 17 Mev γ-ray of Li^7+H^1 have been studied by Bothe and Gentner,[5] who do in fact find that the typical reaction involves the ejection of a neutron. Their estimate, $\sigma_n \sim 10^{-27}$ cm^2, gives at once, since $\lambda^2/\pi \sim 10^{-23}$ cm^2,

$$\Gamma_{\gamma 0}/\Gamma_n \sim 10^{-4}.$$

If we combine with this the estimate of some 100 v for Γ_n at these energies, we find that $\Gamma_{\gamma 0}$ must be of the order of 1/100 of a volt, about a tenth of the total radiative breadth of the resonances found in slow neutron capture. In fact one might expect that $\Gamma_{\gamma 0}$ would not change very much in going from excitations of 8 to 17 Mev; for, on the one hand, it will increase with a high power (probaby the fifth power characteristic of electric quadripole and magnetic dipole radiation) of the frequency; on the other, it will decrease exponentially very roughly with the square root of the energy because of the smaller probability of finding all the excitation energy in a single mode of high frequency.[6] Thus if one supposes that the electric moments associated with these oscillations of varying frequency are of the same type and order of magnitude at 8 and at 17 Mev, the variation of the two factors on which $\Gamma_{\gamma 0}$ depends will tend to cancel. We should then expect that in this range σ_n should increase with decreasing γ-ray energy, and continue to increase until Γ_n becomes equal to the spacing between levels. At this point (γ-ray energy $\sim$10–12 Mev) we should have $\Gamma_{\gamma 0}/\Gamma_n \sim 10^{-2}-10^{-3}$, and a cross section, σ_n, between 10^{-25} and 10^{-26} cm^2. For still lower energies (5) is no longer valid; we must then, as pointed out by Bethe and Placzek, apply (2), i.e., in (5) replace Γ_n by $(2/\pi)s$. In this range the cross section will decrease with decreasing energy, as s increases.

It would thus be interesting to see if such an increase in yield occurs when photodisintegrations are produced by γ-rays of lower energy. Two points must, however, be kept in mind. In the first place there are in the Li spectrum[7] γ-rays of about 14 Mev which may contribute as much to the photoeffect as the 17 Mev line. Moreover, since the yields from 10–12 Mev radiation may be much larger than those at the higher energies, the presence of any appreciable contamination of such degraded radiation in the experiments we have quoted would render their interpretation uncertain, and the maximum cross sections we suggest might be much too large.

In the second place, our discussion has been based on the use of (4); and we know that the validity of this is conditioned by the possibility of disregarding short-lived intermediate states and their contribution to the formation of the compound nucleus. It is clear that as the energy of the γ-ray is indefinitely increased, processes of absorption involving the dipole moment associated with the acceleration of a single particle, will be essential even for those impacts in which a long lived compound nucleus is ultimately formed. To estimate the order of magnitude of the relative contribution of these processes compared to the resonance effects described by (4), one may in (5) replace $\Gamma_{\gamma 0}/\hbar$ by the radiative transition probability to the normal state for a wave packet representing a concentration of all

[5] Bothe and Gentner, Naturwiss. **25**, 90, 126, 191 (1937).
[6] A discussion of these questions is to be published by Bohr and Kalckar.
[7] Delsasso, Fowler and Lauritsen, Phys. Rev. **51**, 391 (1937).

the excitation energy in one particle, and further replace $\hbar/\Gamma_n$ by the nuclear collision time, and must include a factor to take into account the fact that several wave packets of this type can take part in the absorption process. It seems difficult to obtain a good enough evaluation of the quantities involved to tell us for what energies (4) will become inapplicable. As already pointed out however, the fact that the photoelectric yields for 17 Mev radiation from O^{16} and N^{14} are only about one percent of those from heavier nuclei[8] is a strong indication that resonance effects predominate at these energies, since the lifetime of an intermediate state of a light nucleus is so much smaller than that of a heavy nucleus with the same excitation energy that on the basis of (4), and even allowing for a considerable increase in $\Gamma_{\gamma 0}$, one would anticipate much smaller photoelectric yields.

III

We want now to look more closely at the formal derivation of the result (4), and at the relation of our treatment to the more familiar application of dispersion formulae to nuclear problems.

According to Bohr's picture the intermediate nucleus lasts for a time long compared to the mean time between collisions of particles in the nucleus. In attempting to take this fact into account in formulating a dispersion theoretic treatment of collision problems, certain simplifying assumptions must be introduced, which state that the incident particle may only be either elastically scattered at the surface of the nucleus, or captured to form a compound system of long life which subsequently disintegrates. This can be so only when the short-lived compound systems, which are characteristic of surface effects, are not involved in the inelastic scattering or transmutations. The formal consequence of this simplification is that we can then describe the collision in terms of resonance between two quite distinct types of states, each of which may be supposed to give an approximate description of a stationary state of the whole system. One of these sets, ψ_r, corresponds just to discrete excited states of the compound nuclei; the other set, ψ_s, represents asymptotically a definite residual nucleus in a definite state, and definite free particles of given energies. In setting up these states, we may so choose the ψ_r and their energies E_r, that the coupling between the various r states is as far as possible eliminated, and the ψ_s so that we may neglect all terms in the Hamiltonian directly coupling the s states with each other. The long life of the compound nucleus now means that the coupling between the r and s states is so small that the decay time of the r states is very long compared to the nuclear collision time: the condition that in the description of the collision process short-lived compound nuclei do not appear means that the coupling between r and s states is effective only near resonance, and that we need not consider wave packets built up from the ψ_r whose lifetime is much smaller than that of the states ψ_r themselves.

If we now call the matrix elements of the total Hamiltonian $H_{rr'}$, H_{rs}, $H_{ss'}$, our conditions on the ψ_s mean that $H_{ss'}$ may be treated as a diagonal matrix:

$$H_{ss'}=E_s\delta(s-s').$$

The optimal elimination of the coupling between the r states means, that not $H_{rr'}$, but $H_{rr'}$ corrected for the "line shifts" due to the coupling with the s states, is diagonal:

$$H_{rr'}+P\int ds H_{rs}H_{sr'}/(E-E_s)=E_r\delta_{rr'}, \quad (6)$$

where E is the total energy of the system. We now try to find a wave function of the form

$$\psi=\psi_0+\sum_r c_r\psi_r+\int ds c_s\psi_s,$$

where ψ_0 is that one of the ψ_s which represents asymptotically the bombarding particle and the bombarded nucleus, and is normalized so that the incident flux is unity. The wave equation for the c's is then

$$Ec_r=\sum_{r'}H_{rr'}c_{r'}+\int ds H_{rs}c_s+H_{r0}, \quad (7)$$

$$(E-E_s)c_s=\sum_r H_{sr}c_r. \quad (8)$$

[8] We are indebted to Dr. Cockcroft for telling us of these experiments carried out by Goldhaber and his collaborators.

From this, substituting c_s from (8) in (7), and using (6),

$$\chi_r = H_{r0} - \frac{i}{2}\sum_{r'\neq r}\frac{\Gamma_{rr'}\chi_{r'}}{E-E_{r'}+\frac{1}{2}i\Gamma_{r'r'}}, \qquad (9)$$

where $\Gamma_{rr'}=2\pi\sum_s H_{rs}H_{sr'}$, and the sum $\sum_s$ is taken over all states with $E_s=E$, and where we have introduced

$$\chi_r=(E-E_r+\tfrac{1}{2}i\Gamma_{rr})c_r,$$

which varies smoothly with E.

The assumption that no short-lived intermediate nuclei contribute now means that we may neglect the contribution to the sum in (9) of all states r' for which $|E_{r'}-E|\gg\Gamma_{r'r'}$. When the spacing of the levels, s_r, is large compared to Γ_{rr} we then get at once

$$\chi_r=H_{r0} \quad \text{when} \quad E_r\sim E. \qquad (10)$$

In the other limiting case, with $s_r\ll\Gamma_{rr}$, many terms in the sum contribute. We may then suppose that the Γ's vary smoothly from level to level. There may of course be various sets of intermediate states, for example states of given angular momentum, with quite different sets of Γ's; but in general one will expect this only when the different sets of levels belong to different representations of a group of transformations which leave the Hamiltonian approximately invariant, and in this case each such set (i) may be considered separately; there will be no interference between different sets and their contributions to the cross section will be simply additive, so that from now on we shall consider only a single such set. The summation in (9) may thus be replaced by an integral

$$\chi_r=H_{r0}-\frac{i}{2}\int\frac{dE_{r'}}{s_{r'}}\frac{\Gamma_{rr'}\chi_{r'}}{(E-E_{r'}+\frac{1}{2}i\Gamma_{r'r'})}. \qquad (11)$$

If then we neglect the contribution of levels $|E_{r'}-E|\gg\Gamma_{r'r'}$, and the variation over the line breadth of the matrix elements of H, we may replace the integral by its residue. The solution of (11) is then

$$\chi_r=H_{r0}-\frac{\pi\Gamma_{r\rho}H_{\rho 0}}{2s_\rho+\pi\Gamma}\sim\frac{2s_\rho H_{r0}}{\pi\Gamma} \qquad (12)$$

except when $|E_r-E|\gg\Gamma$, and where $E_\rho\sim E$ and $\Gamma=\Gamma_{\rho\rho}$. Because of the assumed asymptotic form of ψ_s, one sees from (8) that the cross section for a process of type k involving the emission of a given particle and leaving the nucleus in a given state is

$$\sigma_k=(2\pi/\hbar)\sum_{s=k}|\sum_r H_{sr}c_r|^2, \qquad (13)$$

where $\sum_{s=k}$ is to be taken over all states s, with $E_s=E$, and leading to a disintegration of type k. From (10), (12) and (13), and treating the sum over r as before, we then get

$$\sigma_k=\frac{8\pi}{\hbar}\frac{|H_{\rho 0}|^2\sum_{s=k}|H_{s\rho}|^2}{\Gamma^2}, \quad \Gamma\gg s_\rho, \quad E_\rho\sim E. \qquad (14)$$

$$=\frac{2\pi}{\hbar}\frac{|H_{\rho 0}|^2\sum_{s=k}|H_{s\rho}|^2}{(E-E_\rho)^2+\frac{1}{4}\Gamma^2}, \quad \Gamma\ll s_\rho$$

Because of the asymptotic form of ψ_s and ψ_0, the matrix elements occurring in (14) are connected with the decay constant Γ_k for the disintegration of type k, and the decay constant Γ_{a0} for the reemission of the incident particle with its initial energy, by

$$\Gamma_k=2\pi\sum_{s=k}|H_{s\rho}|^2,\ \Gamma_{a0}=(4\pi w_A/\hbar\lambda^2)|H_{\rho 0}|^2.$$

We thus have

$$\sigma_k=\frac{\lambda^2}{\pi w_A}\frac{\Gamma_{a0}\Gamma_k}{\Gamma^2}, \quad \Gamma\gg s_\rho$$

$$=\frac{\lambda^2}{4\pi w_A}\frac{\Gamma_{a0}\Gamma_k}{(E-E_\rho)^2+\frac{1}{4}\Gamma^2}, \quad \Gamma\ll s_\rho. \quad E_\rho\sim E.$$

By summing over all sets of intermediate states (i) we get from this (3) and (4). It is clearly not possible by formal arguments alone to decide whether, in a given problem, the incisive conditions necessary for the validity of (3) or (4) are really fulfilled. For this, as in the case of the nuclear photoeffect, a detailed discussion of the physical problem is in general essential.

Note on Resonances in Transmutations of Light Nuclei

F. KALCKAR, J. R. OPPENHEIMER AND R. SERBER
California Institute of Technology, Pasadena, California

(Received May 19, 1937)

It is shown that the sharp resonance effects observed in many transmutations involving light nuclei require the existence of fairly strict selection rules to limit the decay rates of the corresponding compound nuclei. Such selection rules in several cases follow from the slowness of the interconversion of spin and orbital angular momentum. Some consequences of this are discussed for the bombardment of B and F by protons.

WHEN light nuclei are bombarded with protons, the transmutation functions for the various alternative reactions are often radically different. This suggests that, by bombardment of a given nucleus, compound nuclei can be formed which have quite different properties. Thus in the reaction

$$Li^7+H^1\rightarrow(Be_A^8)\rightarrow 2He^4 \qquad (1a)$$

the yield of 8 cm α-particles increases steadily with bombarding voltage, and for low energies, where such considerations are applicable, follows the course expected from the arguments of Gamow on the penetration of the potential barrier by the proton. On the other hand the reaction in which high energy γ-rays are emitted,

$$Li^7+H^1\rightarrow(Be_B^8)\rightarrow Be^8+\gamma, \qquad (1b)$$

exhibits a pronounced and sharp resonance at a bombarding energy of 440 kv.[1]

With the proton bombardment of fluorine, the situation is similar but a little more complicated. Here too the 6 cm α-particle yield from the reaction

$$F^{19}+H^1\rightarrow(Ne_A^{20})\rightarrow O^{16}+He^4 \qquad (2a)$$

increases rapidly with bombarding energy,[2] but the γ-ray transmutation function[1] shows sharp resonances of increasing magnitude at 330 kv, 890 kv, 940 kv. Two reactions have been proposed to account for these γ-rays,

$$F^{19}+H^1\rightarrow(Ne_B^{20})\rightarrow(O_B^{16})+He^4 \rightarrow O^{16}+He^4+\gamma \qquad (2b)$$

$$F^{19}+H^1\rightarrow(Ne_B^{20})\rightarrow(Ne_C^{20})+\gamma \rightarrow\begin{cases}O^{16}+He^4+\gamma\\ Ne^{20}+\gamma+\gamma'\end{cases} \qquad (2b')$$

where again the parentheses indicate excited nuclei. At least for low bombarding energies the γ-rays are approximately monochromatic,[3] with an energy $\sim$6 Mev; the excitation energy of the Ne_B^{20} is more than twice this.

Still more complicated is the bombardment of B^{11} with protons. Here most of the α-particles are to be ascribed[4] to the reaction

$$B^{11}+H^1\rightarrow(C_A^{12})\rightarrow(Be_A^8)+He^4\rightarrow 3He^4, \qquad (3a)$$

where the Be_A^8 has an excitation of a few Mev. The yield of these alpha-particles increases smoothly[5] and without marked evidence of resonance for bombarding energies up to 600 kv. On the other hand both the reactions

$$B^{11}+H^1\rightarrow(C_B^{12})\rightarrow Be^8+He^4 \qquad (3b)$$

$$B^{11}+H^1\rightarrow(C_B^{12})\rightarrow C^{12}+\gamma \qquad (3b')$$

show[5, 6] sharp resonance at 180 kv. The yield of γ-rays increases again markedly[7] at about 700 kv, suggesting the existence of a further resonance level in this neighborhood.

Since in any case the sharpness of resonance is a measure of the lifetime of the compound nucleus formed by the capture of the bombarding particle, the compound nuclei Be_B^8, Ne_B^{20}, C_B^{12} must differ very radically from Be_A^8, Ne_A^{20}, C_A^{12} as to their possibilities and rates of disintegration. Now in each of the cases we are considering,

[1] Hafstad, Heydenburg and Tuve, Phys. Rev. **50**, 504 (1936).
[2] Henderson, Livingston and Lawrence, Phys. Rev. **46**, 38 (1934).
[3] Delsasso, Fowler and Lauritsen, Phys. Rev. **51**, 527, (1937).
[4] Dee and Gilbert, Proc. Roy. Soc. **154**, 279 (1936).
[5] Williams, Wells, Tate and Hill, Phys. Rev. **51**, 434 (1937).
[6] Bothe and Gentner, Zeits. f. Physik **104**, 685 (1937).
[7] Fowler and Lauritsen, private communication.

there are just three energetically possible modes of disintegration:

(1) Reemission of the bombarding proton, with decay constant $\Gamma_p/\hbar$,
(2) emission of an α-particle, $\Gamma_\alpha/\hbar$,
(3) γ-radiation, $\Gamma_\gamma/\hbar$.

The decay constant of the compound nucleus will be just $\Gamma/\hbar=(\Gamma_p+\Gamma_\alpha+\Gamma_\gamma)/\hbar$. The absence of marked resonance effects for the A-reactions shows that Γ must be very large for the A nuclei; Γ_γ is always small, and Γ_p is surely small for low bombarding energies because of the effect of the barrier. Under these circumstances $\Gamma\sim\Gamma_\alpha$, $\Gamma_\alpha\gg\Gamma_\gamma$, $\Gamma_\alpha\gg\Gamma_p$. Thus the sharp resonances observed for the B-reactions show that the B nuclei can disintegrate by α-emission, either not at all, or very much more slowly than the A nuclei. The reaction (3b) shows that in this case at least we have to do with retarded but not forbidden α-decay. What is then the distinction between the A and B nuclei which brings about this great difference in behavior?

For the case of Be_B^8, a satisfactory answer to this question has already been given,[1] for since two unexcited α-particles are necessarily described by a wave function which is even with respect to the mirroring of the coordinates of all particles in the center of mass, a state of Be^8 will not be able to decay into two such α-particles at all if it is odd; we thus account qualitatively for the facts if we say that Be_A^8 is even, Be_B^8 odd. Analogous considerations of parity are however inapplicable to C^{12} and Ne^{20}, since the disintegration products are not in these cases identical nuclei. It is true that arguments of parity may demand that the α-particle come off with a relative angular momentum different from zero; but the energy of the α-particle is so high that this will not alter the order of magnitude of the decay constant. We have thus to ask what other selection rule can so markedly reduce the α-decay rate of the two nuclei C_B^{12}, Ne_B^{20}.

Now there is one feature of nuclear forces which follows quite generally from the fact that the velocities of neutrons and protons are small compared to c, that we have here an essentially nonrelativistic problem. This is that the total spin S of the neutrons and protons, and their total orbital angular momentum L, will vary only very slowly with time;[7a, 8] for the coupling between them which is responsible for their variation is of the order $(v/c)^2$, and corresponds, according to the suggestion of Inglis,[9] merely to the Thomas precession of the spins in accelerated motion ($\omega_T=-(\mathbf{v}\times\dot{\mathbf{v}})/2c^2$). Thus the ideas of Bohr on the ease of energy exchange between particles, and the fact that nuclear forces surely do depend upon the relative spin orientations of the particles, guarantee a rapid exchange on the one hand of the orbital angular momentum among the particles composing the nucleus, and on the other of the individual particle spins, but do not in any way alter the approximate constancy of S and L. In fact, since the rate of conversion of spin into orbital angular momentum should be proportional to the square of the coupling energy, this conversion should take a time larger than the nucleus collision time by a factor of the order $(c/v)^4\sim10^4$.[10]

Now for the α-particle certainly $S=0$. Moreover, for the product nuclei Be^8, O^{16} one would expect from very general symmetry arguments that the lowest states would have paired neutron and proton spins and $S=0$. Thus the normal α-decay products will have vanishing spin, and only when the intermediate nucleus too has $S=0$ will this normal α-decay be rapid; for compound nuclei with $S\neq0$, the possibility of such decay will depend on the interconversion of spin and orbital angular momentum, the decay time will in any case be increased by a factor $(c/v)^4$, and marked resonance effects will appear. The absence of such resonance for the A nuclei shows that for them $S=0$; thus normal F^{19} and B^{11} must have $S=\frac{1}{2}$, as indeed one would expect. We then wish to suggest that Ne_B^{20}, C_B^{12} are triplet states, with $S=1$. More generally, it

[7a] L and S would be constants of the motion for any nuclear Hamiltonian which is invariant under a rotation of the positional coordinates of all particles alone, and of their spins alone. This condition is satisfied for all the types of forces commonly considered in nonrelativistic nuclear theory (Majorana, Heisenberg, Wigner, Bartlett forces).

[8] The importance of the approximate constancy of S for the interpretation of nuclear reactions was first recognized by Goldhaber, Proc. Camb. Phil. Soc. **30**, 361 (1934).

[9] D. R. Inglis, Phys. Rev. **50**, 783 (1936).

[10] This selection rule applies only to the interconversion of spin and orbital momentum; in γ-ray emission, where magnetic dipole radiation can alter the spin, and probably in β-ray emission, transitions involving a change of S by one unit are hardly less probable than those leaving it unaltered.

seems not unlikely that for nuclei of odd atomic weight the normal states will have $S=\frac{1}{2}$, so that when these are bombarded by protons or neutrons, only singlet and triplet states of the compound nucleus will be formed. If states of even higher multiplicity were formed in such reactions, they would be almost stable against normal α-decay.

II

We shall now have to see in greater detail whether this explanation is tenable, and what implications it has for the interpretation of the reactions in question.

The Ne^{20} formed by bombarding F^{19} with protons has an excitation energy of more than 12 Mev. We should thus expect the singlet states, which can decay to $O^{16}+He^4$, to have a short lifetime, since the α-particles emitted have so great an energy that the effects of the potential barrier will be negligible.[11] Since, for instance, for the heavier and less highly excited nucleus P^{31} formed from $Al^{27}+He^4$, the breadth of the levels is $\sim 10^5$ v, we would expect for the singlet levels of Ne^{20}, $\Gamma \sim \Gamma_\alpha \sim 10^5 - 10^6$ v. This breadth is so large that from such states we should surely expect no marked resonance in the yield of long range α-particles.[11] For triplet states of Ne^{20} the long range α-emission will be slowed up by $(c/v)^4$, so that here $\Gamma_\alpha' \sim 100$ v. In order to account on the basis of reaction (2b′) for the fact[12] that the γ-ray yields at ~ 1 Mev are at least ten times the total long range α-particle yield, we should thus have to assume a value of $\Gamma_\gamma \sim 1000$ v. This value is far larger than any which have been found for nuclear γ-rays, and at least 100 times that necessary to account for the far more energetic γ-ray of the simpler nucleus Be_B^8. Moreover, the fact that the γ-ray spectrum consists only of radiation quite near 6 Mev could on this basis be explained only quite artificially. We are thus led to consider the possibility that O^{16} has triplet states lying about 6 Mev above ground, and that the reaction which successfully competes with the emission of long range α-particles is the emission of slow α-particles, without spin change, but with so low an energy that the level breadth Γ_α'', though larger than Γ_α', is still small enough to give sharp resonances ($100 \text{ v} < \Gamma_\alpha'' < 10{,}000$ v). Experimentally one knows that at bombarding energies ~ 400 kv there are no short range α-particles of energy > 2 Mev emitted;[7] and for this process to compete successfully with the long range α-emission, the energy of the particles cannot be far less than 1.5 Mev. A value in this neighborhood is consistent with the energy balance. If this suggestion is correct, one would expect the ratio $\Gamma_\alpha''/\Gamma_\alpha'$ to increase rapidly with energy; and for the lowest resonance level (~ 330 kv) it would seem possible that some long range α-particles could be observed. The absence of other lines in the γ-ray spectrum could then be interpreted in a natural way because of the absence of low-lying excited states in the "closed shell" nucleus O^{16}.

In the case of the $B^{11}+H^1$ reactions, one will again expect that the Γ_α for C^{12} in singlet states will be large, and that with an increase in bombarding energy the yield in (3a) will increase smoothly with Γ_p. Again one will make a triplet C^{12} responsible for the γ-ray emission and the long range α-particles which show marked resonance. But here there is a point which calls for further explanation: why is the ratio of long to short range α-particles so much smaller for C_A^{12} than for C_B^{12}? Since for the low resonance energy the reaction (3a) is far more probable than (3b), and since the long range α-particles are not isotropically distributed in direction,[13] it seems reasonable to assume that C_A^{12} is formed by capture of an s-proton, and is odd, and that C_B^{12} is formed by p-capture, and is even. If the normal state of B^{11} were a ^2P state, C_A^{12} would then be an odd ^1P state; and C_B^{12} an even ^3D state, so that both states could give both α-particle reactions, and one could expect no great difference in the relative yields. If however normal B^{11} is a ^2D, then C_A^{12} is an odd ^1D, and this cannot disintegrate into a normal $Be^8(^1S)$ and an unexcited α-particle at all, whereas C_B^{12},

[11] Since $\Gamma_\alpha \gg \Gamma_p$, and Γ_α varies slowly with bombarding energy, the interpretation of the rapid rise (faster than Γ_p) of the yield in this reaction given in reference (2) cannot be right. If this more rapid rise should be confirmed, one would have to understand it in terms of a residual structure for the singlet levels, or a contribution from high-lying triplet levels, of the compound nucleus.

[12] E. McMillan, Phys. Rev. **46**, 868 (1934).

[13] Neuert, Physik. Zeits. **38**, 122 (1937).

in an even triplet state can. We wish therefore to suggest this interpretation, which is hardly in serious conflict with the calculations[14] based on a Hartree model, according to which the ^2D of B^{11} is only $\sim 2.5\ mc^2$ higher than the ^2P. According to this view the resonance reaction may contribute also to the short range α-particles, and the small yield from this reaction must be ascribed to the smallness of Γ_p for a p-proton at these low energies.

With the Li reactions, one point remains a little puzzling if one accepts the usual interpretation: since normal Li^7 is almost certainly odd, the long range α-reaction must be ascribed to the capture of a p-proton, the Be_B^8 to that of an s-proton. The fact that the long range α-reaction comes from p-capture may in part account[15] for the smallness of the α-particle yield compared to that of the reaction $Li^6+H^1 \rightarrow He^3+He^4$. One would now expect that if the Be_A^8 could be formed in a ^1D state, the corresponding α-particles should be distributed in angle with marked anisotropy; and the fact that the observed distribution[16] seems to be isotropic suggests that such states contribute little to Be_A^8 in the range of energies ($\sim$250 kv) investigated. This could then only be understood if the spacing of levels of different angular momentum in Be^8, even at the high excitation of 17 Mev, were still large compared to the very considerable breadth of these levels.

[14] Feenberg and Wigner, Phys. Rev. **51**, 95 (1937); Feenberg and Phillips, Phys. Rev. **51**, 597 (1937).

[15] Compare M. Goldhaber, Proc. Camb. Phil. Soc. **30**, 561 (1934).

[16] Kirchner, Physik. Zeits. **34**, 785 (1933); Giarratana and Brennecke, Phys. Rev. **49**, 35 (1936).

AUGUST 15, 1937 PHYSICAL REVIEW VOLUME 52

Neutron Scattering Cross Section as a Function of Energy

ALLAN C. G. MITCHELL AND R. N. VARNEY
Physics Department, New York University, University Heights, New York

(Received June 9, 1937)

The study of scattering of neutrons of energy range from 0.02 to 80 volts from Fe, Ni, and Pb has been completed by measuring the activation of Ag, Rh, and CHI_3 detectors. The scattering of C neutrons was determined indirectly by two methods, and the results agreed closely. The scattering cross section for Ni fell off slowly with neutron velocity, that for Pb increased slightly, while that for Fe remained constant over the range from 0.02 to 80 volts. The directional distribution of neutrons emerging from the top of a paraffin cylinder containing a Ra–Be neutron source was investigated by placing detectors at various distances above the top of the paraffin. The results agreed well with those calculated for a cosine distribution law.

PART I. SCATTERING CROSS SECTION

A CONSIDERABLE amount of work has been done recently on the scattering of neutrons from various materials. Mitchell and Murphy[1–2] measured the scattering cross section for a number of elements, while Pontecorvo and Wick[3] measured the reflection of neutrons from several substances and calculated scattering cross sections for a few of these. Furthermore, various materials sensitive to neutrons of different energies have been used as detectors. We have extended our experiments on the scattering of slow neutrons using various detectors and filter combinations so that we now have data on the scattering cross section of neutrons of energies from 0.02 to 80 volts for several different scattering materials.

The method used was that previously described with certain modifications which we shall show to be unessential. A cylindrical block of paraffin, 15 cm in diameter and 17 cm high, contained a source of neutrons located 6 cm from its top surface. Ag, Rh, and CHI_3 were used as detectors of the various groups of neutrons.

[1] A. C. G. Mitchell and E. J. Murphy, Phys. Rev. **48**, 653 (1935); Mitchell, Murphy, and Langer, Phys. Rev. **49**, 400 (1936).

[2] Mitchell, Murphy, and Whitaker, Phys. Rev. **50**, 133 (1936).

[3] B. Pontecorvo and G. C. Wick, Ricerca Scient. **1**, 134, 220 (1936).

The detectors were 6 by 10 cm in area and were irradiated by placing them on the top of the paraffin block for a given length of time. The scattering material, in the present instance Fe, Ni, and Pb, in the form of metallic blocks the same size as the scatterer, was placed above the detector. After irradiation the detectors were counted with the help of a tube counter and recording mechanism. The percentage scattering was plotted as a function of the thickness of the scattering material, after suitable corrections had been made for absorption in the detector.[2]

The detectors used were metallic silver, thickness 0.105 g/cm², for neutrons of groups C and $A+B$; and metallic rhodium, thickness 0.124 g/cm², for neutrons of groups C and D. These detectors were used with and without a cadmium filter, thickness 0.218 g/cm², which completely absorbs neutrons of group C. The neutrons which affect iodine, group I, were detected with the help of CHI_3 deposited in paraffin and mounted between thin aluminum foils. The concentration of iodine was approximately 0.1 g/cm², but varied slightly among the detectors in the group. The iodine detectors were always used with Cd filtering so that only I neutrons were detected. Under these conditions the fraction of neutrons transmitted by the detector was 0.80. The fraction of neutrons transmitted by the other two detectors is tabulated in the previous paper.[2]

In the earlier work the neutron source consisted of a small glass bulb containing beryllium and radon in amounts up to 300 millicuries. In the present work the source consisted of 211 mg of radium, in the form of $RaCl_2$, mixed with 5 grams of beryllium powder, contained in a brass capsule 2 cm in diameter and 5 cm long. The capsule was placed in the paraffin with its axis parallel to the top surface and so that its center was on the axis of the paraffin cylinder. With the axis of the capsule 6 cm below the top surface of the paraffin, the activity of an Ag detector irradiated with the radium-beryllium mixture was compared with that obtained when a mixture of radon and beryllium, of known strength, was used under the same geometrical conditions. The activity per millicurie was found to be the same, to within 10 percent, in either case. Furthermore, certain scattering curves taken with the radon-beryllium source were redone with the radium-beryllium source and the results were in agreement.

Since the activity of the iodine detector was rather weak it was found necessary to place the neutron source closer to the top surface of the paraffin. A new cylinder of paraffin was prepared, having the same dimensions as the previous one, except that the neutron source was placed 4 cm below the surface. Since the relative scattering cross section depends on the geometry of the beam, corrections had to be made so that all cross sections would be on the same basis. This was accomplished by running a scattering curve for Fe with an Ag detector with Cd filtering, first with the arrangement in which the neutron source was 4 cm below the surface of the paraffin and second when it was 6 cm below. The results for the iodine detector were then corrected to standard conditions, i.e., source 6 cm below surface, by multiplying by the ratio.

Source 6 cm below surface/Source 4 cm below surface.

The scattering curves were similar to those previously published[2] and consisted of one portion in which the scattering for small thicknesses of scatterer, was proportional to the thickness, and another portion for larger thicknesses in which the scattering eventually became independent of the thickness. Over the linear portion of the curve the slope may be equated to $N\sigma$, where σ is the relative scattering cross section and N the number of scattering nuclei per cm³. The relative scattering cross sections for the elements Fe, Ni, and Pb for neutrons affecting the various detectors are shown in Table I.

From Table I the scattering cross section for the C neutrons can be obtained in two ways: (1) From the scattering cross sections found with the Ag detector; and (2) from similar results with the Rh detector. The scattering cross section for neutrons of two groups x and y can be calculated from that for the separate groups from the relation

$$\sigma_{x+y}=\frac{n_x}{n_x+n_y}\sigma_x+\frac{n_y}{n_x+n_y}\sigma_y, \qquad (1)$$

where $n_x/(n_x+n_y)$ is the fraction of the activity of the detector due to group x. For the arrangements we have used we find that in the Ag detector the fraction of the activity due to group

TABLE I. *Relative scattering cross sections* $\times 10^{24}$ *cm*^{2}.

Group Element	$A+B+C$	$A+B$	D	I	$C+D$
Fe	10.5	11.6	10.0	10.8	9.3
Ni	18	13.4	11.9	12	17
Pb	7.7	12.3	6.6	13	—

C is 0.75 and that due to $A+B$ is 0.25; while for Rh we find 0.72 due to C and 0.28 due to D. Using this method in conjunction with the results shown in Table I we find:

For Fe

$$(\sigma_c)_{Ag}=10.2 \quad 10^{-24} \text{ cm}^2;$$

and

$$(\sigma_c)_{Rh}=9.1 \quad 10^{-24} \text{ cm}^2.$$

For Ni

$$(\sigma_c)_{Ag}=19.5 \quad 10^{-24} \text{ cm}^2;$$

and

$$(\sigma_c)_{Rh}=18.9 \quad 10^{-24} \text{ cm}^2.$$

The agreement is therefore quite good for σ_c calculated from two different detectors.

The scattering cross section is shown as a function of the energy of the neutrons in Table II. The values for the energy of the various groups are taken from the paper of Goldsmith and Rasetti,[4] who determined these energies from the absorption coefficient in boron.

It will be seen from Table II that, in the case of Fe, the scattering cross section is independent of energy. Ni shows a larger cross section for thermal neutrons than for those of higher velocities, while the reverse is true for Pb. It is known from the work of Breit and Wigner[5] that the scattering cross section will be affected by the positions and widths of the resonance levels of the scatterer. These factors are not known for the elements in question so that it is difficult to predict the dependence of scattering cross section on energy. It would appear that, since the scattering cross section in Pb is small in the region up to 3.5 volts, there are probably resonance levels giving rise to absorption in this region.

[4] H. H. Goldsmith and F. Rasetti, Phys. Rev. **50**, 328 (1936).

[5] G. Breit and E. Wigner, Phys. Rev. **49**, 519 (1936).

TABLE II. *Scattering cross section as a function of neutron energy.*

Group	Energy (volts)	Scattering Cross Section $\times 10^{24}$ cm^2		
		Fe	Ni	Pb
C	0.02	9.8	19.2	6.2
D	1.16	10.0	11.9	6.6
$A+B$	3.5	11.6	13.5	12.3
I	80	10.8	12	13

PART II. DIRECTIONAL DISTRIBUTION OF NEUTRONS EMERGING FROM PARAFFIN

Some time ago Mitchell and Murphy[1] reported experiments in which they attempted to measure the directional distribution of neutrons emerging from the top of the paraffin cylinder. Recently Amaldi and Fermi,[6] from measurements of the activity of detectors at small distances below the top surface of the paraffin cylinder, came to the conclusion that the thermal neutrons issued from the surface of the paraffin according to the law $\cos\theta+\sqrt{3}\cos^2\theta$. We have repeated the experiments of Mitchell and Murphy with the object of testing the above law, through measurements of the intensity of the neutron beam outside of the paraffin.

In the present experiments the top surface of the paraffin was covered with a sheet of Cd, 1 mm thick in the center of which there was a rectangular aperture 6×10 cm. Ag detectors, 6×10 cm., could be placed at various positions above the top surface of the paraffin. Arrangements were also made to place an additional Cd filter (0.218 g/cm^2) over the aperture so that the activity of the Ag detector due to C neutrons could be obtained by the difference in activity with and without the Cd filter. Furthermore, sheets of Ag 1 mm thick were placed on the top of the bucket covering the whole surface except the 6×10 cm opening. This was done to prevent neutrons issuing from the outer edges of the paraffin surface from being recorded by the Ag detector. Direct experiment showed that 1 mm Ag, used as an absorber, diminished the activity of an Ag detector irradiated with neutrons filtered through 0.218 g/cm^2 Cd to 46 percent of its original intensity.

[6] E. Amaldi and E. Fermi, Ricerca Scient. **1**, 11–12, p. 1 (1936); Phys. Rev. **50**, 899 (1936).

With the 211 mg radium-beryllium source, measurements were made with the Ag detector at several different distances above the paraffin surface both with and without the additional filter of Cd. The difference in the activity of the detector with and without Cd filtering (effect due to C neutrons) was plotted as a function of the distance above the top surface of the paraffin. A smooth curve was drawn through the points and the following points taken off the curve are shown in Table III together with points calculated for a theortical neutron distribution, which will be discussed below.

To compare our results with theory we made the following calculations: (1) The number of neutrons emerging from a rectangular aperture of area $dxdy$ and striking a parallel detector area $dx'dy'$ located r_0 cm above the aperture is given by

$$dn = n_0 \cos^2 \theta \, dxdy \, dx'dy'/\pi r^2, \qquad (2)$$

where n_0 is the number emerging per unit area, r is the distance between $dxdy$ and $dx'dy'$, and θ is the angle between r and the normal to $dxdy$. The assumption here is that the neutron intensity falls off as the square of the distance and that the directional distribution follows the simple geometrical cosine law. This equation was integrated over the length and breadth of the aperture and the detector of the same size and shape. The resulting equation is omitted, but the results of the calculations are shown in column 3 of Table III. (Ratio of n/n_0.)

(2) According to Amaldi and Fermi, the distribution of neutrons differs from the cosine law, so that Eq. (2) should read

$$dn = n_0(\cos^2 \theta + \sqrt{3} \cos^3 \theta)dxdy \, dx'dy'/\pi r^2. \quad (3)$$

We have also integrated this equation and find as may be expected that over relatively large detector and aperture areas there is almost no difference between the two resulting distributions. It is also to be expected that the Fermi and Amaldi distribution should give a relatively higher value of n/n_0 at small distances. This is confirmed by comparing the results in columns 3 and 4 of Table III, but the difference is seen to be far below the experimental error of measurement and therefore beyond observation.

Experiments were tried and calculations made for small apertures and large detectors. Because of the weak intensity of the neutron beam, the maximum predicted differences between the results for large and small apertures were of the same size as the experimental error.

The following conclusions can be drawn from these experiments: (1) The experimental results for detectors and apertures of the same size are in essential agreement with the cosine law of distribution. (2) The law of Amaldi and Fermi differs so little from the cosine law for large apertures and detectors that the experiments could not possibly differentiate between them.

Finally, in comparing curves for the total activity of the Ag detectors, activiated by neutrons of groups C, A and B (i.e. with no Cd absorber over the aperture) taken using a radon-beryllium source or the radium-beryllium source, it was found that the points fitted the same curve to better than 5 percent. Since the radon-beryllium mixture was contained in a small bulb about 1 cm in diameter and the radium-beryllium source in a cylinder of much larger dimensions, it follows that the distribution of neutrons issuing from the paraffin is dependent on the amount of paraffin present and the size of the aperture but does not depend critically on the size or shape of the neutron source.

Financial assistance has been received through a grant to one of us (ACGM) from the Penrose Fund of the American Philosophical Society.

TABLE III. *Intensity of neutron beam as a function of distance from upper surface of paraffin.*

DISTANCE (cm)	OBSERVED	INTENSITY CALCULATED ($\cos\theta$)	CALCULATED ($\cos\theta + \sqrt{3}\cos^3\theta$)
0	1.000	1.000	1.000
1	—	0.776	0.787
2	0.590	0.615	0.625
3	0.461	0.488	—
4	0.361	0.400	—
5	0.290	0.322	0.322
6	0.250	0.265	—
7	0.215	0.222	0.227

The Scattering of Neutrons by Ortho- and Parahydrogen

JULIAN SCHWINGER
Columbia University, New York, New York

AND

E. TELLER
George Washington University, Washington, D. C.

(Received June 12, 1937)

Calculations have been performed which indicate that experiments on the scattering of neutrons by ortho- and parahydrogen would enable one to determine the sign of the singlet state binding energy and the range of the neutron-proton interaction, in addition to providing direct information concerning the spin dependence of the neutron-proton interaction. A dependence of the neutron-proton interaction upon the relative spin orientation of the particles will manifest itself in a marked difference between the slow neutron scattering cross sections of orthohydrogen (parallel proton spins) and parahydrogen (anti-parallel proton spins). Neutrons with energy less than 0.068 ev, incident upon *para*-H_2 in its ground state ($J=0$, $v=0$, $S=0$), may be either elastically scattered, or inelastically scattered with excitation of the molecule to the ground state of the *ortho* system ($J=1$, $v=0$, $S=1$). This latter process, requiring 0.023 ev, occurs only if the neutron-proton interaction is spin dependent. When the neutron energy is less than 0.045 ev, the cross section for the scattering of neutrons by *ortho*-H_2 in its ground state will be the sum of the elastic scattering cross section and the cross section for the inelastic process in which the molecule is converted to a *para*-H_2 molecule in its ground state, with the neutron taking up the excess energy. The cross sections of these four processes have been calculated, assuming an interaction range of 2×10^{-13} cm and a virtual singlet state of the deuteron. For liquid-air temperature neutrons ($3kT/2=0.012$ ev), $\sigma_{\text{para}}(0.012)=0.21\times10^{-24}$ cm², while $\sigma_{\text{ortho}}(0.012)=65\times10^{-24}$ cm². The cross sections for neutrons at ordinary temperatures ($3kT/2=0.037$ ev), however, are $\sigma_{\text{para}}(0.037)=19\times10^{-24}$ cm², and $\sigma_{\text{ortho}}(0.037)=50\times10^{-24}$ cm². Therefore, if the present concept of the neutron-proton interaction is valid, one would expect the following results: (a) The *ortho*-scattering cross section for liquid air neutrons should be about 300 times the corresponding *para*-scattering cross section. (b) The *para*-scattering cross section for ordinary thermal neutrons should be roughly 100 times the *para*-scattering cross section for liquid air neutrons. For a real singlet state, however, these ratios are of the order of one. The elastic *para*-scattering cross section is quite sensitive to the value of the range of interaction if the singlet state is virtual. For example, the value of this cross section at liquid air neutron temperatures with zero range of interaction is 1.75×10^{-24} cm², as compared with 0.26×10^{-24} cm² for an interaction range of 2×10^{-13} cm. Hence, from a measurement of the *para* elastic scattering cross section for homogeneous neutrons at some energy less than 0.023 ev, the range of interaction in the triplet state may be inferred with some degree of accuracy. A discussion of the influence of intermolecular forces on the previous results is given.

INTRODUCTION

WIGNER and Bethe and Peierls[1] have given a simple theory of the scattering of neutrons by protons, assuming a short range neutron-proton interaction. The resultant scattering cross section:

$$\sigma=\frac{4\pi\hbar^2}{M}\frac{1}{|E_0|+\frac{1}{2}E}, \tag{1}$$

depends only upon the binding energy $|E_0|$ of the deuteron, and the energy E of the neutron measured in the system in which the proton is initially at rest.

For small neutron energies ($E\ll|E_0|$), Eq. (1) predicts a scattering cross section of 2.40×10^{-24} cm², since $|E_0|=2.2\times10^6$ ev. This is in complete disagreement with the experimental value of $\sigma=13\times10^{-24}$ cm².[2] This discrepancy cannot be explained by using a finite value of r_0, the range of the neutron-proton force. Bethe and Bacher[3] have shown, for a rectangular potential hole, that the Bethe-Peierls formula must be multiplied by $1+\alpha_0 r_0$, i.e.,

$$\sigma=\frac{4\pi\hbar^2}{M}\frac{1+\alpha_0 r_0}{|E_0|+\frac{1}{2}E}, \tag{2}$$

where

$$\alpha_0=(M|E_0|/\hbar^2)^{\frac{1}{2}}=2.29\times10^{12}\ \text{cm}^{-1}. \tag{3}$$

It is easily shown that this formula is practically

[1] E. Wigner, Zeits. f. Physik **83**, 253 (1933); H. A. Bethe and R. Peierls, Proc. Roy. Soc. **A149**, 176 (1935).

[2] E. Amaldi and E. Fermi, Phys. Rev. **50**, 899 (1936).

[3] H. A. Bethe and R. F. Bacher, Rev. Mod. Phys. **8**, 82 (1936).

independent of the shape of the potential well. With a reasonable value of r_0 obtained from the theory of the light nuclei, namely $r_0 = 2 \times 10^{-13}$ cm, this modified Bethe-Peierls formula gives a cross section of 3.50×10^{-24} cm^2, for slow neutrons.

To explain this marked lack of agreement, Wigner[4] advanced the suggestion that the neutron-proton interaction in the singlet state differs from that in the triplet state. From this assumption, it follows that

$$\sigma = \frac{4\pi\hbar^2}{M}\left(\frac{3}{4}\frac{1+\alpha_0 r_0}{|E_0|+\frac{1}{2}E} + \frac{1}{4}\frac{1+\alpha_1 r_0}{|E_1|+\frac{1}{2}E}\right), \quad (4)$$

where $|E_1|$ is the energy of the singlet state, and

$$\alpha_1 = \pm(M|E_1|/\hbar^2)^{\frac{1}{2}}, \quad (5)$$

the plus or minus sign obtaining according as the singlet state is real or virtual, respectively. Since the ground state of the deuteron gives no information about $|E_1|$, it can be chosen to give agreement with the experimental results. The large slow neutron scattering will be explained, therefore, if $|E_1| = 142{,}000$ ev for a real level, or $|E_1| = 114{,}000$ ev for a virtual level.

Fermi[5] has shown that one can determine which of these two possibilities is realized by a measurement of the cross section for radiative capture of neutrons by protons. Such measurements have been performed,[2] and indicate the existence of a virtual singlet state of the deuteron It should be pointed out, however, that on the basis of the β-ray theory of magnetic moments, it is questionable whether Fermi's mechanism of magnetic dipole capture can be correctly treated by simply assuming the additivity of magnetic moments.

It is the purpose of this paper to point out that experiments on the scattering of neutrons by ortho- and parahydrogen would afford a direct means of testing Wigner's hypothesis of a spin-dependent interaction between neutrons and protons. Furthermore, it will be shown that, from the results of such experiments, one can deduce the energy of the singlet state and the range of the forces.

[4] E. Feenberg and J. K. Knipp, Phys. Rev. **48**, 906 (1935).

[5] E. Fermi, Phys. Rev. **48**, 570 (1935); Ricerca Scient. VII-II, 13 (1936).

I

Neutrons of thermal energy have a wave-length which is of the same order as the distance between the protons in H_2. One should therefore observe interference between the neutron waves scattered from the two protons in the hydrogen molecule. If the neutron-proton interaction depends upon the relative spin orientation of the particles, this should manifest itself in a difference between the interference effects in ortho- and parahydrogen, i.e., parallel and antiparallel proton spins, respectively. In addition to demonstrating directly the existence or nonexistence of spin forces, an experimental determination of these scattering cross sections would give the amplitudes of the singlet and the triplet scattered waves, save for a possible common factor of (-1). It should be emphasized that these results can be obtained without a detailed theory of the mechanism of interaction. Making the usual assumptions about the interaction, one can then determine the energy of the singlet level, and the range of the neutron-proton force.

The problem of calculating scattering cross sections is complicated by the presence of inelastic scattering processes. In general, all possible transitions consistent with conservation of energy and momentum will occur. However, a neutron-proton interaction which is independent of spin will only induce transitions between states of the molecule with the same total spin angular momentum, that is, *ortho-ortho* and *para-para* transitions, while spin-dependent interactions will also cause *ortho-para* and *para-ortho* transitions.

It is interesting to note that, for neutrons with energy comparable to the excitation energy of the first few rotational levels, the *ortho*-scattering cross section differs from the *para*-scattering cross section, even if no spin-dependent forces act between neutrons and protons. This is a consequence of the different rotational energy levels of ortho- and parahydrogen. Neutrons with energies large compared with the lowest rotational levels, however, will have the same scattering cross sections in ortho- and parahydrogen. If, on the other hand, the neutron wave-length is large compared with the internuclear separation in hydrogen, the elastic

scattering in ortho- and parahydrogen will differ if spin-dependent forces are present, but will be the same if no such spin forces are operative.

At sufficiently low temperatures, the molecules of H_2 are in their respective ground states, namely $J=0$, $v=0$ for *para*-molecules and $J=1$, $v=0$ for *ortho*-molecules. In the absence of spin-dependent neutron-proton forces, slow neutrons will suffer only elastic collisions. The scattering cross sections of slow neutrons in ortho- and parahydrogen will, therefore, be the same.

If, however, the neutron-proton interaction involves the relative spin orientation of the particles, the cross section corresponding to the conversion of an *ortho*-molecule into a *para*-molecule will also contribute to the *ortho*-scattering cross section, whereas the *para* cross section will still consist of only the elastic cross section. Therefore, at sufficiently low neutron energies, a difference between the scattering of ortho- and parahydrogen should manifest itself.

II

The mathematical treatment of the scattering of neutrons by hydrogen molecules may be given with the aid of a theorem which Fermi[6] utilized in his considerations on the effect of molecular binding forces on the neutron-proton scattering cross section. With neglect of the dependence of the neutron-proton interaction upon the relative spin orientation of the particles, this theorem states that the scattering of a neutron by a bound proton may be calculated with the Born approximation, by using

$$-(4\pi\hbar^2/M)a\delta(\mathbf{r}_n-\mathbf{r}_p) \tag{6}$$

as the effective neutron-proton interaction. Here $\delta(\mathbf{r})$ is the three-dimensional Dirac δ-function, and a is defined by the solution corresponding to zero energy of the wave equation for the relative motion of the particles, namely:

$$1+a/r \quad \text{for} \quad r>r_0. \tag{7}$$

The condition of validity of this result is that there exist a quantity R which is large compared with r_0 and a, but small compared with the de Broglie wave-lengths of the neutron and the proton. This condition is easily satisfied for slow neutrons and the protons in the hydrogen molecule.

The extension of this theorem to an interaction which differs in the singlet state from that in the triplet state is made without difficulty. We need merely replace a in formula (6) by an operator whose eigenvalue for a triplet state is a_1, the value of a calculated for the triplet interaction, and whose eigenvalue for a singlet state is a_0, the value of a calculated for the singlet interaction. Such an operator can be written:

$$\tfrac{1}{2}a_1(1+Q)+\tfrac{1}{2}a_0(1-Q), \tag{8}$$

where Q is an operator with the eigenvalues $+1$ and -1 for triplet and singlet states, respectively. It has been shown by Dirac[7] that Q can be expressed algebraically in terms of $\boldsymbol{\sigma}_n$ and $\boldsymbol{\sigma}_p$, the Pauli matrices of the neutron and the proton, *viz.:*

$$Q=\tfrac{1}{2}(1+\boldsymbol{\sigma}_n\cdot\boldsymbol{\sigma}_p). \tag{9}$$

Therefore, (6) must be replaced by

$$-(\pi\hbar^2/M)(3a_1+a_0 +(a_1-a_0)\boldsymbol{\sigma}_n\cdot\boldsymbol{\sigma}_p)\delta(\mathbf{r}_n-\mathbf{r}_p). \tag{10}$$

The effective interaction between a neutron and the protons in the hydrogen molecule will then be

$$\begin{aligned}&-(\pi\hbar^2/M)(3a_1+a_0 +(a_1-a_0)\boldsymbol{\sigma}_n\cdot\boldsymbol{\sigma}_1)\delta(\mathbf{r}_n-\mathbf{r}_1)\\ &-(\pi\hbar^2/M)(3a_1+a_0 +(a_1-a_0)\boldsymbol{\sigma}_n\cdot\boldsymbol{\sigma}_2)\delta(\mathbf{r}_n-\mathbf{r}_2),\end{aligned} \tag{11}$$

in consequence of the small probability that the protons approach within a distance of the order of R.

It is convenient to separate (11) into two parts which are, respectively, symmetrical and antisymmetrical in the proton spins, namely:

$$\begin{aligned}&-(\pi\hbar^2/M)(3a_1+a_0+(a_1-a_0)\boldsymbol{\sigma}_n\cdot\mathbf{S}) \times(\delta(\mathbf{r}_n-\mathbf{r}_1)+\delta(\mathbf{r}_n-\mathbf{r}_2))\\ &-(\pi\hbar^2/2M)(a_1-a_0)\boldsymbol{\sigma}_n\cdot(\boldsymbol{\sigma}_1-\boldsymbol{\sigma}_2) \times(\delta(\mathbf{r}_n-\mathbf{r}_1)-\delta(\mathbf{r}_n-\mathbf{r}_2)),\end{aligned} \tag{12}$$

where

$$\mathbf{S}=\tfrac{1}{2}(\boldsymbol{\sigma}_1+\boldsymbol{\sigma}_2) \tag{13}$$

represents the total spin angular momentum of the molecule. It is evident that the symmetrical part of the interaction will be responsible for

[6] E. Fermi, Ricerca Scient. VII–II, 13 (1936).

[7] P. A. M. Dirac, *Quantum Mechanics*, second edition (Oxford, 1935).

those transitions in which the spin symmetry of the molecule does not change, that is, *ortho-ortho* and *para-para* transitions. The antisymmetrical part of the interaction, however, will induce *ortho-para* and *para-ortho* transitions.

Consider a scattering process in which a neutron with momentum $\mathbf{p}^0$ collides with a hydrogen molecule with the momentum $-\mathbf{p}^0$, the vibrational quantum number v, the rotational quantum number J, and the quantum number S of the resultant proton spin. We wish to calculate the probability that the neutron is scattered with the momentum $\mathbf{p}$, leaving the molecule in a state described by the set of quantum numbers $-\mathbf{p}$, v', J', S'. The wave function of the initial state, normalized in a volume V, is:

$$\Psi_i = V^{-\frac{1}{2}} \exp\left((i/\hbar)\mathbf{p}^0\cdot\mathbf{r}_n\right)\chi_m V^{-\frac{1}{2}} \exp\left(-(i/\hbar)\mathbf{p}^0\cdot(\mathbf{r}_1+\mathbf{r}_2)/2\right)\phi_{v,\,J,\,m_J}(\mathbf{r}_1-\mathbf{r}_2)\chi_{S,\,m_S}, \tag{14}$$

where $V^{-\frac{1}{2}} \exp\left((i/\hbar)\mathbf{p}^0\cdot\mathbf{r}_n\right)$ is the wave function of a free neutron with momentum $\mathbf{p}^0$, χ_m is the eigenfunction of the z-component of the neutron spin corresponding to the eigenvalue m, $V^{-\frac{1}{2}} \exp\left(-(i/\hbar)\mathbf{p}^0\cdot(\mathbf{r}_1+\mathbf{r}_2)/2\right)$ is the wave function which describes the motion of the center of gravity of the hydrogen molecule with momentum $-\mathbf{p}^0$, $\phi_{v,\,J,\,m_J}(\mathbf{r}_1-\mathbf{r}_2)$ is the wave function of the relative motion of the two protons in a state with vibrational quantum number v, rotational quantum number J and magnetic quantum number m_J, and, finally, $\chi_{S,\,m_S}$ is the eigenfunction of the proton spins corresponding to a resultant spin angular momentum S and an eigenvalue of the z-component of the total spin equal to m_S. Similarly, the wave function of the final state is:

$$\Psi_f = V^{-\frac{1}{2}} \exp\left((i/\hbar)\mathbf{p}\cdot\mathbf{r}_n\right)\chi_{m'} V^{-\frac{1}{2}} \exp\left(-(i/\hbar)\mathbf{p}\cdot(\mathbf{r}_1+\mathbf{r}_2)/2\right)\phi_{v',\,J',\,m'J}(\mathbf{r}_1-\mathbf{r}_2)\chi_{S',\,m'S}. \tag{15}$$

According to the well-known Born formula, the probability of the transition per unit time is given by:

$$(2\pi/\hbar)\,|(\Psi_f,\ U\Psi_i)|^2\rho_E, \tag{16}$$

where U denotes the expression (12) for the interaction, and ρ_E represents the number of neutron momentum states per unit range of the total final energy. Writing $E_{J,\,v}$ for the internal energy of the molecule in a state characterized by the quantum numbers v and J, we have

$$E=(3/4M)p^{0^2}+E_{J,\,v}=(3/4M)p^2+E_{J',\,v'}, \tag{17}$$

by the law of conservation of energy. Therefore, if we consider a process in which the neutron is scattered through an angle Θ into a solid angle $d\Omega$, the number of final states per unit range of the total final energy is

$$\rho_E=\frac{Vp^2}{8\pi^3\hbar^3}\frac{dp}{dE}d\Omega=V\frac{Mp}{12\pi^3\hbar^3}d\Omega. \tag{18}$$

Formula (16) gives the transition probability for definite values of m, m_J, m_S and m', m_J', m_S'. Since we are not interested in the transition probabilites between particular degenerate states, we must sum over all values of m', m_J', m_S' and average with respect to m, m_J, m_S. Therefore, the total transition probability per unit time will be

$$\frac{1}{2(2S+1)(2J+1)}\sum_{m',\,m'_J,\,m'_S}\sum_{m,\,m_J,\,m_S}|(\Psi_f,\ U\Psi_i)|^2\frac{VMp}{6\pi^2\hbar^4}d\Omega. \tag{19}$$

Dividing by the neutron flux relative to the hydrogen molecule, namely

$$3p^0/2MV, \tag{20}$$

we obtain the differential cross section $\sigma_{J',\,v',\,S';\,J,\,v,\,S}(\Theta)d\Omega$ for scattering of a neutron through an angle Θ into the solid angle $d\Omega$ with excitation of the molecule from the state J, v, S to the state

J', v', S', referred to the system in which the center of gravity of the neutron and the molecule is at rest, *viz.*:

$$\sigma_{J',\,v',\,S';\,J,\,v,\,S}(\Theta)d\Omega=\frac{4}{9}\frac{p}{p^0}\frac{1}{2(2S+1)(2J+1)}\sum_{m',\,m'_J,\,m'_S}\sum_{m,\,m_J,\,m_S}\left|\left(\Psi_f,\frac{MV}{2\pi\hbar^2}U\Psi_i\right)\right|^2 d\Omega. \quad (21)$$

The summation with respect to m, m_S and m', m_S' may be performed without difficulty. We consider first those transitions in which the total spin of the molecule remains unchanged, i.e., $S'=S$. Utilizing the expressions (14) and (15) for the initial and final wave functions, we obtain:

$$\left(\Psi_f,\frac{MV}{2\pi\hbar^2}U\Psi_i\right)=-\frac{1}{2V}(m';S,m_S'|3a_1+a_0+(a_1-a_0)\boldsymbol{\sigma}_n\cdot\mathbf{S}|m;S,m_S)$$

$$\cdot\int\exp\left[(i/\hbar)(\mathbf{p}^0-\mathbf{p})\cdot(\mathbf{r}_n-(\mathbf{r}_1+\mathbf{r}_2)/2)\right]\phi^*_{v',\,J',\,m'_J}(\mathbf{r}_1-\mathbf{r}_2)\phi_{v,\,J,\,m_J}(\mathbf{r}_1-\mathbf{r}_2)$$

$$\times(\delta(\mathbf{r}_n-\mathbf{r}_1)+\delta(\mathbf{r}_n-\mathbf{r}_2))d\tau_n d\tau_1 d\tau_2=-(m';S,m_S'|3a_1+a_0+(a_1-a_0)\boldsymbol{\sigma}_n\cdot\mathbf{S}|m;S,m_S)$$

$$\cdot\int\cos\frac{(\mathbf{p}^0-\mathbf{p})\cdot\mathbf{r}}{2\hbar}\phi^*_{v',\,J',\,m'_J}(\mathbf{r})\phi_{v,\,J,\,m_J}(\mathbf{r})d\tau. \quad (22)$$

Therefore,

$$\sum_{m,\,m_S}\sum_{m',\,m'_S}\left|\left(\Psi_f,\frac{MV}{2\pi\hbar^2}U\Psi_i\right)\right|^2=\left|\int\cos\frac{(\mathbf{p}^0-\mathbf{p})\cdot\mathbf{r}}{2\hbar}\phi^*_{v',\,J',\,m'_J}(\mathbf{r})\phi_{v,\,J,\,m_J}(\mathbf{r})d\tau\right|^2$$

$$\cdot\sum_{m,\,m_S}\sum_{m',\,m'_S}|(m';S,m_S'|3a_1+a_0+(a_1-a_0)\boldsymbol{\sigma}_n\cdot\mathbf{S}|m;S,m_S)|^2. \quad (23)$$

Since $3a_1+a_0+(a_1-a_0)\boldsymbol{\sigma}_n\cdot\mathbf{S}$ is diagonal with respect to the total spin of the molecule, the second factor of this expression may be written:

$$\sum_{m,\,m_S}\sum_{m',\,S',\,m'_S}|(m';S',m_S'|3a_1+a_0+(a_1-a_0)\boldsymbol{\sigma}_n\cdot\mathbf{S}|m;S,m_S)|^2, \quad (24)$$

which becomes

$$\sum_{m,\,m_S}(m;S,m_S|(3a_1+a_0+(a_1-a_0)\boldsymbol{\sigma}_n\cdot\mathbf{S})^2|m;S,m_S) \quad (25)$$

by the matrix law of multiplication. Now

$$(3a_1+a_0+(a_1-a_0)\boldsymbol{\sigma}_n\cdot\mathbf{S})^2=(3a_1+a_0)^2+(a_1-a_0)^2\mathbf{S}^2+2(3a_1+a_0)(a_1-a_0)\boldsymbol{\sigma}_n\cdot\mathbf{S}-(a_1-a_0)^2\boldsymbol{\sigma}_n\cdot\mathbf{S}, \quad (26)$$

from which we obtain

$$2(2S+1)((3a_1+a_0)^2+S(S+1)(a_1-a_0)^2) \quad (27)$$

for the sum (25), using the fact that the diagonal sum of an angular momentum matrix is zero.

Collecting our formulae, we obtain finally

$$\sigma_{J',\,v',\,S';\,J,\,v,\,S}(\Theta)d\Omega=(4p/9p^0)((3a_1+a_0)^2+S(S+1)(a_1-a_0)^2)$$

$$\cdot\frac{1}{2J+1}\sum_{m_J,\,m'_J}\left|\int\cos\frac{(\mathbf{p}^0-\mathbf{p})\cdot\mathbf{r}}{2\hbar}\phi^*_{v',\,J',\,m_J'}(\mathbf{r})\phi_{v,\,J,\,m_J}(\mathbf{r})d\tau\right|^2 d\Omega. \quad (28)$$

We may note that Eq. (28) gives a nonvanishing transition probability only if J and v are both even or both odd, since $\phi_{v,\,J,\,m_J}(-\mathbf{r})=(-1)^J\phi_{v,\,J,\,m_J}(\mathbf{r})$. Indeed, this is required by the well-known condition

$$(-1)^J=(-1)^S, \quad (29)$$

imposed by the Pauli exclusion principle. Therefore *ortho-ortho* transitions are associated with transitions between states of odd rotational quantum number, while *para-para* transitions are associated with transitions between states of even J.

A similar calculation shows that the scattering cross sections for transitions in which the total spin of the molecule changes, i.e., $S'=1-S$, are given by:

$$\sigma_{J',\,v',\,1-S;\,J,\,v,\,S}(\Theta)d\Omega=(4p/9p^0)(a_1-a_0)^2(3-2S)\cdot\frac{1}{2J+1}\sum_{m_J,\,m'_J}\left|\int\sin\frac{(\mathbf{p}^0-\mathbf{p})\cdot\mathbf{r}}{2\hbar}\phi^*_{v',\,J',\,m'J}(\mathbf{r})\phi_{v,\,J,\,m_J}(\mathbf{r})d\tau\right|^2 d\Omega. \quad (30)$$

It is evident from (29) that *ortho-para* and *para-ortho* transitions are accompanied by odd-even and even-odd transitions in the rotational quantum number J, respectively.

III

The minimum energy necessary to excite the molecule from the state J, v to the state J', v' is $(2/3)(E_{J',\,v'}-E_{J,\,v})$, if the neutron energy is measured in a system moving with the center of gravity of the neutron and the molecule. Measured in the system in which the molecule is initially at rest, the requisite energy is $(3/2)(E_{J',\,v'}-E_{J,\,v})$ since $\mathbf{p}_0$, the initial momentum of the neutron in the latter system of reference, is given by

$$\mathbf{p}_0=3\mathbf{p}^0/2. \quad (31)$$

For small rotational and vibrational quantum numbers, the energy levels of the molecule, in volts, are:[8]

$$E_{J,\,v}=0.015\tfrac{1}{2}J(J+1)+0.533v. \quad (32)$$

Therefore, if the neutron energy is less than 0.045 ev, the energy necessary to excite the J transition 1→2, the only excitation process which may take place is the J transition 0→1, requiring 0.023 ev.

The most interesting effects are obtained at low temperatures which are such that practically all the hydrogen molecules will be in their respective ground states, namely $v=0$, $J=0$ for *para*-molecules, and $v=0$, $J=1$ for *ortho*-molecules. With these restrictions upon the neutron energy and the initial states of the molecule, the only processes which can occur are those in which the vibrational states remain unexcited and J undergoes any of the four possible transitions: 0→0, 0→1, 1→0, 1→1.

To a sufficient approximation, the probability of these transitions may be calculated by treating the H_2 molecule as a rigid rotator. The wave function appropriate to this model is:

$$\phi_{0,\,J,\,m_J}(\mathbf{r})=\left(\frac{2J+1}{4\pi}\frac{(J-|m_J|)!}{(J+|m_J|)!}\right)^{\frac{1}{2}}\sin^{|m_J|}\vartheta\left(\frac{d}{d\cos\vartheta}\right)^{J+|m_J|}\frac{(\cos^2\vartheta-1)^J}{2^J J!}e^{im_J\varphi}(\delta(r-r_e))^{\frac{1}{2}}/r_e, \quad (33)$$

where r_e, the equilibrium nuclear separation, has the numerical value[8]

$$r_e=0.75\times10^{-8}\text{ cm}. \quad (34)$$

According to the principle of spectroscopic stability, the sums which occur in Eqs. (28) and (30) have a value which is independent of the direction of quantization. It is evident from (33) that, if the direction of quantization is taken to be the direction of the vector $\mathbf{p}^0-\mathbf{p}$, the only nonvanishing terms in these sums are those for which $m_J=m_J'$. Therefore, the number of terms is equal to the rotational multiplicity of the state with smaller rotational quantum number.

The only matrix element which need be evaluated to calculate the elastic scattering from para-hydrogen (0→0), is

$$\int\cos\left(\frac{|\mathbf{p}^0-\mathbf{p}|r\cos\vartheta}{2\hbar}\right)|\phi_{0,\,0,\,0}(r)|^2 2\pi r^2 dr\sin\vartheta d\vartheta=\frac{\sin(|\mathbf{p}^0-\mathbf{p}|r_e/2\hbar)}{|\mathbf{p}^0-\mathbf{p}|r_e/2\hbar}. \quad (35)$$

[8] W. Jevons, *Report on Band-Spectra of Diatomic Molecules* (Cambridge, 1932).

In terms of Θ, the angle of scattering in the system of the center of gravity, this may be written

$$\frac{\sin\left[(p^0r_e/\hbar)\sin\tfrac{1}{2}\Theta\right]}{(p^0r_e/\hbar)\sin\tfrac{1}{2}\Theta}. \tag{36}$$

Therefore,

$$\sigma_{0,\,0,\,0;\,0,\,0,\,0}(\Theta)2\pi\sin\Theta d\Theta=\frac{4}{9}(3a_1+a_0)^2\left(\frac{\sin\left[(p^0r_e/\hbar)\sin\tfrac{1}{2}\Theta\right]}{(p^0r_e/\hbar)\sin\tfrac{1}{2}\Theta}\right)^2 2\pi\sin\Theta d\Theta. \tag{37}$$

The total elastic scattering cross section is

$$\sigma_{0,\,0,\,0;\,0,\,0,\,0}=\frac{32\pi}{9}(3a_1+a_0)^2\left(\frac{\hbar}{p^0r_e}\right)^2\int_0^{p^0r_e/\hbar}\frac{\sin^2 x}{x}dx$$

$$=\frac{16\pi}{9}(3a_1+a_0)^2\left(\frac{\hbar}{p^0r_e}\right)^2\left[\log\frac{2p^0r_e}{\hbar}-Ci\frac{2p^0r_e}{\hbar}+0.5772\right], \tag{38}$$

where

$$Cix=-\int_x^\infty\frac{\cos t}{t}dt. \tag{39}$$

A similar calculation yields the following cross sections for the $0\to1$, $1\to0$, $1\to1$ transitions, respectively:

$$\sigma_{1,\,0,\,1;\,0,\,0,\,0}=32\pi(a_1-a_0)^2\left(\frac{\hbar}{p^0r_e}\right)^2\left[\frac{\sin x}{x}+\frac{\cos x-1}{x^2}+\tfrac{1}{2}\log x-\tfrac{1}{2}Cix\right]_{(p^0-p)r_e/\hbar}^{(p^0+p)r_e/\hbar},\quad p=\left(p^{0^2}-\frac{4M}{3}E_{1,\,0}\right)^{\frac{1}{2}};$$

$$\sigma_{0,\,0,\,0;\,1,\,0,\,1}=\frac{32\pi}{3}(a_1-a_0)^2\left(\frac{\hbar}{p^0r_e}\right)^2\left[\frac{\sin x}{x}+\frac{\cos x-1}{x^2}+\tfrac{1}{2}\log x-\tfrac{1}{2}Cix\right]_{(p-p^0)r_e/\hbar}^{(p+p^0)r_e/\hbar},\quad p=\left(p^{0^2}+\frac{4M}{3}E_{1,\,0}\right)^{\frac{1}{2}};$$

$$\sigma_{1,\,0,\,1;\,1,\,0,\,1}=\frac{16\pi}{3}((3a_1+a_0)^2+2(a_1-a_0)^2)\frac{1}{\xi^2}\left[-\frac{3}{\xi^2}\left(\frac{\sin\xi}{\xi}-\cos\xi\right)^2+\frac{\sin^2\xi}{\xi^2}+\log 2\xi-Ci2\xi-0.4228\right],$$

$$\xi=\frac{p^0r_e}{\hbar}. \tag{40}$$

These four cross sections, calculated for a virtual singlet state of the deuteron and a range $r_0=2\times10^{-13}$ cm, are plotted in Figs. 1, 2 as a function of the neutron energy.[9] The curves for any other choice of the range of interaction and the sign of the binding energy of the singlet state[10] may be obtained by an appropriate change of scale since only the values of a_1 and a_0 need be changed. Thus, if the singlet state is taken as real rather than virtual, the cross sections for the elastic scattering by parahydrogen should be multiplied by 244.

It is evident from these graphs that the present concept of the neutron-proton interaction as a spin-dependent force leading to a virtual state of the deuteron, and of range $r_0=2\times10^{-13}$ cm, implies the following qualitative predictions:

(a) The scattering cross section of parahydrogen for ordinary thermal neutrons ($E=0.037$ ev) should be about 100 times the scattering cross section of parahydrogen for liquid-air neutrons ($E=0.012$ ev);

[9] The quantities a_1 and a_0 are obtained from the free proton triplet and singlet scattering cross sections with the aid of the relations: $\sigma_{\text{triplet}}=4\pi a_1^2$, $\sigma_{\text{singlet}}=4\pi a_0^2$. The sign of a_0/a_1 is positive if the singlet state is real, negative if the singlet state is virtual.

[10] We speak of a positive binding energy if the state is real, a negative binding energy if it is virtual.

(b) The scattering cross section of orthohydrogen for liquid-air neutrons should be roughly 300 times the scattering cross section of parahydrogen for liquid-air neutrons;

(c) The scattering cross section of orthohydrogen for ordinary thermal neutrons should be only 2 or 3 times larger than the scattering cross section of parahydrogen for these neutrons;

(d) The *ortho*-scattering cross section for ordinary thermal neutrons should be about three-fourths of the *ortho*-scattering cross section for liquid-air neutrons.

If, however, the singlet state is real, the parahydrogen scattering cross section for ordinary thermal neutrons should be about $\frac{3}{4}$ of the parahydrogen scattering cross section for liquid-air neutrons, and the orthohydrogen cross section should be approximately 7/5 of the *para*-scattering cross section for liquid-air neutrons. A comparison of these two predictions shows clearly that this, rather than the capture of neutrons by protons, is the ideal method for determining the sign of the deuteron singlet state binding energy.

The parahydrogen elastic scattering cross section varies sensitively with the range of the neutron-proton interaction. This is illustrated in Fig. 3 for a virtual singlet state. It is seen, for example, that the scattering cross section for zero range is 7 times the scattering cross section for a range of $r_0=2\times10^{-13}$ cm. An experimental determination of the parahydrogen scattering cross section for neutrons of some definite energy

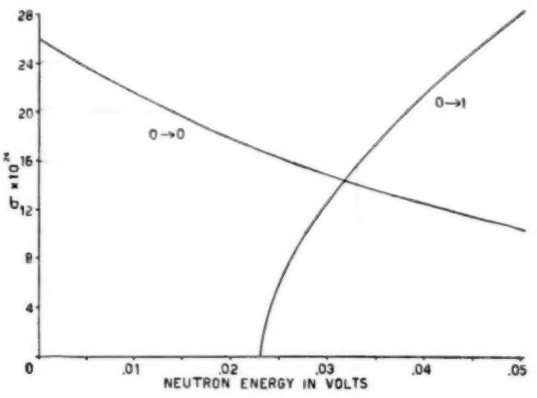

FIG. 1. The elastic (0→0) and inelastic (0→1) scattering cross sections of parahydrogen, calculated for a virtual singlet state of the deuteron and a range of interaction in the triplet state equal to 2×10^{-13} cm. The ordinates of the elastic scattering curve are enlarged 100 fold.

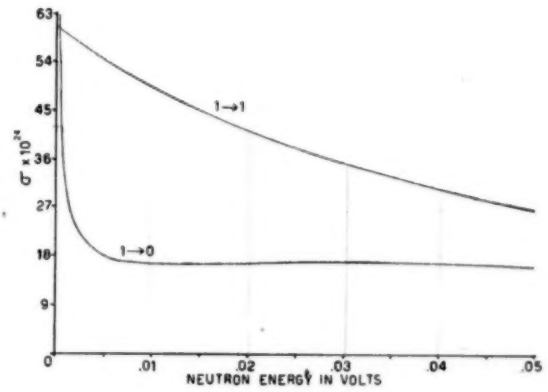

FIG. 2. The elastic (1→1) and inelastic (1→0) scattering cross sections of orthohydrogen, calculated under the same assumptions as Fig. 1.

less than 0.023 ev would, therefore, permit one to calculate the range of the neutron-proton interaction with some degree of accuracy. Neutron beams with a sufficient energy homogeneity can be obtained with a mechanical velocity selector[11] or with the aid of Bragg reflection from crystals.[12]

Unfortunately, this scattering cross section is of the same order as the capture cross section if the singlet state is virtual. This necessitates a theoretical knowledge of the capture cross section if one performs absorption measurements. Since the deuteron formed in a capture process has a recoil energy (~1000 ev) which is very large compared with the molecular binding energy of a proton, the cross section for this process can be calculated by assuming the protons to be free.[13] The capture cross section per molecule, therefore, is twice the free proton capture cross section, and thus has the numerical magnitude[5] 0.6×10^{-24} cm^2 at liquid-air temperatures ($E=0.012$ ev), provided the singlet state is virtual.

IV

The neglect of intermolecular forces in the preceding discussion limits its applicability to the scattering by H_2 in its gaseous state. However, experiments are most easily carried out with liquid or solid hydrogen where intermolecular

[11] G. A. Fink, Phys. Rev. **50**, 738 (1936).
[12] D. P. Mitchell and P. N. Powers, Phys. Rev. **50**, 486 (1936).
[13] An analytical proof has been given by W. E. Lamb, Jr., Phys. Rev. **51**, 187 (1937).

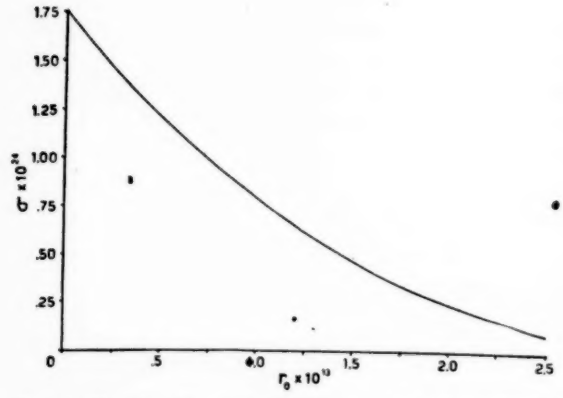

FIG. 3. The elastic scattering cross section of parahydrogen for neutrons of zero energy, as a function of the range of interaction in the triplet state. The singlet state of the deuteron is assumed to be virtual.

forces may have an appreciable effect. The discussion of this effect may be simplified by supposing the molecules to vibrate independently about positions of equilibrium with a frequency ν, given by

$$h\nu = k\Theta_E, \tag{41}$$

where Θ_E, the characteristic Einstein temperature, is related to the characteristic. Debye temperature Θ_D by[14]

$$\Theta_E = 3\Theta_D/4. \tag{42}$$

Experimentally,[15] $\Theta_D = 105°\text{K}$, from which we obtain

$$h\nu = 0.007 \text{ ev}. \tag{43}$$

Consequently, if the neutron energy is large compared with 0.007 ev, the molecules may be treated as if they were free and the preceding results are applicable.

The heat of evaporation and the heat of fusion of normal and parahydrogen agree to within 1 percent,[16] which is good evidence for the free rotation of hydrogen molecules in the liquid and solid phase.[17] This is supported by experiments upon the Raman effect in liquid H_2.[18] We may conclude that intermolecular forces act only upon the center of gravity of a hydrogen molecule, and do not affect its internal motion. Therefore, the appropriate description of the effect of intermolecular forces upon the *elastic* scattering cross sections is obtained by multiplying our previous results by a function $F(E/h\nu)$ which approaches 1 rapidly as E becomes greater than $h\nu$. The limiting value of this function for $E/h\nu \ll 1$ may be obtained by an elementary consideration. When E is small compared with $h\nu$, the effective mass of a molecule is the same as the mass of the whole liquid or solid. Now the scattering cross section is proportional to the square of the reduced mass of the system, that is, $4M^2/9$ for a free molecule, and M^2 for a strongly bound molecule. Therefore $F(0) = 9/4$ so that the elastic scattering cross sections we have obtained should be multiplied by a function which decreases rapidly from 9/4 to 1 with increasing neutron energy.[19] The effect of intermolecular forces upon the $1 \rightarrow 0$ transition will be much less important, for even with $E = 0$ the molecule has a recoil energy of the order of $h\nu$.

If the *ortho*-scattering cross section consisted only of the elastic cross section, the ratio of the *ortho-* to the *para*-scattering would be independent of intermolecular forces, since the interaction between *ortho*-molecules is practically identical with the interaction between *para*-molecules.[20] It is clear, therefore, that the effect of intermolecular forces will not be such as to alter our qualitative comparison between the *ortho-* and *para*-scattering cross sections. Unfortunately, however, the $1 \rightarrow 0$ cross section, with its different dependence upon the intermolecular forces, is added to the elastic ortho-scattering cross section. It is necessary, therefore, to perform measurements at energies which are large compared with $h\nu$, so that intermolecular forces may be neglected, but yet are less than 0.023 ev. A measurement of the scattering cross sections of both ortho- and parahydrogen at some such energy would enable one to calculate the amplitudes a_1 and a_0, from which we may obtain r_0 and the free proton scattering cross

[14] N. F. Mott and H. Jones, *The Theory of the Properties of Metals and Alloys* (Oxford, 1936).
[15] G. Bartholomé, Zeits. f. physik. Chemie **33**, 387 (1936).
[16] A. Farkas, *Orthohydrogen, Parahydrogen and Heavy Hydrogen* (Cambridge, 1935).
[17] The anomalous specific heat of solid orthohydrogen at very low temperatures indicates that, at these temperatures, rotation ceases to be free.
[18] J. C. McLennan and J. H. McLeod, Nature **123**, 160 (1929).
[19] A similar argument enables one to deduce Fermi's result of an increase in the scattering cross section of a proton bound to a heavy molecule by a factor of 4 over the corresponding value for a free proton, in the limiting case of zero neutron velocity.
[20] R. B. Scott and F. G. Brickwedde, Phys. Rev. **51**, 684 (1937).

section, thus permitting a check of the consistency of the whole theory.

Note added in proof: Recently published experiments by J. Halpern, I. Estermann, O. C. Simpson and O. Stern, Phys. Rev. **52**, 142 (1937) indicate that the scattering cross section of *ortho*-H_2 for liquid-air neutrons is much larger than the corresponding *para*-H_2 scattering cross section. This proves conclusively that the singlet state of the deuteron is virtual.

AUGUST 15, 1937 PHYSICAL REVIEW VOLUME 52

Statistics and Nuclear Reactions

V. WEISSKOPF
Institute for Theoretical Physics, Copenhagen, Denmark
(Received March 18, 1937)

It is possible to apply statistical methods to the calculation of nuclear processes provided that the energies involved are large in comparison with the lowest excitation energies of nuclei. Expressions are obtained for the emission probability of neutrons or charged particles by highly excited heavy nuclei. These expressions are built up in a similar way to the formula for the probability of evaporation of a particle from a body at low temperatures. In applying it to the impact of high energy neutrons on heavy nuclei, the mean energy loss per impact turns out to be $E[1-2(a/E)^{\frac{1}{2}}]$ where E is the energy of the incident neutrons and a is dependent on the nuclear structure; we can put approximately $a \sim 0.05$–0.2 MV. The energy distribution of the scattered neutrons is approximately a Maxwellian one with a mean energy of $2(aE)^{\frac{1}{2}}$.

I

THE application of quantum mechanics to the calculation of nuclear reactions in heavy nuclei gives rise to extremely complicated expressions which cannot be treated by ordinary methods, since there is no approximate solution for this complex many-body problem on account of the intense interaction between the constituents of atomic nuclei. On the other hand Bohr[1] has pointed out that just the extreme facility of energy exchange gives rise to a characteristic simplification of the course of every nuclear process initiated by a collision between a particle or a light quantum and a nucleus. It consists in the possibility of dividing the process into two well-separated stages. The first is the formation of a compound nucleus in a well-defined state in which the incident energy is shared among all the constituents, the second is the disintegration of that compound system, which can be treated as quite independent of the first stage of the process. This conception has been extremely fruitful in the treatment of all kinds of nuclear reactions.[2] Qualitative statistical conclusions about the energy exchange between the nuclear constituents in the compound state have led to simple explanations of many characteristic features of nuclear reactions. In particular the use of thermodynamical analogies has proved very convenient for describing the general trend of nuclear processes. The energy stored in the compound nucleus can in fact be compared with the heat energy of a solid body or a liquid, and, as first emphasized by Frenkel,[3] the subsequent expulsion of particles is analogous to an evaporation process.[4]

In this note an attempt is made to apply statistical methods in a more quantitative way to nuclear processes in which heavy nuclei are involved and become highly excited as, for example, in the case of the collision of very fast neutrons with heavy nuclei. The individual properties of the separate nuclear quantum states are then of no interest, on account of the extremely small distance between the energy levels of highly excited heavy nuclei; it is thus possible to obtain statistical information on the behavior of these nuclei by averaging over many quantum states

[1] N. Bohr, Nature **137**, 344 (1936); N. Bohr, Science (1937), in print.

[2] A comprehensive account of the application of the ideas in question to nuclear phenomena will be given in a paper by Bohr and Kalckar to appear shortly in the Proceedings of the Danish Academy.

[3] I. Frenkel, Sov. Phys. **9**, 533 (1936).

[4] A general discussion of the application of thermodynamical conceptions to nuclear processes can be found in the paper by Bohr, Science, reference 1.

of approximately the same energy.[5] A general statistical formula is derived for the emission of particles by highly excited heavy nuclei. It can be shown by means of this expression to what extent it is possible to describe the disintegration of the compound nucleus as an ordinary evaporation process. The statistics of systems with comparatively few particles gives rise to characteristic discrepancies from the ordinary result obtained for the case of macroscopic bodies. We cannot, for example, speak unambiguously of an evaporation temperature of an excited nucleus, since after emitting one particle it has lost such a large amount of energy that often a much lower temperature must be ascribed to the remaining nucleus. Furthermore all the other terms and quantities which are neglected in ordinary statistics on account of the great number of degrees of freedom must be taken into consideration.

The general expression contains, however, several quantities which are closely connected with the special structure of the nuclei considered. The most important is the density of levels as a function of the excitation energy. Our knowledge of the structure of heavy nuclei is so far very restricted, so that the quantitative conclusions which can be drawn have only a very low accuracy. Thus most of the deviations from the ordinary evaporation formula are much smaller than the inaccuracy of the quantities inserted. On the other hand the general expression can be used to draw conclusions about the density of levels from the observed energy distribution of particles emitted by highly excited nuclei.

II

Let us examine the state of a heavy nucleus A when it is excited to an energy E_A which we suppose to be greater than the binding energy of an elementary particle (proton, neutron, α-particle). This excitation may be produced by absorption of a hard γ-ray or by the collision of a nucleus with a neutron or another particle, whereby the compound nucleus A is created. Before the collision the colliding particle must have a kinetic energy E_A-E_0, E_0 being its binding energy when bound to the nucleus A. The cross section for that collision can in general be very simply determined. The validity of the statistical conclusions requires very high incident energies (at least 3 MV for incident neutrons, see below) so that the wave-length of the incident particles is much smaller than the radius r of the nucleus. The collision can therefore be described classically and the cross section will be of the order πr^2.

We consider now the emission of a neutron by the excited nucleus $A(E_A)$.[6] In order to be able to get statistical information there must be a great number of possibilities for the reaction

$$A=B+n$$

the various possibilities differing according to the various excited states of the remaining nucleus $B(E_B)$. The energy E_A must therefore be much greater than the energy E_0 which binds the neutron to the nucleus A—indeed there must be a great many levels of B having an excitation energy less than E_A-E_0. This condition is fulfilled sufficiently well in heavy nuclei (mass number greater than 100), if

$$E_A-E_0>3\text{MV}. \tag{1}$$

There is of course an upper limit for E_A too; it must be small in comparison with the total binding energy of the nucleus. Otherwise the compound state could not be formed at all.

Let us calculate the probability per unit time $W_n(\epsilon)d\epsilon$ of the nucleus A, excited to the energy E_A, emitting a neutron with kinetic energy between ϵ and $\epsilon+d\epsilon$, thus transforming itself into a nucleus B with an excitation energy $E_B=E_A-E_0-\epsilon$. This probability may possibly depend on some special features of the initial excited level of A. Therefore we understand by $W_n(\epsilon)d\epsilon$ the average of this probability over all excited states of A whose energy lies near E_A. The probability $W_n(\epsilon)d\epsilon$ has, of course, no meaning unless the interval $d\epsilon$ is chosen so big that there are a large number of levels of the nucleus B with energies between E_B and $E_B-d\epsilon$. To get a continuous function $W_n(\epsilon)$ it is necessary to average over a number of final states. We shall always assume that the interval $d\epsilon$ is much bigger than

[5] Similar ideas recently have been put forward by L. Landau, Sov. Phys. **11**, 556 (1937).

[6] We shall use the symbols $A(E)$ or $B(E)$ to designate nuclei A or B which are excited by an energy E *above the ground state*.

the distance between the levels of the nuclei in the excited states considered.

It is possible to give an expression for $W_n(\epsilon)d\epsilon$ as a function of the cross section corresponding to the reverse process: i.e., of the mean cross section $\sigma(E_A, \epsilon)$ for the collision of a neutron with energy ϵ with a nucleus $B(E_A-E_0-\epsilon)$ producing a compound nucleus $A(E_A)$. We can write

$$W_n(\epsilon)d\epsilon=\sigma(E_A, \epsilon)\frac{gm\epsilon}{\pi^2h^3}\frac{\omega_B(E_B)}{\omega_A(E_A)}d\epsilon, \qquad (2)$$

where $\omega_A(E)dE$ and $\omega_B(E)dE$ are the numbers of levels of the nuclei A and B, respectively, between E and $E+dE$, the energies being measured *from the ground state* of the particular nucleus under consideration. m is the mass of the emitted particle, h Planck's constant divided by 2π and g denotes the number of states for the spin of the particle considered. ($g=2$ for neutrons and protons, $g=1$ for α-particles. This factor is left undetermined in (2) so that we can apply (2) to the emission of other particles.)

To derive this relation, let us consider the nucleus and the neutron enclosed in a volume Ω. Then

$$W_c=\sigma(E_A, \epsilon)v/\Omega$$

is the mean probability per unit time of the neutron, with an energy between ϵ and $\epsilon+d\epsilon$ and a velocity $v=(2\epsilon/m)^{\frac{1}{2}}$, being captured by the nucleus $B(E_A-E_0-\epsilon)$, forming nucleus A with an energy between E_A and $E_A+d\epsilon$. We then obtain the probability $W_n(\epsilon)d\epsilon$ for the reverse process by dividing W_c by the number $\omega_A(F_A)d\epsilon$ of states in which the neutron can be captured and multiplying by the number of states into which $A(E_A)$ can decay. There are $\omega_B(E_B)d\epsilon$ states of the nucleus B into which $A(E_A)$ can decay if the energy of the neutron lies between ϵ and $\epsilon+d\epsilon$ and there are

$$\frac{\Omega gm}{2\pi^2h^3}(2m\epsilon)^{\frac{1}{2}}d\epsilon$$

quantum states in the volume Ω in the energy range $d\epsilon$ at the disposal of the neutron. Therefore we get

$$W_n(\epsilon)d\epsilon=W_c\frac{\omega_B(E_B)}{\omega_A(E_A)}\frac{\Omega gm}{2\pi^2h^3}(2m\epsilon)^{\frac{1}{2}}d\epsilon$$

which leads at once to (2).

It is convenient to introduce the logarithm of the density of the levels:

$$S_A(E)=\lg\,\omega_A(E), \quad S_B(E)=\lg\,\omega_B(E).$$

$S(E)$ corresponds to the entropy of the nucleus having an energy between E and $E+dE$. We obtain then

$$W_n(\epsilon)d\epsilon=\sigma(E_A, \epsilon)\frac{gm\epsilon}{\pi^2h^3}e^{S_B(E_A-E_0-\epsilon)-S_A(E_A)}d\epsilon. \qquad (3)$$

This is a general expression for the emission of a particle of mass m, from a system having the free energy E_A and a density of levels $\omega_A(E)$, the remaining system having a density of levels equal to $\omega_B(E)$. The usual formula for the probability of evaporation can be derived from (3) by assuming that E_A is much greater than both the binding energy E_0 and the kinetic energy ϵ of the emitted particle ($E_A\gg E_0$, $E_A\gg\epsilon$), and that S_A and S_B are identical functions ($S_A(E)=S_B(E)$). It is then possible to develop

$$S_B(E_A-E_0-\epsilon)=S_A(E_A)-(E_0+\epsilon)(dS_A/dE)_{E_A}.$$

The derivative of S_A can be expressed by means of a temperature, namely

$$dS_A/dE=1/T_A(E), \qquad (4)$$

where $T_A(E)$ is the temperature at which the most probable energy of the body A is equal to E at thermodynamical equilibrium.[7] The temperatures T given here are of the dimensions of an energy, and are equal to the ordinary temperature times the Boltzmann constant k. We can then write

$$W_n(\epsilon)d\epsilon=\sigma(E_A, \epsilon)\frac{gm}{\pi^2h^3}e^{-E_0/T_A(E_A)}\epsilon e^{-\epsilon/T_A(E_A)}d\epsilon. \qquad (5)$$

This is exactly the usual equation for evaporation. The meaning of σ becomes clearer in putting $\sigma=q\cdot\gamma(\epsilon)$ where q is the actual spatial cross section of the vaporizing body and $\gamma(\epsilon)\leqq 1$ gives the ratio of the number of particles captured to the number of incident particles with an energy ϵ. The cross section for elastic reflection is then $q(1-\gamma(\epsilon))$.

If we apply these considerations to the emission of particles by nuclei, we must observe that the assumptions necessary to establish (5) are not realized. E_0 in particular is not small in comparison with E_A. Nevertheless it is possible to

[7] We distinguish here between the most probable energy and the mean energy. Formula (4) is the statistical définition of the former.

transform (3) into an expression similar to (5), by assuming only $\epsilon \ll E_A - E_0$. We can then develop

$$S_B(E_A - E_0 - \epsilon) = S_B(E_A - E_0) - \epsilon/(T_B(E_A - E_0)) - f(\epsilon), \quad (6)$$

where just as in (4) we define:

$$1/T_B(E) = dS_B/dE. \quad (4a)$$

$T_B(E)$ is the temperature at which E is the most probable energy of the nucleus B in thermodynamical equilibrium. $f(\epsilon)$ contains all further terms of the development. We thus obtain

$$W_n(\epsilon)d\epsilon = \sigma(E_A, \epsilon)\frac{gm}{\pi^2\hbar^3}e^{S_B(E_A-E_0)-S_A(E_A)} \times \epsilon e^{-\epsilon/T_B(E_A-E_0)}e^{-f(\epsilon)}d\epsilon. \quad (7)$$

The total probability of a neutron being emitted is obtained by integrating with respect to ϵ; if multiplied by $\hbar$, it is identical with the "neutron breadth" Γ_n of the emitting level of the nucleus A (i.e., that part of the level-breadth which arises from the emission of a neutron):

$$\Gamma_n = \hbar\int W(\epsilon)d\epsilon = \bar{\sigma}\frac{gm}{\pi^2\hbar^2}T_B^2(E_A - E_0) \times e^{S_B(E_A-E_0)-S_A(E_A)}, \quad (8)$$

$\bar{\sigma}$ is a mean value of $\sigma(E_A, \epsilon)e^{-f(\epsilon)}$ averaged over the Maxwell distribution:

$$\bar{\sigma} = \int \epsilon\sigma(E_A, \epsilon)e^{-\epsilon/T_B - f(\epsilon)}d\epsilon \Big/ \int \epsilon e^{-\epsilon/T_B}d\epsilon.$$

In order to get a closer analogy to the evaporation formula (5) we put

$$S_B(E_A - E_0) - S_A(E_A) = -E_0^*/T_A(E_A), \quad (9)$$

where E_0^* is an energy which is only equal to E_0 if $E_0 \ll E_A$ and $S_A(E) = S_B(E)$. When (9) is inserted in (7) the difference between (7) and the evaporation-formula (5) consists in the following: the energy E_0^* is not identical with the binding energy E_0 and the energy-distribution of the neutrons is not of the Maxwell type, but differs from it by the factor $e^{-f(\epsilon)}$. Furthermore the temperature $T_B(E_A - E_0)$ is by no means the temperature of the evaporating compound-nucleus $A(E_A)$ (its temperature is defined by $T_A(E_A)$), but it is the temperature of the remaining nucleus $B(E_A - E_0)$. This difference can also be explained as follows: on the liberation of the neutron a considerable cooling down takes place. The energy-distribution of the neutrons corresponds to the temperature of the remaining nucleus.

The corrections $f(\epsilon)$ and E_0^* can be determined still more exactly. It follows from (4) and (4a) that dS/dE decreases monotonically with increasing E, since this expression is equal to $1/T(E)$. Therefore $S(E)$ as plotted against E is a curve which is concave downwards; from this fact and from (6) we conclude that

$$f(0) = 0, \quad f(\epsilon) \geqq 0$$

and finally that $f(\epsilon)$ increases monotonically. Hence the relative energy-distribution of the emitted neutrons

$$W_n(\epsilon) = \text{const. } \sigma(E_A, \epsilon)\epsilon e^{-\epsilon/T_B}e^{-f(\epsilon)} \quad (10)$$

possesses a maximum which, as compared with the distribution (5), is shifted towards higher energies and has a smaller breadth.

We can apply the same considerations to estimate the difference (9). Assuming $S_A(E) \sim S_B(E)$ we get

$$S_A(E_A) - S_B(E_A - E_0) > E_0/T_A(E_A). \quad (11)$$

This implies that $E_0^* > E_0$.

It may be noticed that the observed neutron energy distribution for a highly excited nucleus $A(E_A)$ can be different from (10) because the remaining nucleus $B(E_B)$ may possibly emit neutrons again. Such double emissions of neutrons have been found by Heyn.[8] If, however, E_A is less than the energy necessary for removing two neutrons the observed distribution should always be represented by (10).

Eq. (7) leads to the following qualitative conclusions concerning collisions between fast neutrons and nuclei: if a neutron with an energy E collides with the nonexcited nucleus B, and gives rise to the nucleus A with energy $E + E_0$, it will be reemitted on an average with a much smaller energy $\sim 2T_B(E)$ and therefore give a great part

[8] F. A. Heyn, Nature **138**, 723 (1936); Physica **4**, 160 (1937).

of its energy to the nucleus B. $2T$ is the mean energy of particles *emitted* with a Maxwell distribution corresponding to a temperature T. Here it is assumed that the cross section $\sigma(E_A, \epsilon)$ does not depend appreciably on ϵ as is shown in the following section. The energy $T_B(E)$ is generally approximately equal to E divided by the number of degrees of freedom of the nucleus B which are excited at this energy. We see that this represents a very inelastic collision.

In applying formula (7) to excitations made by colliding particles or light quanta, we must take into account the fact, that (7) represents an average over all levels of A having an energy of about E_A. But not all of those levels can be excited by the process mentioned above. Excitation is only possible to levels whose angular momentum differs not too much from the momentum of the original nucleus, since a particle or a light-quantum with the momentum p hitting a nucleus cannot transfer a bigger amount of angular momentum than $\sim pr+s$ (r is the radius of the nucleus and s is the spin angular momentum of the incident particle, which is $\hbar/2$ for neutrons and $\hbar$ for photons). We meet here a characteristic difficulty in nuclear statistics. The conservation of angular momentum, which is found in nuclear processes, is not usually taken into consideration in ordinary statistics. It is easy to see that the emission probability from a level with small angular momentum will in general be bigger than the average value (7) over all angular momenta since there are among the levels with energy E_A several which cannot emit at all. The latter are those with an angular momentum $l>L_B+l_\epsilon$. L_B is the maximum angular momentum of the levels in $B(E_B)$ and l_ϵ is the maximal angular momentum the outgoing neutrons can have ($l_\epsilon\sim r(2m\epsilon)^{\frac{1}{2}}+s\ll L_B$). We get a rough estimate of the emission probability $W_n'(\epsilon)d\epsilon$ for levels with low angular momentum by assuming that all the levels with $l<L_B$ emit with the same probability and that the levels with $l>L_B$ do not emit at all. The only change in the formula (7) for $W_n(\epsilon)$ caused by this assumption consists in putting $\omega_A'(E_A)$ instead of $\omega_A(E_A)$. $\omega_A'(E_A)$ being the density of levels with angular momentum less than L_B. In what follows we shall neglect this change, since up to the present it is impossible to say anything about the angular momentum distribution among nuclear levels. All estimates of $\omega_A(E)$ are far too inexact to distinguish between ω_A' and ω_A.

The formula derived above can be applied to the emission of charged particles (protons, α-particles). We need only allow for the fact that the Coulomb field has a strong influence on the cross section $\sigma(E_A, \epsilon)$ for the reverse process, because it repels and deflects the incident charged particles. If the cross section for the reverse process can be roughly determined by the classical conception that any particle hitting the nucleus is absorbed, we get the expression

$$\sigma(E_A, \epsilon)\begin{cases}=\sigma_0(1-V/\epsilon) & \text{for } \epsilon>V\\ =0 & \text{“ } \epsilon<V\end{cases}$$

$$\sigma_0=\pi r^2, \qquad V=ZZ'e^2/r.$$

where Ze and r are the charge and the radius of the nucleus and $Z'e$ the charge of the particle. For $Z=50$ we get approximately $V=7\cdot Z'$ MV. It is better here to use the following expansion instead of (6):

$$S_B(E_A-E_0-\epsilon)=S_B(E_A-E_0-V)$$
$$-(\epsilon-V)/T_B(E_A-E_0-V)-f(\epsilon-V).$$

Instead of (7) we then get

$$W_P(\epsilon)\,d\epsilon=\sigma_0\frac{gm}{\pi^2\hbar^3}e^{S_B(E_A-E_0-V)-S_A(E_A)}(\epsilon-V)$$
$$\times e^{-(\epsilon-V)/T_B(E_A-E_0-V)}\cdot e^{-f(\epsilon-V)}d\epsilon$$

for the emission probability of charged particles, and for the total emission-probability (proton breadth, α-particle breadth)

$$\Gamma_P=\sigma_0\frac{gm}{\pi^2\hbar^2}T_B^2(E_A-E_0-V)e^{S_B(E_A-E_0-V)-S_A(E_A)}. \tag{12}$$

Comparing this with (7) we note that the binding energy E_0 is replaced by E_0+V and the energy distribution is shifted to higher energies by an amount V without any other change in form. This is easily understood because an additional energy V is given to the emitted particle on account of the Coulomb field of the nucleus. For the same reason the binding energy E_0 is increased, since the energy necessary to liberate the particle must appear in our formula without the energy gained when the particle is accelerated in the Coulomb field, being taken into account. The formula has no longer a meaning when $\epsilon<V$, since then, according to the classical considerations made in deriving the expression, the particle cannot leave the nucleus. But if we take into account the quantum-mechanical possibility of passing through the potential wall, one may expect to find for $\epsilon<V$ an emission probability different from zero, though very small.

The general consequences of the electrostatic repulsion in nuclear reactions are discussed in both papers of Bohr.[1] We restrict ourselves therefore to the following two general conclusions:

The binding energy E_0 is generally as large for protons as for neutrons, in so far as we have to deal with isotopes which are stable with regard to β-emission. Thus, when the Coulomb potential V in the exponential of (12) is comparable with E_0^*, we may expect the emission of protons to be in general much less probable than that of neutrons. In fact, no emission of protons from heavy nuclei $Z>30$ is found when excited by neutrons[9] or γ-rays.[10]

The emission probability for α-particles will be much smaller than that of neutrons as long as the nucleus is stable in respect to α-decay since V is then certainly much bigger than the binding energy of neutrons. The latter is about 8 MV, whereas V is at least 14 MV. For radioactive nuclei however the binding energy of α-particles is negative. It can then happen that E_0^*+V is nearly equal for α-particles, to the binding energy of a neutron. The excited nucleus will then be able to emit neutrons and α-particles with probabilities of the same order of magnitude. Thus we should expect an emission of α-particles by heavy nuclei after the capture of a neutron only in nuclei belonging to the radioactive group. In fact a process of this kind has only been found in thorium.[11, 12]

The nuclear reactions resulting from collisions between charged particles and heavy nuclei are outside the scope of the present paper, because the velocity of charged particles is reduced in the Coulomb field, and (in the experiments which have so far been carried out) they do not therefore possess sufficient energy to excite the nuclei strongly enough. The energy of protons or deuterons should be considerably above 7 MV and that of α-particles above 14 MV.

III

Let us now investigate the order of magnitude of the functions $S(E)$ and $\sigma(E_A, \epsilon)$ which appear in (7). It is obvious that this can only be done roughly, owing to the small knowledge we have of nuclei so that the expressions to be given now are much less exact than those of the preceding section. An attempt has been made by Bethe[13] to calculate the density of levels in nuclear spectra. According to his result (32) we get

$$S(E)=(M\cdot E/2.2)^{\frac{1}{2}}-(5/4)\lg E, \qquad (13)$$

where E is measured in MV and M signifies the mass number. On account of the extreme inaccuracy of any nuclear model we shall try to derive expressions for S by means of two other methods which are less exact but perhaps more general than Bethe's method.

A proper way to calculate $S(E)$ is to find $T(E)$ first. If we know the dependence of the most probable energy E of the nucleus upon the temperature in thermodynamical equilibrium, we can put

$$S(E)=\int dE/T(E), \qquad (14)$$

where the constant of integration does not concern in our problem, since we always have to deal with the difference between two values of S. The energy E can in general be represented over a large range as proportional to a power of T:

$$E=T^n/a,$$

where a is a constant. If all the degrees of freedom are excited (classical limiting case), n must be put equal to unity; in the reverse case (i.e., for relatively low temperatures) $n=4$ for solid bodies, and $n=2$ for degenerate gases. In the present problem we can check the power n and the constant a in two almost independent ways:

(1) As an approximation we represent the degrees of freedom of the nucleus under consideration by proper oscillations with frequencies $\nu_1, \nu_2, \cdots, \nu_i \cdots$.[14] Then $E(T)$ can be evaluated from $Z(\nu)$, $Z(\nu)$ being the number of proper frequencies $\nu_i<\nu$ as function of ν.[15] The most probable energy or the mean energy (the approximation is so rough, that this difference has no essential effect) is in the fact approximately

$$E\sim T\cdot Z(T/h).$$

---

[9] E. Fermi and collaborators, Proc. Roy. Soc. **A146**, 483 (1934).
[10] W. Bothe and W. Gentner, Naturwiss. **25**, 30, 126 (1937).
[11] I. Curie, H. v. Halban, and P. Preiswerk, J. d. phys. **7**, 6, 361 (1935).
[12] O. Hahn and L. Meitner, Naturwiss. **23**, 320 (1935).
[13] H. A. Bethe, Phys. Rev. **50**, 332 (1936).
[14] I am indebted to Professor Bohr for the following method of estimating the temperature of an excited nucleus.
[15] In this model the proper oscillations and the quantum states must be distinguished. The number $Z(\nu)$ of the oscillations is different from that of the quantum states for which $E<h\nu$: the former $Z(\nu)$, is smaller than the latter.

This is equivalent to the assumption, that the mean energy of a proper oscillation whose frequency is smaller than T/h, is equal to the classical value T and that the proper frequencies $\nu_i > T/h$ are regarded as nonexcited. For energies E small compared with the binding energy of the particles, $Z(E/h)$ is more or less proportional to the energy E, since the proper frequencies in this energy-domain are still statistically distributed. We then obtain $Z(E/h) = E/a$ and

$$E = T^2/a. \tag{16}$$

Thus we find $n = 2$ where a is an energy which can be considered as equal to the mean energy distance between the lowest proper frequencies $h\nu_i$. The value of a cannot be easily estimated owing to our restricted knowledge of the structure of heavy nuclei. Only for radioactive nuclei does experimental evidence on the spacing of the lowest levels exist. This spacing can roughly be set equal to the frequencies of the lowest proper oscillations. The experiments on α-ray fine structure and on γ-ray spectra lead to nuclear levels the spacing of which is of the order of 0.1 MV. Since no information on nuclear spectra of heavy nonradioactive nuclei is available, we assume that the value of a is of the same order of magnitude for nuclei with mass numbers greater than 100 and put for these nuclei $a \sim 0.1 - 0.2$ MV. This check on a is very uncertain; a dependance on the weight of the nuclei and a variation due to the existence of different kinds of nuclei (odd or even) must be expected.

(2) The other way to check n and a avoids the representation of the dynamics of the nuclei by means of proper oscillations. We try to approximate to the problem from another side, and consider the nucleus as a degenerate gas of particles, with strong interaction forces between them. The energy of a degenerate gas of particles obeying the Fermi-statistics is also given by (16). Since we know from experience of metallic electrons that this law holds in spite of very strong interactions between electrons, we may assume $n = 2$ for nuclei also. The constant a can be checked by means of the expression for the density of levels which follows from (14) and (16):

$$\begin{aligned} S(E) &= 2(E/a)^{\frac{1}{2}} + \text{const.}, \\ \omega(E) &= \text{const.} \cdot \exp\left[2(E/a)^{\frac{1}{2}}\right]. \end{aligned} \tag{17}$$

Thus the value of a can be calculated if we know the density of levels $\omega(E)$ for two values E_1, E_2:

$$a = 4\left(\frac{E_1^{\frac{1}{2}} - E_2^{\frac{1}{2}}}{\lg \omega(E_1) - \lg \omega(E_2)}\right)^2. \tag{18}$$

We have a rough knowledge of the density at an energy $E \sim 8$ MV from the experiments on the capture of slow neutrons. The capturing levels of the compound nucleus have an energy of about 8 MV and their distance apart is about $1 - 10 \cdot 10^{-6}$ MV for heavy nuclei (weight $M \sim 100$) according to Bethe and Placzek.[16] On the other hand we can assume the distance between the lowest nuclear levels to be of the order 0.1 MV. from experiments on γ-ray spectra as stated above. Inserting these two values in (18) we get $a \sim 0.2$ MV. This value may be too high because the actual density of levels at 8 MV is certainly higher than the value inserted, since the experiments on capture of slow neutrons only give information about levels with two fixed successive values of angular momentum.[17] In any case the order of magnitude can hardly be very different since the level densities only appear logarithmically in the expression (18).

The value of a from Bethe's formula (13) is slightly lower than the above results. Neglecting the logarithmic term we get $a = 8.8/M$ expressed in MV. The interpretation of a as the distance between the lowest proper oscillation frequencies may however indicate a weaker dependence on M.

From a comparison of all the results obtained, we may take the following expression for $T(E)$ for nuclei of mass number $M > 100$

$$T(E) = (aE)^{\frac{1}{2}}, \quad 0.05 \text{ MV} < a < 0.2 \text{ MV}.$$

a is certainly nearer to the upper limit than the lower for the lighter nuclei and decreases with increasing mass number.

The cross section $\sigma(E_A, \epsilon)$ can be estimated in the following way: when the energy ϵ of the neutron is high enough for the corresponding magnitude $\lambda\!\!\!^{-} = \lambda/2\pi = h/(2m\epsilon)^{\frac{1}{2}}$ to be smaller than the range of nuclear forces $d = 2 \cdot 10^{-13}$ cm, then we can consider the reverse collision as classical, and put $\sigma = \pi r^2$ independently of E_A and ϵ (r is the radius of the nucleus). This is only fulfilled if

[16] H. A. Bethe and G. Placzek, Phys. Rev. **51**, 450 (1937).

[17] The capture of slow neutrons can only give rise to levels whose angular momentum differs by $h/2$ from the angular momentum of the capturing nucleus.

$\epsilon > 5$ MV. When the magnitude λ cannot be considered as small compared to d, but is still smaller than $r/2 \sim 0.5 \cdot 10^{-12}$ (i.e., $\epsilon > 0.8$ MV), the area πr^2 can be regarded as an upper limit for the cross section. How much σ is less than this upper limit depends on E_A. When the levels of the compound nucleus $A(E_A)$ are separated by large distances, the capture is very selective, which reduces the cross section. But in the case considered here E_A must be very high for $E_A > E_0 + 3$ MV, on account of condition (1). It may generally be expected—and we shall verify it by calculation—that the breadth of the levels is then larger than their distance apart, so that selectivity is no longer possible. No considerable error can then be made in putting

$$\sigma(E_A, \epsilon) = \pi r^2 \quad \text{for} \quad \epsilon > 0.8 \text{ MV}.$$

Since, according to (7) the bulk of the emitted neutrons has an energy $\epsilon \sim 2T_B$, the only interesting value of $\sigma(E_A, \epsilon)$ is that corresponding to this energy. Now the temperatures occurring in nuclear processes which can be handled by statistical methods are generally higher than 0.5 MV. This follows from the fact that a temperature $T \sim 0.55$ MV corresponds to the minimum value of $E_A - E_0$ (see (1)). Thus the mean energy of neutrons will be high enough for putting $\sigma(E_A, \epsilon) = \pi r^2$.

The relative energy distribution of the emitted neutrons is then according to (7):

$$W_n(\epsilon)d\epsilon = \text{const. } \epsilon e^{-\epsilon/T_B(E_A - E_0)} e^{-f(\epsilon)} d\epsilon.$$

This represents a Maxwell distribution with a correction $f(\epsilon)$ in the exponent. According to (6) $f(\epsilon)$ is given by

$$f(\epsilon) = -\frac{\epsilon^2}{2}\left(\frac{d^2 S_B}{dE^2}\right)_{E_A - E_0},$$

the higher derivatives being of no importance. With assumption (17) for S this becomes

$$f(\epsilon) = \epsilon^2 / 4(E_A - E_0) \cdot T_B(E_A - E_0)$$

and the correction $f(\epsilon)$ is therefore smaller than the Maxwell exponent ϵ/T_B itself in the ratio $\epsilon/4(E_A - E_0)$. The Maxwellian mean value of ϵ is given by $\bar{\epsilon} = 2T_B(E_A - E_0)$ so that

$$\frac{\bar{\epsilon}}{4(E_A - E_0)} = \frac{1}{2}\left(\frac{a}{E_A - E_0}\right)^{\frac{1}{2}} \ll 1$$

in virtue of (1). Consequently we see that the correction $f(\epsilon)$ has no great influence. The energy distribution of particles emitted by highly excited nuclei will therefore be nearly a Maxwellian one. When neutrons with energy E fall on a nucleus B they will be reemitted with a mean energy of $2(aE)^{\frac{1}{2}}$. Hence the mean energy loss per impact is $E[1 - 2(a/E)^{\frac{1}{2}}]$. Neutrons of 10 MV will for example be reemitted with a mean energy of only 1.4 − 2.8 MV.

Let us now calculate from (9) the total probability for the emission of neutrons from the excited nucleus $A(E_A)$. This probability expressed in energy-units, is equal to the neutron-breadth of the emitting levels. The fact must be allowed for that the statistical expressions are only valid when $E_A - E_0$ is large, i.e., when the nucleus B can remain excited after the emission of the neutron in many different ways. Consequently the formula cannot be applied to levels resulting from the capture of slow neutrons. From (8) and (17) it follows that

$$\Gamma_n = \frac{a(E_A - E_0)}{\pi E_K} \exp\{2[(E_A - E_0)/a]^{\frac{1}{2}} - [E_A/a]^{\frac{1}{2}}\},$$

where $E_K = h^2/2mr^2 \sim 0.2$ MV. To get an idea of the dependence on E_A and on the assumed value of a we calculate Γ_n for several values of E_A and a, putting $E_0 = 8$ MV. The values of Γ_n in electron volts (not in MV) are given in Table I.

TABLE I. *Values of probability of emission of neutrons given in electron volts (breadth of emitting levels).*

a \ E_A	11 MV	15 MV	20 MV	25 MV
0.05 MV	0.2	18	120	680
0.1 MV	22	450	4800	10000
0.2 MV	860	10000	38000	97000

For increasing mass number E_0 as well as a gets smaller and consequently the values of Γ_n will not depend essentially upon the mass number within the low accuracy of this calculation. It should be noticed from this result that the neutron breadths of the level of $A(E_A)$ are much larger than the mean distances of the levels at the corresponding energy.

The probability of emitting a neutron is much higher than that of emitting a γ-ray. We know the latter, however, only for comparatively low

values of E_A from experiments on capture of slow neutrons. The γ-ray breadth is according to Bethe and Placzek[13] about 10^{-7} MV for an excitation energy of ~ 8 MV. If it is permissible to assume this value valid also for higher excitation, the capture of high energy neutrons ($E > 3$ MV) will be extremely improbable. Even a transition of the compound nucleus to a less energetic unstable state by emission of a γ-ray will be an improbable process since according to the above table the probability of neutron emission is in general several orders of magnitude greater than that for radiation.

I would like to express my thanks to Professor N. Bohr and to Dr. F. Kalckar for the fruitful collaboration which led to the production of this paper. I would also like to thank Drs. G. Placzek, L. Landau, and H. Bhabha for many valuable discussions I have had with them, and the Rask Oersted Fond for the opportunity to work at the Institute for Theoretical Physics at Copenhagen.

AUGUST 15, 1937 PHYSICAL REVIEW VOLUME 52

The Beta-Ray Spectrum of Radium E

JOHN S. O'CONOR, S. J.*
Massachusetts Institute of Technology, Cambridge, Massachusetts

(Received May 15, 1937)

The beta-ray spectrum of radium E was examined with a magnetic spectrometer, by using coincidence counting, under various conditions of source strength, mounting and aperture of defining slits. It is concluded that the experimental high energy end point depends on the source strength used, as well as the width of the defining slits. Data from all but very strong sources gave a K.U. plot which was linear within the limits of error set by statistical fluctuations and finite slit widths. Extrapolation of the K.U. plot gave 1.25 ± 0.03 Mev as the high energy end point.

SINCE the original work of Schmidt[1] in 1907 more than a score of workers[2–24] have made measurements on the beta-ray spectrum of radium E with none too concordant results. The disagreement between observers may be appreciated by consulting Table I wherein one finds values for the high energy end point which range from 4500 $H\rho$ up to 12,000 $H\rho$.

The importance of obtaining the true energy distribution curve for the disintegration electrons from radioactive bodies has been recently enhanced by the tentative success of the Konopinski-Uhlenbeck[25] modification of the Fermi[26] theory of beta-disintegration, especially as applied to the lighter artificially radioactivated elements. The present investigation was undertaken with the purpose of securing data from one-of the naturally radioactive elements which could be used after the manner proposed by Kurie, Richardson and Paxton[27] as a further criterion in determining more conclusively the validity of the theory.

Fermi's original formula (44), reference[26] gives the probability of disintegration with the emis-

* Now at Woodstock College, Woodstock, Maryland.
[1] H. W. Schmidt, Physik. Zeit. **8**, 361 (1907).
[2] Baeyer, Hahn and Meitner, Physik. Zeits. **11**, 488 (1910); **12**, 273 (1911); **13**, 264 (1912).
[3] J. A. Gray, Proc. Roy. Soc. **87**, 487 (1912).
[4] J. Danysz, Ann. Chim. Phys. S8, **30**, 241 (1913).
[5] Kovarik and McKeehan, Phys. Rev. **8**, 574 (1916).
[6] A. V. Douglas, Proc. Roy. Soc. Canada **16**, 113 (1922); B. W. Sargent, P. C. P. S. **25**, 514 (1929).
[7] Curie and d'Espine, Comptes rendus **181**, 31 (1925).
[8] Yovanovitch and d'Espine, J. de phys. et rad. **8**, 276 (1927).
[9] E. Madgwick, P. C. P. S. **23**, 982 (1927).
[10] Gray and O'Leary, Nature **123**, 568 (1929).
[11] F. R. Terroux, Proc. Roy. Soc. **A131**, 90 (1930).
[12] N. Feather, Phys. Rev. **35**, 1559 (1930).
[13] B. W. Sargent, P. C. P. S. **28**, 538 (1932).
[14] F. C. Champion, Proc. Roy. Soc. **A134**, 672 (1932).
[15] J. A. Chalmers, P. C. P. S. **28**, 319 (1932).
[16] B. W. Sargent, Proc. Roy. Soc. **A139**, 659 (1933).
[17] H. O. W. Richardson, Proc. Roy. Soc. **A147**, 442 (1934).
[18] F. A. Scott, Phys. Rev. **48**, 391 (1935).
[19] Alichanow *et al.*, Nature **137**, 314 (1936); Physik. Zeits. Sowjetunion, Band 10, Heft. 1, p. 78 (1936).
[20] Ho and Wang, Chinese J. Phys. **2**, 1 (1936).
[21] Champion and Alexander, Nature **137**, 744 (1936).
[22] M. Lecoin, Comptes rendus **205**, 171 (1936).
[23] E. M. Lyman, Phys. Rev. **51**, 1 (1937).
[24] Langer and Whitaker, Bull. Am. Phys. Soc. **12**, No. 2, p. 32 (1937).
[25] Konopinski and Uhlenbeck, Phys. Rev. **48**, 7 (1935).
[26] E. Fermi, Zeits. f. Physik **88**, 161 (1934).
[27] Kurie, Richardson and Paxton, Phys. Rev. **48**, 167 (1935); **49**, 203 (1936).

sion of an electron having momentum between η and $\eta+\Delta\eta$, and the expression used therein is an approximation applicable to elements whose atomic number is in the neighborhood of 82.

By grouping all constants under the symbol K and writing for the probability of disintegration the number N, which is proportional to this probability, we may express Fermi's formula as follows:

$$N=K(\eta+0.355\eta^2)[(1+\eta_0^2)^{\frac{1}{2}}-(1+\eta^2)^{\frac{1}{2}}]^2. \quad (1)$$

Here $\eta=H\rho/1700$; where ρ is the radius of curvature of the electron trajectory in a magnetic field of strength H. η_0 is the maximum value of η.

The relation between the momentum η and the kinetic energy ω in mc^2 units may be expressed as follows:

$$\eta=(2\omega+\omega^2)^{\frac{1}{2}}; \quad \omega=(1+\eta^2)^{\frac{1}{2}}-1. \quad (2)$$

By substituting for $(1+\eta^2)^{\frac{1}{2}}$ its value $(\omega+1)$ and similarly for $(1+\eta_0^2)^{\frac{1}{2}}$ we can write $[\omega_0-\omega]^2$ for the last bracket of Fermi's equation; which yields:

$$c[N/(\eta+0.355\eta^2)]^{\frac{1}{2}}=\omega_0-\omega. \quad (3)$$

In the case of the heavy elements the only difference between the original Fermi formula and the modification introduced by Konopinski and Uhlenbeck is a change in the exponent of the final bracket which appears raised to the fourth instead of the second power.

If $[N/(\eta+0.355\eta^2)]^{\frac{1}{2}}$ be plotted against the energy of the disintegrating electrons a straight line should result if the Fermi theory be correct; and the intercept on the axis of abscissa will give the value of ω_0, the maximum energy

TABLE I. *Results of various observers on the high energy end point and number maximum of the continuous beta-ray spectrum of radium E.*

INVESTIGATOR	YEAR	NUMBER MAXIMUM $H\rho$	HIGH ENERGY END POINT $H\rho$	METHOD	REMARKS
Schmidt[1]	1907	2500	5500	Absorption and Magnetic deflection (photographic)	
Baeyer, Hahn and Meitner[2]	1911	"	"	Magnetic deflection (photographic)	
Gray[3]	1912		5150–5450	Absorption	
Danysz[4]	1913		5500	Magnetic focusing (photographic)	Found a doubtful band between 6000 and 12000 $H\rho$
Kovarik and McKeehan[5]	1916	2000	7000 (ca)	Magnetic focusing (point counter)	
Douglas[6]	1922		4990–5080	Absorption	Results converted by Sargent in 1929
Curie and d'Espine[7]	1925	2900	4500	Magnetic deflection (photographic)	Also found feeble band between 7000 and 10,000 $H\rho$
Yovanovitch and d'Espine[8]	1927		4500	Magnetic deflection, magnetic focusing (photographic)	Feeble band or group of lines between 7000 and 10,000 $H\rho$
Madgwick[9]	1927	2200	5000	Magnetic focusing (ionization chamber)	
Gray and O'Leary[10]	1929		less than 8200	Combination absorption and deflection (ionization chamber)	Estimate less than one atom in 25000, gives ray of 8200 $H\rho$ or greater; possibly none at all
Terroux[11]	1930		11,200	Cloud chamber	Probable error of 50%
Feather[12]	1930		5300	Absorption	
Sargent[13] from data of Varder and Madgwick	1932	1750	5100	Absorption	
Champion[14]	1932		5500	Cloud chamber	Estimates that beta-rays over 5500 $H\rho$ are less abundant than 1 in 2000
Chalmers[15]	1932			Absorption	Interprets "kink" in absorption curve near high energy end point as region of most rapid change of slope of distribution curve and not true end point
Sargent[16]	1932		5100 5000 5500	Absorption Magnetic Cloud chamber	Summary of all work done by various methods. Prefers value from cloud chamber
Richardson[17]	1934	850 (?)		Cloud chamber	Finds number of electrons in range between 0.01 and 0.065 Mev exceeds number attributed to usual maximum between 0.3 and 0.4 Mev
Scott[18]	1935	2480	6604±98	Magnetic focusing (Geiger-Müller counter)	
Alichanow *et al.*[19]	1935	1100 (ca)	5400	Magnetic focusing (Geiger-Müller counter)	No pronounced number maximum. Many low energy electrons
Ho and Wang[20]	1936		7500	Cloud chamber	Relatively few tracks; large probable error
Champion and Alexander[21]	1936		5975	Cloud chamber	End point value from extrapolation of K.U. plot of 1932 data[14]
Lecoin[22]	1936	1450	5100	Cloud chamber	Sharp number maximum with rapid decline on low energy side
Lyman[23]	1937	1750	5280±20 6050 (K.U.)	Magnetic focusing (G-M Counter)	
Langer and Whitaker[24]	1937		5330±70 6250 (K.U.)	Magnetic focusing (coincidence counting)	
O'Conor	1937	1650	5350±130 5650 (K.U.)	Magnetic focusing (Geiger-Müller single and coincidence counters)	

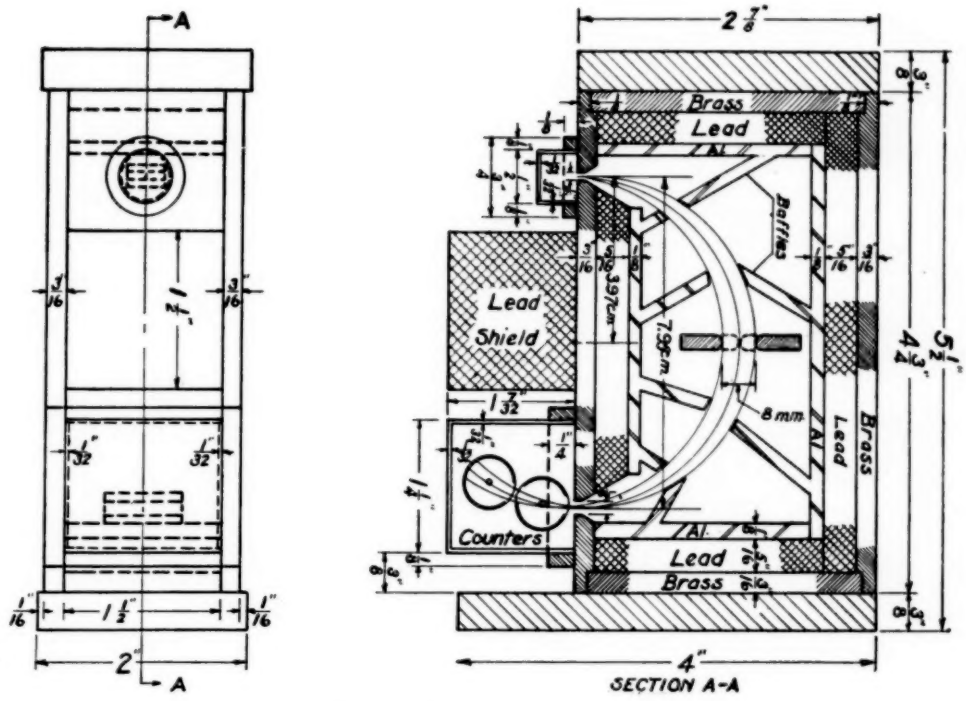

FIG. 1. Magnetic spectrometer.

possible for electrons from this particular type of disintegration.

Likewise a plot of the fourth root of the same function *versus* electron energy should show linearity if the Konopinski-Uhlenbeck modification of the Fermi theory be the correct one.

EXPERIMENTAL OBJECTIVE

The distribution in energy of electrons from radium E was observed over an extended period of time, under varying conditions of source strength, source mounting and defining slit widths so that the effect of the changes in these experimental factors might be followed and thus help to trace and eventually lead to the causes responsible for the discrepancies existing between the results of previous experimenters.

CONSTRUCTION AND OPERATION OF APPARATUS

The spectrometer proper is essentially the same as that originally used by Rutherford and Robinson.[28] The improvements which were adopted from those made by Henderson[29] and Alichanow[30] include special precautions in the form of baffles to prevent scattering as well as the use of Geiger-Müller double coincidence counters for detection purposes.

A diagram of the spectrometer is shown in Fig. 1. Electrons emerging from the source have their paths bent into the arc of a circle by a magnetic field applied at right angles to the plane of the paper.

The position of the receiving slit in front of the counters is fixed at a definite distance from the source (7.95 cm). This determines (within limits set by the finite widths of the defining slits) the radius of curvature which the electron track must possess in order that the electron itself may enter the counting chamber.

An electron of mass m and charge e, initially projected with a determined speed v, at right angles to the lines of force of a homogeneous magnetic field of strength H, will describe a circle of radius ρ.

Under such conditions the electron will be in dynamic equilibrium which may be represented

[28] Rutherford and Robinson, Phil. Mag. **26**, 717 (1913).
[29] W. J. Henderson, Proc. Roy. Soc. **A147**, 572 (1934).
[30] Alichanow *et al.*, Zeits. f. Physik **90**, 249 (1934); J. phys. et rad. S VII, Tome VII, No. 4, 163 (1936).

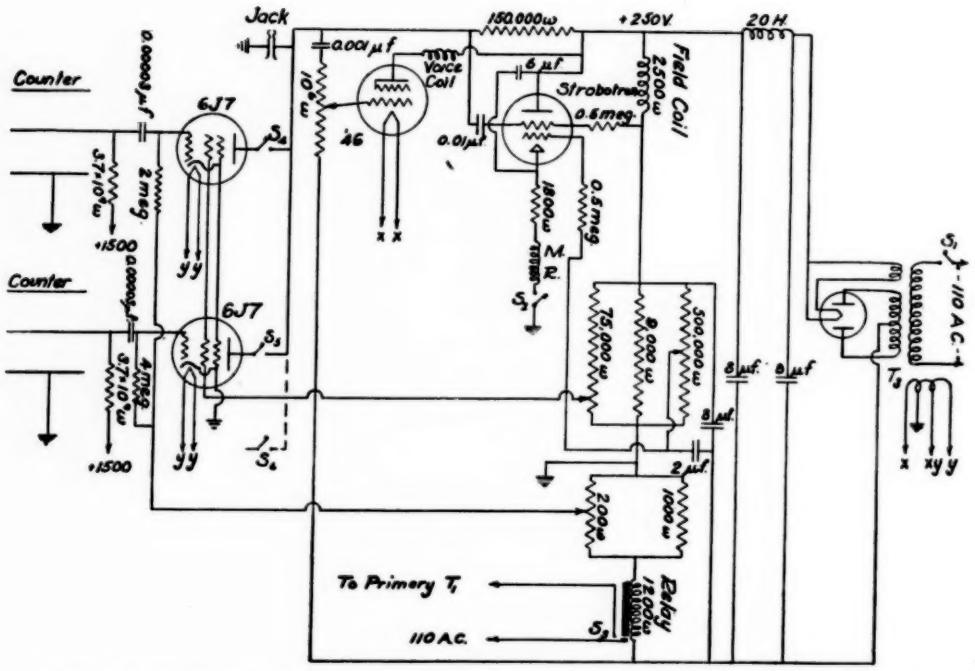

FIG. 2. Coincidence counter amplifier and power supply. S_3 acts as a time delay switch which retards the application of the potential in the high voltage circuit (not shown) until after the filament of the rectifier in that circuit is heated.

by the equation:

$$H\rho = mv/e. \tag{4}$$

If we use the relativistic form for the mass of the electron (required because of the high velocity of the beta-rays), $H\rho$ may be expressed in terms involving the kinetic energy, E, and the velocity of light c, as follows:

$$H\rho = (1/ce)(E^2+2mc^2E)^{\frac{1}{2}}. \tag{5}$$

Expressed in absolute electrostatic units (5) becomes:

$$H\rho = (1/e)(E^2+2mc^2E)^{\frac{1}{2}}. \tag{6}$$

SPREAD IN $H\rho$ DUE TO FINITE SOURCE AND SLIT WIDTHS

If in a spectrometer such as is shown in Fig. 1 we consider a receiving slit of width ϵ, a central defining slit of width δ and a source of width ξ it may be shown that to a first approximation:

$$\Delta\rho \leqq \epsilon/2+\xi/2+\delta/8\rho_0. \tag{7}$$

ρ_0 is the radius of curvature corresponding to $\frac{1}{2}$ the distance from the center of the source to the outer edge (high velocity side) of the receiving slit.

The value of the above spectrometer constants as determined for computation and corrections made in this report are as follows:

ϵ, receiving slit width = 3.18 mm,
ξ, source width (Ra E on Ni) = 0.8 mm,
ξ', defining slit at source = 1.59 mm,
δ, central defining slit: variable from 0 to 8 mm
" " " Width = 1 mm for all readings except certain high energy end point readings specially noted,
ρ_0 = 40.54 mm,
ρ_m = 39.95 mm.

The mean value ρ_m is used in computing $H\rho$ for the distribution curves, and is one-half the measured distance between the outside edge of the source mounting and the center of the receiving slit.

The spread, which is determined from Eq. (7) gives the uncertainty in any mean value of $H\rho$ which will be $= \pm\frac{1}{2}H\Delta\rho$.

It is evident from Eq. (7) that the contribution to the spread in $H\rho$ due to the width of the central slit δ is small compared to that from the terms involving ϵ and ξ but, as will be shown later, the presence of this central slit system cuts down scattering between the two halves of the spectrometer chamber and for that reason all

readings, except certain special measurements on the high energy end point, were made with $\delta = 1$ mm.

Counting System

The circuit used for coincidence counting is a modification of that proposed by Rossi.[31] Type 6J7 tubes are used for the first stage of amplification. It was found that with the type '57 tubes used originally there was a complete paralysis of the tube action when the magnetic field of the spectrometer exceeded 4000 oersteds. With the metal tubes this paralyzing action was appreciably reduced, although the tubes were mounted directly over the spectrometer and magnet; and an additional cylindrical iron shield placed over the metal housing made it possible to attain a field well over 8000 oersteds without measurably disturbing the normal operation of the 6J7 tubes. The complete circuit, which uses a strobotron (neon filled, double grid, cold cathode discharge tube) to actuate the message register, is given in Fig. 2.

The high voltage supply for the Geiger-Müller counters is obtained by use of a circuit identical with that described by Gingrich.[32]

The necessary slits cut in the counter cathodes for the admission of beta-rays resulted in a distortion of the electric field and a consequent instability of the counters. This was remedied by covering the slits with aluminized Cellophane. The Cellophane used was obtained through the courtesy of the duPont Cellophane Co. and is 12.7 microns thick; equivalent to 0.00175 g/cm.^{2} Aluminum was deposited on it by evaporation to a thickness of the order of 0.1 micron. The material was then fastened over the slits with scotch tape in such a way that the metallized surface was in contact with the cathode cylinder beyond the limits of the slit.

The Cellophane with its aluminum coating is opaque to ultraviolet light and this serves the purpose of isolating the counters as well as stabilizing them.

In addition to the three aluminized windows covering the slits, a fourth (not metallized), is used to separate the counter chamber from the spectrometer proper. Such separation was necessary since the counters were operated at a pressure of 10.5 cm of Hg whereas the spectrometer was connected to a Hyvac pump which kept the pressure well under 1 mm of Hg during operation.

Correction for Stopping Power of Cellophane Windows

The correction giving the number of particles stopped by the windows for various electron energies, which must be added to the registered count, was made in a manner similar to that described by Scott.[18] Counting rates for beta-rays of various energies, in the region where this effect was known to be appreciable, were determined with three different thicknesses of Cellophane interposed between spectrometer and counter chamber. By plotting counting rate against Cellophane thickness for each definite energy a set of curves were obtained and under the assumption of linearity could be extrapolated back to give a counting rate for zero thickness of Cellophane. The correction became inappreciable above 2000 $H\rho$ and hence was applied only below that value.

An additional conclusion of importance resulting from the experimental determination of the stopping power of the Cellophane windows is the fact that there exists an apparent effective range for electrons in Cellophane practically identical with that found by Schonland[33] for aluminum. For despite certain irregularities in the counting rates (due to the difficulty of reproducing identical conditions of counter operation after changing window thickness), the cut-off at the low energy end was definitely abrupt.

This sharp cut-off at low energies is a powerful argument in favor of the absence of scattering in the spectrometer in which the measurements were made. For if electrons of energy higher than that proper to the beam being measured were being scattered onto the counter window, they would penetrate the same and be registered by the counting system,—thus rendering impossible the sharp low energy cut-off that was actually found.

Scott's Cellophane correction table does not reveal a similar cut-off despite the fact that the

[31] B. Rossi, Nature **125**, 636 (1930).
[32] N. S. Gingrich, R. S. I. **7**, 207 (1936).
[33] B. F. J. Schonland, Proc. Roy. Soc. **A104**, 235 (1923); **108**, 187 (1925).

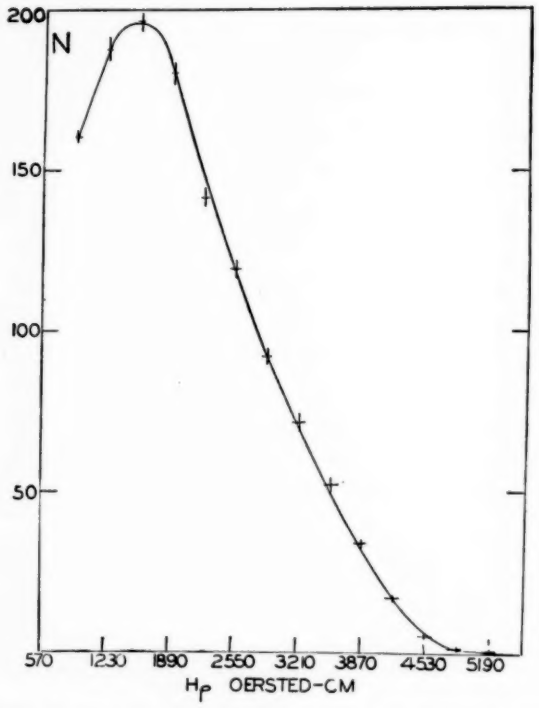

FIG. 3. Momentum ($H\rho$) distribution of electrons from radium E. Readings taken with source of intermediate strength and with central slit width of 1 mm. Corrections made for background, Cellophane absorption and finite resolving time of counters. Ordinates divided by their respective H values.

Cellophane used by him is twice as thick (linear dimension) as that used by the writer. Even allowing for the fact that there is not a linear relation between ordinary thickness and g/cm² for different grades of stock, an examination of Scott's tabulation of variation in counting rate with Cellophane thickness for various electron energies, would lead one to believe that electrons were getting into his counter far below the $H\rho$ cut-off value found by Schonland for the equivalent g/cm² of aluminum.

Finite Resolving Time of Counters

The determination of the actual number of particles reaching the counter from the number recorded by the message register requires a correction for counts missed due to the finite resolving time of the counter and associated recording apparatus.

The method for making this correction is treated by Schiff[34] and the procedure outlined by him was followed here.

[34] L. I. Schiff, Phys. Rev. **50**, 88 (1936).

The resolving time was determined by observing the maximum counting rate as a gamma-ray source was slowly brought in close proximity to the counter from a distance where the counting rate was well below this maximum. The relation $t=1/N_{max}e$ then gives the resolving time, where N_{max} is the maximum counting rate in counts per second. The value of t thus determined was 0.076 sec.

Measurement of the Magnetic Field

The magnetic field was first measured with a flip coil and flux meter. The constants of the flip coil were calculated from its dimensions, and the flux meter readings were corrected from a calibration curve made for the instrument in the department of electrical engineering. A plot of H *vs.* I was made and found to be linear throughout the region to be used for examination of the radium E spectrum.

An estimate of the inhomogeneity of the field was made from a flux plot of Dr. H. B. Dwight, professor of electrical machinery, of the department of electrical engineering, and it was found that in the region of greatest variation traversed by the electrons the inhomogeneity was less than 2 percent.

The plot of field strength against current was then checked against the four most prominent lines of the thorium B+C+C″ spectrum. A mean value for the $H\rho$ of each of these lines was taken from the recent determinations of Ellis[35] and Wang.[36] The true value of H at which these lines were recorded was determined by dividing their accepted $H\rho$ value by the radius of curvature of the spectrometer in use, and these four values of H were plotted, using the current values at which the lines came in as abscissae, and the mean value of H (obtained from the data of Ellis and Wang as explained above) for ordinates. These points coincided with the line from the flux meter data within an accuracy of 0.6 percent.

Measurements on the Radium E Spectrum

The radium E source was prepared on three different mountings; nickel, palladium and platinum. The nickel mounting consisted of a

[35] C. D. Ellis, Proc. Roy. Soc. **A138** 318, (1932).
[36] K. C. Wang, Zeits. f. Physik **87**, 633 (1933).

flattened wire 6 mm long, 3 mm wide and 0.8 mm thick. The Pd and Pt mountings were of the same dimensions in lengths and width; the thickness of the Pt being 0.5 mm and that of the Pd 0.4 mm.

The flattened face of each mounting was so oriented in the spectrometer housing that its plane made a grazing angle with the plane passing perpendicularly through the center of the source slit.

The spectrum from the source mounted on nickel was examined on two occasions separated by an interval of three months. The first test consisted of twenty-five explorations of the spectrum which were continued over the period of a month, the initial source strength being such that the total emission was approximately 10^7 beta-particles per second. Additional tests were then made with source mountings of Pd and Pt. In these latter cases the intensity of total emission was relatively weak compared to the maximum activity of the source on the nickel mounting. Several more tests, with a new source mounted on nickel of strength slightly greater than the original one, were then made as a final check.

Results

We may summarize the results as follows: Comparing source strengths of the same magnitude; no difference in the shape of the energy distribution curve resulted from changing the source mounting from nickel to platinum. The data from the source mounted on palladium are meager, but all indications were that the distribution was unaffected by the substitution of this mounting. These findings seem to eliminate any possibility of error from selective reflection due to the type of source mounting used.

The similarity of the distribution curves taken from sources mounted on the three materials extends from the high energy maximum down to 900 $H\rho$. Below 1000 $H\rho$ the error from the correction for absorption due to the cellophane windows was of such magnitude as to obscure any difference due to absorption in or selective reflection from the material of the source mounting.

In the explorations which attempted to cover the entire spectrum in an uninterrupted run, a source strength giving a total emission of less than 6×10^5 particles per second was employed.

For this limited source strength and below it all momentum (and energy) distribution curves were in agreement from the lower observable limit, 900 $H\rho$ (0.067 Mev), up to 4860 $H\rho$ (1.03 Mev). Beyond 1.03 Mev the shape of the distribution curve definitely became a function of the central defining slit width as well as of source strength.

A typical momentum ($H\rho$) distribution curve from weak and intermediate source strengths is shown in Fig. 3, while Fig. 4 shows the effect of variation in slit width on the experimental high energy end point.

In the case of the complete distribution curve, background readings have been subtracted, and necessary corrections for absorption in cellophane windows as well as for finite resolving time of counters have been made. Each counting rate has also been divided by the corresponding magnetic field strength, thus reducing the effective slit width to a common value for all parts of the spectrum.

The high energy end point readings of Fig. 4 are plotted as registered, without corrections.

When the source strength used was of the order of, or greater than, a total emission of 10^7 particles per second, only the high energy portion of the spectrum could be satisfactorily examined, because as the number maximum of the distribution curve was approached the increase in counting rate produced paralysis of the recording system. As the source strength was increased the "tail" of the distribution curve continued to extend to higher and higher energies (even with

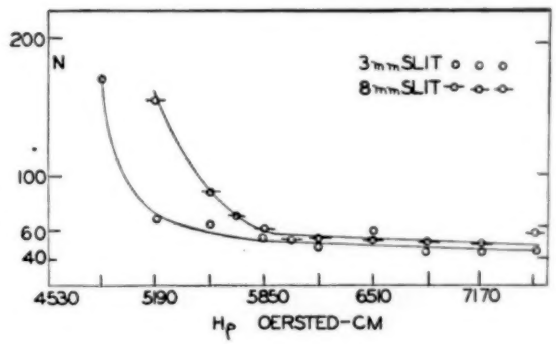

Fig. 4. End point counting rates with 3 and 8 mm central slit widths. Single G-M counter, with fairly strong source. Background included.

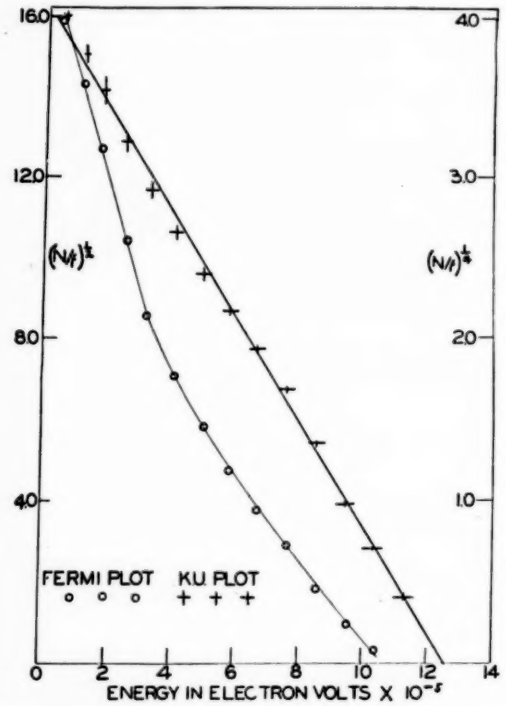

FIG. 5. Fermi and K.U. plots. Radium E. Number data averaged from four sets of readings.

minimum central slit width of 1 mm), until with the maximum strength available, counting rates unquestionably above the background could be detected (in five minute runs) out as far as 9500 $H\rho$ (2.4 Mev).

This effect is somewhat similar to that obtained by Curie and d'Espine[7] as well as by Yovanovitch and d'Espine.[8] These workers used extremely strong sources with photographic detection, and found a feeble band between 7000 and 10,000 $H\rho$ which they hesitated to interpret as an actual continuation of the main continuous spectrum. The interpretation offered by the writer is that the effect is due to multiple reflection from the walls, baffles or slit systems of the spectrometer; the geometry of these reflecting surfaces producing broken trajectories for electrons of certain preferred intermediate energies which results in an apparent but spuriously large radius of curvature in the case of photographic registration.

That this scattering is not indiscriminate seems to follow from the fact that with the present apparatus, using fixed radius of curvature and variable magnetic field, different apparent maxima can be found for each source strength, beyond which the counting rate with the source shutter entirely closed does not differ from that obtained with the shutter wide open. It is again worth noting that this scattering is entirely absent at low energies, as deduced from the sharp cut-off (previously mentioned) produced by absorption in the Cellophane windows.

It also seems reasonable to presume that this postulated selective scattering drops below the background level for weak sources and becomes negligible in the main portion of the spectrum; otherwise it would produce discrepancies between the curves from weak and intermediately strong sources, and such discrepancies were not found.

The above reasoning leads to the rejection of the high energy end points obtained with excessively strong sources as unreliable, and also to the rejection of the distribution curves made from data taken with slit widths which give a fractional resolution ($\Delta\rho/\rho$) poorer than 0.05.

Under these restrictions the best value of the experimental end point was estimated as 5350 ± 130 $H\rho$ (1.175 ± 0.04 Mev). From the previous discussion it would seem that any attempt to fix the experimental end point with greater accuracy would be unwarranted under conditions imposed by the spectrometer in use.

FERMI AND K.U. PLOTS

A plot of $[N/(\eta+0.355\eta^2)]^{\frac{1}{2}}$ against the energy of the electrons yields the curved line shown to the left of Fig. 5, indicating that the Fermi function does not correctly represent the experimental distribution in energy of electrons from radium E. In the same figure the line to the right represents the plot of $[N/(\eta+0.355\eta^2)]^{\frac{1}{2}}$ *versus* electron energy and shows a degree of linearity which appears to indicate substantial agreement between the experimental distribution

TABLE II. *Expected energy-number distribution (N calculated from values of the function $(N/f)^{\frac{1}{2}}$ as determined from the extrapolation of the straight line graph of Fig. 5).*

$(N/f)^{\frac{1}{2}}$	N	Mev
0.99	5	0.945
0.69	1.33	1.036
0.38	0.134	1.132
0.093	0.0005	1.224

and the theoretical one predicted by Konopinski and Uhlenbeck.

Data from several distribution curves obtained with both single and double coincidence counting and with both nickel and platinum source mountings all yield K.U. plots whose extrapolated high energy end points coincide at the value of 1.25 ± 0.03 Mev. This is but 6 percent higher than the most probable experimental value for the end point.

It is also of interest to note that the straight line plot of $(N/f)^{\frac{1}{2}}$ *vs.* energy continues through to fairly low energies and does not curve downward as in the plots from the data of Scott[18] and Lyman.[23]

Omission of the previously listed corrections only increases by an additional 5 percent the divergence between the experimental and extrapolated end points determined in this work.

Comparison Between Values of High Energy End Point from Experimental Distribution Curve and Extrapolation of K.U. Plot

If the Konopinski-Uhlenbeck theory have any validity, then the experimentally determined end point should always be found at a value which is considerably lower than the one determined from extrapolation of the K.U. plot. The reason for this is the fact that the K.U. theory requires a fourth order contact between the energy distribution curve and the energy axis, thus limiting the number of electrons close to the end point to a value which makes their detection by present methods most improbable.

Thus within the limits of the source strengths used we cannot expect experimental points beyond 1.13 Mev. This may be readily shown by calculating the relative expected counting rates for points on the K.U. plot beyond this energy value. This has been done and the results are tabulated in Table II.

If we take the ratios of successive pairs of predicted counting rates we notice that between 1.036–1.132 and 1.132–1.224 Mev the ratio of successive counting rates should drop from 10 : 1 to 373 : 1. Thus if the counting rate is near the limit of sensitivity of the detector at the former values, it is hopelessly below it for the latter.

Thus a counting rate of 5 per min. at 1.036 Mev would give (on K.U. predictions) a rate of $\frac{1}{2}$ count per min. at 1.132 Mev.

This latter would not be recognized above the background in a normal 5-minute run. And as a matter of fact no electrons above 1.036 Mev were found with the 1 mm slit width.

With a three mm slit width, which because of a larger solid angle gives a higher counting rate, we obtain a counting rate of between 150 and 200 a minute which would be cut to only 15 to 20 per min. at 1.132 Mev. This rate is well within

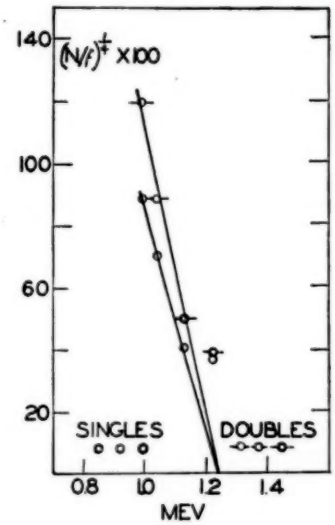

Fig. 6. K.U. plot in end point region. Number data taken with central slit width 3 mm.

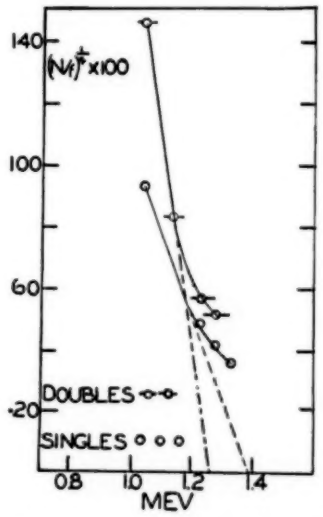

Fig. 7. K.U. plot in end point region. Number data taken with central slit width 8 mm.

the limits of detection. Electrons in the correct abundance were found at this energy and with the three mm slit.

Extending the reasoning to higher energies we find that with counting rates obtainable with a 3 mm slit width we have a predicted drop on K.U. theory from 150 counts per min. at 1.132 Mev to less than $\frac{1}{2}$ count per min. at 1.224 Mev.

This is the first energy at which there is found a disagreement between K.U. prediction and experimental count; the departure being relatively slight in the case of the 3 mm slit when the probable error in N and H is considered. Beyond 1.22 Mev there is no further count recorded above background with the 3 mm slit, and the recorded readings from the 8 mm slit above these energies depart still more from the K.U. predictions.

If the experimental counting rates near the end point be used for a plot of the K.U. function, it is found, as may be seen in Fig. 6, that for a 3 mm slit width all the points but the last one lie on the straight line which gives the same extrapolated end point as does the line which was plotted from the average of several runs (taken with 1 mm slit) over the entire range of the spectrum.

On the other hand with the 8 mm slit (Fig. 7), there is a definite curving away from linearity exhibited by the last three or four points; and this trend is such as to indicate an *excess* of electrons over the amount predicted by the K.U. theory.

The most plausible interpretation seems to be that the departure seen in Fig. 7 is due to scattering as a result of the use of a wide slit; and this effect becomes more noticeable as the ratio between scattered electrons and those of energy proper to the beam being measured increases.

We may sum up the previous discussion by saying:

(1) All counting rates at energies amenable to measurement with source strength below a total emission of 10^6 electrons per second and 1 mm slit width, are in full agreement with predictions of the K.U. theory.

(2) Only the last measurable counting rate taken with the 3 mm slit width is in disagreement with the predictions of the K.U. theory, and this discrepancy may be partially explained by the spread in $H\rho$ due to finite slit widths.

(3) Measurable counting rates taken with the 8 mm slit width and at energies higher than the maximum found with the 3 mm slit width, are in complete disagreement with the K.U. predictions, and the disagreement increases with increasing energy.

Keeping in mind the probability of scattering with wide slits, the logical conclusion from the above seems to be that the reliability of the end point measurements is in inverse proportion to the central slit width, and that the rejection of those readings taken with wide slits, which are in disagreement with the predictions of the Fermi-K.U. theory, is justified.

Position of Number Maximum

Measurements progressing in the direction of decreasing energy show that the distribution curve continues to rise until a value of 1650 ± 40 $H\rho$ (0.182 Mev) is reached. This differs considerably from the early estimates of the number maximum but agrees with the trend of more recent observers to place the number maximum at lower energies. Because of the uncertainty in the corrections for absorption, no great confidence can be placed in the way the curve behaves on the low energy side of the maximum. Errors in the corrections may exaggerate the height of the peak, but it is not displaced with respect to the energy axis; its abscissa being the same with or without the corrections.

Comparison of End Points Obtained by Various Observers

The evidence for a true experimental end point appreciably above 5500 $H\rho$ seems both dubious and untrustworthy. Terroux's[11] abnormally high value of 11,200 $H\rho$ (from cloud chamber data), according to a footnote in a subsequent article,[37] is admittedly an overestimate due to an improper criterion for the rejection of tracks whose radii of curvature had been altered by collision with nuclei.

In addition any estimate such as that of Terroux, which attributes an $H\rho$ of over 5000 to as many as 4 percent of the particles, is in disagreement with the work of Ellis and Wooster[38]

[37] F. R. Terroux, P. C. P. S. **28**, 115 (1932).
[38] Ellis and Wooster, Proc. Roy. Soc. **A117**, 109 (1927).

and of Meitner and Orthman.[39] These investigators determined the mean energy of the continuous spectrum of radium E by calorimetric methods, and its value absolutely precludes the possibility of so many high energy electrons.

The paucity of tracks and large probable error in the work of Ho and Wang[20] does not tend to convince one of the objectivity of an end point at 7500 $H\rho$.

Among the recent spectrometer measurements we have the results of Alichanow,[19] Lyman,[23] Langer and Whitaker[24] and the writer all in agreement to the extent of placing the most probable value of the experimental end point between 5300 and 5400 $H\rho$.

Scott's high energy end point of 6600 $H\rho$ is far beyond that found in the present investigation with a source strength of the same order of magnitude (280 counts per min. at the number maximum of the spectrum).

It also exceeds most other values obtained from spectrometer measurements.

The possibility of scattering being increased by the small radius of curvature (2 cm) and lack of baffle system in his spectrometer seems to receive confirmation from the lack of sharp cut-off at the low energy end of the spectrum, as mentioned previously in the paragraph on the correction for absorption in the Cellophane windows.

While all workers on beta-ray spectra agree in the rejection of the Fermi function, because of its inability to satisfy the criterion established by Kurie, Richardson and Paxton, there is no such unanimity concerning the shape of the K.U. plot and consequent validity of that theory.

Champion and Alexander[21] have found the K.U. plot linear for both radium E and thorium C″, with an extrapolated end point for the former only 9 percent above their experimental one of 5500 $H\rho$.

Scott's data, when used for making the K.U. plot, show linearity for the main body of the graph, and this line gives an extrapolated end point value almost identical with his rather high experimental one. However, there are serious departures from linearity at both low and high energy portions of this same plot; the upward curvature at the high energy end indicating an excess of electrons over the number predicted by the K.U. theory. Lyman on the contrary finds a deficiency of electrons near the end point which causes his K.U. plot to drop to the energy axis more rapidly than the theory requires.

Lyman as well as Langer and Whitaker find the K.U. extrapolated end point more than 14 percent higher that the experimental one, while the results of the present investigation indicate a difference of only 6 percent.

Table III summarizes the results just discussed.

The different values obtained for the extrapolated end point by various workers indicate that the shape, even of the main portion, of the distribution curve from which the data are taken must be seriously distorted by some of the spectrometers in use; for independently of the truth or error of the theory, plots of the identical function from the data secured by four different spectrometers from the same radioactive substance should yield curves which have the same intercept on the energy axis. Such agreement is not found in the four last cases listed above.

In view of such discrepancies it would be difficult to justify the rejection of the Konopinski-Uhlenbeck theory until there is better agreement concerning the experimental distribution with which it may fail to conform.

Some modification, such as that proposed by Richardson,[40] may be necessary if the agreement between Lyman[23] and Langer and Whitaker[41] regarding the deficiency of high energy electrons, with respect to the K.U. plot, be taken to indicate a real rather than instrumental effect. While it is possible that such a deficiency might be obscured by lack of fine resolution (in the present investigation $\Delta\rho/\rho \leqq 0.05$) the results here re-

TABLE III. *Comparison of experimental and extrapolated K.U. end points obtained by recent observers.*

Investigator	Experimental End Point $H\rho$	Extrapolated K.U. End Point $H\rho$	Percentage Difference
Champion and Alexander[21]	5500	5975	9%
Scott[18]	6600	6600 (?)	—
Lyman[23]	5300	6050	14%
Langer and Whitaker[24]	5330	6250	17%
O'Conor	5350	5650	6%

[39] Meitner and Orthman, Zeits. f. Physik **60**, 143 (1930).

[40] H. O. W. Richardson, Nature **139**, 505 (1937).

[41] Langer and Whitaker, Phys. Rev. **51**, 713 (1937).

corded for the major portion of the distribution curve can be conservatively interpreted as contributing limited support to the K.U. theory.

ACKNOWLEDGMENTS

The writer wishes to express his sincere appreciation for the inspiration to begin the above investigation and the encouragement to carry it to completion which was given by Professor Robley D. Evans, under whose direction the work was done.

It is also a pleasure to acknowledge the cooperation of Professor A. F. Kovarik of Yale University who was kind enough to prepare a thorium B source on two occasions. This source was used for the calibration of the magnetic field and determination of the efficiency of the spectrometer.

The radium E sources were obtained from Dr. L. R. Hafstad of the Department of Terrestrial Magnetism, Carnegie Institution of Washington, as well as from Professor J. A. Bearden and Dr. W. R. Kanne of the Johns Hopkins University.

It was only the continued courtesy of those just named that made it possible to study the radium E beta-ray spectrum under the various conditions reported in this paper.

For data concerning the design and operation of the spectrometer as well as for information concerning the Fermi and Konopinski-Uhlenbeck theories the writer is also deeply indebted to Dr. L. I. Schiff.

A like debt of gratitude is owed to Dr. N. S. Gingrich and Dr. E. J. Schremp for advice on the electrical circuits used in the counting apparatus.

AUGUST 15, 1937 PHYSICAL REVIEW VOLUME 52

Extreme Ultraviolet Series in Cr VI, Mn VII and Fe VIII[1]

P. GERALD KRUGER AND S. G. WEISSBERG
University of Illinois, Urbana, Illinois

(Received June 14, 1937)

Lines in the extreme ultraviolet region involving the $3d\,^2D$, $4p\,^2P$, $5s\,^2S$, $6s\,^2S$, and several $nf\,^2F$ terms have been identified in the spectra of Mn VII and Fe VIII. In Cr VI the first member of the $3d\,^2D-nf\,^2F$ series has been found. These spectra have been photographed with a twenty-one foot grazing incidence vacuum spectrograph. Identification was facilitated by the use of constant second difference displaced frequency diagrams.

THE spectra of highly ionized chromuim, manganese and iron have been photographed in the extreme ultraviolet with a twenty-one foot grazing incidence vacuum spectrograph. The instrument and source of power have been described in previous reports.[2, 3]

Heretofore the identification of the extreme ultraviolet spectra of isoelectronic ions by the use of the constant second difference law, has been greatly facilitated by the fact that the lines involved were among the very strongest in the region. However, when an attempt was made to extend the K I–Cr VI isoelectronic sequence to Mn VII, an extrapolation of the displaced frequency diagram (see Fig. 1) for the resonance multiplet $3d\,^2D_{3/2,\,5/2}-4p\,^2P_{1/2,\,3/2}$ led into a thickly populated region, with no prominent lines. This was in contrast to the appearance, on our plates, of the very strong $3d\,^2D_{3/2,\,5/2}-4p\,^2P_{1/2,\,3/2}$ multiplets in V V and Cr VI.[4] That Mn VII might not be excited would indeed be curious, since spectra both from Mn VI and Mn VIII have been identified on the same plates, and lines from both of these ions are intense. One must conclude, therefore, that the above multiplet is among the lines of intermediate intensity in Mn VII.

From the identification of the multiplet $4s\,^2S_{1/2}-4p\,^2P_{1/2,\,3/2}$, Gibbs and White had already found the fine structure interval in the

[1] Preliminary report given by P. G. Kruger and S. G. Weissberg, Phys. Rev. **49**, 873A (1936).
[2] P. G. Kruger, Rev. Sci. Inst. **4**, 128 (1933).
[3] P. G. Kruger and W. E. Shoupp, Phys. Rev. **46**, 124 (1934).
[4] Previously reported by R. C. Gibbs and H. E. White, Proc. Nat. Acad. Sci. **12**, 598, 675 (1926).

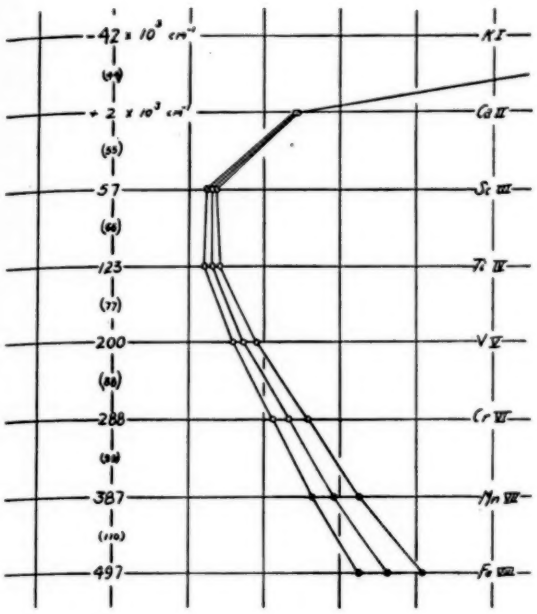

FIG. 1. Displaced frequency diagram with constant second difference of 11,000 cm^{-1} for resonance multiplet $3d\,^2D_{3/2,\,5/2}-4p\,^2P_{1/2,\,3/2}$. Horizontal scale: 1 div. = 4000 cm^{-1}.

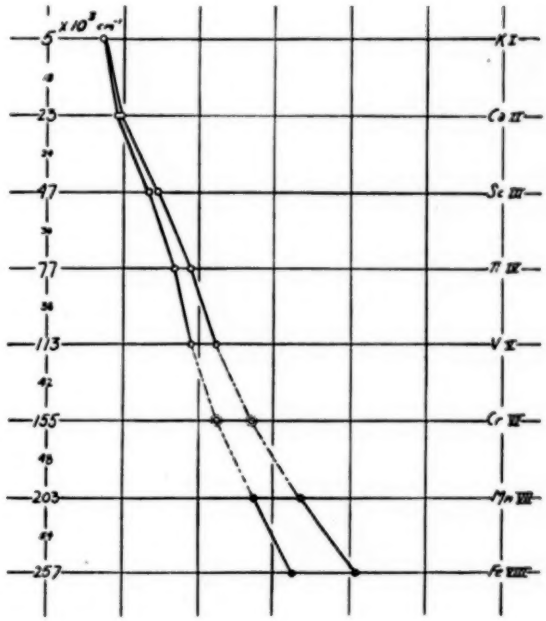

FIG. 2. Displaced frequency diagram with constant second difference of 6000 cm^{-1} for $4p\,^2P_{1/2,\,3/2}-5s\,^2S_{1/2}$. Horizontal scale: 1 div. = 4000 cm^{-1}.

$4p\,^2P$ term in Mn VII to be 2464.7 cm^{-1}. This interval was verified by us with the discovery of the $4p\,^2P_{1/2,\,3/2}-5s\,^2S_{1/2}$ and $4p\,^2P_{1/2,\,3/2}-6s\,^2S_{1/2}$ multiplets, their approximate location being predicted with the use of displaced frequency diagrams. (See Figs. 2, 3.)

An approximate value (1340 cm^{-1}) of the $3d\,^2D$ fine structure interval was found graphically by extrapolating a σ *vs.* Z graph, where σ and Z are related by the regular doublet law, $\Delta\nu = R\alpha^2(Z-\sigma)^4/n^3l(l+1)$. The resonance multiplet selected yielded 2467 cm^{-1} for the ^2P interval and 1344 cm^{-1} for the ^2D interval.

On one of our Mn plates, a series of four pairs of lines with nearly the same frequency difference appeared. These were fitted to the formula

$$\nu_m = 961{,}517 - 49R/(m-0.092)^2,$$

where $m=6$, 7, 8, 9. (This formula is for the lower ν of the pairs.) The close fit of this limit with the limit predicted for the $3d\,^2D$ terms by the use of a Moseley diagram, and the similarity of the frequency intervals (1341, 1323, 1353, 1355 cm^{-1}) to the $3d\,^2D$ interval of 1344 cm^{-1} suggested strongly that the series had $3d\,^2D$ as the common lower state. There were two possibilities, namely a $3d\,^2D-nf\,^2F$ and a $3d\,^2D-np\,^2P$ series. Members of the ^2P series would normally consist of three lines with relative intensities (ν increasing) of 5, 9, 1, and with the

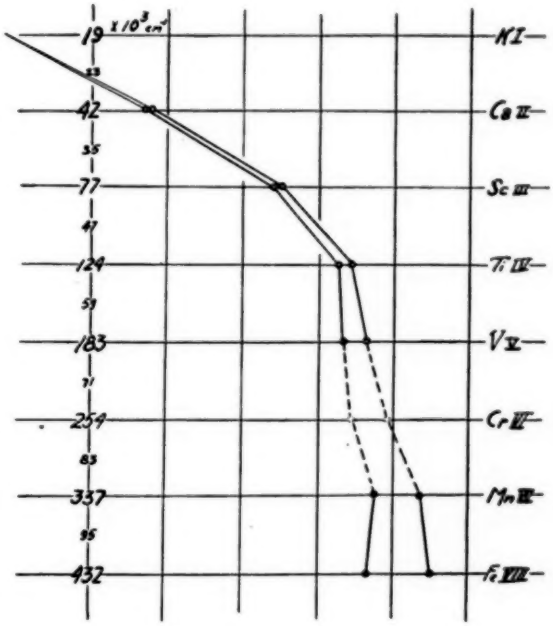

FIG. 3. Displaced frequency diagram with constant second difference of 12,000 cm^{-1} for $4p\,^2P_{1/2,\,3/2}-6s\,^2S_{1/2}$. Horizontal scale: 1 div. = 4000 cm^{-1}.

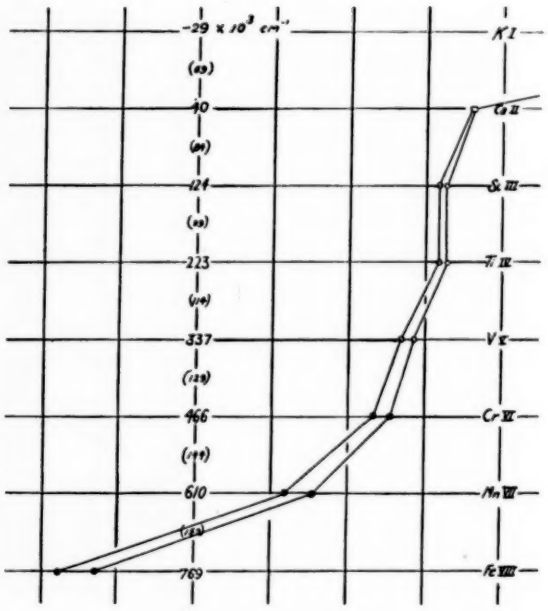

FIG. 4. Displaced frequency diagram with constant second difference of 15,000 cm^{-1} for first members of the $3d\ ^2D_{3/2,\ 5/2}-nf\ ^2F_{5/2,\ 7/2}$ series. Horizontal scale: 1 div. = 4000 cm^{-1}.

^2P interval nearly twice the ^2D interval. Members of the ^2F series, on the other hand, would consist of three lines, with relative intensities (ν increasing) of 5, 100, 70, but with the ^2F interval very much smaller than the ^2D interval. Hence, if only two lines appeared, members of the ^2P series would show the line of shorter wave-length to be the more intense, whereas the opposite would be the case for a ^2F series. In the series at hand, the more intense line in each pair is of longer wave-length. This points to identification of the series as a $3d\ ^2D-nf\ ^2F$ series.

The term values were calculated for this ^2F series by fitting the lines $\nu=806{,}419$, 847,515, and 874,181 cm^{-1} to a Ritz-Rydberg formula given by

$$\nu_m=A-Z^2R/(m+\mu+\alpha T_m)^2=A-T_m,$$

where A is the series limit, m is an integer, $\mu=-0.1370$ and $\alpha=2.68\times10^{-7}$, and T_m is the term value.

Once these terms were established, and the trend of the variation of the quantum defects known, the identification of the $3d\ ^2D-4f\ ^2F$ and $3d\ ^2D-5f\ ^2F$ lines offered no difficulty. Identification of the first member was assisted somewhat by the displaced frequency diagram (Fig. 4).

TABLE I. *Observed lines and transitions.*

TRANSITION	λ(A)	INT.	ν(cm^{-1})	Δν(cm^{-1})
Mn VII				
$4p\ ^2P_{3/2}-5s\ ^2S_{1/2}$	467.662	30	213830	2450
$4p\ ^2P_{1/2}-5s\ ^2S_{1/2}$	462.363	15	216280	
$4p\ ^2P_{3/2}-6s\ ^2S_{1/2}$	284.059	10	352040	2450
$4p\ ^2P_{1/2}-6s\ ^2S_{1/2}$	282.095	3	354490	
$3d\ ^2D_{3/2}-4p\ ^2P_{1/2}$	251.479	1	397647	2467
$3d\ ^2D_{5/2}-4p\ ^2P_{3/2}$	250.771	4	398770	
$3d\ ^2D_{3/2}-4p\ ^2P_{3/2}$	249.929	2	400114	1344
$3d\ ^2D_{5/2}-4f\ ^2F_{5/2}$	162.707	30	614602	151
$3d\ ^2D_{5/2}-4f\ ^2F_{7/2}$	162.667	60	614753	
$3d\ ^2D_{3/2}-4f\ ^2F_{5/2}$	162.349	80	615957	1355
$3d\ ^2D_{5/2}-5f\ ^2F_{5/2}$	135.425	2	738416	174
$3d\ ^2D_{5/2}-5f\ ^2F_{7/2}$	135.393	25	738590	
$3d\ ^2D_{3/2}-5f\ ^2F_{5/2}$	135.177	20	739771	1355
$3d\ ^2D_{5/2}-6f\ ^2F_{7/2}$	124.005	15	806419	1341
$3d\ ^2D_{3/2}-6f\ ^2F_{5/2}$	123.799	10	807760	
$3d\ ^2D_{5/2}-7f\ ^2F_{7/2}$	117.992	5	847515	1323
$3d\ ^2D_{3/2}-7f\ ^2F_{5/2}$	117.808	3	848838	
$3d\ ^2D_{5/2}-8f\ ^2F_{7/2}$	114.393	2	874181	1353
$3d\ ^2D_{3/2}-8f\ ^2F_{5/2}$	114.216	1	875534	
$3d\ ^2D_{5/2}-9f\ ^2F_{7/2}$	112.260	1	892387	1355
$3d\ ^2D_{3/2}-9f\ ^2F_{5/2}$	111.889	0	893742	
Cr VI				
$3d\ ^2D-4f\ ^2F$	210.288	6	475312	
$3d\ ^2D-4f\ ^2F$	209.978	4	476240	

The complete list of wave-lengths identified in Mn VII is given in Table I. Two new lines have been assigned to Cr VI, namely the two strong lines of the $3d\ ^2D-4f\ ^2F$ transitions.

The analysis of the Fe VIII lines presented the same problems met in Mn VII with the addition that the $4p\ ^2P$ fine structure interval was unknown. Reliance was placed on the screening constant extrapolation for an approximate value of the $4p\ ^2P\Delta\nu$. The $^2P-{}^2S$ lines were easily

TABLE II. *Observed lines and transitions. Fe VIII.*

TRANSITION	λ(A)	INT.	ν(cm^{-1})	Δν
$4p\ ^2P_{3/2}-5s\ ^2S_{1/2}$	370.432	10	269955	3364
$4p\ ^2P_{1/2}-5s\ ^2S_{1/2}$	365.873	4	273319	
$4p\ ^2P_{3/2}-6s\ ^2S_{1/2}$	223.870	4	446688	3379
$4p\ ^2P_{1/2}-6s\ ^2S_{1/2}$	222.189	4	450067	
$3d\ ^2D_{3/2}-4p\ ^2P_{1/2}$	196.046	15	510084	3363
$3d\ ^2D_{5/2}-4p\ ^2P_{3/2}$	195.476	20	511572	1875
$3d\ ^2D_{3/2}-4p\ ^2P_{3/2}$	194.762	5	513447	
$3d\ ^2D_{5/2}-4f\ ^2F_{7/2}$	131.242	9	761951	1763
$3d\ ^2D_{3/2}-4f\ ^2F_{5/2}$	130.939	8	763714	
$3d\ ^2D_{5/2}-5f\ ^2F_{7/2}$	108.083	8	925214	1810
$3d\ ^2D_{5/2}-5f\ ^2F_{5/2}$	107.872	8	927024	
$3d\ ^2D_{5/2}-6f\ ^2F_{7/2}$	98.522	4	1015002	1826
$3d\ ^2D_{3/2}-6f\ ^2F_{5/2}$	98.345	4	1016828	
$3d\ ^2D_{5/2}-7f\ ^2F_{7/2}$	93.374*	3	1071000	1846
$3d\ ^2D_{3/2}-7f\ ^2F_{5/2}$	93.217*	3	1072765	

* Absolute values of λ probably in error by 0.01A.

TABLE III. *Term values and effective quantum numbers.*

Mn VII

	$n=3$	4	5	6	7	8	9
$^2S_{1/2}$		643267 2.8912	348067 3.9304	209857 5.0618			
$^2P_{1/2}$		564354 3.0867					
$^2P_{3/2}$		561889 3.0935					
$^2D_{3/2}$	962001 2.3642						
$^2D_{5/2}$	960646 2.3658						
$^2F_{5/2}$		346044 3.9419	222230 4.9190	154241 5.9044	113163 6.8932	86467 7.8859	68259 8.8755
$^2F_{7/2}$		345893 3.9430	222056 4.9209				

Fe VIII

	$n=3$	4	5	6
$^2S_{1/2}$			435958 4.0137	259225 5.2051
$^2P_{1/2}$		709276 3.1467		
$^2P_{3/2}$		705913 3.1542		
$^2D_{3/2}$	1219360 2.3999			
$^2D_{5/2}$	1217485 2.4018			
$^2F_{5/2}$		455646 3.9260	292336 4.9015	202532 5.8887
$^2F_{7/2}$		455539 3.9264	292276 4.9020	202483 5.8894

found with the aid of the displaced frequency diagrams (Fig. 2). The $3d\ ^2D$ splitting was then obtained from the $^2D-{}^2F$ series. This permitted the definite location of the resonance lines $3d\ ^2D-4p\ ^2P$. The complete list of wave-lengths of Fe VIII is given in Table II.

Term values and effective quantum numbers are listed in Table III, and the ionization potentials for the entire sequence are shown in Table IV. The value 526,006 cm^{-1} for the $3d\ ^2D$ term in V V is our estimate based on the data of Gibbs and White.[5] This results from fitting a Ritz-Rydberg term formula to the ^2S terms, as was done by Russell and Lang with Ti IV.[6] Our estimate is likely to be slightly too deep. This statement is based on the fact that a limit calculation from the ^2S terms in Mn VII and Fe VIII leads to a value which is too deep as compared to the more accurate calculation based on the third, fourth, and fifth members of the ^2F series in Mn VII and the second, third, and fourth members of the ^2F series in Fe VIII.

The ionization potentials in the sequence increase with a nearly constant second difference. Heretofore short range extrapolations of the ionization potential have been made by assuming a constant second difference. This practice is supported by the results of exact series calculations made possible by the identification of several members of the ^2F series.

[5] Bacher and Goudsmit, *Atomic Energy States.*

TABLE IV. *Ionization potentials in the isoelectronic sequence K I–Co IX.**

ION	$3d\ ^2D_{3/2}$ cm^{-1}	IONIZATION POTENTIAL VOLTS	FIRST DIFFERENCE VOLTS	SECOND DIFFERENCE VOLTS
K I	13470.26	1.6618		
			8.4662	
Ca II	82097.8	10.1280		6.0404
			14.5066	
Sc III	199693	24.6346		3.84
			18.3499	
Ti IV	348433	42.9845		3.56
			21.9065	
V V	526006	64.891		(3.37)
			(25.279)	
Cr VI	(730940)	(90.17)		(3.23)
			(28.507)	
Mn VII	962001	118.677		(3.24)
			31.750	
Fe VIII	1219360	150.427		(3.22)
			(34.97)	
Co IX	(1503000)	(185.4)		

* Values in parentheses are estimated from a Moseley diagram. The value for V V has been recalculated from data of Gibbs and White, Phys. Rev. **33**, 157 (1929).

[6] A. N. Russell and R. J. Lang, Acous. J. **66**, 13 (1927).

Ultraviolet Spectra of BeH and BeH$^+$

WILLIAM W. WATSON AND R. F. HUMPHREYS
Sloane Physics Laboratory, Yale University, New Haven, Connecticut

(Received June 12, 1937)

A BeH band system analogous to the $B^2\Pi \rightarrow X^2\Sigma$ MgH system is reported. Observed bands are the (0,0) at 1960A, (1,0) at 1882A and (1,1) at 1956A. Each consists of a single Q branch (negligible spin doubling), P and R branch transitions being eliminated by predissociation from the $^2\Pi$ state into a neighboring unstable $^2\Sigma$ state. For the $^2\Pi$ state $B_0 = 10.65$ cm^{-1} and $\omega_e - 2x_e\omega_e = 2133.4$. The complex BeH spectrum from 3100A to 3600A consists only of an extension of the known $^1\Sigma^+ \rightarrow {}^1\Sigma^+$ BeH$^+$ system. Analyses of the principal BeH$^+$ bands in this region yield revised values for the band constants.

THERE has been but a single band system, a $^2\Pi \rightarrow {}^2\Sigma$ transition with principal head at 5000A, so far reported for the neutral BeH molecule.[1] In addition an extensive system of bands due to BeH$^+$, covering practically all of the quartz ultraviolet region of the spectrum, has been partially analyzed.[2] Since for the corresponding MgH molecule two more electronic transitions are known, it was thought likely that as yet undiscovered BeH systems existed. In particular we have searched for and found in the near vacuum ultraviolet BeH bands analogous to the $B^2\Pi \rightarrow X^2\Sigma$ system of MgH. This new BeH system forms the second member of a Rydberg series, the first member of which is the green $^2\Pi \rightarrow {}^2\Sigma$ system, has its principal head at 1960A and exhibits the same interesting predissociation observed in the MgH bands near 2430A. In fact, although these new BeH bands represent a $^2\Pi \rightarrow {}^2\Sigma$ system, due to this predissociation they possess Q branches only. We give the details below.

In the region 3100A–3600A there is a considerable accumulation of hydride band lines, especially about the $3p\ ^3P$–$3s\ ^3S$ multiplet of Be I at 3321A. Although this "many-lined" spectrum was believed to be made up in part of an extension of the known BeH$^+$ system to higher v'' levels, it was suspected that it also contained another BeH system. Our quantum analysis shows, however, that almost all of the lines of appreciable intensity in this region are assignable to BeH$^+$ bands. The great density of band lines is due to the tendency for the spacing of successive bands in sequences $\Delta v = -3$, -4, etc. to be reduced to zero with increasing v. There may be another BeH system composed of fainter lines in this region, but it is not evident.

Recently Guntsch[3] has found a $^2\Sigma^- \rightarrow A^2\Pi$ MgH band at 4400A. The corresponding BeH band would be expected to occur at about 4050A. Near this wave-length on our spectrograms we find many band lines but, owing partly to the presence of band structure of impurities, and partly to the lack of obvious band branches, we have not attempted the analysis.

The spectrograms of the 1960A system were made with a vacuum spectrograph having an aluminized speculum metal grating with a 10-foot radius of curvature and giving a dispersion of 5.5A per mm. A hollow cathode discharge employing a molybdenum cylinder charged with small pieces of beryllium as a cathode carrying 0.8 ampere either in pure hydrogen or in hydrogen-helium mixtures at about 5 mm pressure produced the 1960A band very well. More intense spectrograms were obtained with a 220-volt d.c. arc between Be electrodes in a hydrogen atmosphere at 5 cm pressure, the light being focused on the slit with a large fluorite lens. A fluorite window covered the slit in all the exposures. The hollow cathode discharge showed also the H_2 continuum as well as the H_2 many-lined spectrum beginning at 1650A. Atomic lines of Be I and Be II together with lines of Al II and Al III always present in our Be spectra served as standards for the wave-length measurement. The BeH$^+$ spectrum in the 3100-3600A range was

[1] For references cf. W. Jevons, *Report on Band Spectra of Diatomic Molecules*.

[2] Cf. 1. Also E. Bengtsson Knave, Dissertation, Uppsala, 1932.

[3] A. Guntsch, Zeits. f. Physik **104**, 584 (1937).

photographed with a dispersion of 1.58A per mm, using the 220-volt d.c. Be arc as a light source.

The 1960A BeH Bands

The principal feature of this new BeH system is a single strong band branch degrading to higher frequencies from a head at 1960A. From the closeness of the rotational line spacing it is to be concluded that the band could only originate in the light BeH molecule providing it represents a Q branch of a transition between two states of nearly the same B_v value. There is no trace of a P branch in the region just to the red of this 1960A head. Now experimentally we find that both Be and hydrogen are necessary to produce the band. Similar hollow cathode discharges in a mixture of H_2 and He but with Al or graphite cathodes or with boron in a molybdenum cathode as well as the Be hollow cathode discharge running in He alone all failed to show the band. The only appreciable impurity lines are those of Al, but on the intense BeH arc exposures the AlH bands at 2033A and 2254A do not appear.

Furthermore, calculation shows that the BeH analog of the $B^2\Pi \rightarrow X^2\Sigma$ 2430A MgH band should occur at approximately this wave-length. The $A^2\Pi \rightarrow X^2\Sigma$ system of MgH has its (0,0) band at 19,271 cm^{-1}, making the interval between the two $^2\Pi$ states 21,966 cm^{-1}. If we assume that the ratio of this interval for MgH to that for BeH is the same as that of the ionization potentials of the two molecules and use for the I.P. the value for the united atom in each case, we calculate the $B^2\Pi - A^2\Pi$ interval for BeH to be 30,516 cm^{-1}. This places the $B^2\Pi \rightarrow X^2\Sigma$ (0,0) band of BeH at 50,547 cm^{-1}, or very close to the frequency 50,980 at 1960A. A rough Rydberg series calculation with the $A^2\Pi \rightarrow X^2\Sigma$ system at 20,031 cm^{-1} as the first member and with the limit placed at the I.P. of the united atom (B, I.P. = 67,068 cm^{-1}) indicates that the second member should be found at 49,924 cm^{-1}, again fairly near to the frequency of the observed band.

We therefore take this 1960A band to be indeed the second member of a Rydberg series of $^2\Pi \rightarrow {}^2\Sigma$ bands for BeH. In the corresponding MgH system, the P and R branches of the (0,0) and (0,1) bands end abruptly at $J = 11$ while the Q branches proceed normally to higher J values.[4] The (1,1) and (1,0) bands possess Q branches only. This sudden cessation of P and R branch transitions has been attributed[5] to the fact that radiationless transitions occur from these particular upper levels to the continuum of a $^2\Sigma^+$ state. In BeH the continuum of this interacting $^2\Sigma^+$ state must begin below the level $J = 1$, $v = 0$ of the $B^2\Pi$ state, for no P and R branches at all are to be found.

In Table I we list the frequencies and quantum assignments of the lines in this Q branch of the (0,0) $B^2\Pi \rightarrow X^2\Sigma$ band. The J numbering has been made by extrapolating through the region of unresolved lines near the head with the aid of the average second difference between successive lines. Since the spin doubling is negligible in both states, we may apply the formula for the Q-branch frequencies of a $^1\Pi \rightarrow {}^1\Sigma$ band to obtain values of $B' - B''$ from frequency differences between lines of known J values. By an averaging process, using lines with $J < 20$, we compute $B_0' - B_0'' = 0.4882$. Since $B_0'' = 10.1622$,[6] $B_0' = 10.65$ cm^{-1}. The accuracy of measurement is insufficient for the determination of D_0'.

The (1,0) and (1,1) bands are definitely present but with low intensity in the spectrum of the Be arc. Again only the Q branches occur, the (1,0) head coming at 1882.75A or 2133.4 cm^{-1} from the (0,0) head. It should be noted that this value of $\Delta G(\frac{1}{2})$ is almost as large as that for the ground state of BeH$^+$, 2140.4 cm^{-1}, whereas the value for the $A^2\Pi$ state is 2007.9 cm^{-1}. The (1,1) head

TABLE I. *Frequencies and quantum assignments of the lines of the Q branch of the* (0,0) $B^2\Pi \rightarrow X^2\Sigma$ *BeH band at 1960A.*

J	ν	J	ν
1	50,980.4	22	51,226.1
⋮	⋮	23	45.8
6	50,997.8	24	67.1
7	51,005.3	25	92.8
8	13.1	26	316.8
9	21.2	27	39.7
10	31.9	28	67.9
11	42.5	29	93.3
12	54.3	30	416.8
13	66.5	31	47.5
14	78.8	32	74.8
15	94.7	33	500.7
16	109.6	34	29.4
17	27.4	35	57.8
18	45.4	36	92.7
19	64.0	37	
20	83.0	38	657.2
21	202.8		

[4] R. W. B. Pearse, Proc. Roy. Soc. **122**, 442 (1929).

[5] R. deL. Kronig, Zeits. f. Physik **62**, 300 (1930).

[6] W. W. Watson, Phys. Rev. **32**, 600 (1928).

TABLE II. *Quantum assignments in the* $^1\Sigma \rightarrow {}^1\Sigma$ *system of* BeH^+.

	(2,5)		(3,6)		(3,7)	
J''	$P(J)$	$R(J)$	$P(J)$	$R(J)$	$P(J)$	$R(J)$
1		32,052.46		31,710.60		
2	31,987.36	057.21		713.36	30,010.50	30,077.1
3		057.21		713.36	29,988.32	081.6
4		053.56	31,590.60	710.60	961.96	081.9
5	895.47	045.53	556.23	702.18	932.19	078.7
6	855.88	032.34	518.94	692.26	899.69	072.00
7	812.53		478.64	677.24	864.13	063.16
8	764.87	31,994.51	434.43	658.17	825.54	050.79
9	713.36		386.71	636.70	784.70	034.25
10	658.17		335.42	610.72	740.51	014.76
11	599.10		280.93	581.15	693.17	29,993.94
12	536.08	868.35	224.00	547.84	644.58	969.32
13	470.06	826.97	163.26	511.12	593.00	941.78
14	399.93	781.31		470.06	538.85	911.60
15	326.60	732.25	031.06	427.24	483.00	878.80
16	250.42	679.67	30,960.92	380.45	424.63	843.53
17	170.59	623.01	888.32	330.94	364.18	806.54
18	088.32	563.51		277.64	302.64	766.09
19	003.38	500.70		222.00	238.98	724.01
20	30,915.75	434.43		163.26	173.90	680.08
21	825.46	365.45		102.30	107.88	634.43
22	733.37	293.80		039.32	040.61	589.00
23	639.28	219.35		30,973.63	28,972.78	538.85
24	542.44	142.49		904.86	904.23	488.97
25	444.35	063.37			835.19	
26	344.92	30,982.21			765.81	
27	244.01	899.29			696.89	
28		815.05			628.11	
29					560.09	
30					492.52	

	(4,8)		(5,9)		(6,10)	
J''	$P(J)$	$R(J)$	$P(J)$	$R(J)$	$P(J)$	$R(J)$
1						
2						
3						
4					29,512.65	29,622.19
5	29,733.33	29,876.24			490.59	625.67
6	703.80	872.02	29,561.69	29,725.44	466.94	625.67
7	671.53	865.27	530.63	721.71	441.74	625.67
8	636.64	855.92	500.04	714.29	413.52	620.80
9	599.56	843.53	466.66	703.80	385.16	615.33
10	559.70	828.45	431.55	693.17	354.97	608.09
11	518.40	810.63	394.90	680.08	323.32	599.93
12	474.55	790.90	356.48	664.51	290.36	588.86
13	428.62	768.60	316.49	647.38	256.74	577.58
14	380.70	744.10	274.96	628.31	222.11	564.65
15	331.09	717.97	232.32	608.09	186.02	549.90
16	280.02	688.62	187.87	585.00	149.50	534.66
17	227.37	657.64	143.67	561.69	112.83	518.40
18	173.90	625.67	097.73	536.80	075.45	500.04
19	118.50	591.07	051.77	510.54	038.36	483.00
20	062.51	555.23	005.01	483.00	001.17	464.05
21	005.81	518.40	28,957.97	455.54	28,964.48	445.55
22	28,948.63	480.69	911.12	426.87	928.15	426.87
23	891.18	441.74	864.31	398.16	892.70	408.41
24	833.60	402.24	818.09	369.13	858.46	389.77
25	776.07	362.12	772.61	340.04	825.60	373.34
26	718.97	321.69	728.07	311.64	794.46	
27	662.45	280.02	684.87			
28	606.84	238.98	642.83			
29	552.62					
30	499.52					

TABLE III. *Band origins in the* $^1\Sigma \rightarrow {}^1\Sigma$ *BeH+ system.*

(v', v'')	ν	(v', v'')	ν
0,0	39,051.4	2,5	32,028.26
0,1	36,911.5	3,0	43,284.5
0,2	34,852.5	3,6	31,682.46
0,3	32,875.3	3,7	30,048.86
1,0	40,496.4	4,0	44,621.7
1,3	34,320.4	4,8	29,841.10
1,4	32,426.9	5,9	29,689.23
2,0	41,908.3	6,10	29,587.06

TABLE IV. *BeH+ constants from the rotational term differences.*

v'	B_v'	$-D_v'$	v''	B_v''	$-D_v''$
0	7.129		0	10.659	
1	6.988		1	10.346	
2	6.835	0.00060	2	10.028	
3	6.680	0.00060	3	9.701	
4	6.521	0.00060	4	9.373	
5	6.353	0.00062	5	9.019	0.00093
6	6.158	0.00062	6	8.684	0.00099
			7	8.333	0.00098
			8	7.955	0.00097
			9	7.586	0.00103
			10	7.185	0.00106

TABLE V. *BeH+ band constants.*

ELECTRONIC STATE	B_e	α_e	$-\gamma_e$	$-D_e$	ω_e	$\omega_e x_e$	$-y_e\omega_e$	ν_e
$^1\Sigma^+$ (lower)	10.7996	0.2935	0.0049	0.000987	2221.7	39.79	0.021	
$^1\Sigma^+$ (upper)	7.1835	0.1249	0.0054	0.000608	1476.1	14.8	0.038	39,417.0

should come at $53{,}113.8 - 1987.5 = 51{,}126.3$ cm^{-1}, and we do observe a series of weaker lines converging to just about this frequency. Because of the incompleteness of the present data on the (1,0) and (1,1) bands, however, we omit their tabulation. The (0,1) band of this system cannot be detected because of the presence of a multitude of lines of the BeH^+ spectrum.

It is well known that an increase in the H_2 pressure in the light source tends to introduce the radiation transitions that are eliminated by predissociation at low gas pressure. To study this effect we ran the Be arc with H_2 pressures up to 70 cm, but the very strong pressure broadening of the several higher members of the diffuse series of Be I which lie in this spectral region obliterated the molecular spectrum. Incidentally, several of the Be I and Be II lines on these spectrograms show extremely large pressure broadenings, some shading to the blue, others to the red. The details of these effects should be investigated.

THE BeH+ SPECTRUM

The $^1\Sigma \rightarrow {}^1\Sigma$ system of the BeH^+ molecule is very extensive, as already noted, but to date only the more obvious bands in the center portion of the system have been analyzed.[2, 6] In our present search for new BeH spectra in the region from 3100A to 3600A we have added the (2,5), (3,6), (3,7), (4,8), (5,9) and (6,10) bands. The quantum assignments for these bands are given in Table II and the array of known band origins is displayed in Table III. A considerable number of bands of this system remain unanalyzed, but the data now available are complete enough to enable us to calculate all the constants for both electronic states with considerable accuracy.

In Table IV are listed the constants of the rotational energy term formulas for the known vibrational levels. These constants have been determined from the combination differences by the usual semigraphical method. The values of B_v for $v'=0$ and 1 and $v''=0$ to 4 are taken from the work of E. Bengtsson Knave.[2] The constants in the relation $B_v = B_e - \alpha(v+\frac{1}{2}) + \gamma(v+\frac{1}{2})^2$ representing the variation of these B values with v differ somewhat from those given in reference 2, showing the influence of the added data. We can detect no definite variation of D_v with v, and there is no appreciable effect of a fifth power term in the rotational energy in the range of J values available. Cubic terms in the vibrational energy formula are necessary in both states, the coefficients being markedly smaller than those given by Bengtsson. All band constants are collected in Table V. The more rapid decrease of these constants with v for the lower state tends to close up the gap between corresponding constants for the two states, thus accounting for the convergence of the bands in the sequences, the overlapping of structure from different bands and the general complexity of the red end of this spectrum.

The Efficiency of Counters and Counter Circuits

ARTHUR E. RUARK AND FOREST E. BRAMMER
University of North Carolina, Chapel Hill, North Carolina

(Received June 17, 1937)

Existing formulas for correcting counter data for "missing" are found to apply to conditions which often cannot be realized in practice. Let τ_c, τ_i, and τ_r be the recovery times of the counter, amplifier and recording unit. It is shown that excellent performance can be obtained by using an amplifier which controls the voltage recovery of the counter so that $\tau_c=\tau_i=$constant. When the counter receives f particles/sec., capable of activating it, the efficiency of the entire apparatus is $(1+f\tau_i)^{-1}$ if $\tau_r<\tau_i$. It is $e^{-f(\tau_r-\tau_i)}/(1+f\tau_i)$ if $\tau_r>\tau_i$ and the recorder is not influenced by any impulse which reaches it while it is operating.

1

THERE has been considerable misunderstanding as to the correction of counter data for particles missed because of the finite recovery times of the counter and of its recording circuits. Formulas for this purpose published by different authors are not identical and closer inspection shows that they really refer to different arrangements of apparatus. These formulas can be used to correct data obtained under the conditions assumed in their derivations, but often these conditions are not realized in practice. All formulas proposed up to the present contain only a single recovery time. Some authors have considered the recovery time of a counter fed with a random distribution of events, paying no attention to the recording circuits. Correction equations obtained in this way can be used only when the recovery times of the circuit-elements are negligible compared to that of the counter. Conversely, other authors have discussed the behavior of a hypothetical recording circuit characterized by a single recovery time, neglecting the counter recovery time and the fact that the impulses from a counter do not form a random distribution. In this paper we derive new formulas, taking into account all recovery times which affect the over-all counting efficiency, and show how apparatus can be arranged to make these formulas valid.

Suppose that on the average a counter receives f particles per unit of time, following the Bateman distribution law, and that the recovery time is τ_c. This quantity is variable and its highest value will be called $\tau_{c\,\max}$. For present purposes we can treat the amplifier as a single unit with recovery time τ_i, and the recorder as another unit with recovery time τ_r. The word "recorder" includes both the mechanical recorder and any circuit which precedes it to scale down the counts. In such a case τ_r is the recovery time of the first stage in the scaling-down circuit.

The number of counts recorded per unit of time is f', and the problem is to get f from observations of f' and of the three recovery times, $\tau_{c\,\max}$, τ_i, and τ_r.

Skinner[1] has given correction formulas and curves for the tube counter itself. Of necessity, his very complete analysis is based on certain reasonable assumptions about the mechanism of recovery, derived partly from Danforth's[2] experiments on the variation of counter voltage during a "kick." To avoid extreme complexity, Skinner neglects the variation of efficiency with voltage, and the fact that τ_c cannot be less than the duration τ_d of the discharge in the tube counter. Nevertheless, his treatment is the best we have, and until detailed experimental work indicates the necessity of modifications, it may be used to correct counter data when certain conditions are satisfied. First, the recovery times of the amplifier and recorder should be small compared with $\tau_{c\,\max}$. Second, the average counting rate should be small compared with the reciprocal of τ_d.

2. Efficiencies of Recorders Fed with Random Events

We now consider cases in which the counter and amplifier are very fast compared with the

[1] Skinner, Phys. Rev. **48**, 438 (1935).
[2] Danforth, Phys. Rev. **46**, 1026 (1934).

recorder. More specifically, it is supposed that the recorder receives a Bateman distribution of impulses. Previous authors have not pointed out that there are two types of recorders, with different efficiencies.

Type I is exemplified by the Cenco recorder. Suppose that a current impulse excites the magnet of such a recorder, moving the ratchet wheel ahead one tooth, and that the ratchet pawl starts to fall back. If a second impulse arrives before the cycle of movement is complete, the pawl simply slides up over the tooth on which it is riding, and starts back again. The result is that the second impulse is not counted, and the recovery time after the second impulse is shorter than that required for the whole cycle of movement. Thus a recorder of this type has a variable recovery time when counting random impulses. The average recovery time depends on the counting rate and on the details of the ratchet motion, so no general statements can be made about it. Nevertheless the efficiency can be obtained, for an impulse coming at an arbitrary instant will be recorded only if the recorder has not received another in a period equal to the maximum recovery time τ_r. This simple argument was given by Volz[3] but he did not mention the fact that it applies only to ratchet-like recorders. His efficiency formula is

$$f'/f=e^{-f\tau_r}. \tag{1}$$

Type II. The second type of recorder is one which goes through its cycle after an impulse without paying any attention to the arrival of additional ones. A properly designed thyratron set approximates this behavior closely. (This is true even when a ratchet-type recorder is used after the final pair of tubes, provided the recovery time of this pair is larger than that of the mechanical recorder.) The efficiency formula is

$$f'/f=1/(1+f\tau_r). \tag{2}$$

Skinner mentioned this result, but did not give the simple proof, which is as follows. Consider the interval τ_r following the arrival of an impulse. The average number of impulses lying in this interval is $f\tau_r$, but there are f' such intervals per second, so $f'f\tau_r$ impulses are missed per second. Thus $f=f'+f'f\tau_r$, which gives Eq. (2).

As f increases, the counting rate of a Type I recorder passes through a maximum value, $1/e\tau_r$, and decreases again; the recorder is said to "jam." A Type II recorder simply goes up to the maximum possible counting rate, $1/\tau_r$, which is e times larger than the value for a Type I recorder. In this laboratory we have counting outfits which behave approximately in this way. For one of them, we found a recovery time of 3.5 milliseconds from oscillograph observations. The maximum counting rate was very close to 300/sec., leading to a recovery time of 3.3 milliseconds. Such high-speed tests can be avoided if one has two similar radioactive sources of known ratio, and of suitable strength. If the numbers of particles supplied to the counter by the sources are f_1 and f_2, we write $R=f_2/f_1$. Then Eq. (2) shows that

$$\tau_r=(Rf_1'-f_2')/[(R-1)f_1'f_2']. \tag{3}$$

3. Desirable Characteristics of an Apparatus for Fast Counting

We now consider how the entire counting apparatus can be designed to make it follow simple efficiency formulas to a high degree of approximation. There are two general types of amplifying equipment. The first is exemplified by any amplifier which has the conventional input and no arrangements by which the amplifier can control the course of voltage recovery in the counter. By "conventional input" we mean that the counter wire is separated from ground by a high resistance and is coupled to the grid of the first tube through a condenser, a grid resistance of the order of 1 megohm being provided. As an idealization, one may say that the grid has no influence on the recovery of the counter, and it will be assumed that the remainder of the amplifier follows the first stage perfectly. It is easy to arrange matters so that the recovery time of the input grid obeys the conditions $\tau_d<\tau_i<\tau_{c\,\max}$, or alternatively the condition $\tau_{c\,\max}<\tau_i$. No matter which choice we make, we can see from Skinner's discussion that the impulses handed on to the recorder will not form a Bateman distribution.

To avoid this complicated situation, one must

[3] Volz, Zeits. f. Physik **93**, 539 (1935); Schiff, Phys. Rev. **50**, 88 (1936).

use the Neher-Harper circuit[4] or any similar circuit which automatically lowers the counter voltage when a count occurs and raises it briskly to a level above threshold after the discharge ceases.[5] The important point is that the conditions $\tau_i = \tau_c = \text{constant}$ should be satisfied. Then the counter and amplifier will work together as a single unit with a definite recovery time. If the counter misses an event, the amplifier also does, and conversely the amplifier cannot miss any impulse from the counter. The amplifier gives $f/(1+f\tau_i)$ impulses per second and the value of the recorder efficiency depends on the relative sizes of the recovery times. If τ_r is less than τ_i the recorder follows the amplifier perfectly, no matter whether it is of Type I or Type II. Thus the efficiency of the entire counting apparatus is given by Eq. (2). If τ_r is greater than τ_i and the recorder is of a kind which cannot be reexcited while it is in action (Type II), the efficiency of the apparatus is

$$f'/f = e^{-f(\tau_r-\tau_i)}/(1+f\tau_i). \tag{4}$$

To see this, we consider the interval τ_r following an amplifier pulse at time zero. There is certainly no additional pulse until time τ_i and the probability that none occurs in the interval τ_i to τ_r is $e^{-f(\tau_r-\tau_i)}$. This, then, is the probability that the recorder catches the next pulse, and the efficiency (4) of the whole apparatus is gotten by multiplying this factor by the efficiency of the counter and the amplifier. When $\tau_r > \tau_i$, the efficiency of a ratchet recorder (Type I) depends on the detailed nature of its cycle of motion. The only general statement which can be made is that the efficiency of the entire apparatus is not less than that given by Eq. (4).

When Eq. (4) holds true the counting rate rises to a maximum as f increases. This maximum occurs when

$$2\tau_i f = -1+(1+4\tau_i/(\tau_r-\tau_i))^{\frac{1}{2}}. \tag{5}$$

We are now in a position to make definite recommendations for choosing the essential constants of a counting apparatus which operates without jamming and with minimum loss up to the highest possible speed, and which has the simple correction formula (2) with τ_i substituted for τ_r. The amplifier should control the voltage recovery of the counter itself, and should feed the recorder unit with pulses whose duration is less than τ_r. The recovery time τ_r should be less than τ_i, and τ_i should be made as short as possible, always keeping in mind the requirement that deionization of the counter must be complete before the amplifier returns to its initial state. Circuits which fulfill these requirements will be described in another communication.

A word of caution as to the discharge time of tube counters is desirable. Different authors[6] have found wide variations in this time, depending on the size of the counter and the nature of the gas. Values from 10^{-2} to 2×10^{-5} seconds have been reported for counters operating at a few cm of mercury. It is not possible to say whether the higher values reported are due to the use of voltages too far above the threshold. However, we have observed a value of about 0.003 second for a counter 3.25 cm in diameter and 15 cm long, filled with dry tank hydrogen at atmospheric pressure. Larger counters filled in the same way are still slower.

The experimental work which led to the writing of this paper was facilitated by a grant from the National Research Council to one of us (A.E.R.). This aid is gratefully acknowledged.

[4] Neher and Harper, Phys. Rev. **49**, 940 (1936). We have employed a multivibrator circuit which is a modification of one described by Gingrich, Evans and Edgerton, R. S. I. **7**, 450 (1936); see their Fig. 6.

[5] If τ_i is made less than τ_d, reexcitation occurs. We have found it convenient to adjust τ_i to the optimum value by oscillographic observations. Starting with a low value, τ_i is increased until double amplifier pulses are eliminated.

[6] Medicus, Zeits. f. Physik **74**, 350 (1932); Hummel, Physik. Zeits. **35**, 997 (1934); Trost, Physik. Zeits. **36**, 801 (1935).

Domain Theory of Ferromagnetics Under Stress: Part I

WILLIAM FULLER BROWN, JR.
Columbia University, New York, New York

(Received June 3, 1937)

The statistical domain theory of ferromagnetism, introduced by Heisenberg and extended by others, is developed in a general form capable of application to any ferromagnetic, crystalline or polycrystalline. Formulas are derived by which the magnetization and strain components can be computed to the first order in the stresses, provided the magnetization curve at zero stress is known. The analysis is valid at any magnetization below that at which the rotation process begins, and the six stress components may have arbitrary values. The formulas are then specialized to nickel crystals; the results reduce to those of Gans and v. Harlem, and of Akulov and Kondorsky, for the special cases treated by them, except for one formula of the former authors and one of the latter. In these cases the original formula is shown to be in error, and the corrected formula leads to better agreement with experiment.

INTRODUCTION

THE statistical domain theory by which Heisenberg[1] calculated the magnetostriction curves of iron crystals has been successfully extended to other fields by Gans and v. Harlem[2] and by Bozorth.[3] A similar calculation carried out by Akulov and Kondorsky,[4] and leading to formulas for the variation of Young's modulus with magnetization and of magnetostriction with tension, has been less successful; for although the authors found fair agreement with certain data, and although Girenchin[5] has recently presented data apparently in good agreement with the theoretical formulas, the results of Siegel and Quimby[6] indicate a need for emendation of the theory. Moreover the formulas are valid only to the third order in the magnetization.

It was recently pointed out by the writer[7] that because of the magnetic skin effect, measurements of Young's modulus by a dynamical method give approximately the value at constant flux density (B), while static methods give the value at constant magnetizing field (H). It is therefore important, before applying theoretical formulas to such data, to ascertain to which of these two values the formulas correspond. Another source of uncertainty is the inaccuracy of any method of averaging over the constituent crystals of polycrystalline material; the true average may be expected to lie somewhere between the values obtained by assuming uniform stress and by assuming uniform strain, but Akulov and Kondorsky give only the first of these. It seems desirable, therefore, to carry out the theoretical calculation under various assumptions in regard to the constancy of magnetic quantities during the strain, and by both methods of averaging over the crystals. To do this by the original method of Akulov and Kondorsky would involve tedious calculations, as would any attempt to apply the method to the calculation of the variation of rigidity with magnetization, or to obtain a higher degree of approximation in the formulas. The need for a more flexible procedure is also evident from the fact that so far, every writer who has attempted a further application of Heisenberg's method has gone through a complete derivation of a distribution function for the particular type of crystal and the particular magnetic and mechanical situation under investigation. The method has now proved useful in such a variety of problems that it seems desirable to obtain, once for all, general formulas applicable to any ferromagnetic crystal under the action of any field and stress system.

The application of the theory to polycrystalline material may be made in several different ways, depending on the nature of the material. If each of the constituent crystals contains many

[1] W. Heisenberg, Zeits. f. Physik **69**, 287 (1931).
[2] R. Gans and J. v. Harlem, Ann. d. Physik **15**, 516 (1932); **16**, 162 (1933).
[3] R. M. Bozorth, Phys. Rev. **42**, 882 (1932).
[4] N. Akulov and E. Kondorsky, Zeits. f. Physik **78**, 801 (1932); **85**, 661 (1933).
[5] B. K. Girenchin, Physik. Zeits. Sowjetunion **10**, 689 (1936).
[6] S. Siegel and S. L. Quimby, Phys. Rev. **49**, 664 (1936).
[7] W. F. Brown, Phys. Rev. **50**, 1165 (1936).

domains, the results for crystals may be averaged; this is the procedure followed by Akulov and Kondorsky. If the size of the crystals is of the same order of magnitude as the size of the domains, then, following Gans,[8] we may regard the substance as an aggregate of crystalline domains with their axes oriented at random. If the crystals are much smaller than the domains, the domains can no longer be regarded as crystalline; they may be isotropic, or may have an anisotropy due to nonrandom orientation of the crystal axes or to other causes. The theory should be flexible enough to apply to any of these cases.

The first object of the present paper is to derive general formulas by which the strains (or stresses) and certain other quantities can be calculated rigorously as functions of the magnetization, and to the first order in the stresses (or strains), for any ferromagnetic under various assumptions regarding the constancy of magnetic quantities during the strain. (The assumption of uniform stress or of uniform strain will enter implicitly, according as one or the other is taken as independent variable.) The formulas will then be applied to nickel crystals; the results will be compared with those of previous writers, especially of Akulov and Kondorsky, and with experimental data.

General Theory

Using Heisenberg's simple model, we regard a ferromagnetic specimen as consisting of domains of equal size, N of them in unit volume; these may be divided into classes in accordance with the nature of their anisotropy, so that of the N domains, N^τ are of class τ: then $\sum_\tau N^\tau = N$. For a single crystal, all the domains will belong to a single class, so that the superscript τ and the summation sign $\sum_\tau$ may be omitted in all equations. For a polycrystalline specimen as viewed by Gans, the orientation of fixed axes with respect to the crystal axes of a domain may be specified by Eulerian angles ϕ, θ, ψ; a particular class τ will then consist of those domains for which the direction ϕ, θ is within a solid angle $d\omega$ and for which ψ is within $d\psi$, and N^τ will be $Nd\omega d\psi/8\pi^2$.

[8] R. Gans, Physik. Zeits. **33**, 15 (1932).

Each domain of class τ will have certain directions of easy magnetization; we are concerned with magnetizations below the knee of the J-H curve, so that rotation of the magnetization vector out of these directions of easy magnetization may be neglected, and the magnetization process may be assumed to proceed entirely by changes of the spontaneous magnetization in individual domains from one of these directions to another. In the limiting case of isotropic domains, every direction is a direction of easy magnetization, and the transitions degenerate to continuous rotations. A particular microscopic state of the specimen could be described by giving the direction of the magnetization of each domain; those states for which the number of domains of class τ with magnetization in direction σ is a specified number N_σ^τ for each τ and σ are macroscopically indistinguishable and together constitute a macroscopic state of statistical weight

$$W=\prod_\tau (N^\tau!)/\prod_\tau\prod_\sigma (N_\sigma^\tau!),$$

or by use of Stirling's approximation,

$$\log W=\text{const.}-\sum_\tau\sum_\sigma N_\sigma^\tau \log N_\sigma^\tau.$$

All variations of the partition numbers N_σ^τ are subject to the conditions

$$\sum_\sigma N_\sigma^\tau = N^\tau. \tag{1}$$

We take, as the independent variables of the system, quantities y_r, each of which is either a thermodynamic coordinate or the negative of a thermodynamic force. Let V be the thermodynamic potential per unit volume corresponding to this choice of independent variables, for isothermal or for adiabatic changes. Then $Y_r=\partial V/\partial y_r$ will be the thermodynamic force corresponding to y_r as coordinate, or the coordinate corresponding to $-y_r$ as force, and these quantities will consequently satisfy the thermodynamic relations

$$\partial Y_r/\partial y_s=\partial Y_s/\partial y_r. \tag{2}$$

V for the specimen as a whole will consist of a part made up of contributions from individual domains, and a part resulting from interaction of the domains. In the contribution of a par-

ticular domain to the former, terms independent of the direction of the spontaneous magnetization may be disregarded for present purposes, and the remainder, in all cases in which we are interested, may be regarded as linear in the y_r's. Thus the value of V for a domain of class τ and magnetization-direction σ is

$$V_\sigma^\tau = \sum_r Y_{r\sigma}^\tau y_r, \tag{3}$$

where the quantities $Y_{r\sigma}^\tau$ are constants, in general different for different σ's as well as for different τ's. The value of Y_r for such a domain then consists of a part independent of the magnetization-direction plus a part $\partial V_\sigma^\tau/\partial y_r = Y_{r\sigma}^\tau$ dependent on this magnetization-direction.

If q is any quantity whose observed value for the specimen as a whole is an average of values for the individual domains and whose value for a domain of class τ and magnetization-direction σ is q_σ^τ, then

$$q = \sum_\tau n^\tau \sum_\sigma n_\sigma^\tau q_\sigma^\tau, \tag{4}$$

where
$$n^\tau = N^\tau/N, \quad n_\sigma^\tau = N_\sigma^\tau/N^\tau. \tag{5}$$

In particular, the macroscopic quantities Y_r are given by

$$Y_r = Y_{r0} + \sum_\tau n^\tau \sum_\sigma n_\sigma^\tau Y_{r\sigma}^\tau = Y_{r0} + Y_r', \tag{6}$$

where Y_{r0} is the part independent of the distribution of magnetization-directions; and the value of the thermodynamic potential V for the specimen is

$$V = V_0 + \sum_\tau n^\tau \sum_\sigma n_\sigma^\tau V_\sigma^\tau + V'' = V_0 + V' + V'', \tag{7}$$

where V_0 is independent of the distribution of magnetization-directions, V'' is due entirely to interaction between domains, and V' is the part contributed by the separate domains and dependent on their magnetization-directions. V' is given by

$$V' = \sum_\tau n^\tau \sum_\sigma n_\sigma^\tau V_\sigma^\tau = \sum_r y_r \sum_\tau n^\tau \sum_\sigma n_\sigma^\tau Y_{r\sigma}^\tau = \sum_r Y_r' y_r. \tag{8}$$

It is to be noted that the Y_{r0}'s and the Y_r''s satisfy (2) separately, since $Y_{r0} = \partial V_0/\partial y_r$ and $Y_r' = \partial(V' + V'')/\partial y_r$.

The values of the N_σ^τ's for which $\log W$ is a maximum, for a specified value of V', are determined by

$$\frac{\partial}{\partial N_\sigma^\tau}\{\log W + \sum_\tau L^\tau \sum_\sigma N_\sigma^\tau + L' V'\} = 0,$$

where the L^τ's and L' are Lagrangian multipliers and the N_σ^τ's are independent variables in the differentiation. We thus find for the most probable distribution consistent with a prescribed V' and with (1),

$$n_\sigma^\tau = \exp(LV_\sigma^\tau)/\sum_\rho \exp(LV_\rho^\tau), \tag{9}$$

where L is determined as a function of V' by

$$\sum_\tau n^\tau \{\sum_\sigma V_\sigma^\tau \exp(LV_\sigma^\tau)/\sum_\sigma \exp(LV_\sigma^\tau)\} = V'. \tag{10}$$

It, of course, does not follow that this is the actual distribution; it can be said only that this is the one we are safest in predicting on the basis of a knowledge of V', in the absence of definite knowledge of the form of the interaction term V''. If V'' were known, we should merely find the distribution making $V' + V''$ a minimum.

Equation (6), together with (9) and (10), now determines the Y_r''s as functions of the y_r's and of the prescribed value of V'. The completion of the analysis requires a knowledge of V' or of L as a function of the y_r's. This we do not have. We do know, however, that whatever the nature of this function, it must lead to values of the Y_r''s satisfying (2). If one of the Y_r''s, say Y_0', is known as a function of the corresponding variable y_0 when all the other y_r's are zero, then V' and hence all the Y_r''s are determined when $y_r = 0$ $(r > 0)$. The derivatives $\partial Y_r'/\partial y_s$ are then, as we shall see, completely determined by (2), and thus the Y_r''s are determined to the first order in the y_r's. Thus from a knowledge of the magnetization curve at zero stress we can calculate the magnetization and the strains as functions of the field, not merely at zero stress, but to the first order in the stresses.

For convenience, we introduce the definitions

$$\begin{aligned} S^\tau &= \sum_\sigma \exp(LV_\sigma^\tau), \\ S_r^\tau &= \sum_\sigma Y_{r\sigma}^\tau \exp(LV_\sigma^\tau), \\ S_{rs}^\tau &= \sum_\sigma Y_{r\sigma}^\tau Y_{s\sigma}^\tau \exp(LV_\sigma^\tau). \end{aligned} \tag{11}$$

We then have, from (6),

$$Y_r - Y_{r0} = Y_r' = \sum_\tau n^\tau S_r^\tau / S^\tau, \tag{12}$$

and from (10),

$$\sum_\tau n^\tau \sum_r y_r S_r^\tau / S^\tau = V'. \tag{13}$$

When $y_r = 0$ $(r > 0)$, LV_σ^τ becomes $L^0 Y_{0\sigma}{}^\tau y_0$, and (13) becomes, by virtue of (8),

$$\sum_\tau n^\tau S_0^{\tau 0} / S^{\tau 0} = Y_0{}'^0, \tag{13'}$$

an equation identical with that one of Eqs. (12) for which $r = 0$. This determines L^0 and the S's, and the rest of Eqs. (12) then determines the quantities

$$Y_r{}'^0 = \sum_\tau n^\tau S_r^{\tau 0} / S^{\tau 0}. \tag{12'}$$

To evaluate the Y_r''s to the first order in the y_s's we differentiate (12) with respect to y_s, using (11), and then set all the y_r's except y_0 equal to zero. This gives (we omit the primes)

$$\partial Y_r / \partial y_s = LP_{rs} + (\partial L / \partial y_s) P_{r0} y_0, \tag{14}$$

where $$P_{rs} = \sum_\tau n^\tau P_{rs}{}^\tau,$$

$$P_{rs}{}^\tau = S_{rs}{}^\tau / S^\tau - S_r{}^\tau S_s{}^\tau / S^{\tau 2} = P_{sr}{}^\tau. \tag{15}$$

In these formulas, superscript zeros have been dropped, but it is to be understood that all quantities occurring in the equations are to be evaluated for $y_r = 0$ $(r > 0)$, after the differentiations have been performed. We note also the useful relation

$$P_{r0} = \partial Y_r^0 / \partial (Ly_0). \tag{15'}$$

For a given Y_i and y_j, with i and $j \geq 0$, we can obtain from (14) four equations, by setting, in turn, $r = s = 0$; $r = j$, $s = 0$; $r = 0$, $s = j$; $r = i$, $s = j$. In addition we have, by (2), $\partial Y_0 / \partial y_j = \partial Y_j / \partial y_0$. By elimination of these two quantities and of $\partial L / \partial y_0$ and $\partial L / \partial y_j$, we get

$$\left(\frac{\partial Y_i}{\partial y_j}\right)_{v0} = L\left(P_{ij} - \frac{P_{i0}P_{j0}}{P_{00}}\right) + \frac{P_{i0}P_{j0}}{P_{00}^2}\frac{\partial Y_0}{\partial y_0}, \tag{16}$$

where y_0 has been written as a subscript to indicate that it is the independent variable held constant in the differentiation.

For the derivative at constant Y_0, we have

$$\left(\frac{\partial Y_i}{\partial y_j}\right)_{Y_0} = \left(\frac{\partial Y_i}{\partial y_j}\right)_{v0} - \frac{\partial Y_i}{\partial y_0}\frac{\partial Y_j}{\partial y_0} \Big/ \frac{\partial Y_0}{\partial y_0}$$

$$= L\left(P_{ij} - \frac{P_{i0}P_{j0}}{P_{00}}\right). \tag{17}$$

By a similar analysis we may obtain the formulas to be used if a certain number of the Y_r's, say those for which $r \leq m$, are known as functions of the corresponding y_r's when the other y_r's $(r > m)$ are zero. In this case the functions must of course be such as to satisfy the thermodynamic relations (2), and they must also be such that the m Eqs. (12), with $r \leq m$, give consistent values of L. For the derivatives at constant y_r $(r \leq m)$ we get

$$\left(\frac{\partial Y_i}{\partial y_j}\right)_{y_r} = LP_{ij} + \frac{Q_iQ_j}{Q_rQ_s}\left(\frac{\partial Y_r}{\partial y_s} - LP_{rs}\right), \tag{18}$$

where $$Q_i = \sum_{t=1}^{m} P_{it} y_t. \tag{19}$$

Here r and s may have any values (not necessarily different) $\leq m$; if the consistency requirements just mentioned are satisfied, the uniqueness of the result is insured. For the derivatives at constant Y_r $(r \leq m)$, we get

$$\left(\frac{\partial Y_i}{\partial y_j}\right)_{Y_r} = L(P_{ij} - T_{ijtu}) - L^2 \sum_\tau \sum_s \frac{\partial y_r}{\partial Y_s} R_{ist} R_{jru}, \tag{20}$$

where

$$T_{ijtu} = (Q_iQ_uP_{jt} + Q_jQ_tP_{iu} - Q_iQ_jP_{tu})/Q_tQ_u,$$

$$R_{ist} = P_{is} - Q_iP_{ts}/Q_t. \tag{21}$$

In the differentiations, the independent variables are the Y_r's $(r \leq m)$ and the y_j's $(j > m)$. Formula (20) is required for the evaluation of the strains to the first order in the stresses when the *vector* magnetization remains constant during the strain.

We have, finally (restoring the primes),

$$Y_i = Y_{i0} + Y_i{}'^0 + \sum_j (\partial Y_i' / \partial y_j) y_j, \tag{22}$$

where the derivatives will be those at constant y_r or at constant Y_r, according as one or the other set of quantities is assumed to remain constant as the y_j's vary.

Nickel and Iron Crystals

To apply the general theory to single crystals of nickel and iron, we begin with the thermodynamic potential F_{He} per unit volume of a single domain, defined by

$$\delta F_{He}=-\sum J_i\delta H_i+\sum X_{ii}\delta e_{ii}+\sum X_{jk}\delta e_{jk}. \quad (23)$$

Here the H_i's ($i=1, 2, 3$) are the components of magnetic field, the J_i's the components of magnetization, along the crystal axes; $X_{ij}=X_{ji}$ is the x_i-component of stress exerted across a surface normal to Ox_j; $e_{ii}=\partial u_i/\partial x_i$, $e_{jk}=\partial u_j/\partial x_k+\partial u_k/\partial x_j$ ($k\neq j$), where the u_i's are components of displacement. The summation, in this and in subsequent expressions, is over the three sets of values $(i, j, k)=(1, 2, 3); (2, 3, 1); (3, 1, 2)$. For ferromagnetic crystals $J_i=J_s\alpha_i$, where J_s is the spontaneous magnetization and $\alpha_i=\cos(J_s, Ox_i)$. Keeping all the terms that it has been found necessary to introduce in order to account satisfactorily for experimental results,[9] we have by virtue of the cubic symmetry

$$\begin{aligned}F_{He}=&-J_s\sum H_i\alpha_i+2K_1\sum\alpha_j^2\alpha_k^2+K_2\alpha_1^2\alpha_2^2\alpha_3^2\\&+k_0\sum e_{ii}+k_1\sum e_{ii}\alpha_i^2+2k_2\sum e_{jk}\alpha_j\alpha_k\\&+k_3(\sum e_{ii})(\sum\alpha_i^4)+k_4\sum e_{ii}\alpha_i^4\\&+k_5\sum e_{ii}\alpha_j^2\alpha_k^2+k_6\sum e_{jk}\alpha_i^2\alpha_j\alpha_k\\&+\tfrac{1}{2}c_{11}\sum e_{ii}^2+c_{12}\sum e_{jj}e_{kk}+\tfrac{1}{2}c_{44}\sum e_{jk}^2.\end{aligned} \quad (24)$$

The thermodynamic potential F_{HX} defined by

$$\begin{aligned}\delta F_{HX}&=\delta(F_{He}-\sum X_{ii}e_{ii}-\sum X_{jk}e_{jk})\\&=-\sum J_i\delta H_i-\sum e_{ii}\delta X_{ii}-\sum e_{jk}\delta X_{jk}\end{aligned} \quad (23')$$

is given by a formula obtainable from (24) by substituting $-X_{ij}$ for e_{ij}, and new constants K_i', κ_i, $-s_{ij}$ for K_i, k_i, c_{ij}. The relations between the two sets of constants are easily obtained, and need not be given here. The K's are the constants of magnetic anisotropy, the c's and s's are the elastic constants and moduli, and the k's and κ's determine the magnetostrictive stresses or strains. F_{He} is to be used when the strain is assumed uniform, F_{HX} when the stress is assumed uniform.

[9] F. Bitter, Phys. Rev. **42**, 697 (1932); **43**, 655 (1933); R. Gans, Physik. Zeits. **33**, 924 (1932); reference 2. The k_1 of reference 2 is our $2\kappa_2$. The k_5-term is really superfluous, since $\alpha_j^2\alpha_k^2=\frac{1}{3}-\alpha_i^2+\alpha_i^4-\frac{1}{3}\Sigma\alpha_i^4$.

The actual values of the α_i's are those that make F_{He} or F_{HX} a minimum; but since we are neglecting the small rotation produced by the field and the strains, we have for nickel $\alpha_i=p_i/\sqrt{3}$, where p_i is either $+1$ or -1 for each value of i; and for iron $\alpha_i=+\delta_{ir}$ or $-\delta_{ir}$, where $\delta_{ii}=1$, $\delta_{ij}=0$ ($j\neq i$), and r may be 1, 2, or 3. Omitting the terms that are the same for all the directions of easy magnetization, and using the condition that the average strains must vanish in the demagnetized state, we get for the part of F_{HX} dependent on the direction of magnetization of the domain

$$\text{(Ni)}\quad F_{HX}'=-(J_sH/\sqrt{3})\sum p_il_i-(2\kappa_2/3+\kappa_6/9)\sum p_ip_kX_{jk}, \quad (25)$$

$$\text{(Fe)}\quad F_{HX}'=\mp J_sHl_r-(\kappa_1+\kappa_4)\sum(\delta_{ir}-\tfrac{1}{3})X_{ii}, \quad (25')$$

where the l_i's are the direction-cosines of the field. For the parallel component of magnetization, J_p, and for the part of the strains depending on the magnetization-direction, we have

$$J_p=-\partial F_{HX}'/\partial H, \quad e_{ij}'=-\partial F_{HX}'/\partial X_{ij};$$

or

$$\text{(Ni)}\quad J_p=(J_s/\sqrt{3})\sum p_il_i, \quad e_{ij}'=(2\kappa_2/3+\kappa_6/9)p_ip_j \quad (j\neq i); \quad (26)$$

$$\text{(Fe)}\quad J_p=\pm J_sl_r, \quad e_{ii}'=(\kappa_1+\kappa_4)(\delta_{ir}-\tfrac{1}{3}). \quad (26')$$

Gans and v. Harlem found it necessary to include the quantities denoted here by κ_4 and κ_6, in order to obtain a good fit at saturation. For our purposes the coefficients of p_ip_j and of $(\delta_{ir}-1/3)$ are merely constants, and they will therefore be written hereafter as $2\kappa_2/3$ and κ_1 respectively, in conformity with Akulov's notation. They may be determined from the saturation magnetostriction in the [111] and [100] directions, by the relations

$$\kappa_2=3\lambda_{111}/2, \quad \kappa_1=3\lambda_{100}/2. \quad (27)$$

Assuming uniform strain rather than uniform stress, we need only replace e, $-X$, κ by X, e, k respectively in the analysis to follow. The new κ's defined by (27) are related to the corresponding k's by the formulas

$$-k_2/\kappa_2=c_{44}=1/s_{44}, \quad -k_1/\kappa_1=c_{11}-c_{12}=1/(s_{11}-s_{12}). \quad (27')$$

Nickel Crystals

The calculation is simplified and the symmetry of the equations increased, if the field is assumed to remain constant in direction and to vary only in magnitude. Equivalent results are obtained by treating the three field-components as independent variables; Eq. (18) must then be used instead of (16). We shall present only the simpler derivation. By comparison of Eqs. (25) and (3), we see that for a nickel crystal, assuming uniform stress, we may take F_{HX}' as V', and write

$$\begin{aligned} &y_0=-H, \quad y_1=-X_{ij}, \quad y_2=-X_{jk} \quad (k\neq i),\\ &Y_0=J_p, \quad Y_1=e_{ij}, \quad Y_2=e_{jk},\\ &Y_{0\sigma}=(J_s/\sqrt{3})\textstyle\sum p_i l_i, \quad Y_{1\sigma}=2\kappa_2 p_i p_j/3,\\ &\qquad\qquad Y_{2\sigma}=2\kappa_2 p_j p_k/3. \end{aligned} \tag{28}$$

The first of Eqs. (11) becomes

$$\begin{aligned} S=\sum_p \exp\left[(-LHJ_s/\sqrt{3})\textstyle\sum p_i l_i\right]\\ =\sum_p \exp\left[\eta\textstyle\sum p_i l_i\right], \end{aligned}$$

$$\text{where} \qquad \eta=-LHJ_s/\sqrt{3}; \tag{29}$$

the outside summation is over the eight combinations of values $(p_1, p_2, p_3)=(1, 1, 1)$; $(1, 1, -1)$; $\cdots$ $(-1, -1, -1)$, so that

$$S=8\cosh\eta l_1\cosh\eta l_2\cosh\eta l_3. \tag{30}$$

The evaluation of the other sums is facilitated by noting that p_j, multiplying the exponential factor, is equivalent to $\partial/\partial(\eta l_j)$, which may be taken outside the summation sign $\sum_p$; moreover $[\partial/\partial(\eta l_j)]^n$, operating on S, is equivalent to 1 if n is even and to $\tanh\eta l_j$ if n is odd. Writing for brevity $t_i=\tanh\eta l_i$, $s_i=\operatorname{sech}\eta l_i$, we have

$$\begin{aligned} &S_0/S=(J_s/\sqrt{3})\textstyle\sum l_i t_i,\\ &S_1/S=2\kappa_2 t_i t_j/3,\\ &S_2/S=2\kappa_2 t_j t_k/3; \end{aligned} \tag{31}$$

$$\begin{aligned} &P_{00}=J_s{}^2\textstyle\sum l_i{}^2 s_i{}^2/3,\\ &P_{10}=(2\kappa_2 J_s/3\sqrt{3})(l_i s_i{}^2 t_j+l_j s_j{}^2 t_i),\\ &P_{20}=(2\kappa_2 J_s/3\sqrt{3})(l_j s_j{}^2 t_k+l_k s_k{}^2 t_j),\\ &P_{11}=(4\kappa_2{}^2/9)(1-t_i{}^2 t_j{}^2),\\ &P_{22}=(4\kappa_2{}^2/9)(1-t_j{}^2 t_k{}^2),\\ &P_{12}=(4\kappa_2{}^2/9)t_i s_j{}^2 t_k. \end{aligned} \tag{32}$$

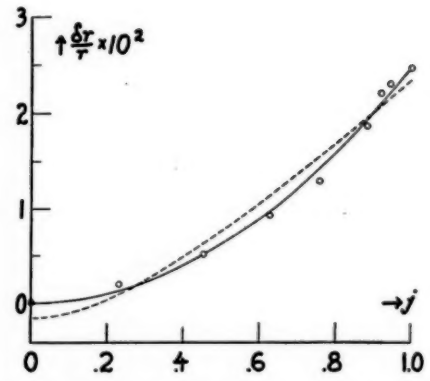

Fig. 1. Variation of longitudinal resistivity with magnetization for nickel crystal magnetized in [111] direction. Points, experimental values of Kaya as plotted by Gans and v. Harlem. Dashed curve, formula of Gans and v. Harlem; solid curve, corrected formula. Each curve has been fitted separately to the data by least squares.

Eqs. (12′) and (13′) therefore become

$$e_{ij}{}'^0=2\kappa_2 t_i t_j/3, \quad j_p{}^0=J_p{}^0/J_s=(1/\sqrt{3})\textstyle\sum l_i t_i. \tag{33}$$

Eqs. (16) and (17) become

$$\begin{aligned} \partial e_{ij}'/\partial X_{ij}=L_0(P_{11}-P_{10}{}^2/P_{00})+\alpha\chi P_{10}{}^2/P_{00}{}^2,\\ \partial e_{ij}'/\partial X_{jk}=L_0(P_{12}-P_{10}P_{20}/P_{00})\\ +\alpha\chi P_{10}P_{20}/P_{00}{}^2, \end{aligned} \tag{34}$$

where $\chi=\partial J_p{}^0/\partial H$; $L_0(=-L)$ is determined as a function of H by (29), the second of Eqs. (33), and the magnetization curve at zero stress; α is 1 if the differentiation is at constant H, 0 if at constant J_p; and the P_{ij}'s are given by Eqs. (32).

The two Eqs. (33) give in parametric form the functional relation between the magnetostrictive strain components $e_{ij}{}'^0$ and the magnetization $J_p{}^0$ in the field direction. The parameter η runs from 0 at demagnetization to ∞ at pseudo-saturation ($j_p{}^0=\sum|l_i|/\sqrt{3}$). The magnetostrictive elongation in direction (v_1, v_2, v_3) is

$$e_v{}'^0=\textstyle\sum e_{jk}{}'^0 v_j v_k=2\kappa_2\sum v_j v_k t_j t_k/3, \tag{35}$$

and a similar formula holds for the magnetization-dependent part of the electrical resistivity. The magnetization components (see Eq. (4)) are given by

$$j_i{}^0=J_i{}^0/J_s=t_i/\sqrt{3}. \tag{36}$$

Eq. (35) may therefore be written

$$e_v{}'^0=2\kappa_2\textstyle\sum v_j v_k j_j{}^0 j_k{}^0=2\kappa_2 j^{0\,2}\sum v_j v_k\sigma_j\sigma_k, \tag{37}$$

where J^0 is the magnitude of $\mathbf{J}^0$ (not to be confused with the parallel component $J_p{}^0$), $j^0=J^0/J_s$,

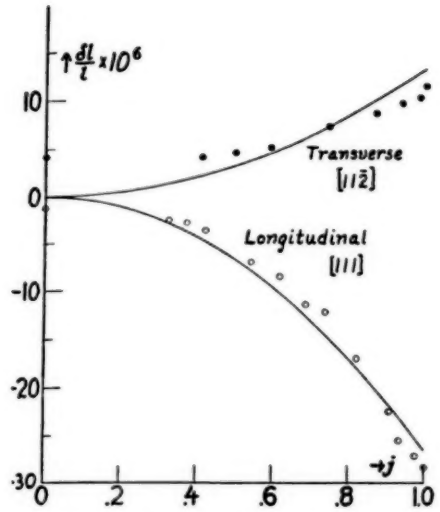

FIG. 2. Variation of longitudinal and transverse ([11$\bar{2}$]) magnetostriction with magnetization for nickel crystal magnetized in [111] direction. Points, experimental values of Mashiyama as plotted by Gans and v. Harlem. Curves, corrected formula. The curves have been fitted to the data by least squares with a single value of κ_2, 39.9×10^{-6}.

and the σ_i's are the direction cosines of the magnetization. This formula is useful only when it is known from symmetry considerations that the magnetization direction $(\sigma_1, \sigma_2, \sigma_3)$ coincides with the field direction (l_1, l_2, l_3). This is the case when the field is in one of the directions [100], [110], [111]; for these three cases, the right member of (37) reduces to

$$[100]\,0,\ [110]\,\kappa_2 j^{0^2} v_1 v_2,\ [111]\,2\kappa_2 j^{0^2}\textstyle\sum v_j v_k/3. \quad (38)$$

The first two of these agree with the formulas of Gans and v. Harlem, but in their [111] formulas[10] our factor j^{0^2} is replaced by $\frac{1}{2}[(8j^{0^2}+1)^{\frac{1}{2}}-1]$. The discrepancy is traceable to their erroneous assumption[11] that when the resultant magnetization is in the [111] direction, the same number of domains are magnetized in each of the directions $[\bar{1}11]$, $[1\bar{1}1]$, $[11\bar{1}]$ on the one hand, and in each of the directions $[1\bar{1}\bar{1}]$, $[\bar{1}1\bar{1}]$, $[\bar{1}\bar{1}1]$ on the other.

Figure 1 shows the improved agreement between theory and experiment obtained by using the corrected formula for the longitudinal resistivity.

[10] See Eq. (6) of their first paper and Eqs. (11), (12) of their second (reference 2). R. H. Fowler, *Statistical Mechanics*, second edition (1936), p. 520, gives correct formulas and curves for the longitudinal magnetostriction in these three special directions.

[11] See the third of Eqs. (5), first paper, reference 2.

The agreement with the data on longitudinal and transverse magnetostriction is less satisfactory (see Fig. 2), but still constitutes an improvement over the original formula.

The distribution functions n_σ do not occur explicitly in any of the present formulas; they may, however, be found from Eq. (9). Thus the fractional number of domains with magnetization along $(p_1/\sqrt{3}, p_2/\sqrt{3}, p_3/\sqrt{3})$ when the stresses are zero is given by

$$\begin{aligned} n^0{}_{p_1p_2p_3} &= [\exp(\eta\textstyle\sum l_i p_i)]/S \\ &= (1/S)\textstyle\prod_i(\cosh\eta l_i + p_i\sinh\eta l_i) \\ &= [1+\textstyle\sum p_i l_i + \sum p_i p_k l_i l_k \\ &\qquad + p_1p_2p_3 l_1 l_2 l_3]/8 \qquad (39) \\ &= [1+\sqrt{3}j^0\textstyle\sum p_i\sigma_i + 3j^{0^2}\sum p_i p_k \sigma_i\sigma_k \\ &\qquad + 3\sqrt{3}j^{0^3} p_1p_2p_3\sigma_1\sigma_2\sigma_3]/8. \end{aligned}$$

This reduces to formulas identical with those of Gans and v. Harlem[12] for the special case $\mathbf{J}\|[110]$, and it is identical with the formulas obtained from those of Akulov and Kondorsky[13] by setting the tension equal to zero. The present derivation shows however that the formula thus obtained is rigorous to all orders in the magnetization, and not merely a third-order approximation as might be expected from Akulov and Kondorsky's derivation.

Equations (34) give the variation of the effective elastic moduli s_{ij}' of the crystal with magnetization. We see that the tension-elongation moduli are unaffected by the magnetization, but that the relations between shearing stress and shearing strain are altered: the field destroys the cubic symmetry and leads to relations of the more general type

$$e_{12} = s_{66}'X_{12} + s_{64}'X_{23} + s_{65}'X_{31}.$$

In (34), α is to be set equal to 1 if the moduli are measured by a static method. The same equations with $\alpha=0$ give the values when the direction of the field and the component of magnetization (and hence approximately of flux density) in this direction remain constant during the strain. This will be the case, in a dynamic measurement of the elastic moduli, only if the

[12] First paper, Eqs. (5), reference 2.

[13] Akulov and Kondorsky, Zeits. f. Physik **85**, 661 (1933), Eq. (22).

field-direction and the stress system have such symmetry with respect to the crystal axes that the magnetization and the field are in the same direction even during the strain. This condition can be satisfied by utilizing the longitudinal vibrations of a thin crystalline cylinder with cylinder axis in one of the orientations [100], [110], [111]. In general, however, the values at constant *vector* magnetization must be obtained by means of Eq. (20).

Since experimental data are not available, it is not yet possible to test these theoretical conclusions in regard to the elastic properties of ferromagnetic crystals. When experiments of this nature are undertaken, it should be remembered that the theory takes no account of magnetic hysteresis, and that therefore the use of the actual magnetization curve may lead to erroneous results. Since the stress-strain relations are themselves nearly reversible,[7] it seems plausible that so far as these are concerned the actual specimen may be equivalent to a reversible specimen whose differential susceptibility, at any magnetization, is equal to the *reversible* susceptibility[14] of the actual specimen. This, as well as the usual magnetization data, should therefore be determined for the specimens used in the elastic measurements.

The theory should apply rigorously to data obtained anhysteretically: that is, by shaking the specimen into its most stable state before each reading. This is usually accomplished by applying an alternating magnetic field and gradually reducing it to zero. The writer has found, however, that in obtaining anhysteretic magnetization curves it is safer not to rely on a single reduction of this sort, but to vary the alternating field rapidly between zero and its maximum value, several times, in order to insure the penetration of the field to the interior of the specimen. In order that the data may be truly anhysteretic, it is of course necessary that this procedure be followed whenever either field or stress is changed; *vibrations* at a point on the anhysteretic magnetization curve will not give an anhysteretic value of Young's modulus.

[14] R. Gans, Physik. Zeits. **12**, 1053 (1911); Ann. d. Physik **61**, 379 (1920); P. Debye, *Handbuch der Radiologie* (1925), Vol. 6, 721.

We shall now use the results already obtained to derive formulas corresponding to those of Akulov and Kondorsky for the ΔE effect at low magnetizations.

Third-Order Approximation

We assume that the magnetization components J_i^0 under zero stress are known as functions of the field components H_i, to the fourth order. The assumed functional relations are subject to three types of restriction: (a) those imposed by thermodynamics; (b) those imposed by the cubic symmetry; (c) the restriction, already mentioned, that Eqs. (36) with $i=1, 2, 3$ must yield a unique value of η. The thermodynamic conditions may be satisfied by deriving the J_i's from the thermodynamic potential $F=F_{H,\ \chi=0}$, which must be expressed to the fifth order in the H_i's. The cubic symmetry then requires that this be in the form

$$-F=\tfrac{1}{2}\chi_0 H^2+\tfrac{1}{4}\chi_1 H^4+\tfrac{1}{4}\chi_2\sum H_i^4,$$

where the χ's are constants. Hence

$$\begin{aligned} J_i^0 &= -\partial F/\partial H_i = H_i[\chi_0+(\chi_1 H^2+\chi_2 H_i^2)] \\ &= H l_i[\chi_0+(\chi_1+\chi_2 l_i^2)H^2]. \end{aligned} \tag{40}$$

By expansion of the hyperbolic tangent to the fourth order in η, we get from Eq. (36)

$$J_i^0=(J_s/\sqrt{3})\eta l_i(1-\eta^2 l_i^2/3). \tag{41}$$

If we equate the right members of (40) and (41) and solve for η to the fourth order in H, the result, by restriction (c), must be the same for $i=1$, 2, and 3. This requires

$$\chi_2=-\chi_0^3/J_s^2; \tag{42}$$

then

$$\begin{aligned} \eta &= (\sqrt{3}\chi_0 H/J_s)[1+(\chi_1/\chi_0)H^2], \\ J_i^0 &= H_i[\chi_0+\chi_1 H^2-(\chi_0^3/J_s^2)H_i^2], \\ J_p^0 &= \sum J_i^0 l_i = H[\chi_0+(\chi_1-\chi_0^3\textstyle\sum l_i^4/J_s^2)H^2]. \end{aligned} \tag{43}$$

In terms of j_p^0 we have

$$\begin{aligned} \eta &= \sqrt{3}\, j_p^0[1+(\textstyle\sum l_i^4) j_p^{0^2}], \\ L_0 &= (3\chi_0/J_s^2)[1+(\chi_1 J_s^2/\chi_0^3) j_p^{0^2}]. \end{aligned} \tag{44}$$

From (33) and (34) we now get, to the third order in j_p^0,

$$e_{ij}'^0=2\kappa_2 l_i l_j j_p^{0^2},$$

$$\left(\frac{\partial e_{ij}'}{\partial X_{ij}}\right)_H=\frac{4\kappa_2^2\chi_0}{3J_s^2}\left\{1+\frac{\chi_1 J_s^2}{\chi_0^3}j_p^{0^2}\right\},$$

$$\left(\frac{\partial e_{ij}'}{\partial X_{jk}}\right)_H=\frac{4\kappa_2^2\chi_0}{J_s^2}l_i l_k j_p^{0^2},\qquad(45)$$

$$\left(\frac{\partial e_{ij}'}{\partial X_{ij}}\right)_{J_p}=\frac{4\kappa_2^2\chi_0}{3J_s^2}\left\{1-\left(12l_i^2l_j^2-\frac{\chi_1 J_s^2}{\chi_0^3}\right)j_p^{0^2}\right\},$$

$$\left(\frac{\partial e_{ij}'}{\partial X_{jk}}\right)_{J_p}=\frac{4\kappa_2^2\chi_0}{J_s^2}l_i l_k(1-4l_j^2)j_p^{0^2}.$$

Although these results have been written for convenience in terms of j_p^0, they can be expressed in terms of H by replacing j_p^0 by $\chi_0 H/J_s$. The corresponding formulas when the magnetization components are the independent variables are

$$e_{ij}'^0=2\kappa_2\sigma_i\sigma_j j^2\quad(j=J/J_s),$$

$$\left(\frac{\partial e_{ij}'}{\partial X_{ij}}\right)_J=\frac{4\kappa_2^2\chi_0}{3J_s^2}\left\{1-\left[3(\sigma_i^2+\sigma_j^2)-\frac{\chi_1 J_s^2}{\chi_0^3}\right]j^2\right\},\qquad(46)$$

$$\left(\frac{\partial e_{ij}'}{\partial X_{jk}}\right)_J=0.$$

These may be obtained by use of Eq. (20); or they may be derived from Eqs. (45) by first writing the complete expression for e_{ij}' to the third order in the H_i's and to the first order in the stresses, and then substituting for H_i its value to the second order in the J_i's and to the first in the stresses. This is obtained by inversion of the formula

$$J_i=\chi_0 H_i+c(H_j X_{ij}+H_k X_{ik}),$$

where

$$c=\frac{1}{H_j}\left(\frac{\partial J_i}{\partial X_{ij}}\right)_H=\frac{1}{H_j}\frac{\partial e_{ij}'^0}{\partial H_i}=\frac{2\kappa_2}{J_s^2}\chi_0^2.\qquad(47)$$

From the formulas just given, we can derive the following formulas for the elongation e_v' in direction (v_1, v_2, v_3) when the stress-system consists merely of a tension T in the same direction $(X_{ij}=v_i v_j T)$:

$$e_v'^0=2\kappa_2 j_p^{0^2}\sum l_j l_k v_j v_k,$$

$$\left(\frac{\partial e_v'}{\partial T}\right)_H=-\frac{4}{3}\frac{\kappa_2^2\chi_0}{J_s^2}\sum v_j^2 v_k^2+\frac{4\kappa_2^2\chi_0}{J_s^2}j_p^{0^2}\times\left[2\sum v_i^2 v_j v_k l_j l_k+\frac{1}{3}\frac{\chi_1 J_s^2}{\chi_0^3}\sum v_j^2 v_k^2\right].\qquad(48)$$

In $(\partial e_v'/\partial T)_{J_p}$, the quantity in square brackets is replaced by

$$[2\sum v_i^2 v_j v_k l_j l_k-4\sum l_j^2 l_k^2 v_j^2 v_k^2-8\sum l_i^2 l_j l_k v_i^2 v_j v_k+\tfrac{1}{3}(\chi_1 J_s^2/\chi_0^3)\sum v_j^2 v_k^2].\qquad(49)$$

If the magnetization components are taken as independent variables, we have

$$e_v'^0=2\kappa_2 j^2\sum\sigma_j\sigma_k v_j v_k,$$

$$\left(\frac{\partial e_v'}{\partial T}\right)_J=-\frac{4}{3}\frac{\kappa_2^2\chi_0}{J_s^2}\sum v_j^2 v_k^2-\frac{4\kappa_2^2\chi_0}{J_s^2}j^2\times\left[\left(1-\frac{1}{3}\frac{\chi_1 J_s^2}{\chi_0^3}\right)\sum v_j^2 v_k^2-\sum\sigma_i^2 v_j^2 v_k^2\right].\qquad(50)$$

The last formula should agree with that of Akulov and Kondorsky. In their formula, however, the quantity $-\sum\sigma_i^2 v_j^2 v_k^2$ is replaced by $+2\sum v_i^2 v_j v_k\sigma_j\sigma_k$. The difference appears to be due to the omission of terms in the tension, in certain of their formulas in which such terms should be present: particularly in the assumed relation between the J_i's and the H_i's, where no account is taken of the effect of the tension upon the magnetization curve.

The formulas to be used when the direction of the tension coincides with that of the field or of the magnetization are obtained by setting $v_i=l_i$ in (48–49) or $v_i=\sigma_i$ in (50). It is easily verified that (49) and (50) then lead to identical results when this direction is [100], [110], or [111].

Polycrystalline Nickel

Before averaging for polycrystalline material, we must decide which quantities are to be assumed constant during the stress, and also which quantities are to be assumed uniform from crystal to crystal. In the dynamical measurement of Young's modulus, it is the value at constant B that is measured; this however differs inappreciably from the value at constant J. This con-

stancy of flux density is due to macroscopic eddy currents, whose field neutralizes the tendency of the stress to change the flux density. It is evident from the relation $\partial J/\partial T=\partial e_v/\partial H$ and from (50) that this neutralization cannot be exact in each crystal: only the *average* magnetization remains constant. We therefore average (48) at uniform H and then use, for the polycrystalline material as a whole, the relation

$$\left(\frac{\partial e_v}{\partial T}\right)_J=\left(\frac{\partial e_v}{\partial T}\right)_H-\left(\frac{\partial e_v}{\partial H}\right)_T^2\Big/\chi. \quad (51)$$

This gives, when the tension is in the field direction,

$$e_v'^0=2\kappa_2 j^{0^2}/5, \quad (52)$$

$$\left(\frac{\partial e_v'}{\partial T}\right)_H=\frac{4}{15}\frac{\kappa_2^2\chi_0}{J_s^2}\left[1+3j^{0^2}\left(\frac{2}{7}+\frac{1}{3}\frac{\chi_1 J_s^2}{\chi_0^3}\right)\right], \quad (53)$$

$$\left(\frac{\partial e_v'}{\partial T}\right)_J=\frac{4}{15}\frac{\kappa_2^2\chi_0}{J_s^2}\left[1-3j^{0^2}\left(\frac{18}{35}-\frac{1}{3}\frac{\chi_1 J_s^2}{\chi_0^3}\right)\right]. \quad (54)$$

(It is no longer necessary to distinguish between j_p^0 and j^0.) The value of the derivative at constant B may be found by a similar method; it differs from the last expression only in that the fraction 18/35 is multiplied by $(1-5\epsilon/9)/(1+\epsilon)$, where $\epsilon=1/4\pi\chi_0\doteq 0.004$. This justifies the statement made above, that these two values differ inappreciably.

Equation (54) agrees with the formula of Akulov and Kondorsky in the constant term, and therefore leads to the same formula for the total change of Young's modulus between demagnetization and saturation. The term in j^{0^2}, however, has 18/35 where their formula has 9/7. Neglecting the term in χ_1, we get, in terms of the saturation magnetostriction λ_{111} in the [111] direction,

$$\begin{aligned}(E_\infty-E_0)/E_0&=a/(1-a),\\ (E-E_0)/E_0&=54aj^{0^2}/35,\end{aligned} \quad (55)$$

where E_0, E, E_∞ are, respectively, the values of Young's modulus when $J=0$, J, J_s, and

$$a=3\lambda_{111}^2\chi_0 E_0/5J_s^2. \quad (56)$$

We see that the ratio of $(E_\infty-E_0)/E_0$ to the coefficient of j^{0^2} in $(E-E_0)/E_0$ should be approximately equal to 35/54, or 0.65, instead of the value $7/27=0.26$ predicted by the original theory. The observed ratio in Siegel's experiments[6] was 0.67. The new formula therefore removes satisfactorily the discrepancy between theory and experiment.

It is to be noted that the term in j^{0^2}, which in (54) is opposite in sign to the constant term, in (53) has the same sign. This means that, while Young's modulus at constant J increases steadily from demagnetization to saturation, the value at constant H should *decrease* when small fields are applied. This explains the apparent discrepancy between Siegel's results, in which a steady increase of E is observed, and the older results of Honda and Terada[15] (obtained by a static method), in which E first decreases, and subsequently increases. It may be remarked (see Eqs. (45)) that this initial decrease results from the appearance of effective elastic constants s_{45}', s_{56}', and s_{64}' in the (elastically) very anisotropic state ensuing when the crystal is slightly magnetized. As saturation is approached, all such effects disappear, and the crystal returns to cubic symmetry, with a higher value of Young's modulus than in the demagnetized state.

The writer plans in subsequent papers to apply the theory to iron crystals, and to polycrystalline material in the manner indicated in the introduction; also to suggest a thermodynamic interpretation of the theory, and to show its relation to Gans's theory[14] of reversible susceptibility. He wishes to acknowledge his indebtedness to Professor S. L. Quimby for helpful suggestions and criticisms made after reading the first draft of this paper.

[15] K. Honda and T. Terada, Phil. Mag. **13**, 36 (1907).

Static Universe and Nebular Red Shift

S. SAMBURSKY
The Hebrew University, Jerusalem, Palestine
(Received March 10, 1937)

Hubble's recent nebular counts have brought the question of a static universe into the forefront. The red shift of the nebulae in a static universe can be explained if instead of postulating a growing world radius we proceed on the assumption of a shrinkage of the universal lengths of atomic physics, this being equivalent to a decrease with time of the quantum of action. A new quantity, $\dot{h}$, is thereby defined and, if introduced into the Dirac equation of the electron, leads to gravitation. The consequences of this connection and other features of the theory are discussed and compared with experience.

1

HUBBLE'S systematic nebular counts and his subsequent discussion of the consequences which follow for the various cosmological theories[1] give rise to grave doubts regarding the validity of the conception of an expanding universe. The uniform spatial distribution of nebulae up to a distance of about $1.6 \cdot 10^8$ parsecs suggests the idea of a static universe and reopens the question as to the physical causes of the red shift.

Before going into this question let us again regard the models of a closed world with an increasing radius R and try to determine the meaning of the assertion "the radius of the world increases with time." According to Laue[2] all bodies participate in the expansion, every material area being proportional to R^2. That would mean that the question of the dependence of the world radius on time could in principle be answered only by physical observation of processes in other parts of space (which for practical purposes must be at a very large distance from the observer), e.g., nebular distribution, Doppler effects and by considering certain statements capable of being proved by experiment with regard to the propagation of light in an expanding universe. On the other hand, according to this view, no answer could be obtained regarding the question of expansion by measuring physical processes at different times at one and the same point of space, seeing that together with every element of space its physical substance also undergoes a similarity transformation.

As against this the question must be asked whether the assertion "the radius of the world increases with time" does not in principle involve the existence of a constant, reproducible standard of length, compared with which R, or the distance between two nebulae, increases as time goes on. Such a standard of length cannot be looked for within the framework of the theory of relativity, which does not contain any assumption regarding the physical nature of matter, or, to be more exact, its atomistic structure. On the other hand, the universal lengths of atomic physics and the quantum theory are to be regarded as standard units to which the increase of R stands in relation. In other words, the assertion that R increases can have a meaning only if R is measured in units of the radius of the electron e^2/mc^2 or the Compton wave-length h/mc or the radius of the hydrogen atom in its ground state $h^2/(4\pi^2me^2)$. If, however, one accepts this relation to a standard length, the above mentioned assertion can also be formulated as follows: "Expressed as fractions of the constant world radius R, the radius of the electron and the other universal lengths shrink with time." This assertion is equivalent to the above one; it has, however, the advantage of postulating a static cosmos which is in accordance with Hubble's nebular counts. The dynamics of expansion are transferred into the dimensions of atomistic phenomena where expansion appears as its reverse-shrinkage.

Now it is well known that the atomistic quantities of the dimension of a length are re-

[1] Nature **138**, 1001 (1936).
[2] Laue, Berl. Ber. 1931, 123; Zeits. f. Astrophys. 208 (1936).

ductible to the two universal lengths e^2/mc^2 and $\hbar/mc$, the quotient of which represents the fine structure constant $\alpha=2\pi e^2/hc$. It can be said, therefore, that all these lengths are proportional to Planck's h, the main significance of which, as has often been pointed out,[3] lies in the introduction of a new standard of length into physics. We shall now try to interpret the shrinkage of the atomic standards of length as a decrease with time of the quantum of action. Assuming the velocity of light to remain constant and taking into consideration the fact that the dimensionless fine structure constant also must remain constant with time for reasons of quantum mechanical stability, it follows that the elementary quantum of electricity also undergoes a shrinkage in such a way that e^2 shrinks at the same rate as h.

We therefore postulate that a static universe with a quantum of action decreasing with time is equivalent to an expanding universe with a constant quantum of action. This equivalence does not, of course, signify an isomorphy of the two models; that is evident from the above mentioned fact that the first model correctly describes the observed constant nebular density, while the second finds itself in contradiction to this phenomenon. The new model must, however, describe those features of the expanding universe which relate to the propagation of light, particularly the nebular red shifts which increase with the distance. That it does do so is evident under the assumption that the energy $\epsilon=h\nu$ connected with every definite quantum process remains constant in time. The more remote the observed nebula is, the more remote in time therefore the quantum process which produced the light which we observe, the greater must have been Planck's h, the smaller therefore the emitted frequency. The propagation of light in empty space and its measurement at the point of observation, which in practice is carried out by dispersion or diffraction, can be described by means of the wave theory. And since the proper time of the light wave is zero, the emitted frequency ν is transmitted to us without undergoing any change; this frequency, as compared with that which is produced today by the respective quantum process, therefore displays a red shift.

The decrease with time of h can be calculated from Hubble's distance red shift relation of spiral nebulae. By differentiating $\epsilon=h\nu$ with respect of time we get

$$0=\dot{h}\nu+h\dot{\nu}$$

or
$$\dot{h}=-h\frac{\dot{\nu}}{\nu}=-h_0\frac{\dot{\nu}}{\nu_0}=-\frac{h_0}{\nu_0}\frac{\nu_0-\nu}{t_0-t}.$$

The indices refer to the present time. Furthermore we have

$$\nu=\nu_0(1-u/c),$$

where u is the radial velocity of the nebula and c the velocity of light. We, therefore, get

$$\dot{h}=-h_0\frac{u/c}{t_0-t}. \tag{1}$$

Because of the uncertainty in determining the distances of the nebulae, the velocity of expansion, as is well known, is known to us only with a low degree of accuracy. According to Ten Bruggencate[4] the error can be as great as 50 percent. Of late the value has been estimated as 560 km/(sec. 10^6 parsec). For reasons which will soon be clear to us we shall assume the true value to be about 14 percent lower, e.g. 485 km/(sec. 10^6 parsec). Then there follows from (1)

$$\dot{h}=-1.03\cdot10^{-43}\text{ erg}. \tag{2}$$

For obvious reasons a linear decrease of h makes no sense except as a first approximation, say for a period of 10^8 years. The true form of the function $h(t)$ can only be such that h vanishes asymptotically for $t=\infty$. We are not contradicted by experience if we assume an exponential decrease of h, i.e. $h=h_0\cdot e^{-\kappa t}$. The quotient $\kappa=\dot{h}/h$ is then a constant, i.e., the well-known Hubble factor.

2

The hypothesis of a static universe with shrinking quantum of action which replaces a constant by a decreasing physical quantity, however slow the decrease, can only be justified either by the discovery of new physical relations,

[3] B. Podolsky, Phys. Rev. **46**, 734 (1934); compare e.g., the quotation from L. L. Whyte mentioned there.

[4] Ten Bruggencate, Naturwiss. **24**, 609 (1936).

e.g., between quantum and cosmic phenomena or if it permits a simpler description of certain empirical facts.

The shrinkage of h could be proved, in principle, by measuring the wave-length of a spectral line, which is produced at the same point at two different times, since the decrease of h provides us with a new way for distinguishing the future from the past. The frequency of every spectral line is in the course of time shifted towards the violet. It can easily be shown that the wave-length of the red cadmium line would decrease within 350 years by one unit of the third decimal; in other words, we cannot, for the time being, count on this experimental proof.

It is possible to establish a relation between the new quantity $\dot{h}$ and gravitation, since the gravitational constant G can be shown to be proportional to $\dot{h}$. Since $\dot{h}$ has the dimension of an energy we must have

$$[G]=[l/m^2]\cdot\dot{h}.$$

The lengths as well as the masses must be atomic quantities. By assuming $\dot{h}$ to be equal (2) we in fact get

$$G=\frac{2\pi e^2\dot{h}}{M^2mc^2}, \tag{3}$$

where e is the charge of the electron, M and m the masses of the proton and the electron respectively and c the velocity of light. If one writes (3) in the form

$$\frac{GMm}{e^2}=\frac{2\pi\dot{h}}{Mc^2}, \tag{4}$$

it becomes evident that the relation of the gravitational energy of the hydrogen atom to its Coulomb energy which stands on the left side of the equation can be expressed by $\dot{h}$ and the rest energy of the atom.

The relation between G and $\dot{h}$ which is expressed in equations (3) and (4) can also be derived by introducing h as a function of time, and generally, by introducing the exponential shrinkage of all lengths into the quantum mechanical calculus and by correspondingly transforming the Dirac equation of the electron.[5] This operation yields an additional term for the energy of the system which can be interpreted, in accordance with (3) or (4), as the gravitational energy of the hydrogen atom. If we also take into account that Dirac's coefficients α_κ are now functions of the coordinates, and if we substitute for

$$\alpha_i\alpha_\kappa+\alpha_\kappa\alpha_i=2\delta_{i\kappa}$$

the more general relation $\alpha_i\alpha_\kappa+\alpha_\kappa\alpha_i=2g_{i\kappa}$, then the $g_{i\kappa}$ which results from the new α_κ yields the metric of the world which contains the shrinking hydrogen atom. The result is a hyperbolic world with the constant radius

$$R=hc/\dot{h}=1.9\cdot10^{27}\text{ cm}. \tag{5}$$

The value of (5) is in good agreement with the other values of R which have been obtained in different ways. From Eqs. (5) and (3) it can also be deduced that, if h is constant, gravitation vanishes and the finite curved universe degenerates into an infinite Euclidean space.

The attempt has often been made to establish relations between G and various combinations of the fundamental units of atomic physics. Stewart[6] makes the assumption that the red shift can be expressed by $\nu=\nu_0\cdot e^{-x/H}$ and gets the result that the length H which is identical with the world radius can easiest be expressed, with a 20 percent deviation from the experimental data, by the combination $H=e^6/(hGm^3c^3)$. The fact that the introduction of $\dot{h}$ permits the so much simpler relation (3) or (5), is an argument in favor of the reality of $\dot{h}$.

3

The relation between $\dot{h}$ and gravitation leads to further consequences which are susceptible of experimental proof. According to (3) G is not a constant, but, since it is proportional to e^2 and $\dot{h}$, a quantity which decreases with h^2. If one considers that the effect of the gravitational forces upon the dynamics of the creation of stars and stellar systems is determined by the product GM, where M is the mass of the system,

[5] This calculation and the following ones in which I was greatly aided by Mr. M. Schiffer, with whom I also had many valuable discussions of the problem, will be given more fully in a separate paper.

[6] Stewart, Phys. Rev. **38**, 2070 (1931).

it becomes obvious that, on the basis of an average value for GM, the masses of those stars which originated earlier must have been smaller in the proportion in which G was greater. The most reliable data on stellar masses have been obtained by the observation of binary stars. Nernst[7] has recently investigated the statistical material relative to about 60 binary stars. In doing so he makes two assumptions which today are shared probably by most astrophysicists: 1. The Russell diagram is a purely evolutionary diagram; 2. The duration of life of a star is approximately 10^{10} years. Nernst arrives at the result that in the course of their development the stars lose considerably more of their mass than can be accounted for by radiation, on the basis of Einstein's law of equivalence. According to Table II[7] this decrease in mass is about 100 : 1 in 10^{10} years, compared with which the relativistic decrease is negligible.

On the basis of the above considerations, the "nonrelativistic" decrease in mass can now be explained in the simplest way. Taking a mean GM as a basis, the older binary stars were characterized by a larger G, and therefore must have had a smaller mass. Numerical calculations lead to a satisfactory agreement with the data given by Nernst from a qualitative point of view, and for a period of 10^8 years there is also quantitative agreement.

As regards the influence of the expansion of the universe on the luminosity of distant sources of light which is dealt with by Laue in the above mentioned papers, there is no difficulty in tracing its analog within the framework of our theory, if one assumes the sources of light (nebulae) to be black radiators. The constant of Wien's law of displacement $\lambda_{max} \cdot T = \text{const}$ is, as is well known, proportional to h and therefore decreases continuously. The wave-length λ_{max} of a nebula of a certain effective temperature therefore undergoes a shift towards the red in proportion to its distance from us and at the same time its luminosity is changed in such a way as though it belonged to an object the temperature of which was smaller by the factor $e^{\varkappa t}$.

The energy density u of a nebula is proportional to T^4, where T is its effective absolute temperature. The factor of proportionality, according to Planck's law, is inversely proportional to h^3. We, therefore, get

$$u/\nu^3 = \text{const.} \tag{6}$$

Against this increase in the energy density of radiation with time, there is a decrease in the gravitational energy of the cosmic masses (decrease of G), which probably has its origin in the reciprocal action of both energies in the nebulae; the increase of the one is compensated by the decrease of the other. The energy of radiation undergoes no change during its propagation, while in an expanding universe it decreases on its way through space in the measure in which it participates in the expansion.

It has already been pointed out that the assumption of a shrinking h entails a new physical criterion for distinguishing the future from the past. Of two states of the universe the one with the smaller h is to be regarded as the later. Without any doubt there is a connection between this criterion and the entropy law. At any rate, there is no contradiction between the two. The entropy constant of an ideal monoatomic gas, e.g., is proportional to $\log 1/h^3$. For this reason the entropy of a gas of this kind increases in a static universe with decreasing h, even if it is subject only to reversible changes of state.

The question of how far the hypothesis whose fundamentals have been outlined here is tenable and capable of being developed further, depends not only on its compatibility with experience but also to a very high degree on the progress of quantum mechanics and quantum electrodynamics, and in particular on the possibility of a more exact treatment of the many-electron problem within the framework of Dirac's theory.

[7] Nernst, Zeits. f. Physik **97**, 511 (1935).

The Lattice Energies and Transition Temperatures of Caesium Chloride and Ammonium Chloride*

ALBERT MAY
The Catholic University of America, Washington, D. C.
(Received May 27, 1937)

The lattice energies of CsCl and NH_4Cl are calculated for both the CsCl type and NaCl type lattices, and the temperatures of transition between these two crystal forms determined from the equality of the free energies. This requires the computation of the elastic constants and proper frequencies. In determining the lattice energies, use is made of the method of Born and Mayer, four constants in the lattice energy expression being evaluated from experimental data. To obtain results consistent with known lattice constants, compressibilities and heats of transition, it is found necessary to multiply the van der Waals constants derived by Mayer by about 3.5 and to make the constant coefficient in the repulsion term for nearest like ions about 0.6 that for nearest (unlike) ions. Some success is attained in computing transition temperatures comparable with those known from experiment, but the temperature dependence found for the proper frequencies appears to be faulty.

INTRODUCTION

EXPERIMENT shows that at normal temperatures CsCl and NH_4Cl are stable in the CsCl type lattice, which is body-centered, and at higher temperatures in a simple lattice of the NaCl type. The transition temperatures are 184.3°C for NH_4Cl,[1] and about 445°C for CsCl.[2]

According to thermodynamics the form with the lowest free energy is stable. At low temperatures the free energy is practically equal to the total energy or to the negative lattice energy, $-U$, plus the zero point energy of the vibrations, so that at such temperatures the stable form is that which has the highest lattice energy. The stability of another form at higher temperatures requires that it have the lower free energy at those temperatures or, essentially that it have a higher entropy.

The free energy calculations require a knowledge only of the difference of lattice energies in the two forms and of the proper frequencies (acoustic and optical) of the lattices. To determine the difference of lattice energies, the shape of the potential energy curve must be known. The calculation of the frequencies requires also the computation of the elastic constants.

The lattice energy of the normally stable body-centered type has been calculated for NH_4Cl by Bleick[3] and for CsCl by Huggins and Mayer.[4] Born and Mayer,[5] Wasastjerna[6] and Jensen[7] have compared the lattice energies of the body-centered and simple lattice types of CsCl and have thus investigated the stability. Since none of these comparisons has resulted in the proper stability, the lattice energies have been recalculated. Apparently no previous attempt has been made to determine theoretically the temperature of transition.

LATTICE ENERGIES

In calculating the lattice energy, U, as a function of the lattice constant, r_0, that is, the smallest distance between ions in the lattice, Huggins and Mayer[4] and Bleick[3] have used the form

$$-U+\tfrac{1}{2}h\nu_0=\Phi(r_0)=-\alpha\epsilon^2/r_0-C/r_0^6 \\ -D/r_0^8+B(r_0)+\tfrac{1}{2}h\nu_0. \quad (1)$$

The five terms included are, respectively: the electrostatic energy, the energies of the dipole-

* A dissertation submitted in partial fulfillment of the requirements of the Ph.D. degree at The Johns Hopkins University.

[1] P. W. Bridgman, Am. Acad. Proc. **52**, 91 (1916); F. E. C. Scheffer, Proc. Roy. Acad. Sci. Amsterdam **18**, 446 (1915).

[2] G. Wagner and L. Lippert, Zeits. f. physik. Chemie **31B**, 263 (1936); S. Zemczuzny and F. Rambach, Zeits. f. anorg. allgem. Chemie **65**, 403 (1910).

[3] W. E. Bleick, J. Chem. Phys. **2**, 160 (1934).

[4] M. L. Huggins and J. E. Mayer, J. Chem. Phys. **1**, 643 (1933).

[5] M. Born and J. E. Mayer, Zeits. f. Physik **75**, 1 (1932).

[6] J. A. Wasastjerna, Soc. Scient.-Fennica, Comm. Phys.-Math. vol. 8 No. 21 (1935).

[7] H. Jensen, Zeits. f. Physik **101**, 164 (1936).

TABLE I. *Constants which depend only on the lattice type.*

	Type of Lattice	
	CsCl	NaCl
α	1.7627	1.7476
S_6'	8.7088	6.5952
S_6''	3.5445	1.8067
S_8'	8.2077	6.1457
S_8''	2.1476	0.8001
M	8	6
M'	6	12
a	1.1547	1.4142
Δ	$(2r_0/\sqrt{3})^3$	$2r_0^3$

dipole and dipole-quadrupole van der Waals interactions, the repulsion component and the zero point energy of the vibrations. e is the electronic charge. The values of Madelung's constant, α, for the two lattice types involved are given in Table I.

The van der Waals constants C and D are of the forms[8]

$$C=S_6'c_{+-}+S_6''(c_{++}+c_{--})/2;$$
$$D=S_8'd_{+-}+S_8''(d_{++}+d_{--})/2$$

where the S's are numbers depending on the type of lattice and the c's and d's are constants characteristic for the interaction of a pair of ions. Table I lists the values of S obtained from the summations of Jones and Ingham.[9]

While the van der Waals terms constitute only a small part of the total energy, they change rapidly with variation of the lattice separation and are important for considerations of stability.

In this paper the constants c and d are, at first, given the values derived by Mayer[8] for CsCl from optical data, and by Bleick[3] for NH_4Cl. They are listed in Table II. The values of c obtained by Mayer for CsCl are considerably higher than those previously given by Mayer and Helmholz.[10]

It is assumed that the repulsion energy between two ions has the form $be^{-r/\rho}$ as given by Born and Mayer.[5] Because of the rapid decrease of the exponential form with increase of separation, it is necessary to include only the repulsion between a given ion and those ions nearest to it (unlike ions) and those at the next smallest distance (like ions). These we shall call first and second neighbors of that ion. The complete form assumed for the repulsion component, $B(r_0)$, will be considered in detail later.

The constants b and ρ can be evaluated if the compressibility, β, and lattice constant, r_0, are known, by forming the first and second derivatives of Eq. (1) with respect to r_0,

$$r_0\frac{\partial\Phi}{\partial r_0}=\frac{\alpha e^2}{r_0}+\frac{6C}{r_0^6}+\frac{8D}{r_0^8}+r_0\frac{\partial B}{\partial r_0}=R, \tag{2}$$

$$-r_0^2\frac{\partial^2\Phi}{\partial r_0^2}=\frac{2\alpha e^2}{r_0}+\frac{42C}{r_0^6}+\frac{72D}{r_0^8}-r_0^2\frac{\partial^2 B}{\partial r_0^2}=-S, \tag{3}$$

where, at absolute zero, $R=0$ and $S=9V/N\beta$. Since r_0 and β are not known at absolute zero, Born and Mayer derived the expressions

$$R=\frac{3T}{N\beta}\left(\frac{\partial V}{\partial T}\right)_P, \tag{2'}$$

$$S=\frac{9V}{N\beta}\left[1+\frac{T}{\beta}\left(\frac{\partial\beta}{\partial T}\right)_P+\frac{T}{\beta^2V}\left(\frac{\partial V}{\partial T}\right)_P\left(\frac{\partial\beta}{\partial P}\right)_T+\frac{2}{3}\frac{T}{V}\left(\frac{\partial V}{\partial T}\right)_P\right]. \tag{3'}$$

V is the mole volume; N, Avogadro's number; and P the pressure. With these expressions, the values at temperature T are used for all quantities occurring in (2) and (3). The calculations reported in this paper, except where otherwise noted, were made for 273°K.

At the temperatures involved, the classical value has practically been reached by the specific heats and therefore the heat energies have absorbed the zero point energies and become equal for the two lattice types. Since we shall be concerned primarily only with the difference of the energies in the two forms, the heat energy, and consequently the zero point energy, has been dropped.

The compressibility data for NH_4Cl were calculated from information supplied by Professor P. W. Bridgman to supplement that published[11] and the volume-temperature coefficient for CsCl was computed from the measurements of Wagner and Lippert.[12] All other quantities occurring in (2') and (3') have been taken from Huggins and

[8] J. E. Mayer, J. Chem. Phys. **1**, 270 (1933).
[9] E. Jones (Lennard-Jones) and A. E. Ingham, Proc. Roy. Soc. **A107**, 636 (1925).
[10] J. E. Mayer and L. Helmholz, Zeits. f. Physik **75**, 19 (1932).
[11] P. W. Bridgman, Phys. Rev. **38**, 182 (1931).
[12] Wagner and Lippert, reference 2.

Mayer and from Bleick. These data are listed in Table II.

The lattice constants of the body-centered and simple lattice types have been measured for both CsCl[12] and NH_4Cl,[13] but not at 273°. For the body-centered type we have only to correct for the change between room temperatures and 273°, but values for the simple lattices are available only at high temperatures and the thermal expansion coefficients are not known. The values given in Table II are approximations obtained by extrapolating from the measured data by means of the expansion coefficients of the body-centered type.

We shall write

$$B(r_0)=b_1Me^{-r_0/\rho}+b_2M'e^{-ar_0/\rho}, \qquad (4)$$

so that

$$r_0\partial B/\partial r_0=-(r_0/\rho)(b_1Me^{-r_0/\rho}+b_2aM'e^{-ar_0/\rho}) \qquad (5)$$

and

$$r_0^2\partial^2 B/\partial r_0^2=(r_0^2/\rho^2)(b_1Me^{-r_0/\rho}+b_2a^2M'e^{-ar_0/\rho}). \qquad (6)$$

The two terms represent the interactions with first and second neighbors and b_1 and b_2 are the corresponding values of b. M and M' are the numbers of first and second neighbors of an ion, and a is the ratio of the distances of second and first neighbors. Values of M, M' and a, which depend only on the type of lattice, are given in Table I.

It is to be expected that b will vary with the ions involved, so that it has been customary to introduce the two constants b_+ and b_-, one for each type of ion, and in place of b, to write b_+b_-, b_+b_+, or b_-b_- for interactions between two unlike ions, two positive ions or two negative ions, respectively. Then $b_1=b_+b_-$ and $b_2=(b_+b_++b_-b_-)/2$. Since there are now three unknowns, b_+, b_- and ρ, their evaluation requires the use of a third known quantity, in addition to the compressibility and lattice constant of the body-centered type at 273°. Born and Mayer[5] have used the experimentally determined "ionic radii" of Goldschmidt,[14] and Huggins and Mayer[4] and Bleick[3] have assumed ρ to have the average value, 0.345×10^{-8} cm, found for the alkali halides by Born and Mayer. For CsCl and NH_4Cl, Huggins and Mayer[4] and Bleick[3] have found b_+ and b_- to be only slightly different and the use of a single value of b appears entirely justified. Hence we shall, at first, assume that $b_1=b_2$.

b and ρ were determined for both salts from the compressibilities and lattice constants with Eqs. (2) and (3) for the body-centered type. Higher lattice energies were found for the NaCl type than for the CsCl type lattice for both salts and the former type should therefore be stable. This is contrary to experience. The values obtained are given in Table II under the heading "Original Data."

The conviction expressed by Mayer[8] that the van der Waals constants used provide stability for the body-centered form of CsCl is not confirmed. Born and Mayer,[5] starting with the smaller van der Waals constants already mentioned,[10] obtained the proper stability by an arbitrary doubling of the van der Waals energy but neglected the large effect of this change on the repulsion constants.

The fact that expression (1) fails to give the proper differences of lattice energies, may be due to the incorrect form of some of the terms as functions of r_0, to an inaccurate determination of the constants or to the omission of important components. The error is, of course, greatly magnified by taking small differences between large quantities.

The repulsion term should certainly be of more complicated form than that used. Wasastjerna[6] has attempted to arrive at a suitable form empirically, but has not obtained stability of the proper lattice type for CsCl. This he ascribes not to the incorrectness of the form used for the repulsion energy of individual ions, but to failure of additivity of the contributions of these pairs to the repulsion, when many ions are accumulated in a lattice. This would indicate the need, with the expression for the repulsion which he uses, for an additional term having a strong dependence on the lattice type, or for an equivalent modification of the form employed for the repulsion energy.

Jensen[7] has determined the lattice energies quantum mechanically, the repulsion being cal-

[12] G. Bartlett and I. Langmuir, J. Am. Chem. Soc. **43**, 84 (1921).

[14] V. M. Goldschmidt, Skrifter Norske Videnskaps Akad. Oslo, No. 2 (1926), No. 8 (1927); Fortschr. d. Min. **15**, 73 (1931).

culated, without an empirical evaluation of constants, by Fermi statistics. He also found the simple lattice type stable for CsCl.

Since the method described, employing only two unknowns, b and ρ, failed to yield the proper stability, an attempt was next made to improve the results by increasing the number of constants that could be varied.

As mentioned before, the difference of lattice energies may, with sufficient accuracy, be assumed equal to the heat of transition at the equilibrium temperature. Experimentally determined values of the heats of transition for CsCl and NH_4Cl are given in the *International Critical Tables* and these are listed as "$\Delta\Phi$ kcal./mole (meas.)" in Table II.

This was now used to permit the evaluation of a third constant, a numerical factor inserted in both parts of the van der Waals energy and, of course, the same for both lattice types. It was found that the factors required to give the proper heat of transition for CsCl and NH_4Cl are 7 and 8.5, respectively. It is improbable that the van der Waals energies can be as large as these factors indicate.

More reasonable results are secured by changing the magnitude of the van der Waals terms and also admitting different coefficients in the repulsion terms of the first and second neighbors (that is, $b_1 \neq b_2$) without changing the form of any term. In order to determine the four constants now available, an additional relation was obtained by using the lattice constant of the NaCl lattice type at absolute zero in Eq. (2). A linear extrapolation from the known values of the lattice constant of the NaCl type lattice at high temperatures by means of the expansion coefficient of the body-centered type, gives 3.372×10^{-8} cm for CsCl and 3.184×10^{-8} cm for NH_4Cl and it was assumed that the correct values might be slightly higher than these.

It was found necessary to multiply the quantities c and d given in Table II, under the heading "Original Data," by factors of 3.6 and 3.5 for CsCl and NH_4Cl, respectively, and to assign values of 0.70 and 0.55 to the ratio b_2/b_1, the fraction by which the coefficient in the repulsion term for the first neighbors must be multiplied to obtain the coefficient for the second neighbors. The results for the two salts are rather similar, but the van der Waals factors are unsatisfactorily large. The complete results are given in Table II under the heading of "Adjusted" data.

By quantum mechanical methods, Neugebauer and Gombas[15] found the principal part of the polarization energy and the first van der Waals component for CaCl to be almost identical in magnitude as well as form. In the method we have used, such a polarization energy would be indistinguishable from the van der Waals energy and the value derived for C would be twice its true value. It is quite possible that for CsCl and NH_4Cl the polarization energy may be large enough to explain completely the large values found for C and D.

Wasastjerna[16] has neglected the repulsion contribution of the second neighbors as inconsiderable based on the empirical expression which he derived for the repulsion energy. If, in the process described using four unknowns, we drop the repulsion of the second neighbors, i.e., set $b_2=0$, we can, of course, still obtain the proper heat of transition, but for both salts, the equilibrium lattice constant of the simple lattice type at absolute zero is found to be unreasonably large, requiring a thermal expansion coefficient for the simple lattice type less than half that for the body-centered type. The experimentally determined values of the lattice constants in the vicinity of the transition point indicate that the two expansion coefficients do not differ greatly.

In this determination of four unknowns, the values were not obtained by exact solution, but were found after numerous trials to give suitable agreement. The procedure followed was to choose values of the factor inserted in the van der Waals terms and of the ratio of the repulsion coefficients in the terms of the second and first neighbors, i.e., b_2/b_1, and then by substitution to ascertain whether suitable values were obtained for the difference of lattice energies, ΔU, in the two crystal types and for the lattice constant of the simple lattice type at absolute zero.

In addition to the methods already described, an investigation was made for CsCl to see what results would be obtained by taking as the four

[15] Th. Neugebauer and P. Gombas, Zeits. f. Physik **89** 480 (1924).

[16] J. A. Wasastjerna, Soc. Scient.-Fennica. Comm. Phys.-Math. vol. 8, No. 9 (1935).

constants, two values of ρ, ρ_1 and ρ_2 for the first and second neighbors, together with the van der Waals factor and a single value of b.

The form used for $B(r_0)$ was essentially that of Born and Mayer,[5]

$$B(r_0)=b\times10^{-12}[Mb_+b_-e^{-r_0/\rho_1}+\tfrac{1}{2}(1.25b_+^2+0.75b_-^2)e^{-ar_0/\rho_2}],$$

b_+ and b_- having the values found by Huggins and Mayer.[4] The results obtained were $b=1.73$, $\rho_1=0.364\times10^{-8}$ cm, $\rho_2=0.310\times10^{-8}$ cm and the van der Waals factor $=3.2$.

Subsequent calculations based on this method were found to differ little from those of the previous method of four constants, being slightly less satisfactory.

Elastic Constants and Acoustic Frequencies

The elastic constants c_{11}, c_{12} and c_{44} were computed by the method of Born[17] from the expressions:

$$c_{11}=\frac{1}{\Delta}\sum\frac{1}{r}\frac{d}{dr}\left(\frac{1}{r}\frac{d\phi}{dr}\right)x^4+\frac{1}{2}\frac{dU}{d\Delta},$$

$$c_{12}=\frac{1}{\Delta}\sum\frac{1}{r}\frac{d}{dr}\left(\frac{1}{r}\frac{d\phi}{dr}\right)x^2y^2,$$

$$c_{44}=\frac{1}{2}\frac{dU}{d\Delta}+c_{12},$$

where $$\frac{1}{2}\frac{dU}{d\Delta}=\frac{1}{6\Delta}r_0\frac{dU}{dr_0}=\frac{R}{6\Delta},$$

Δ is the volume per molecule and ϕ the mutual energy of a pair of ions. The summations are made by assuming a "reference" ion and summing over all other ions in the lattice. The electrostatic part of c_{11} is

$$(c_{11})_e=\frac{3e^2}{\Delta}\sum_{l_1l_2l_3}\frac{x^4}{r^5}(-1)^{l_1+l_2+l_3}. \qquad (7)$$

The indices l_1, l_2 and l_3 are defined by the equa-

[17] M. Born, *Dynamik der Krystallgitter* (Leipzig 1923), p. 536, 548, 554; M. Born and M. Goeppert-Mayer, *Handbuch der Physik*, Vol. 24 (Berlin 1933), p. 630.

TABLE II. *Calculations are for $T=273°K$ unless otherwise specified.*

Substance	CsCl				NH_4Cl			
	Orig. Data		Adjusted		Orig. Data		Adjusted	
Crystal Type	CsCl	NaCl	CsCl	NaCl	CsCl	NaCl	CsCl	NaCl
c_{++}	152	152			98	98		
c_{--}	129	129			127	127		
c_{+-} } $\times 10^{60}$ erg cm^6	129	129			98	98		
d_{++}	278	278			150	150		
d_{--}	260	260			266	266		
d_{+-} } $\times 10^{76}$ erg cm^8	250	250			177	177		
$C\times10^{60}$ erg cm^6	1621	1105	5836	3978	1251	850	4378	2975
$D\times10^{76}$ erg cm^8	2630	1751	9468	6304	1898	1254	6643	4389
$r_0\times10^8$ cm (meas.)	3.553	3.430	3.553	3.442	3.339	3.227	3.339	3.230
$\beta\times10^{12}$ barye^{-1}	5.9				5.602			
$\beta^{-1}(\partial\beta/\partial T)_P\times10^4$ deg.$^{-1}$	6				14.6			
$\beta^{-1}(\partial\beta/\partial P)_T\times10^{11}$ barye^{-1}	−0.30				−2.75			
$V^{-1}(\partial V/\partial T)_P\times10^4$ deg.$^{-1}$	1.887				1.42			
R	1.82	1.08	1.82	1.51	1.19	2.01	1.19	1.04
S	124.9				113.7			
$\alpha e^2/r_0$ } $\times10^{12}$ ergs per molecule	11.29	11.59	11.29	11.55	12.01	12.32	12.01	12.31
C/r_0^6	0.81	0.68	2.90	2.40	0.93	0.75	3.16	2.62
D/r_0^8	0.10	0.09	0.37	0.32	0.12	0.11	0.43	0.37
$\rho\times10^8$ cm	0.290	0.290	0.365	0.365	0.319	0.319	0.374	0.374
b_1	28930	28930	5734	5734	6170	6170	3131	3131
b_2	28930	28930	4014	4014	6170	6170	1722	1722
$B_1(r_0)$	1.09	1.25	2.70	2.75	1.40	1.50	3.32	3.34
$B_2(r_0)$ } $\times10^{12}$ ergs per molecule	0.12	0.02	0.31	0.07	0.21	0.05	0.34	0.10
U	10.99	11.09	11.55	11.45	11.42	11.63	11.94	11.86
ΔU	−0.10		0.10		−0.21		0.08	
$\Delta\Phi$ kcal./mole (calc.)	−1.4		1.4		−3.0		1.2	
$\Delta\Phi$ kcal./mole (meas.)	1.34		1.34		1.03		1.03	
$r_0\times10^8$ cm 0°K (calc.)		3.386		3.399		3.159		3.202

TABLE III. *Summations used to calculate the van der Waals forces.*

SUMMATION	SIGN OF IONS	LATTICE TYPE: CsCl	LATTICE TYPE: NaCl
$1/r^6$	like	3.5446	1.8067
	unlike	8.7088	6.5952
$1/r^8$	like	2.1977	0.8001
	unlike	8.1575	6.1457
$1/r^{10}$	like	1.5250	0.3847
	unlike	8.0394	6.0414
$(-1)^{l_1+l_2+l_3}3x^4/r^5$	both	1.8406[1]	−3.226[3]
$(-1)^{l_1+l_2+l_3}3x^2y^2/r^5$	both	−1.8016[2]	0.739
x^4/r^{10}	like	1.0200	0.3204
	unlike	1.0413	2.0972
x^2y^2/r^{10}	like	0.0808	0.1409
	unlike	0.9308	0.0506
x^4/r^{12}	like	0.6831	0.1376
	unlike	0.9236	2.0213
x^2y^2/r^{12}	like	0.0247	0.0646
	unlike	0.8978	0.0136
r_0 = unit length			

[1] M. Goeppert-Mayer and A. May, Phys. Rev. **50**, 99 (1936).
[2] M. Goeppert-Mayer and A. May, Phys. Rev. **52**, 242 (1937).
[3] Born, reference 17, p. 738.

tions $x=l_1a$, $y=l_2a$, $z=l_3a$, where a, for both the CsCl type and NaCl type lattices, is half the distance between nearest like ions. For the CsCl type all l's must be even or all odd.

The van der Waals contribution to c_{11} is

$$(c_{11})_v=-\frac{48}{\Delta}\left(\frac{c_{++}+c_{--}}{2}\sum_{\text{like ions}}\frac{x^4}{r^{10}}+c_{+-}\sum_{\text{unlike ions}}\frac{x^4}{r^{10}}\right)$$
$$-\frac{80}{\Delta}\left(\frac{d_{++}+d_{--}}{2}\sum_{\text{like ions}}\frac{x^4}{r^{12}}+d_{+-}\sum_{\text{unlike ions}}\frac{x^4}{r^{12}}\right). \quad (8)$$

As in calculating the lattice energies, only the first and second neighbors are included in the repulsion. We obtain

$$(c_{11})_r=(1/\Delta\rho^2)[(8/9)b_1r_0(r_0+\rho)e^{-r_0/\rho}$$
$$+2b_2ar_0(ar_0+\rho)e^{-ar_0/\rho}] \quad (9)$$

for the CsCl type lattice, and

$$(c_{11})_r=(1/\Delta\rho^2)[2b_1r_0(r_0+\rho)e^{-r_0/\rho}$$
$$+8^{\frac{1}{2}}b_2r_0(ar_0+\rho)e^{-ar_0/\rho}] \quad (10)$$

for the NaCl type.

Similarly we have

$$(c_{12})_r=(b_1/\Delta\rho^2)(8/9)r_0(r_0+\rho)e^{-r_0/\rho}$$
(CsCl type), (11)

$$(c_{12})_r=(b_2/\Delta\rho^2)\sqrt{2}r_0(ar_0+\rho)e^{-ar_0/\rho}$$
(NaCl type). (12)

Nothing is contributed to $(c_{12})_r$ by the first neighbors for the NaCl type, nor by the second neighbors for the CsCl type. The other components of c_{12} differ from the sum in c_{11} only in the substitution of the factor x^2y^2 for x^4.

The value of R needed for the calculation of c_{44} has already been obtained for the body-centered lattice. For the simple lattice it is calculated from Eq. (2).

The van der Waals sums were computed directly to spheres of radii seven times the lattice constant, integrated to infinity and then corrected by comparison with the inverse power

TABLE IV. *Elastic constants* $\times 10^{-11}$ *ergs/cm*^{3}.

	CsCl					
	CsCl TYPE			NaCl TYPE		
	c_{11}	c_{12}	c_{44}	c_{11}	c_{12}	c_{44}
electrostatic	1.707	−1.671		−2.615	0.599	
van der Waals C	−3.453	−1.634		−4.021	−0.335	
van der Waals D	−0.681	−0.379		−0.972	−0.037	
repulsion	6.638	4.548		11.358	0.151	
$R/6\Delta$	0.044			0.031		
	4.255	0.864	0.908	3.781	0.378	0.409
	NH_4Cl					
electrostatic	2.188	−2.142		−3.372	0.772	
van der Waals C	−4.585	−2.122		−5.302	−0.457	
van der Waals D	−0.966	−0.519		−1.355	−0.056	
repulsion	8.046	5.710		14.139	0.205	
$R/6\Delta$	0.035			0.023		
	4.718	0.927	0.962	4.133	0.464	0.487

summations of r of Jones and Ingham[9] by using the relation

$$3\Sigma\frac{x^4+2x^2y^2}{r^{n+4}}=\Sigma\frac{1}{r^n},\quad (n=6,\ 8)$$

as was done by Herzfeld and Goeppert-Mayer.[18] The summations for like ions of the body-centered type are obtained, by a change of scale, from the like and unlike ion summations for the simple lattice.

The summations are given in Table III and the resulting constants in Table IV.

In averaging the sound velocities over all directions, the method of Born and Kármán[19] cannot be used since it requires that the quantity $(3c_{12}-c_{11})/(c_{11}-c_{12})$ be small. Herzfeld and Goeppert-Mayer[18] substituted a geometric mean for the average

$$3(1/w^3)_{Av}=(1/w_1^3)_{Av}+(1/w_2^3)_{Av}+(1/w_3^3)_{Av}$$

proposed by Debye. Because of the relatively small values of c_{12} and c_{44}, the several sound velocities will differ considerably and the geometric mean would be too high. The averages, $(1/w^3)_{Av}$, where w is the sound velocity, were obtained by the method of Hopf and Lechner[20] which is especially applicable to the case where c_{12} and c_{44} are small.

The acoustic frequency limit is found from Debye's formula

$$\nu_m^3=3/4\pi\Delta(1/w^3)_{Av}.$$

The velocity averages and corresponding frequencies calculated for 273° are given in Table V.

The frequencies corresponding to various temperatures may be of interest in connection with the calculation of the transition points, and

TABLE V.

	$(1/w^3)_{Av}\times10^{17}$ (cm/sec.)$^{-3}$		$\nu_m\times10^{-12}$ sec.$^{-1}$	
	CsCl	NH_4Cl	CsCl	NH_4Cl
CsCl type	14.4	3.14	2.86	5.10
NaCl type	26.9	5.08	2.21	4.12

[18] K. F. Herzfeld and M. Goeppert-Mayer, Phys. Rev. **46**, 995 (1934).
[19] M. Born and Th. von Kármán, Physik. Zeits. **14**, 15 (1913); Born, reference 17, p. 647.
[20] L. Hopf and G. Lechner, Verh. d. D. phys. Ges. **16**, 643 (1914); Born, reference 17, p. 649.

TABLE VI. *Elastic constants and acoustic frequency limits (ν_m) at various temperatures.*

	CsCl TYPE				*NaCl* TYPE			
	c_{11}	c_{12}	c_{44}	ν_m	c_{11}	c_{12}	c_{44}	ν_m
	$\times10^{-11}$			$\times10^{-12}$	$\times10^{-11}$			$\times10^{-12}$
CsCl								
0°K	4.820	1.205	1.205	3.18	4.606	0.392	0.392	2.24
135°	4.638	1.090	1.106	3.08	4.305	0.387	0.399	2.23
273°	4.254	0.864	0.908	2.86	3.781	0.378	0.409	2.21
718°	3.284	0.340	0.447	2.19	2.436	0.350	0.431	2.12
NH_4Cl								
0°K	5.104	1.179	1.179	5.50	4.684	0.474	0.474	4.12
273°	4.718	0.927	0.962	5.10	4.133	0.464	0.487	4.12
500°	4.340	0.692	0.758	4.67	3.565	0.455	0.501	4.04

a number of values are included in Table VI. In their computation the lattice constants obtained for these temperatures by means of the expansion coefficients, have been used.

Calculating these frequencies by the Hopf and Lechner method is a long task, but this may be obviated by using an approximation developed by Blackman.[21] His formula can be written

$$\nu_m=k[c_{11}(c_{44})^2\Delta]^{1/6}/M^{1/2} \qquad (13)$$

where k is a constant and M is the molecular weight. From a number of frequencies previously calculated by the Hopf and Lechner method, the constant was found to have the value, $k=21.8$, for the elastic constants expressed in the unit 10^{11} ergs/cm^3, Δ in 10^{-23} cm^3, and ν_m in 10^{12} sec.$^{-1}$. Since the longer method involves the small differences of large quantities, the accuracy which it yields is generally poor, and since the deviations between results obtained by the two methods amount to only a few percent, the approximation appears quite satisfactory.

OPTICAL FREQUENCIES

The optical frequencies are derived by a method similar to that already described. Following Born[22] we first evaluate the D "bracket-symbols,"

$$D=\frac{1}{\Delta}\Sigma\left[\frac{1}{r}\frac{d\phi}{dr}+\frac{1}{r}\frac{d}{dr}\left(\frac{1}{r}\frac{d\phi}{dr}\right)x^2\right], \qquad (14)$$

where the summation is over unlike ions only.

[21] M. Blackman, Proc. Roy. Soc. **A148**, 400 (1935).
[22] Born, reference 17, pp. 536, 568, 738, 740.

TABLE VII. *Optical frequencies (273°K). D (Born)* $\times 10^{-26}$ *ergs/cm*^{3}.

LATTICE TYPE	*CsCl*		*NH*$_4$*Cl*	
	CsCl	NaCl	CsCl	NaCl
electrostatic	−1.975	−1.433	−2.901	−2.098
van der Waals *C*	−2.114	−1.776	−3.160	−2.640
van der Waals *D*	−0.595	−0.533	−0.942	−0.839
repulsion	7.658	6.648	10.721	9.063
frequencies ($\times 10^{-12}$)	2.974	2.906	3.718	3.486
	3.368	3.607	5.232	5.494

Using Ewald's method, Born found for the electrostatic part

$$D_e = -4\pi e^2/3\Delta^2. \tag{14a}$$

The van der Waals contributions are:

$$D_v = \frac{6c_{+-}}{\Delta}\sum\frac{1}{r^8} - \frac{48c_{+-}}{\Delta}\sum\frac{x^2}{r^{10}} + \frac{8d_{+-}}{\Delta}\sum\frac{1}{r^{10}} - \frac{80d_{+-}}{\Delta}\sum\frac{x^2}{r^{12}},$$

where again the summations are limited to unlike ions. For both crystal types involved

$$3\sum\frac{x^2}{r^{n+2}} = \sum\frac{1}{r^n}, \quad (n=8, 10)$$

so that

$$D_v = -\frac{10c_{+-}}{\Delta}\sum\frac{1}{r^8} - \frac{56}{3}\frac{d_{+-}}{\Delta}\sum\frac{1}{r^{10}}. \tag{14b}$$

The summations over inverse powers of r are given by Jones and Ingham[9] and are listed in Table III.

Since only the interactions between unlike ions are included, the repulsion part contains only the first neighbors:

$$D_r = (bM/3\Delta\rho^2 r_0)(r_0 - 2\rho)e^{-r_0/\rho}. \tag{14c}$$

The frequencies were calculated from Born's formula, which assumes that they are monochromatic: $2\pi\nu = (\Delta D/m)^{\frac{1}{2}}$ m is the reduced mass of the ions, i.e. $1/m = 1/m_1 + 1/m_2$, where m_1 and m_2 are the masses of the two ions. The components of D for 273° and the corresponding frequencies are listed in Table VII.

The infrared absorption limit of CsCl as measured by Barnes[23] is 102.0 microns, corresponding to a frequency of 2.94×10^{12} sec.$^{-1}$. The value 3.37×10^{12} differs from this by fifteen percent.

[23] R. B. Barnes, Zeits. f. Physik **75**, 723 (1932).

TABLE VIII. *Optical frequencies—various temperatures.* $D\times10^{-26}$, $\nu_r\times10^{-12}$.

	CsCl				*NH*$_4$*Cl*			
	CsCl type		NaCl type		CsCl type		NaCl type	
T°K	*D*	ν_r	*D*	ν_r	*D*	ν_r	*D*	ν_r
0	3.797	3.04	3.528	3.27	4.354	4.37	3.944	4.55
273	2.974	2.69	2.906	2.99	3.718	3.96	3.486	4.30
500					3.125	3.61	3.017	3.98
718	1.786	1.99	1.914	2.43				

Heckmann[24] has derived a formula for computing the effect on the frequencies, of the electron polarization which has been neglected in the method just used. This formula can be written

$$\nu_r^2 = \nu_e^2 - \frac{e^2}{3\pi m\Delta}\frac{\alpha}{1-\alpha} \tag{15}$$

by putting $\beta=1$ in the form given by Heckmann. ν_r is the actual maximum of absorption; ν_e, the frequency which we have calculated from the elastic properties; e, the electronic charge; Δ, the volume per molecule; m, the reduced mass of the ions, and $\alpha=(n^2-1)/(n^2+2)$ is the electronic polarizability, n being the visible refractive index. For optical frequencies the index of refraction of the CsCl type lattice is practically the same[25] for CsCl and NH_4Cl, and in both cases we have used $n=1.620$, obtained for CsCl by Born and Heisenberg[26] by extrapolation to zero frequency.

We find for CsCl, $\nu_e^2-\nu_r^2=4.11\times10^{24}$ and $\nu_r=2.69\times10^{12}$ sec.$^{-1}$, which differs from Barnes' value by eight percent.

The optical frequencies corresponding to a number of temperatures are included in Table VIII. ν_r was calculated on the assumption that α is inversely proportional to Δ, and that in other respects the value of α for the NaCl type lattice is the same as for the CsCl type.

[24] G. Heckmann, Zeits. f. Krist. **61**, 250 (1924).
[25] *International Critical Tables*, Vol. I, p. 165.
[26] M. Born and W. Heisenberg, Zeits. f. Physik **23**, 407 (1924).

The Transition Temperature

The transition temperature is now calculated from the equality of the free energies.

Because of the high temperatures involved, the free energies can be computed from two expressions of the form

$$F=-NU+3RT\ln h\nu_m/kT+3RT\ln h\nu_r/kT,$$

where ν_m and ν_r are the acoustic and optical frequencies, h is Planck's constant and k the gas constant per molecule.

The temperature at which the free energies are equal is given by

$$T=\frac{(U_1-U_2)}{3k\ln(\nu_m\nu_r)_1/(\nu_m\nu_r)_2}, \qquad (16)$$

where the subscripts 1 and 2 refer to the CsCl type and NaCl type lattices, respectively.

By using the frequencies calculated for 0°K, the transition temperatures obtained are 810°K for CsCl and 700°K for NH_4Cl, as compared with the experimental values, 718° and 457°. These results must be regarded as satisfactory in view of the small accuracy to be expected. Slightly better values are obtained if the corrections for the electron polarization are not made.

In calculating the transition temperatures from Eq. (16), the frequencies used should be those corresponding to the temperature T.

Because of the rapid decrease of ν_m for the CsCl type lattice as indicated in the values of Table VI, no transition point is obtained if the temperature dependence of the frequencies is considered. It appears quite probable that it is the temperature dependence of the frequencies that is incorrect rather than the values found for absolute zero.

Acknowledgment

The author wishes to acknowledge his indebtedness to Professor K. F. Herzfeld and to Dr. Maria Goeppert-Mayer for suggesting the present problem and for rendering much assistance during its solution.

AUGUST 15, 1937 PHYSICAL REVIEW VOLUME 52

Coercive Force in Single Crystals

K. J. Sixtus
Research Laboratory, General Electric Company, Schenectady, New York

(Received June 7, 1937)

The coercive force H_c of ten single crystal disks of silicon-iron has been measured in different directions in their planes. In any one disk, H_c changes with the direction; it is mainly determined by the angle α_3 between the field and the [001] axis nearly normal to the disk, and has a minimum value when that angle is 90°. The angle α_1 between the field direction and another cubic axis which lies nearly in the plane of the disk and close to the field direction has a smaller effect on H_c. The relation $H_c=A/\cos\alpha_1+B\cos\alpha_3$ represents very closely the curves taken on well annealed disks; A and B are constants with values close to 0.1 and 0.4, respectively. The effect on H_c of varying the disk shape and of increasing the internal strains by carburization has been studied. Finally it has been shown that H_c values calculated from the empirical relation are in good agreement with data on single crystal wires and strips (Kaya, Ruder).

1. Introduction

MAGNETIC theory can at present account satisfactorily for the behavior of ferromagnetic material near technical saturation. Our understanding, on the other hand, of what happens in low fields in general, and of the phenomenon "coercive force" in particular, is still very limited and vague. It was recognized early that internal strains in a ferromagnetic material caused by cold work or by impurities increased the coercive force. This was proved systematically by Kussmann and Scharnow.[1] Contributions from the theoretical side were made by R. Becker, N. Akulov and by F. Bloch. Bloch[2] in referring to experiments by K. J.

[1] A. Kussmann and B. Scharnow, Zeits. f. Physik **54**, 1 (1929).

[2] F. Bloch, Zeits. f. Physik **74**, 295 (1932).

Sixtus and L. Tonks[3] assumed that only inhomogeneous internal strains affect the coercive force H_c and gave an atomic picture in which he showed qualitatively how local variations in atomic spacing by their effect on the exchange integral determine the energy necessary for reversal of magnetization and thus H_c.

One could expect that a study of H_c in single crystals might yield new and useful information. Sizoo[4] has measured a number of iron and nickel crystals without finding a relation between coercive force and crystal orientation. The spread of H_c values for crystals with similar orientation betrayed the presence of different strains in those crystals. Kaya[5] also made measurements on iron single crystals, in wire form, but gave no relation for H_c. The first evidence of a definite dependence of H_c on crystal orientation is contained in a paper by Ruder.[6] Kaya's and Ruder's results will be discussed later in the light of our findings.

In the present investigation[7] it was decided to use single crystal specimens in the form of disks. This shape makes it possible to obtain a dependence of H_c on orientation, within certain limits, in one specimen by applying the field in various directions in the plane of the disk. It eliminates, at the same time, all doubt as to variations in strain state which arises when several different specimens are compared. Since H_c can be measured directly without applying corrections in samples of any shape, there are no difficulties due to the high demagnetizing factor of disks.

TABLE I. *Data for single crystal disks. ϑ is the angle between an axis and its projection on the disk, φ the angle between this projection and an arbitrary disk diameter used as reference line.*

No.	Diameter in cm	Thickness in cm	[100]		[010]		[001]	
			φ_1	ϑ_1	φ_2	ϑ_2	φ_3	ϑ_3
2M	2.35	0.043	317	19.5	224	9	20	68.5
3M	2.35	.047	23	12	291	11	156	73.5
4M	2.30	.048	2	15	268	17	129	67
6M	2.38	.047	132	38.5	44	2.5	320	51
7M	2.20	.035	250	10	158	9	27	76.5
8M	2.33	.046	277	4	187	12	19	77
9M	2.14	.044	17.5	5.5	286	9.5	133	79
10M	2.35	.049	25.5	3.5	294	23.5	122	66.5
11M	2.35	.048	321	23	226	12	109	63
12M	2.77	.048	307	17	215	5	110	72

2. Material

The crystals were produced in iron-silicon sheets by a strain-anneal method consisting of a two percent extension of hot rolled strips followed by a two-hour anneal at 1300°C. The crystals were carefully cut from the sheet on a lathe, polished and reannealed at 1100°C in pure dry hydrogen. In a few disks very fine crystals had grown on the circumference because of excessive strain developed during cutting. These small crystals were cut off in a lathe with greater precautions than before and no new crystal growth was visible after another 1100° anneal. Chemical analysis gave the following elements besides iron (by weight percentage): Si: 2.8· C: 0.02; Mn: 0.10; S: 0.021; P: nil. The diameters of the disks were between 2 and 2.5 cm; the original thickness ranged around 0.05 cm.

Table I gives dimensions and orientations of the 10 disks used. The orientations were determined from Laue patterns, with an accuracy of $\pm 1°$ and are referred to an arbitrary line along a diameter of the disk. Crystals No. 1M and No. 5M were omitted because they each contained a small included crystal which affected the results considerably.

3. Method of Measurement

The coercive force was measured directly as that value of applied field at which the induction I became zero. A coil, 17.5 cm long with a constant of 99.0 oe./amp. supplied the field in which the single crystal disk could be so adjusted that the reference line drawn on it made any angle (azimuth) with the field direction while its plane was always horizontal and therefore always in the direction of the field. A search coil of 4500 turns fitted closely around the center of the disk; it could be moved away from the disk parallel to itself and to the field. The earth's magnetic field was, at the place of the disk, compensated by a pair of Helmholtz coils. For convenience the magnetizing field was applied, and H_c was measured, in a direction at right angles to the horizontal component of the earth's field.

[3] K. J. Sixtus and L. Tonks, Phys. Rev. **37**, 930 (1931).
[4] G. J. Sizoo, Zeits. f. Physik **56**, 649 (1929).
[5] S. Kaya, Zeits. f. Physik **84**, 705 (1933).
[6] W. E. Ruder, Trans. Am. Soc. for Metals **22**, 1120 (1934).
[7] A short abstract has appeared in Phys. Rev. **50**, 395 (1936).

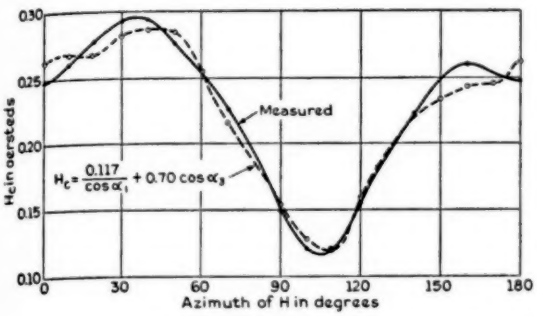

FIG. 1. Coercive force *vs.* azimuth in single crystal disk No. 8M.

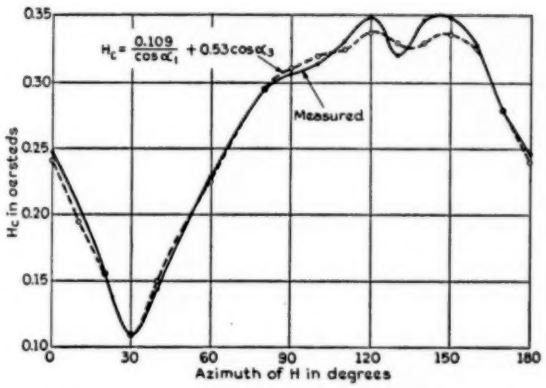

FIG. 2. Coercive force *vs.* azimuth in single crystal disk No. 10M.

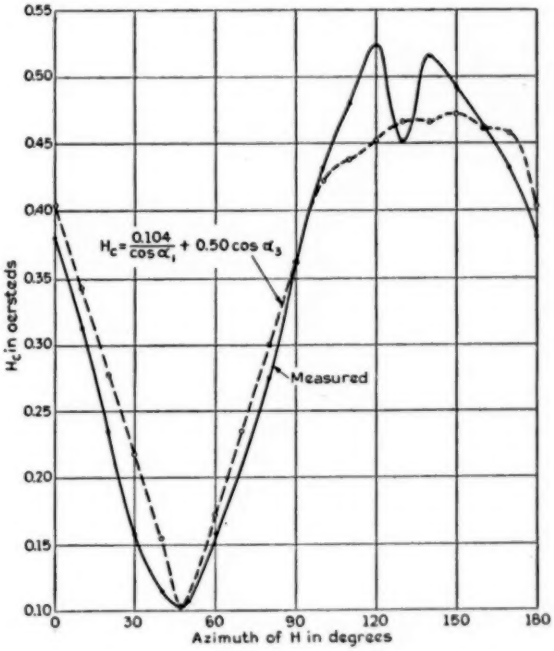

FIG. 3. Coercive force *vs.* azimuth in single crystal disk No. 6M.

The sample was first magnetized to 1000 oersteds which brought it to a point on the reversible part of the magnetization curve near saturation. The field was then slowly reduced to zero and increased in the opposite direction until vanishing deflection in the galvanometer circuit upon withdrawal of the coil from the sample indicated that the coercive force had been reached. The whole procedure was repeated every time in opposite field direction; a disagreement between the measured values of coercive force in the two directions would then reveal the presence of a stray field with a component in the measuring direction.

It was found at the start of the investigation that fields of even several times the strength of the earth's field did not affect H_c as long as they were applied perpendicular to the direction in which H_c was measured. Although this finding eliminated the necessity for compensating the earth's field, all measurements were made with compensation.

The measured values of H_c could be reproduced consistently within one percent if mechanical and magnetic shocks were avoided. The latter condition was fulfilled by reducing the field current gradually from its maximum value to zero with a potentiometer.

4. RESULTS

In Figs. 1, 2 and 3 curves for three disks are given whose surface normal made increasing angles with the [001] axis which was most nearly normal to the surface. (No. 8M: 13°, No. 10M: 23°, No. 6M: 39°.) In each disk the coercive force shows considerable variation with azimuth of H. The range of variation obviously increases with the angle between [001] and the surface normal. The minimum of H_c occurs in every disk at that azimuth, where H was at right angles to [001]. This made it evident at once that the main factor in determining the shape of H_c curves was the [001] axis while the orientation of the other two cubic axes lying more nearly in the surface had a smaller influence (Fig. 4).

An analytical expression for the curves was derived by trial and error. Satisfactory fits even with regard to detail were found by taking into account only the angles between H and the

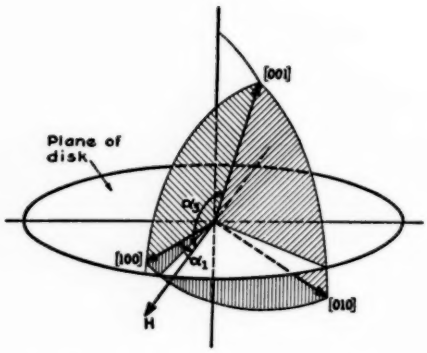

FIG. 4. [100] and [010] are cubic axes lying nearly in the plane of the disk, [001] is nearly perpendicular to it. Measurements show that α_3 has a large, α_1 only a small, influence on the coercive force.

nearest cubic axis (α_1) and between H and the [001] axis nearly normal to the surface (α_3), always measured as acute angle, and combining them in the following equation:

$$H_c = A/\cos\alpha_1 + B\cos\alpha_3. \qquad (1)$$

This approximation could be expected to give the best agreement when α_1 was close to 0 and α_3 close to 90°, because only in that case was the omission of the third axis really justified. In Figs. 1 and 2, the calculated and observed curves agree quite closely, but in Fig. 3 where α_3 assumes values as low as 51° the agreement is less satisfactory. In the second term one might have expected—from symmetry considerations—a second power rather than a first power law. Such a law was actually found in one disk where H_c had been increased by diffusion of carbon (Section 6).

The constants A and B in Eq. (1) are given in Table II. The small variation from disk to disk indicates that the basic state of strain in the different disks was approximately the same and justifies comparisons between H_c values taken on different disks. On this basis we can illustrate the decisive influence of the direction of the [001] axis expressed in Eq. (1) by a striking example. We compare the coercive force in a direction as close as possible to the dodecahedral axes in disks No. 8M and 6M. In the first case where the surface is nearly parallel to a cubic plane, these values are 0.27 oe. and 0.22 oe., respectively; in the second, where the surface lies approximately in a dodecahedral plane, the value is 0.5 oe.

5. Reduction in Diameter and Thickness

The following experiments were undertaken in order to obtain the variation of the constants A and B in Eq. (1) with changes in dimensions.

Disk No. 12M was reduced on the lathe from a diameter of 2.56 cm to 2.04 cm, thus lowering its diameter to thickness ratio from 58 to 42. The constants A and B, measured after anneal, were negligibly larger. They had increased from 0.119 to 0.124, and from 0.40 to 0.42, respectively.

Etching in concentrated nitric acid with following anneal was chosen as the most suitable method of reducing the thickness. The etching left the surface smooth and even, and any absorbed hydrogen was presumably driven off during the anneal. Table III gives the variation of constants A and B for decreasing thickness in disks No. 2M and 4M. Both constants increase, A at a greater rate than B.

The observations on disk No. 12, together with the results on wires and strips reviewed in Section 7, indicate that the shape of samples may be varied within certain limits without affecting the correctness of Eq. (1) and even without much effect on the constants A and B. An extreme case for which Eq. (1) would obviously change into another one, symmetrical with respect to α_1, α_2, and α_3, would be met with in a sphere. The value of A and B, but not the form of Eq. (1), changes when the thickness of the samples decreases below 0.2 mm. Our results on disks No. 2M and 4M indicate that H_c for any given azimuth begins to increase considerably when the disks are thinned down below this value. The same effect has been noted before in polycrystalline material although the critical thickness was found to be smaller. This is presumably due largely to the presence of high internal strains in the materials used in those investigations.[8]

TABLE II. *The constants A and B in Eq. (1) for different disks.*

Disk No.	2M	3M	4M	6M	7M	8M	9M	10M	11M	12M
A	0.096	0.119	0.109	0.104	0.108	0.117	0.113	0.109	0.130	0.119
B	.43	.43	.30	.50	.50	.70	.68	.53	.42	.40

[8] Cf. W. Elenbaas, Zeits. f. Physik **76**, 829 (1932).

6. Carburization

The question arose whether the variation of coercive force would persist in crystals with large internal strains and accordingly high absolute values of coercive force. If the strain energy exceeded the lattice energy by a large amount and if the strains were isotropic, one should expect that the anisotropy of magnetic properties would disappear.

Chemical hardening rather than a plastic deformation of the material appeared most likely to produce strains of a random character. Disk No. 12M was heated in a mixture of charcoal and sodium carbonate for six hours at a temperature of 785° which kept it just below the γ-range for any amount of carbon which it might take up. At that temperature 0.06 percent C can be absorbed in solid solution. During slow cooling to room temperature where only 0.03 percent C can be held in solution under equilibrium conditions the excess carbon will precipitate as carbide. Quenching will preserve the high temperature condition and therefore produce a state of strain in the material.

The original H_c curve and the curves after slow cooling from 785° and after quenching in water from that temperature are shown in Fig. 5. Curve 3 obviously follows a simpler law than curve 1; the hump at 160° which is quite evident in 1 does not appear in 3. Accordingly an equation of the type of Eq. (1) no longer represents the experimental findings satisfactorily. The following expressions were found to give the best fit:

Curve 1: $H_c = 0.124/\cos\alpha_1 + 0.42\cos\alpha_3$
Curve 2: $H_c = 0.186 + 5.0\cos^2\alpha_3$
Curve 3: $H_c = 0.93 + 6.1\cos^2\alpha_3$.

Table III. *Variation of A and B (Eq. (1)) with reduction in thickness.*

Disk No. 2M			Disk No. 4M		
Thickness in mm	A	B	Thickness in mm	A	B
0.43	0.096	0.43	0.48	0.109	0.30
0.30	0.114	0.43	0.30	0.138	0.33
0.18	0.159	0.47	0.16	0.184	0.45
0.13	0.254	0.53			
After Anneal					
0.13	0.298	0.60			

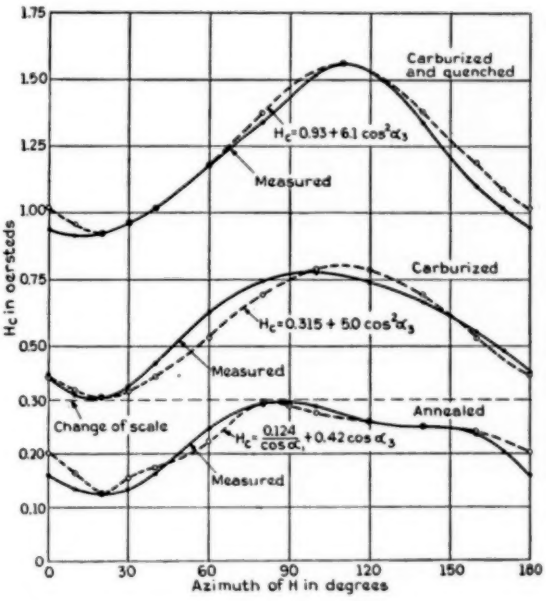

Fig. 5. The effect of carbon on H_c in disk No. 12M.

The fact that the influence of the [100] and the [010] axis on H_c has been eliminated while the effect of the [001] axis persists can be explained in two ways. First, the carbon may diffuse into the lattice in such a fashion as to set up an anisotropic strain condition. Secondly, the strain may still be insufficient to entirely overcome the original anisotropy of the lattice. The second cause appears more plausible; a decision could very likely be made with crystals of nickel whose magnetic crystal energy is only about one-tenth that of iron.

Incidentally, an anneal first at 785° and then at 1100° in pure dry hydrogen returned the crystal to its original condition. The values of H_c in this final state did not differ more than five percent from those plotted in Curve 1.

7. Discussion

The generality of Eq. (1) has been further tested by applying it to Kaya's[5] and Ruder's[6] data on the coercive force of single crystal wires and strips. Kaya's data on wires of electrolytic iron are given in Table IV, together with H_c values calculated from the equation $H_c = 0.08/l + 0.4n$. l, m and n in Tables IV and V stand for $\cos\alpha_1$, $\cos\alpha_2$ and $\cos\alpha_3$, respectively; α_1 being the smallest, α_3 the largest of the angles which the

TABLE IV. *Coercive force of single crystal wires of electrolytic iron as measured by Kaya, compared with calculated values (wire thickness 0.2 cm).*

No.	l	m	n	H_c (OERSTEDS) MEAS.	H_c (OERSTEDS) CALC.
1	0.901	0.416	0.130	0.19	0.14
2	0.926	0.374	0.045	0.14	0.11
3	0.855	0.432	0.284	0.20	0.21
4	0.718	0.696	0.039	0.11	0.13
5	0.665	0.612	0.425	0.21	0.29
8	0.779	0.627	0.001	0.11	0.11
10	0.996	0.065	0.054	0.10	0.10
16	0.901	0.334	0.277	0.24	0.20
18	0.796	0.527	0.296	0.22	0.22
19	0.754	0.598	0.275	0.22	0.22
21	0.894	0.441	0.067	0.12	0.12

TABLE V. *Measured and calculated values of coercive force for Ruder's single crystal strips. Dimensions of the N-series: 1.55×0.054×25.0 cm³; O-series: 1.35×0.054×25.0 cm³.*

No.	l	m	n	H_c (OERSTEDS) MEAS.	H_c (OERSTEDS) CALC.
1-*N*	0.857	0.500	0.087	0.15	0.15
2-*N*	0.743	0.656	0.191	0.21	0.21
3-1-*N*	0.799	0.588	0.191	0.16	0.20
4-*N*	0.819	0.500	0.242	0.20	0.22
5-*N*	0.914	0.423	0.122	0.13	0.16
5-1-*N*	0.914	0.423	0.122	0.13	0.16
6-*N*	0.707	0.695	0.105	0.17	0.18
7-*N*	0.927	0.391	0.070	0.15	0.14
9-*N*	0.934	0.358	0.000	0.12	0.11
10-*N*	0.982	0.156	0.122	0.12	0.15
8-*O*	0.966	0.259	0.052	0.14	0.12
13-*O*	0.755	0.602	0.259	0.21	0.23
17-*O*	0.961	0.292	0.052	0.13	0.12
18-*O*	0.719	0.643	0.326	0.22	0.27

three {100} axes make with the wire or strip axis. Ruder's data on strips of 3.5 percent silicon iron could not be used for our purpose in their original form since his H_c values were obtained from loops with a maximum induction of only 10,000 gauss. Mr. Ruder kindly supplied us with those strips which were still available (N series) and some additional new ones (O series). They were reannealed, their H_c measured after saturation, and their orientation determined more accurately from x-ray patterns. Table V contains the new data which differ not materially from the old ones and the H_c values calculated from $H_c=0.1/l+0.4n$. It should be noted that n does not refer to the cubic axis most nearly perpendicular to the width of the strip but to that axis most nearly perpendicular to the axis of the strip. The agreement between calculated and measured values in Tables IV and V is, in general, satisfactory; the discrepancy in the case of No. 5, Table IV and No. 18–O, Table V is accounted for by the large values of n, for which our empirical equation cannot be expected to hold.

A complete theory would have to explain, in the first place, the particular type of relation between the variables expressed in Eq. (1). While the dependence of H_c on α_1 is obviously due to the fact that only the field component in the direction of the [100] axis is operative in reversing the magnetization along that axis, its dependence on α_3 could be accounted for only after an analysis of the distribution of elementary districts together with a consideration of their demagnetizing fields.

In connection with the constants of Eq. (1) which a theory also has to deal with we want to mention here only the remarkable agreement between the values of A and B found with three different kinds of samples as given above. Considering only A—which measures H_c along a cubic axis—this may imply that H_c is approaching a lower limit. On the basis of a nucleus concept of coercive force[9] such a limiting value would follow naturally from the presence of minimum size nuclei.

[9] K. J. Sixtus, Phys. Rev. **48**, 425 (1935).

Precise Magnetic Torque Measurements on Single Crystals of Iron*

L. P. TARASOV AND F. BITTER
Massachusetts Institute of Technology, Cambridge, Massachusetts

(Received June 11, 1937)

A rugged balance of sufficiently high sensitivity and a rotating magnet capable of producing a field of over 3000 oersteds are used to make magnetic torque curves. The equations for the torque curve of a single crystal disk of any orientation whatsoever are derived on the assumption that the magnetic anisotropy is adequately described by a single constant. Furthermore, a method is developed for predicting the orientation from a knowledge of the angles of zero torque alone, and both the experimental and theoretical limitations of this method are discussed. It is shown experimentally that the use of cylindrical disks introduces errors that may be avoided by using ellipsoids. An experimental torque curve for a single crystal ellipsoid of 2.8 percent Si iron gave excellent agreement with the curve calculated on the basis of just the first anisotropy constant, $a_F = 1.70 \times 10^5$ ergs/cc. Corrections for magnetization not being parallel to applied field are briefly discussed, and it is shown that in practical cases, the magnetization cannot deviate appreciably from the plane of the specimen. The possibility is mentioned of computing a fictitious value of the second anisotropy constant because of error in interpreting experimental data. It is proposed that the anisotropy constants be obtained directly from accurate torque measurements, in order to furnish data for the computation of magnetization curves to be checked against experiment.

INTRODUCTION

THE purpose of this and succeeding papers is to develop magnetic measurements as a tool in studying the grain orientation of ferromagnetic materials so that, in the first place, the physical condition of any given sample may be better and more conveniently defined than is at present possible and, in the second place, so that the physical effect of the various mechanical and thermal treatments to which metals are subjected may be studied in greater detail in the hope of throwing some much needed light on the processes of plastic deformation and recrystallization. The magnetic attack on the problem seems to offer promise because the magnetic properties depend on grain orientation to a marked degree, and because the theory is now sufficiently developed to permit a fairly accurate mathematical description of many phenomena.[1]

In order to develop an interpretation of the magnetic properties of polycrystalline aggregates, especially when directional characteristics are involved, it is essential that we be absolutely certain of the corresponding treatment of single crystals. The following paper discusses this point in some detail.

ENERGY OF SATURATED CRYSTALS

In discussing ferromagnetism it is customary to assume that small regions are spontaneously magnetized to saturation in different directions, and that the observed magnetization of a macroscopic sample is the resultant effect of these regions. In general it is not possible to say how the directions of magnetization of these regions are distributed. The only simple case is the one in which the entire sample is magnetized to saturation in some one direction, so that all the small regions are magnetized in this same direction. In this paper, we shall confine our attention to this case.

The fundamental quantity determining the magnetic behavior of saturated crystals is the energy E_θ which we shall express in terms of ergs/cc. It can be shown[2] that for cubic ferromagnetic crystals in the absence of external forces,

$$E_\theta = a_F \Sigma' \alpha_i^2 \alpha_j^2 + a_F' \alpha_1^2 \alpha_2^2 \alpha_3^2 + \cdots, \qquad (1)$$

where the α's are the direction cosines of the saturation magnetization I_S with respect to the cubic axes, the summation being taken for $i = 1, 2, 3$, $i \neq j$. In terms of a notation commonly used,[3] $a_F = \frac{1}{2}K_1$, $a_F' = K_2$. The number of constants a_F,

* This article forms part of a doctoral thesis to be submitted by L. P. T. to the department of physics, M. I. T.

[1] The reader can find references in E. C. Stoner's *Magnetism and Matter* (Methuen, 1934), p. 434.

[2] For a complete discussion which takes into account the effects of magnetostrictive distortion and which explains more fully the basis of our notation, see *Introduction to Ferromagnetism*, by F. Bitter (McGraw-Hill, 1937).

[3] R. M. Bozorth, Phys. Rev. **50**, 1076 (1936).

a_F', $\cdots$ required to describe E_θ must be determined experimentally for each material, since addition of alloying elements to pure iron or nickel may greatly change the values of these constants.

Let us assume for the present that E_θ can be accurately represented by the first term alone, which we have found experimentally to be true for silicon iron, as will be discussed later in the paper. Then Eq. (1) reads

$$E_\theta = a_F \Sigma' \alpha_i^2 \alpha_j^2. \tag{2}$$

The surface defined by this equation for $a_F > 0$ is shown in Fig. 1 where the length of a line from the center of the model to the surface represents the energy of a crystal magnetized to saturation in the corresponding direction. (A constant term has been added to the expression for E_θ to make it easier to construct a physical model.) The minima occur in the [100] directions, the maxima in [111]. If a_F were negative, as for nickel, the maxima and minima would change places. In general, E_θ is a function of the distortion of the crystal and of the temperature, but we shall consider only crystals kept at one temperature and undistorted except for magnetostriction, the effects of which are taken into consideration in the derivation of Eq. (1).

In order to magnetize a single crystal to saturation in a single direction, it is necessary to apply an effective field H of the order of 10^3 oersteds. The experimentally observed energy is no longer E_θ but $E_{\theta,H}$ where

$$E_{\theta,H} = E_\theta - HI_S \cos \psi, \tag{3}$$

ψ being the angle between H and I_S. Except for certain directions, ψ is not zero, although it tends to approach zero as H becomes indefinitely large and we shall show later how to correct experimental results to give us E_θ. If Eq. (2) is correct, then an experimental determination of E_θ for a single crystal would at once fix its orientation.

If, however, the crystal to be examined has the form of a disk, or more properly of an ellipsoid, it is convenient to confine the observations to the plane of the disk, and the interpretation of the results is somewhat more complicated. Essentially the observation that can be made is the shape of the curve which is formed by the intersection of the model of Fig. 1 with a plane passing through its center, and the problem is to deduce the orientation of the plane from the shape of the resulting curve. This problem has been solved by the methods outlined below.

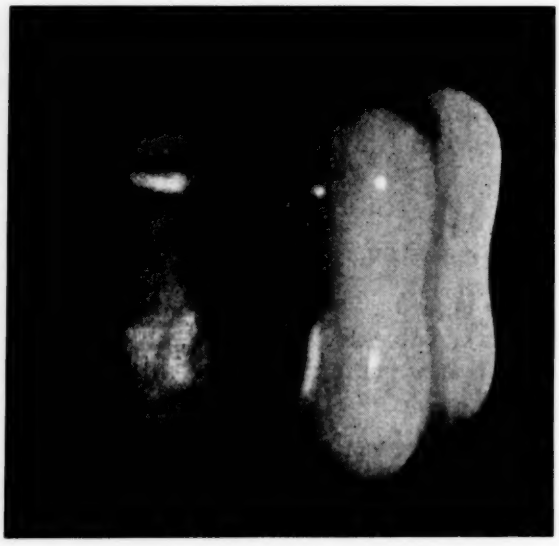

FIG. 1. Model of E_θ for iron, $a_F > 0$.

TORQUE-MEASURING APPARATUS

The experimental observations may most conveniently be made by measuring the torque T acting about the axis of the disk[4] when it is magnetized to saturation along any diameter. If θ measures the direction of magnetization in the plane of the disk, we have $T = -\partial E_\theta / \partial \theta$, and E_θ may be found by integrating the experimentally found torque curve, after it has been corrected for the deviation of I_S from H. We shall see, however, that it is more convenient to work with the torque curve itself rather than to bother with integrating it.

Apparatus for measuring such torque curves has been in use for more than twenty years. That which we have used was designed to give somewhat greater accuracy than has generally been needed, and to produce sufficiently intense fields so that the sample is practically saturated since under such conditions the observed torque becomes independent of the magnitude of the applied field. A photograph of the apparatus is

[4] As we shall see later, the incomplete saturation of the edges of a disk makes it necessary to substitute an ellipsoid for a disk so as to secure best results; hence, in all that follows, "disk" should read "ellipsoid" if strict accuracy is wanted.

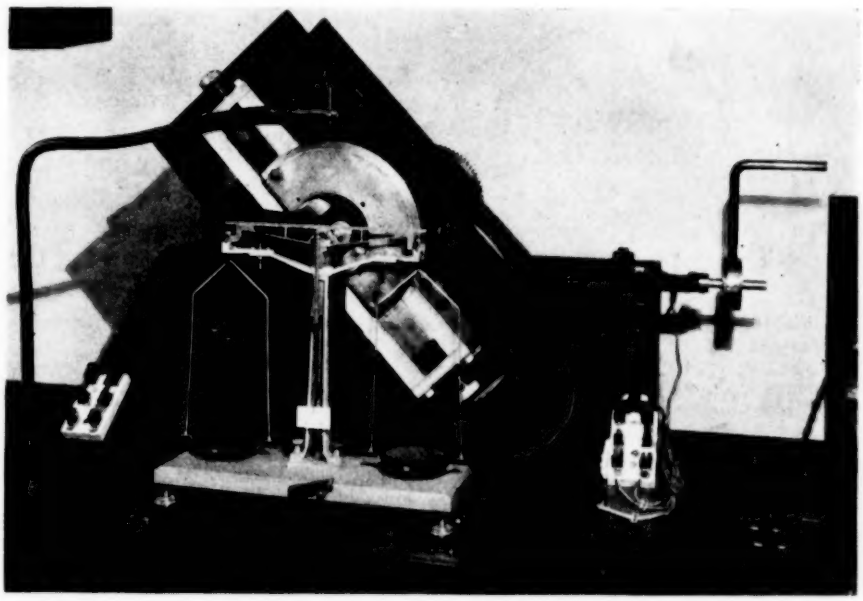

FIG. 2. Experimental set-up showing torque balance and rotating pole pieces.

shown in Fig. 2. The sample, a one-inch disk, is mounted in a light aluminum chuck with its axis accurately in line with the knife-edges of a small balance from which all ferromagnetic parts were carefully removed. Slight traces of ferromagnetism can be corrected for by a test run without a specimen. When the balance is in position, the sample is between the poles of an electromagnet which can be turned so as to produce magnetization along any diameter of the disk. Specially shaped poles are used to produce as uniform a field as possible.[5] The sample is in unstable equilibrium halfway between the poles, and any error in the alignment will cause the sample to jump to one pole face or the other. The labor in making this adjustment may be considerably lessened without sacrificing needed sensitivity by using heavy lead-weight pans. The sensitivity of the balance was in fact purposely reduced by attaching a brass weight to the pointer of the balance so that readings could be made for unstable orientations of the disk in the field. Even with these alterations, a change of 5 mg in the balancing weight could be easily detected, corresponding to a precision of better than 0.2 percent of the maximum weight which was about 3 g for several different disks. Other forms of torque-measuring apparatus may be found described elsewhere.[6]

[5] We wish to thank Professor H. B. Dwight for his assistance in designing these pole pieces.

THEORETICAL TREATMENT OF TORQUE CURVES

Since the theory on which are based the studies of preferred orientation of polycrystalline materials is developed from E_θ as given by Eq. (2), it is important to find the effect of neglecting both the higher order terms and the distortion of the curve arising from lack of parallelism between I_S and H.

As the first step let us investigate the possibility of exactly determining the orientation of a single crystal disk on the assumption that Eq. (2) holds exactly. An obvious limitation on the uniqueness of the solution is the fact that the two sides of the disk are magnetically indistinguishable, so that for any given orientation of the cubic lattice in the disk there is always a twin orientation with the plane of the disk serving as the reflection plane, the two orientations giving identical magnetic results. Since $T=-\partial E_\theta/\partial\theta$ and $E_\theta=a_F\Sigma'\alpha_i^2\alpha_j^2$, it is easily shown that

$$T/4a_F=\Sigma\alpha_i^3\partial\alpha_i/\partial\theta. \qquad (4)$$

[6] E. Dahl and F. Pfaffenberger, Zeits. f. Physik **71**, 93 (1931); N. Akulov and N. Brüchatov, Ann. d. Physik **15**, 741 (1932); K. J. Sixtus, Physics **6**, 105 (1935); H. J. Williams, R. S. I. **8**, 56 (1937).

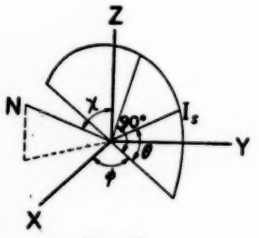

FIG. 3.

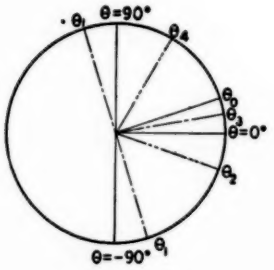

FIG. 4.

FIG. 3. Angles defining orientation of disk. X, Y, Z are the cubic axes of the crystal; N is the normal to the disk; I_S is the direction of the magnetization in the plane of the disk; θ is the angle measured in the plane of the disk.
FIG. 4. Positions of zero torque in plane of the disk.

In terms of the angles defined in Fig. 3,

$$\begin{aligned}\alpha_1&=\cos\theta\cos\phi-\sin\theta\sin\phi\cos\chi,\\ \alpha_2&=\cos\theta\sin\phi+\sin\theta\cos\phi\cos\chi,\\ \alpha_3&=\sin\theta\sin\chi.\end{aligned}\tag{5}$$

The angle θ is measured experimentally from an arbitrary diameter of the disk but in the derivation of the theory it is measured from the intersection of the disk with the XY plane. The X, Y, Z axes are of the form $<100>$.

From Eqs. (4) and (5) it can be shown that[7]

$$T/a_F=A_1\sin 2\theta+A_2\sin 4\theta+B_1\cos 2\theta+B_2\cos 4\theta,$$

where

$$\begin{aligned}A_1&=\tfrac{1}{4}\sin^2\chi[(1-7\cos^2\chi)-(1+\cos^2\chi)\cos 4\phi],\\ A_2&=-(7/8)\sin^4\chi-[(1/8)\sin^4\chi+\cos^2\chi]\cos 4\phi,\\ B_1&=-\tfrac{1}{2}\sin^2\chi\cos\chi\sin 4\phi,\\ B_2&=-\tfrac{1}{2}(1+\cos^2\chi)\cos\chi\sin 4\phi.\end{aligned}\tag{6}$$

The general behavior of a curve fulfilling the conditions of Eq. (6) is illustrated in Fig. 7. The quantities which can be determined with the greatest experimental accuracy are the four angles of zero torque occurring within an angle of 180°. Two of these positions correspond to energy minima and give stable zeros, while the other two give unstable zeros. There is no difficulty in distinguishing between the two types of zeros experimentally.

[7] Similar equations were obtained independently by S. L. Burgwin (private communication) but were not developed further. R. M. Bozorth, Phys. Rev. **50**, 1076 (1936), has obtained analogous equations for the torque but with the constants expressed in terms of the Miller indices of simple crystallographic planes and directions.

USE OF TORQUE ZEROS IN ESTABLISHING ORIENTATION

The four distinct values of θ for which $T=0$ can be found by successive approximations for any pair of values of χ and ϕ. Because of symmetry, it is necessary to investigate only those values of χ and ϕ which lie within the spherical triangle whose corners are [100], [110] and [111]. This was done for 5° intervals both of χ and ϕ, with some smaller intervals where needed. Since actual measurements of the angles of zero torque have to be made with respect to an arbitrary reference direction, it is necessary to consider not the angles, but rather the differences between them.

Let us take the angles as in Fig. 4, where $\theta=0°$ gives the reference line on the disk; $\theta=+90°$ and $-90°$ establish the sense of rotation; at θ_1 and θ_3 are found the stable zeros, at θ_2 and θ_4 the unstable zeros; and at θ_0 is the line of intersection of the disk with the XY plane (see Fig. 3). We assume from now on that $a_F>0$ as for iron; if $a_F<0$, as for nickel, then the stable and unstable zeros exchange places, but otherwise the argument is the same. If for convenience we let θ_{ij} be the absolute value of the *acute* angle between θ_i and θ_j, the experimental determination of the angles of zero torque gives θ_{13} and θ_{24} in the new notation. These two angles can be found immediately from the calculated values of θ_1, θ_2, θ_3 and θ_4. The simplest way of expressing the relation between orientation of the axes in the disk and the θ's was found to be the plotting of two families of contours, $\theta_{13}=$constant and $\theta_{24}=$constant, on a projection of the spherical triangle mentioned above. This map is shown in Fig. 5. The projection of the spherical triangle is not the commonly used stereographic one, but one in which the meridians are distorted into parallel lines in order that ordinary graph paper can be used.

A study of the map shows that appreciable changes of orientation near the [100] and [110] directions will not noticeably affect the values of θ_{13} and θ_{24}, as could be expected from the shape of the energy surface shown in Fig. 1. In about a third of the triangle the orientation is not defined uniquely on account of the double intersection of many of the θ_{13} curves with some of the

θ_{24} curves. This occurs only for $\theta_{24}<76°$. To distinguish between two such possible orientations it is necessary to calculate A_1, A_2, B_1 and B_2 for each, substitute in Eq. (6), and by using the known value of a_F for the material in question, to compare with the experimental torques. The closer the orientation approaches to the [111] corner, the less will be the magnitude of the torques, the torques finally vanishing for all angles when the disk normal becomes the [111] direction.

It is clear from Figs. 3 and 4 that the orientation of the disk with respect to the cube axes can be specified completely (except for the twinning position) only if θ_0 can be located. Exactly as was done for θ_{13}, a map was constructed for θ_{01}, as shown in Fig. 6. In order to locate θ_0 it is necessary to have some means of distinguishing between θ_1 and θ_3, and also between θ_2 and θ_4. Inspection of the calculated θ's of zero torque showed that θ_{41} is always the largest of the angles between any two consecutive zeros, except for a narrow range of orientations in which $\theta_{41}=\theta_{12}$. When there is a largest angle, as is usually the case, θ_4 and θ_1 are immediately identified, and this also fixes θ_3 and θ_2. θ_0 always lies between θ_4 and θ_3, so that it is uniquely located. In case $\theta_{41}=\theta_{12}$ it is unnecessary to distinguish between θ_2 and θ_4 since θ_{01} is found to be 90° to within a small fraction of a degree, making it immaterial in what direction from θ_1 it is measured.

To summarize here, we have obtained two families of curves relating the orientation to the angles of zero torque on the assumption that the energy of magnetization is given by Eq. (2). If

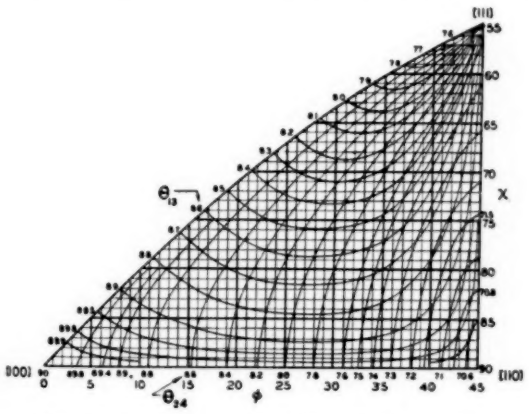

FIG. 5. θ_{13} and θ_{24} as functions of orientation.

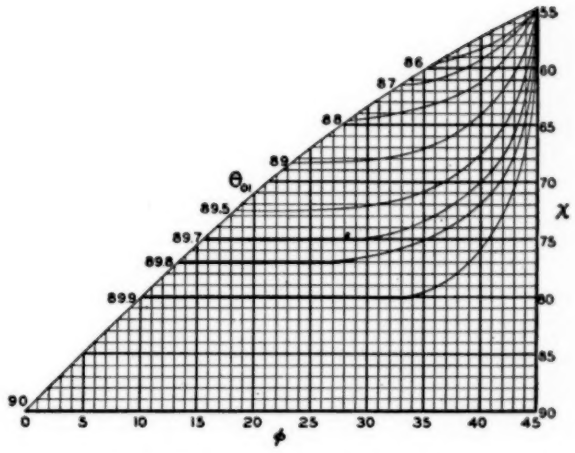

FIG. 6. θ_{01} as function of orientation.

we measure experimentally θ_{13} and θ_{24}, then χ and ϕ can be read off from Fig. 5, and θ_{01} can be found for this value of χ and ϕ from Fig. 6. An uncertainty may be introduced for a certain region of orientations on account of the double intersection of the curves θ_{13} with the curves θ_{24}, but the proper choice of χ and ϕ can be made if a_F is known. Unfortunately, a given χ and ϕ determine not one but two orientations on account of the inherent magnetic similarity of the opposite faces of the disk.

Although the method outlined above has at most a limited application as a practical means of determining the orientation of a single crystal disk, it should prove to be quite useful in studying the form of the energy anisotropy, because the knowledge of θ_0 gained by this method makes it possible to measure precisely the harmonic coefficients of the experimental torque curve. If these are compared directly with the coefficients calculated for the known x-ray orientation according to Eq. (6), we can determine a precise value of a_F in case the agreement is good. On the other hand, if we find any discrepancies to exist in the 2θ and 4θ terms or if higher harmonics, i.e. terms in 6θ, 8θ, etc. are present, we can more easily proceed to evaluate the higher order anisotropy constants such as a_F'. We shall return to the subject of more accurate forms of E_θ later. It should be pointed out here that the 2θ and 4θ terms arising from the presence of higher order anisotropy constants will make the orientation wrong to the extent that these terms interfere with the ones calculated according to Eq. (6).

Correction to Measured Torque Curves

The direction of I_S is found by setting $\partial E_{\theta,H}/\partial\theta=0$ since in this case the torque $T=-\partial E_\theta/\partial\theta$ is balanced by the component of I_S perpendicular to H. Letting $\psi=\theta_H-\theta$ where θ_H determines the direction of H, we can find from Eq. (3) that

$$\sin\psi=-T/I_SH. \tag{7}$$

For fields of the order of 2500 oersteds, the maximum value of the correction will be only 2° or 3° so that the angular correction is proportional to the torque. If we are determining the orientation of a crystal by means of the torque zeros, then the correction obviously disappears.

We have assumed in the derivation of Eq. (7) that I_S always lies in the plane of the disk even though I_S and H, are not parallel and we shall now show that in all practical cases I_S does not deviate by more than a fraction of a degree from the plane of the disk.

Let us place the disk in the XY plane and have the external field H in the Y direction. The saturation intensity I_S will, in general, make a small angle ω with the XY plane, and the projection of I_S on XY will make a small angle ψ with Y. The deviation of I_S from XY is determined by minimizing $E_{\theta,H}$ so we have $\partial E_\theta/\partial\omega-\partial(\mathbf{H}\cdot\mathbf{I})/\partial\omega=0$. Letting, L, M, N be the demagnetizing factors along X, Y, Z, the components of the field are of the form H_X-LI_X, where $H_X=H_Z=0$, $H_Y=H$, $I_X=I_S\cos\omega\sin\psi$, $I_Y=I_S\times\cos\omega\cos\psi$, $I_Z=I_S\sin\omega$, and $L=M$. Then $\mathbf{H}\cdot\mathbf{I}=HI_S\cos\psi\cos\omega-I_S^2(M\cos^2\omega+N\sin^2\omega)$ and

$$\partial E_\theta/\partial\omega=I_S\sin\omega[2I_S(M-N)\cos\omega-H\cos\psi]. \tag{8}$$

In the most unfavorable case ω is given by the largest value of $\partial E_\theta/\partial\omega$ which is $\pm1.12a_F$; this occurs when I_S is in the direction of maximum torque in the (110) plane. Setting $\cos\omega=1$ and $\cos\psi=1$,

$$\sin\omega=\frac{-1.12a_F}{I_S[2I_S(M-N)-H]}. \tag{9}$$

For the ellipsoid used in our experiments, $a_F=1.70\times10^5$, $I_S=1625$, $M-N=-12.03$ (the ratio of diameter to thickness was 54.4). For these constants, Eq. (9) becomes

$$\sin\omega=117/(39{,}100+H).$$

For $H=0$, $\omega=10'$ and for $H=5000$, $\omega=9'$. If we had used an ellipsoid whose diameter to thickness ratio was ony ten, we would find $\omega=13'$ and $11'$ for the largest possible deviations in the two cases.

We have thus shown quantitatively that the demagnetizing field normal to the plane of the disk (ellipsoid, to be exact) is so strong as to make appreciable deviations from magnetization in the plane of the disk impossible.

Experiments on Single Crystals

Preliminary experiments were carried out with seven single crystals of silicon iron,[8] which were all in the form of disks about 2 cm in diameter and 0.05 cm thick. An external field of about 2700 oersteds was used, making the effective field about 2400 oersteds.

The values of χ and ϕ as deduced from the angles of zero torque, did not check at all satisfactorily with the x-ray orientations (obtained by the usual back-reflection method), which were known to an accuracy of 1°. The discrepancies ranged from $1\frac{1}{2}$° to $5\frac{1}{2}$° and corresponded to errors in θ_{13} and in θ_{24} of 1° to 2°. As the latter could be measured to an accuracy of about 0.1°, torque curves of two specimens were analyzed on a Coradi harmonic analyzer, and terms of small but not at all negligible amplitude were found in addition to the expected terms in 2θ and 4θ.

The maximum torque had been observed to increase as much as 2 percent on changing the external field from 2700 to 3100 oersteds, and as this was not a shift of the curve in the manner of Fig. 7 but a real increase in the maximum, we filed one of the disks into an ellipsoid of revolution in order to avoid the complicated effects of nonsaturation in a disk. The proper shape was found by projecting the magnified image of the disk which was fixed on a rotating shaft onto a screen containing a drawing of an ellipse of the proper size. After the filing operation, at least

[8] These disks were kindly lent by Dr. K. J. Sixtus of the General Electric Co. Research Laboratories. The chemical analysis of the disks was: 2.8 percent Si; 0.02 percent C; 0.10 percent Mn; 0.021 percent S; P, nil.

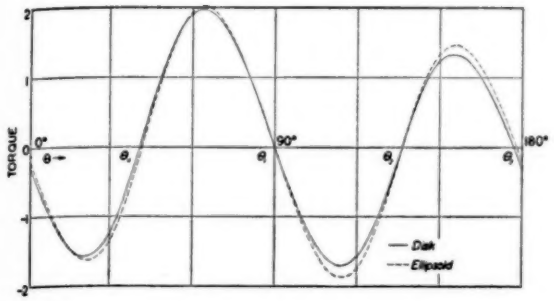

FIG. 7. Experimental torque curves for single crystal in disk and in ellipsoid form.

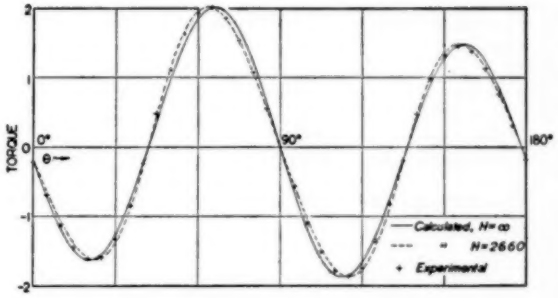

FIG. 8. Torque curves calculated for infinite field and for $H=2660$ oersteds, together with experimental points for ellipsoid.

some of the distorted surface layer was removed by applying a piece of waste soaked in $6N$ nitric acid to the rotating sample. Although any remaining distorted material might affect the results, it seems reasonable to believe that this material was randomly oriented and gave rise to no net torque; thus the only result would be to decrease the effective mass of the sample.

Torque measurements made on the ellipsoid for positions of torque maxima showed no detectable change when the field was increased as previously, so that the crystal could be assumed to be completely saturated. Torque curves of this single crystal both in the form of a disk and of an ellipsoid are shown in Fig. 7. The x-ray orientation of the sample is given by $\chi=84°$, $\phi=17\frac{1}{2}°$. Not only do the curves differ in their peaks (the curves are for the same mass of sample and the torques are in arbitrary units) but the zeros of torque do not coincide. The torque zeros of the ellipsoid curve given an orientation of $\chi=82.8°$, $\phi=18.0°$, or $1\frac{1}{2}°$ away from the x-ray orientation, while for the same sample in the form of a disk $\chi=80.2°$ and $\phi=20.3°$, a discrepancy of about $4\frac{1}{2}°$. Since the assumed x-ray orientation may itself be in error by 1°, the discrepancy of $1\frac{1}{2}°$ in the case of the ellipsoid is reasonably small and we can say that the agreement is very satisfactory.

In Fig. 8 two torque curves have been drawn, one calculated for $H=\infty$ and the other for $H=2660$ oersteds, the external field in the experimental work on the ellipsoid. Both curves were calculated for the orientation of the ellipsoid as given by x-rays, and the ordinate scale was calculated for the experimental value of a_F. The experimental points are shown as crosses, and it is seen that they fall fairly accurately on the dashed curve, the one for $H=2660$. Close inspection reveals that in some places the correction for the field is a little too large, but this slight disagreement very likely arises from the use of an inexact x-ray orientation in calculating the curve for $H=\infty$.

RESULTS OF TORQUE MEASUREMENTS

In order to show the changes that occur in the torque curves, it may be worth while to give the results of the harmonic analyses for the disk, for the ellipsoid and also for the ellipsoid when corrected according to Eq. (7). In Table I, one unit corresponds to 200 mg as weighed on the balance, so that the last decimal place is not to be regarded too seriously. The harmonic analyses could be checked within 0.01 or 0.02 unit. The torque curve is of the form $\Sigma A_n \sin 2n\theta + B_n \cos 2n\theta$. We see from this table that for this orientation at least the higher harmonics present

TABLE I. *Values of the coefficients in the harmonic analysis for the disk, for the ellipsoid, and for the ellipsoid corrected for H.*

	DISK	ELLIPSOID	ELLIPSOID, CORRECTED FOR H
A_1	1.52	1.48	1.44
A_2	−8.22	−8.87	−8.87
A_3	−0.16	−0.11	0.04
A_4	0.41	0.54	−0.06
A_5	0.04	0.00	—
A_6	—	0.03	—
B_1	−0.82	−0.52	−0.53
B_2	−0.77	−0.54	−0.62
B_3	0.04	0.03	−0.02
B_4	0.07	0.07	0.01
B_5	0.02	0.01	—
B_6	—	−0.01	—

in the disk and ellipsoid curves disappear when the field correction is applied. On the other hand, this correction does not greatly affect the value of the 2θ and 4θ terms, from which a_F is obtained; but the shape of the sample does affect the value of a_F.

The value of a_F derived for the ellipsoid is 1.70×10^5 ergs/cc and the estimated uncertainty is 0.01×10^5 ergs/cc, provided the randomly distorted surface is negligible in thickness. For the disk, a_F was calculated to be 1.60×10^5 ergs/cc, which is 6 percent too low, as would be expected because the disk near its edges is not properly magnetized to contribute its share of the torque.

In view of the possible experimental errors, the agreement between the experimental and calculated torque curves for the ellipsoid is highly satisfactory and it would be unwarranted to seek further information about the form of the anistropy from the minute discrepancies that may be left.[9] As for the disk, its shape affects not only the value of a_F but may in some cases give rise to a fictitious second anisotropy constant to take care of the 6θ and 8θ terms which occur because of the shape.

To summarize, we found that $a_F=1.70\times10^5$ ergs/cc for 2.8 percent silicon iron and that our results are adequately described by this single constant.

Results of Other Investigators

In discussing Webster's[10] torque measurements on a single crystal of iron cut as a fairly thick disk parallel to the (100) plane, Bitter[11] found an apparent increase of a_F with the field, even at very high fields of several thousand oersteds. This can now be explained satisfactorily by the incomplete saturation of a disk-shaped sample.

Gans[12] used the results of Honda and Kaya[13] to calculate a value of a_F' for pure iron. In the curves given by Honda and Kaya $\theta_{13}=87°$ instead of 90°, as should be the case for the ellipsoid used, which had [110] for its axis of revolution; this leads to an uncertainty in the angular measure. Also an effective field of only 507 oersteds may be insufficient to eliminate small low field deviations from the curve which would be obtained at several thousand oersteds. Bozorth[14] shows in Fig. 1 of his paper the slight effect on the torque curve of a value of a_F' similar to the value found by Gans. The uncertainties in the original data seem to be large enough to make them unsuitable for extracting information about the magnitude of a_F'.

Williams[15] has made torque measurements on a disk cut parallel to the (110) plane. The discrepancy between his calculated and experimental curves can be explained by reference to Figs. 7 and 8.

The existence of a second anisotropy constant has been postulated to explain the existence of ferromagnetic alloys with [110] as a direction of easy magnetization. In order that we can have more than a qualitative check of the magnetization curves, such as has been obtained by Bozorth,[14] it is necessary to determine accurately the form of the anisotropy and this is possible only if the pitfalls discussed above are avoided. With a really accurate knowledge of the anisotropy constants, as obtained directly from torque measurements on single crystal ellipsoids cut in the proper directions, it should be possible to construct quite accurate magnetization curves. In such a case, any discrepancy between theory and experiment would call for a re-examination of the basic magnetization theory rather than cast doubt upon the correctness of the anisotropy constants which are involved.

[9] We found that by letting $a_F'=0.5\times10^5$ erg/cc (see Eq. (1)), $A_3=0.04$ and $B_3=-0.025$, which would agree nicely indeed with the values in the last column of Table I. Yet if we introduce a_F' to account for these very small coefficients, we should introduce an energy term of the form $a_F''\times$(eighth order terms in α) in order to account for A_4, which is of the same size as A_3. The introduction of these higher order terms would account not only for harmonics that may be of an entirely accidental nature, but would give rise to appreciable terms in 2θ and 4θ, which in turn would affect the calculated value of a_F. Thus the addition to E_θ of a correction term in a_F' alone does not seem justifiable, at least in the present case.

[10] W. L. Webster, Proc. Roy. Soc. **107**, 496 (1925).

[11] F. Bitter, Phys. Rev. **39**, 371 (1932).

[12] R. Gans, Physik. Zeits. **33**, 924 (1932).

[13] K. Honda and S. Kaya, Tôhoku Univ. Sci. Reports **15**, 721 (1926).

[14] R. M. Bozorth, reference 7.

[15] H. J. Williams, reference 6.

Effect of Time-Reversal Symmetry on Energy Bands of Crystals

CONYERS HERRING
Princeton University, Princeton, New Jersey
(Received June 16, 1937)

In the Hartree and Fock approximations the description of the electronic state of a crystal can be made in terms of one-electron wave functions and one-electron energies, which have a band structure. It is known that in addition to the "sticking together" of these energy bands caused by the spatial symmetry of the crystal, additional "sticking" may be necessitated by the fact that the Hamiltonian of the problem is real. In this paper a criterion is developed to facilitate calculation of when and how such additional degeneracy will occur. The consequences of the reality of the Hamiltonian are tabulated for a number of cases. It is pointed out that the same "sticking together" of bands occurs in the theory of the frequency spectrum of the normal modes of vibration of a crystal.

SINCE much of the work now being done on the electron theory of metals is based on the theory of Brillouin zones, i.e., on the picture of almost free electrons or on the Hartree approximation with or without corrections for exchange, it is desirable that the properties of the wave functions and energy values occurring in this type of approximation be clearly understood. An important one of these properties, namely the "sticking together" of energy bands because of the symmetry of the crystal, has recently been discussed by Bouckaert, Smoluchowski, and Wigner.[1] Additional coincidences in the energies of different wave functions are sometimes necessitated by the fact that the Hamiltonian of the problem is real, as these authors have also noted. It has been shown by Hund[2] that for close-packed hexagonal crystals important coincidences in the energies of wave functions with the same wave vector are necessitated by this reality property. We may class as "accidental" any coincidences in the energies of different wave functions with the same wave vector which are not attributable either to the symmetry or to the reality of the Hamiltonian. In this paper a general theory of coincidences due to the reality of the Hamiltonian will be presented; accidental coincidences will be taken up in the following paper.

In Hartree's equations for a crystal the one-electron wave functions ψ_i satisfy

$$(-\hbar^2/2m\nabla^2+V)\psi_i=E_i\psi_i,$$

where $V(\mathbf{r})$ is the potential of the positive nuclei plus the potential due to the charge distribution of all the electrons. The function $V(\mathbf{r})$ has all the periodicities and symmetries of the lattice. In Fock's equations the ψ_i satisfy

$$(-\hbar^2/2m\nabla^2+V-A)\psi_i=E_i\psi_i,$$

where V is as above and A is the Fock exchange operator. It is not hard to show that solutions of Fock's equations exist for which the operators V and A have all the periodicities and symmetries of the given lattice of nuclei, and for which the operator A as well as V is real, i.e., takes every real wave function into a real wave function. Let us restrict ourselves to the consideration only of those solutions of Fock's equations for which V and A possess the symmetry and reality just mentioned. Now all the considerations to be made below apply to the eigenfunctions and eigenvalues of any real Hamiltonian operator commuting with the space group of the crystal. The results of this paper will therefore apply to the one-electron ψ_i and E_i occurring in the solution of Hartree's or of Fock's equations.

As is well known, the wave functions of an electron moving in the trebly periodic force field of a crystal can be taken to be eigenstates of the three fundamental translations of the crystal lattice, and as such may be written in the form $\psi_k=\exp(i\mathbf{k}\cdot\mathbf{r})u_k$, where u_k is a periodic function of position with the three periodicities of the lattice. This equation leaves $\mathbf{k}$ undetermined by 2π times any translation of the reciprocal lattice; the shortest vector $\mathbf{k}$ with which a given wave function can be written in this form is called the

[1] Bouckaert, Smoluchowski, and Wigner, Phys. Rev. **50**, 58 (1936).
[2] F. Hund, Zeits. f. Physik **99**, 119 (1936).

"reduced wave vector" of the wave function, or in the following simply its "wave vector." The set of all vectors $\mathbf{k}$ having the property that no vector of shorter length can be reached from any of them by adding a vector 2π times a translation of the reciprocal lattice will cover the interior and surface of a polyhedron called the first Brillouin zone, for which the abbreviation B-Z will be used hereafter. Any point $\mathbf{k}$ on the surface of the B-Z is reachable from one or more other points $\mathbf{k}'$ of the surface of the B-Z by 2π times a translation of the reciprocal lattice, and it will be convenient to speak of any function $\exp(i\mathbf{k}\cdot\mathbf{r})u_k$ as possessing the same wave vector as another function of the form $\exp(i\mathbf{k}'\cdot\mathbf{r})u_{k'}$; i.e., two wave functions will be said to possess the same wave vector when they have the same eigenvalues of the operations of the translation group of the crystal.

In the following the terms "linear manifold" and "subspace of Hilbert space" will be used synonymously to denote the set of all linear combinations of any given basic set of wave functions, and the set of all linear combinations of the wave functions of several linear manifolds will be called the "subspace spanned by" these manifolds. The symbol (ψ_1, ψ_2) will be used for the scalar product $\int\int\int \psi_1^* \psi_2 d\tau$ of any two wave functions ψ_1 and ψ_2.

The coincidences among the energies of the various eigenfunctions which are due to the reality of the Hamiltonian of any problem have been discussed by Wigner.[3] These coincidences, as well as those due to the spatial symmetry of the Hamiltonian, turn out to be connected with the properties of the various representations of the spatial symmetry group of the Hamiltonian, which for the present problem is the space group of the crystal. Some mathematical theorems on the irreducible representations of space groups have been given by Seitz.[4] From references 1, 3, and 4 the following facts may be noted:

The set of all operations of the space group which take every wave function characterized by a particular wave vector $\mathbf{k}$ into the same or another wave function with the same wave vector forms a subgroup G^k of the space group, which may be called the "group of the wave vector." If one forms the subspace of Hilbert space spanned by a manifold σ^k of wave functions with wave vector $\mathbf{k}$ which reduces G^k together with the $(M-1)$ other manifolds into which σ^k is transformed by the operations of the space group, this subspace will be transformed irreducibly into itself by the whole space group. The set of wave vectors occurring in an irreducible representation of the space group may be referred to as the "star" of the representation.

For all wave vectors $\mathbf{k}$ except those lying in certain planes, lines, or isolated points in the B-Z, the group G^k consists only of the translation group, so that for a particular $\mathbf{k}$ all representations of G^k are equivalent and one-dimensional. For wave vectors lying in certain planes but avoiding certain lines and points, G^k may consist of the translation group plus a reflection or glide plane operation. Further symmetry elements, leading to the existence of multidimensional representations of G^k, may be present when $\mathbf{k}$ terminates on certain lines or assumes certain isolated values.

The conclusions of Wigner are based on the fact that whenever the Hamiltonian of a problem is real, the complex conjugate of any eigenfunction is also an eigenfunction with the same energy. The operation of taking the complex conjugate is to be interpreted as an operation which takes a wave function employed by one observer to describe some state of the system into a wave function which could be employed to describe the same physical state by an observer whose space axes coincide with those of the first, but whose time axis is oppositely directed. Wigner shows that if in any linear manifold of eigenfunctions the representation of the spatial symmetry group of the Hamiltonian is irreducible and equivalent to a representation by means of real matrices only, then the wave functions of the manifold will, in general, have an energy different from the energies of all other wave functions; an irreducible manifold the representation in which cannot be made real must however always have the same energy as the complex conjugate manifold, which will be linearly independent of it and in which the representation D^* of the symmetry group may be either equivalent or inequivalent to the original representation D.[5]

It will be convenient to have a criterion by which from a knowledge of the combination laws of the group elements and their characters in any irreducible representation it can be decided whether that representation is inequivalent to its complex conjugate, is equivalent but cannot be made real, or can be made real. Such a criterion can be obtained by using a theorem first proved by Frobenius and Schur.[6] This theorem states that if D is any irreducible representation of a finite group G, of order N, and if $\chi_D(R)$ is the character in D of the group element R, then

[3] E. Wigner, Gött. Nachr. (1932), p. 546.
[4] F. Seitz, Ann. of Math. **37**, 17 (1936).

[5] These statements are valid when, as in the present case, the wave function does not contain spin. When spin is included the time-reversal operation takes a more complicated form.
[6] Frobenius and Schur, Berl. Ber. (1906), p. 186.

$$\left.\begin{aligned}
\textstyle\sum \chi_D(T^2) = N \quad & \text{if } D \text{ is equivalent to a representation by means of real matrices,}\\
= 0 \quad & \text{if } D \text{ and } D^* \text{ are inequivalent,}\\
= -N \quad & \text{if } D \text{ is equivalent to } D^* \text{ but not to any representation consisting entirely of real matrices.}
\end{aligned}\right\} \quad (1)$$

The summation in (1) is to be extended over all elements T of G. The first possibility will from now on be referred to as case (a), the second as case (b), and the third as case (c).

To apply this result to any space group let the space group be replaced by a group containing the same elements with the same combination rules except that the νth power of any translation operation is the identity. This group has only a finite number of elements, so that the summation on T in (1) can be carried out. If, as is usually done, the representation space is made to consist of all wave functions which are unchanged when displaced by ν times any fundamental translation, all representations of the space group will be identical with corresponding representations of the finite group. Any element of the group which belongs to the coset defined by any Q_0 into the translation group is of the form $Q_i = Q_0 t_i$ where t_i is some operation of the translation group. So the element $Q_i^2 = Q_0^2(Q_0^{-1} t_i Q_0) t_i$ belongs to the coset defined by Q_0^2. The summation over all elements Q_i of the group may be broken up into a summation on t_i and a summation over the different cosets, which may be labeled by the corresponding point group operations Q. If a basis is chosen reducing the translation group,

$$\sum_{Q_i} \chi_D(Q_i^2) = \sum_{\mathbf{k},\mu} \sum_{Q} \sum_{\mathbf{t}_i} [\psi_{k\mu},\, Q_0^2 \times \exp(-i\mathbf{k}\cdot(Q\mathbf{t}_i + \mathbf{t}_i))\psi_{k\mu}],$$

where the operation t_i replaces the vector $\mathbf{r}$ by $(\mathbf{r}-\mathbf{t}_i)$ and where μ labels the different basis functions when two or more have the same wave vector $\mathbf{k}$. The summation on $\mathbf{k}$ is, of course, over all wave vectors in the star of D. Now

TABLE I.

Q_0	Relation D to D^*
J	(a)
C_2	(a)
$\bar{C}_2$	(a), (c)
C_2, J	(a)
$\bar{C}_2$, J	(a), (b)

$$\sum_{\mathbf{t}_i} \exp(-i\mathbf{k}\cdot(Q\mathbf{t}_i + \mathbf{t}_i)) = \sum_{\mathbf{t}_i} \exp(-i(Q^{-1}\mathbf{k}+\mathbf{k})\cdot\mathbf{t}_i)$$
$$= 0 \quad \text{if } Q^{-1}\mathbf{k} \neq -\mathbf{k} + 2\pi\mathbf{g},$$
$$= \nu^3 \quad \text{if } Q^{-1}\mathbf{k} = -\mathbf{k} + 2\pi\mathbf{g},$$

where $\mathbf{g}$ is any translation of the reciprocal lattice. Also, since all the vectors of the star are similar, all terms in the summation on $\mathbf{k}$, which is to be carried out last, are equal. So if h is the order of the macroscopic symmetry group and M the number of distinct wave vectors in the star of D, (1) becomes

$$\sum_{Q}\sum_{\mu} (\psi_{k\mu},\, Q_0^2 \psi_{k\mu}) = \pm h/M \quad \text{or} \quad 0, \qquad (2)$$

where in the summation on Q only those point group operations Q are to be included which take $\mathbf{k}$ into a vector equivalent to $-\mathbf{k}$, and where Q_0 may be any single space group operation belonging to the coset corresponding to Q. Only one wave vector $\mathbf{k}$ of the star is to be used. The steps in applying (2) are thus:

Determine an irreducible representation of G^k.

Select those operations Q of the point group of the crystal which take $\mathbf{k}$ to a vector equivalent to $-\mathbf{k}$.

To each of the operations Q so chosen, there will correspond a coset in the space group; from each such coset choose an operation Q_0 of the space group arbitrarily.

Evaluate the character of each Q_0^2 in the irreducible representation of G^k, and sum over the different Q_0's. Then, according to whether the result is h/M, 0, or $-h/M$, case (a), (b), or (c) obtains for the irreducible representation D of the space group of which the above irreducible representation of G^k is a part.

When $\mathbf{k}$ is a general point of the B-Z, G^k is the translation group, and if an operation Q is present taking $\mathbf{k}$ to a wave vector equivalent to $-\mathbf{k}$, it can only be the inversion. In such case Q_0^2 is the identity, and the positive sign must occur in (2). So for the general point of the B-Z either D and D^* have different stars or else D can be made real; time-reversal symmetry never causes the energies of two wave functions with the same wave vector $\mathbf{k}$ to coincide when $\mathbf{k}$ is a general point of the B-Z.

Consider next what can happen when $\mathbf{k}$ is a general point of some plane in the B-Z, so that every operation Q which takes $\mathbf{k}$ to a point equivalent to $-\mathbf{k}$ takes any other point $\mathbf{k}'$ of this plane into one equivalent to $-\mathbf{k}'$. The only point operations Q which can take every point of

TABLE II.

Q	RELATION D TO D^*
J, $2S_6$	(a) or (b)
J, $2S_6$, $2S_3$, S_2	(a) or (b)
S_2, $2S_3$	(a) or (b)
$2S_4$	(a) or (c)
J, S_2, $2S_4$	(a) or (b)
$2C_2$, $2S_4$	(a) or (b)

a plane into a point equivalent to its inverse are the inversion J and the rotation C_2 about a twofold axis perpendicular to the plane. If no such operation is present D and D^* must of course be inequivalent with different stars. When D and D^* have the same star their relationship is easily verified to be as given in Table I. The first column contains the coset representatives, one for each point group operation taking $\mathbf{k}$ to a vector equivalent to $-\mathbf{k}$. All representations of the space group belonging to the star of $\mathbf{k}$ are of the type denoted by the letter in the second column. In the third and last lines the first letter refers to the case where $\mathbf{k}$ is in a plane inside the B-Z, the second to the case where $\mathbf{k}$ is in a boundary plane. The symbols J, C_2 stand, respectively, for an inversion and a pure rotation through π about some axis. The symbol $\bar{C}_2$ is used for a twofold screw axis of such nature that no operation $\bar{C}_2 t$ of the same coset as $\bar{C}_2$ is a pure twofold rotation without an accompanying translation.

Table I shows therefore that: first, if a boundary plane of the B-Z is perpendicular to a twofold screw axis no element of whose coset is a pure twofold rotation, then the energy bands must stick together in pairs at the points of this plane; secondly, under no other circumstances do the symmetry and reality of H require that two eigenfunctions with the same wave vector $\mathbf{k}$ have the same energy when $\mathbf{k}$ is a general point of a plane of symmetry.

When $\mathbf{k}$ is a general point of a line of symmetry there are so many possibilities for the constitution of the group G^k that it is not convenient to list them all. When $\mathbf{k}$ is an interior point of the B-Z, however, the situation is rather simpler than when the line of which $\mathbf{k}$ is a general point lies in a boundary plane of the B-Z. For such an interior point it is not difficult to find out whether representations of types (b) or (c) can occur. Consider one of the terms $(\psi_{k\mu}, Q_0{}^2\psi_{k\mu})$ occurring in (2). If this is not to equal $+1$, then either $Q^2 \neq E$, i.e., the square of the point group operation Q is not the identity, or else $Q_0{}^2 = t$, where t is a translation in a direction not perpendicular to $\mathbf{k}$. The second possibility is excluded by the fact that Q takes any vector in the direction of $\mathbf{k}$ into one in the opposite direction (if $\mathbf{k}$ were a point on the boundary of the B-Z this would not have to be the case). Now it is easily verified that the only operations Q which occur in any of the crystalline point groups and which have the properties, first, that $Q^2 \neq E$, and secondly, that there exists a direction in space taken into the opposite direction by Q, are the following:

$$Q = S_4, \text{ giving } Q^2 = C_2,$$
$$Q = S_6 \text{ or } S_3, \text{ giving } Q^2 = C_3.$$

Here C_2 and C_3 stand for two- and threefold proper rotations, and S_3, S_4, and S_6 for three-, four-, and sixfold rotations followed by reflection in a plane perpendicular to the axis of rotation. It is easily established that when $\mathbf{k}$ is a general point of a line of symmetry inside the B-Z the positive terms in (2) must always overbalance the complex and negative terms, except in the six cases listed in Table II. This means that if $\mathbf{k}$ is a point of this type whose star contains $-\mathbf{k}$, all representations of the space group belonging to this star are of type (a) unless the set of point operations Q taking $\mathbf{k}$ to $-\mathbf{k}$ is exactly one of the sets listed. In all the cases listed some of the representations having the star of $\mathbf{k}$ are of type (a) and some are of one of the other types; for this reason (a) is always included in the second column.

It can be seen that for all the rows of Table II except the last G^k is cyclic. So we can say that when $\mathbf{k}$ lies along a three-, four-, or sixfold axis, only case (a) can occur if G^k is not cyclic, i.e., only case (a) can occur if a reflection plane passes through the axis. Further, if the space group contains an inversion, only case (a) can occur if $\mathbf{k}$ is along a twofold axis.

In conclusion it should be pointed out that the results listed above have consequences not only for the electronic energy spectrum of the crystal, but also for the frequency distribution of its normal modes of vibration. For it can be shown that the normal modes of a crystal correspond to

basis vectors for a real representation of the space group of the crystal, and that the normal modes, belonging to a representation which is irreducible in the field of real numbers, even though reducible in the complex field, must all have the same frequency.[7] Thus mathematically the theory of normal modes and their frequencies is just like the theory of electronic wave functions and their energies: frequency can be plotted as a function of wave vector, and sticking together of two or more of these frequency bands will occur at wave vectors $\mathbf{k}$ where G^k has multidimensional representations or where case (b) or case (c), as defined above, occurs.

It is a pleasure for me to express my thanks to Professor E. Wigner, who suggested this problem.

[7] Cf. E. Wigner, Gött. Nachr. (1930), p. 133.

AUGUST 15, 1937 PHYSICAL REVIEW VOLUME 52

Accidental Degeneracy in the Energy Bands of Crystals

CONYERS HERRING
Princeton University, Princeton, New Jersey
(Received June 16, 1937)

The circumstances are investigated under which two wave functions occurring in the Hartree or Fock solution for a crystal can have the same reduced wave vector and the same energy. It is found that coincidence of the energies of wave functions with the same symmetry properties, as well as those with different symmetries, is often to be expected. Some qualitative features are derived of the way in which energy varies with wave vector near wave vectors for which degeneracy occurs. All these results, like those of the preceding paper, should be applicable also to the frequency spectrum of the normal modes of vibration of a crystal.

IN previous papers, by Bouckaert, Smoluchowski, and Wigner,[1] and by the author,[2] certain properties of the wave functions and energy values of an electron moving in the periodic field of a crystal were derived. These properties were the properties necessitated by the symmetry of the crystal and by the reality of the Hamiltonian. The two questions to be discussed in this paper are:

(1) In the solution of Hartree's or Fock's equations for a crystal to what extent may one expect to encounter accidental coincidences in energy between two one-electron wave functions with the same wave vector? By "accidental" coincidences are to be understood coincidences not necessitated by the symmetry and reality of the Hamiltonian.

(2) If the energies of two or more bands coincide at wave vector $\mathbf{k}$, whether accidentally or for reasons of symmetry and reality, how may the energies of these bands be expected to vary with wave vector in the neighborhood of $\mathbf{k}$?

The analysis necessary to answer these questions is rather tedious. Despite this and the fact that it may not be of practical significance to bother about too fine details in an approximate theory, the discussion to be given below may be of value in forming pictures of the energy band structures of metals, especially of multivalent ones. In particular, it is hoped that the complete determination of energy as a function of wave vector by interpolation from the results of calculations of the Wigner-Seitz-Slater type will be facilitated and made more reliable. The results of this paper also apply, as did those of I, to the frequency spectrum of the normal modes of vibration of a crystal; however numerical calculation of these frequencies has not yet advanced as far as has the calculation of electronic bands.[3]

The notation to be used is the same as in I. In addition, the symbol $[M^1, M^2]$ will be introduced to represent the subspace of Hilbert space spanned together by any two linear manifolds of wave functions M^1 and M^2.

[1] Bouckaert, Smoluchowski, and Wigner, Phys. Rev. **50**, 58 (1936), hereafter referred to as BSW.
[2] Preceding paper, hereafter referred to as I.
[3] Calculations for a simple cubic lattice have been made by M. Blackman, Proc. Roy. Soc. **A159**, 416 (1937).

1. Preliminary Definitions

In order to discuss accidental energy coincidences it is first necessary to group together all those eigenfunctions which because of the symmetry and reality of the Hamiltonian necessarily have the same energy. If $\psi_k{}^i$ is any eigenfunction with wave vector $\mathbf{k}$ and energy $E^i(\mathbf{k})$, application to $\psi_k{}^i$ of the operations of the space group and the operation K of taking the complex conjugate will generate a linear manifold of wave functions all eigenfunctions of H with energy $E^i(\mathbf{k})$. Such a linear manifold of eigenfunctions which can be generated from an eigenfunction with wave vector $\mathbf{k}$ will, if it is irreducible under K and the space group, be designated by a symbol $M^i(\mathbf{k})$; of course it will in general contain wave functions with wave vectors different from $\mathbf{k}$. Any $M^j(\mathbf{k})$ will be called equivalent to $M^i(\mathbf{k})$ when the representation of the space group in $M^j(\mathbf{k})$ is equivalent to that in $M^i(\mathbf{k})$. As explained in I, the representation of the space group in $M^i(\mathbf{k})$ may be irreducible (case (a)), reducible into two inequivalent parts (case (b)), or reducible into two equivalent parts (case (c)).

Now the occurrence of an accidental coincidence in energy means simply that for some particular $\mathbf{k}$ two independent manifolds $M^i(\mathbf{k})$ and $M^j(\mathbf{k})$ can be found whose energy values coincide. Such an accidental energy coincidence will be called for brevity a "contact," and $\mathbf{k}$ will be called a "contact point." Two kinds of contacts may occur, according to whether $M^i(\mathbf{k})$ and $M^j(\mathbf{k})$ are inequivalent or equivalent. These will be discussed, respectively, in Sections 2 and 4. In this paper we are not interested in all the types of contacts which are possible with specially chosen forms for the potential energy function occurring in the Hamiltonian, but only in those which may be expected to occur in the Hartree or Fock solution for an actual crystal. For example, it is not hard to find a potential $V=V_0(x, y, z)$ for which the locus of the points of contact between the two lowest energy bands is a two-dimensional surface in $\mathbf{k}$-space. However, almost any infinitesimal change which may be made in the function V will give rise to a new Hamiltonian whose spectrum has no contacts at all.[4] For an actual crystal, the factors determining the potential energy function V are quite unrelated to the conditions V must satisfy in order that there exist a contact region of the type just mentioned; consequently it is safe to assert that no actual crystal will be encountered for which V has the form V_0. In general, it will be legitimate to characterize any property of a contact or a contact region (e.g., the property of the contact region being a two-dimensional surface) as "vanishingly improbable" if it ceases to exist after some infinitesimal change is made in the form of the function V which does not alter the symmetry of V. This concept will be used principally in giving precise formulation to the theorems of Section 4.

2. Contacts of Inequivalent Manifolds

The way in which contacts of wave functions with different symmetry properties come about is most easily seen by considering some particular examples. Consider first the energies of two wave functions whose wave vectors $\mathbf{k}$ lie in a plane of symmetry in the B-Z. Let one of these, say $\psi_k{}^i$, be even with respect to reflection in this plane and the other, $\psi_k{}^j$, be odd. Suppose it is known that at some point $\mathbf{k}_1$ of this plane the even function has higher energy than the odd, and that at another point $\mathbf{k}_2$ the odd has higher energy than the even. Then, since the energy of the odd function and the energy of the even function are both continuous functions of wave vector in this plane, there must be a curve in the plane along which the two energies are equal. It must be impossible to get from $\mathbf{k}_1$ to $\mathbf{k}_2$ without crossing this curve. Therefore this curve must be a closed ring about either $\mathbf{k}_1$ or $\mathbf{k}_2$, or else it must extend to infinity when energy is plotted as a periodic function of wave vector in the infinite reciprocal lattice space. It may happen, of course, that part of this curve coincides with a line of symmetry in the B-Z, along which sticking together of the even band and the odd band is necessitated by symmetry.

For another example consider the band structure of sodium. The graph of energy against k

[4] A simple example occurs when the potential is separable in rectangular coordinates. A two-dimensional contact region will occur when a crossing of energy curves occurs in one of the one-dimensional problems to which the three-dimensional problem is reduced, and it is well known that almost any small perturbation will dissolve such a crossing in one dimension. Cf. v. Neumann and Wigner, Physik. Zeits. **30**, 467 (1929).

when $\mathbf{k}$ lies along a fourfold axis of the B-Z is qualitatively as shown in Fig. 1. It is known[5] that for $\mathbf{k}=0$ the lowest state of the valence electron is the $3s$-like state, which belongs, in the notation of BSW, to the irreducible representation Γ_1 of the full cubic group. The next lowest state at $\mathbf{k}=0$ arises from the atomic $3d$ level; this splits in the crystal field into a triply degenerate level Γ_{25}' and a double degenerate one Γ_{12}. For definiteness it will be assumed here that Γ_{25}' lies lower, although the two are so close together that the usual methods of calculation ignore their separation altogether. At the corner of the B-Z, G^k is again the whole space group. The lowest level is the $3p$-like level Γ_{15}, and the $3s$-like level Γ_1 comes next, a little higher. This information alone suffices to determine the way in which the curves should be drawn between the end points 0 and $2\pi/d$. For we may label the different symmetry types of wave functions at intermediate points by the irreducible representations Δ of the group of their wave vectors. The form of the curves is determined by the fact that the Δ belonging to any curve cannot change suddenly at any place between 0 and $2\pi/d$, and the fact that each Γ contains only certain representations Δ. Note that Γ_{12}, which must connect with Γ_1, lies higher than Γ_{25}', which must connect with something at $2\pi/d$ which is above Γ_1. Therefore the curves of types Δ_2', Δ_1, must cross at some intermediate point.

Considerations of the same sort apply to any path of points in the B-Z whose G^k contains rotations or reflections, provided the path is such that all the representations of the space group vary continuously along the path and bear the same relationships to their complex conjugates. The order in energy of the different types of manifolds $M(\mathbf{k}_1)$, $M(\mathbf{k}_2)$, at the end points may necessitate contacts of inequivalent manifolds at intermediate points. And if either end point, say $\mathbf{k}_1$, has a G^{k_1} of which the G^k of the intermediate points is a subgroup, the types of manifolds at intermediate points which can connect with any $M(\mathbf{k}_1)$ can be determined group-theoretically, with due regard for the consequences of time-reversal symmetry.

[5] Approximate values for the energies of the different eigenfunctions at the center and corner of the B-Z can be obtained from J. C. Slater, Phys. Rev. **45**, 794 (1934), Fig. 1.

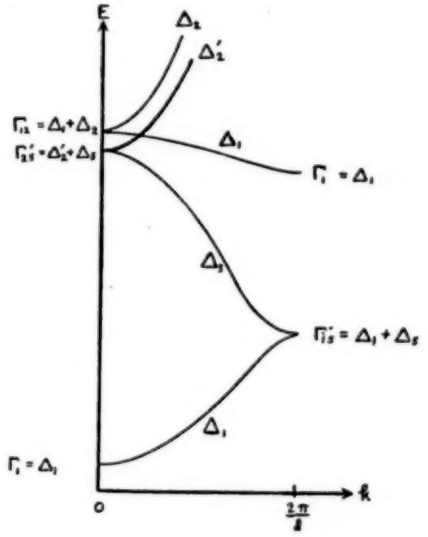

FIG. 1. The representations Δ_1, Δ_2, Δ_2', are one-dimensional, Δ_5 is two-dimensional.

Calculations made for more complicated metals show such contacts of inequivalent manifolds of eigenfunctions along axes of symmetry in the B-Z.[6] Naturally, however, not all such contacts which occur can be predicted from a knowledge of the energies of the different manifolds at the two ends of the axis.

3. Variation of Energy Near Contacts

If all the wave functions which have wave vector $\mathbf{k}$ and a single energy $E^i(\mathbf{k})$ are known, the neighboring energies of the wave functions which have a wave vector $(\mathbf{k}+\boldsymbol{\kappa})$ in the neighborhood of $\mathbf{k}$ can be determined to the first order in κ by perturbation theory. For, since any

$$\psi_k=\exp(i\mathbf{k}\cdot\mathbf{r})u_k$$

where u_k has the periodicities of the lattice,

$$\exp(-i\mathbf{k}\cdot\mathbf{r})H\psi_k=\{-\hbar^2/2m\nabla^2 -i\hbar^2/m\mathbf{k}\cdot\nabla+\hbar^2k^2/2m+V\}u_k=E_ku_k \quad (1)$$

and the term $-i\hbar^2/m\boldsymbol{\kappa}\cdot\nabla$ can be treated as a perturbation. Eq. (1) holds when the Hamiltonian H is of the Hartree type; when we are interested in the solution of Fock's equations we must introduce the exchange operator $-A$

[6] H. M. Krutter, Phys. Rev. **48**, 664 (1935), (copper); Manning and Krutter, Phys. Rev. **51**, 761 (1937), (calcium).

into H, and this means that

$$-A_k = -\exp(-i\mathbf{k}\cdot\mathbf{r})A\exp(i\mathbf{k}\cdot\mathbf{r})$$

must be added to the operator in the brackets. There is then an added perturbation $-\boldsymbol{\kappa}\cdot\partial A_k/\partial\mathbf{k}$.

It will be convenient in the following to use the symbol $m^i(\mathbf{k})$ for the linear manifold spanned by the wave functions u_k which can be obtained by multiplying by $\exp(-i\mathbf{k}\cdot\mathbf{r})$ those wave functions ψ_k of $M^i(\mathbf{k})$ which have wave vector $\mathbf{k}$. If $M^i(\mathbf{k})$ and $M^j(\mathbf{k})$ have the same energy, the neighboring energies at $(\mathbf{k}+\boldsymbol{\kappa})$ are determined to within terms of the order of κ^2 by the solution of a secular equation involving the matrix elements of $i\nabla$ (for the Hartree case) in $[m^i(\mathbf{k}), m^j(\mathbf{k})]$.

When two wave functions $\psi_k{}^i$, $\psi_k{}^j$, and no more, have the same $\mathbf{k}$ and the same energy, the solution of the second order secular equation gives for the energy separation δE at $(\mathbf{k}+\boldsymbol{\kappa})$ of the two bands which come into contact at $\mathbf{k}$

$$\delta E(\mathbf{k}+\boldsymbol{\kappa}) = [(\boldsymbol{\kappa}\cdot\mathbf{f})^2+4|\boldsymbol{\kappa}\cdot\mathbf{g}|^2]^{\frac{1}{2}}+O(\kappa^2), \quad (2)$$

where the vectors $\mathbf{f}$ and $\mathbf{g}$ are defined, for the Hartree case, as

$$\left.\begin{aligned}\mathbf{f} &= -i\hbar^2/m[(u_k{}^i, \nabla u_k{}^i)-(u_k{}^j, \nabla u_k{}^j)],\\ \mathbf{g} &= i\hbar^2/m(u_k{}^i, \nabla u_k{}^j),\end{aligned}\right\} \quad (3)$$

and for the Fock case are these quantities plus matrix elements of $\partial A_k/\partial\mathbf{k}$.

When the degeneracy at $\mathbf{k}$ is threefold it is less simple to give an explicit formula for the energies of the three bands at $(\mathbf{k}+\boldsymbol{\kappa})$. It is, however, possible in most cases to derive a criterion which will tell us whether, for a given direction of $\boldsymbol{\kappa}$, the separation of every pair of the bands is of the order of κ as $\kappa\to 0$, as in (A), Fig. 2, whether two of them have a separation of the order κ^2, as in (B), or whether all the separations are of the order κ^2, as in (C). To do this we start from the following fact:[7] if a third order secular equation $\det(H_{\mu\nu}-\lambda\delta_{\mu\nu})=0$ with $H_{\mu\nu}$ real and equal to $H_{\nu\mu}$ possesses two coincident roots $\lambda=\lambda_1$, then the equation obtained by setting to zero the minor of any element in $\det(H_{\mu\nu}-\lambda\delta_{\mu\nu})$ must have λ_1 as a root. Conversely if every minor has λ_1 as a root, the secular equation must have λ_1 as a double root, since in this case the derivative of the secular determinant with respect to λ will have λ_1 as a root. Now the condition that the minors of H_{12}, H_{13}, and H_{23} have the same root turns out to be the same as the condition that for $\mu\neq\nu=1, 2, 3$ the root of the minor of $H_{\mu\nu}$ be also a root of the minor of $(H_{\mu\mu}-\lambda)$. This condition is

$$\begin{aligned}H_{12}H_{13}H_{23}H_{11}-H_{12}{}^2H_{13}{}^2 &= H_{12}H_{13}H_{23}H_{22}\\ -H_{23}{}^2H_{12}{}^2 &= H_{12}H_{13}H_{23}H_{33}-H_{13}{}^2H_{23}{}^2. \quad (4)\end{aligned}$$

So when none of the three quantities H_{12}, H_{13}, H_{23} vanishes, the satisfaction of (4) implies that all minors of the secular determinant have a common root, and thus that the secular equation has a double root. When (4) is satisfied by virtue of the vanishing of two of the three nondiagonal elements, however, two of the nondiagonal minors vanish identically in λ. In this case it cannot be concluded that the principal minors have a root in common, since concerning one of the principal minors nothing more is known than that it has a root in common with a polynomial which vanishes identically. To insure that all the principal minors have a common root it will be sufficient to use the conditions that for μ, ν, σ all different and running from 1 to 3 the minor of $(H_{\mu\mu}-\lambda)$ have a root in common with that of $H_{\nu\sigma}$. These are

$$\left.\begin{aligned}(H_{22}+H_{33})(H_{23}H_{11}-H_{13}H_{12})H_{23}&\\ -(H_{23}H_{11}-H_{13}H_{12})^2&\\ -H_{23}{}^2(H_{22}H_{33}-H_{23}{}^2)=0,&\\ \text{Permutations of this}=0.&\end{aligned}\right\} \quad (5)$$

Thus the satisfaction of (5) as well as (4) insures existence of a double root except in the trivial case where $H_{12}=H_{13}=H_{23}=0$.

In the present case the matrix elements $H_{\mu\nu}$ will be the matrix elements of $-i\hbar^2/m\boldsymbol{\kappa}\cdot\nabla$ or of $-i\hbar^2/m\boldsymbol{\kappa}\cdot\nabla-\boldsymbol{\kappa}\cdot\partial A_k/\partial\mathbf{k}$. The criteria (4), (5), will be applicable if a basis can be found in $[m^i(\boldsymbol{\kappa}), m^j(\mathbf{k})]$ with respect to which all these matrix elements are real.

In order to apply (2), (4) and (5) it is necessary to know what restrictions are placed on the matrix elements of the vector operator $i\nabla$, or of $\partial A_k/\partial\mathbf{k}$, by the fact that all the basis functions ψ_k are eigenfunctions of a real Hamiltonian H which has the symmetry of the crystal. These restrictions can be obtained in a straightforward manner from the fact that the three components

[7] Burnside and Panton, *Theory of Equations*, Vol. II, p. 66.

of the vector operator in question are pure imaginary operators plus the fact that they form a basis for a representation of the space group which is characterized by wave vector zero and which therefore is simply the point group representation for a polar vector. For the various cases which will be needed later on the most general forms consistent with the spatial and time-reversal symmetry restrictions, which the matrix elements of an imaginary Hermitian polar vector operator $\mathbf{F}$ can assume, are listed in Tables I to IV. The basic wave functions to which these matrix elements are referred have been chosen as follows:

All the basis functions have the same wave vector $\mathbf{k}$.

Each basis function is an eigenfunction of some operation in G^k, as is indicated explicitly in connection with each of the tables.

When an inversion J is present in the space group, the phases of the basis functions are so chosen that the operation JK takes each basis function into itself, K being the time-reversal operator which takes every function into its complex conjugate.

When no inversion is present but a twofold rotation C_2 or $\bar{C}_2$ is included among the operations $Q_{(k)0}$ which take $\mathbf{k}$ into a wave vector equivalent to $-\mathbf{k}$, the phases are to be so chosen that C_2K or $\bar{C}_2K$ takes each basis function into itself.

When neither an inversion nor a twofold axis is included among the $Q_{(k)0}$, the phases of the basis functions do not matter.

Table I gives the matrix elements of a vector operator $\mathbf{F}$ of the type described above in the subspace spanned by two wave functions $\psi_k{}^i$ and $\psi_k{}^j$. Each matrix element of $\mathbf{F}$ is a vector. In the first three rows the manifolds $M^i(\mathbf{k})$, $M^j(\mathbf{k})$, to which $\psi_k{}^i$, $\psi_k{}^j$, belong cannot be inequivalent; in the last two, however, the functions $\psi_k{}^i$, $\psi_k{}^j$, may be both even with respect to reflection in the plane of symmetry, both odd, or one even and one odd. The symbol listed first in each of the columns for $\mathbf{F}_{ij}$ refers to the case where both are even or both odd, the second symbol to the the case where one is even and the other odd. The symbol $\perp$ means that the vector in question must be perpendicular to the twofold axis (or perpendicular to the normal to the reflection plane) but is otherwise unrestricted. The symbol $\parallel$ means that the vector must be parallel to this axis. As in I, $\bar{C}_2$ stands for a twofold screw axis, and $\bar{S}_2$ stands for a glide plane. In the column headed "case" $M^i(\mathbf{k})$ and $M^j(\mathbf{k})$ are classified according to their time-reversal properties, as in Table I of I; some of the possibilities are however omitted from the present table.

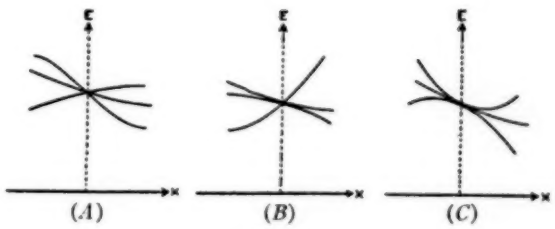

FIG. 2.

Tables II, III, and IV apply along various symmetry axes of the B-Z for simple, body-centered, and face-centered cubic crystals. An inversion is assumed to be present in the space group. Tabulated is the vector $(\psi_k{}^i, \mathbf{F}\psi_k{}^j)$ for the different possible representations of G^k to which $\psi_k{}^i$ and $\psi_k{}^j$ may belong. The notation for these representations is that of BSW. The quantities ρ are arbitrary real numbers, and the ϵ's are unit vectors. Table II is for points $\mathbf{k}$ on a twofold symmetry axis; here ϵ is parallel to the axis of C_2, ϵ_a is perpendicular to the axis of C_2 in the plane taken into itself by $JC_4{}^2$, and ϵ_b is perpendicular to the axis of C_2 and to ϵ_a. Table III is for points $\mathbf{k}$ on a threefold axis. It is supposed that one of the three symmetry planes JC_2 passing through the axis has been singled out; + and − refer, respectively, to eigenfunctions even and odd with respect to reflection in this plane; ϵ is parallel to the axis of C_3, ϵ_a is perpendicular to the axis of C_3 in the plane of the JC_2 selected, and ϵ_b is perpendicular to the axis of C_3 and perpendicular to the plane of the JC_2. Table IV is for points $\mathbf{k}$ on a fourfold axis. It is as before supposed that one of the two symmetry planes JC_2 containing the axis has been chosen; + and − refer to eigenfunctions even and odd with respect to reflection in this plane; ϵ is parallel to the axis of C_4, ϵ_a is perpendicular to the axis of C_4 in the plane of the JC_2 selected, and ϵ_b is perpendicular to the axis of C_4 and to the JC_2.

Table II, given for the representations Σ of the group possessed by points on a twofold axis inside the B-Z may be used also for the representations of the groups belonging to the general points S, Z, G, D, of lines in the boundaries of the B-Z of Figs. 2, 3, and 4 of BSW. The groups of Z and of D do not contain the same operations

as the other two; for these the ϵ's must be oriented relative to the corresponding symmetry planes.

From (2), (3), and the two last lines of Table I we can calculate δE for points in $\mathbf{k}$-space near a curve of contact of even and odd wave functions in a symmetry plane. When no inversion is present in the space group we may expect that as we go out from any point $\mathbf{k}$ of the contact curve the energy separation $\delta E(\mathbf{k}+\boldsymbol{\kappa})$ is of the order κ for any direction of $\boldsymbol{\kappa}$ not in the plane of symmetry. This is because it can safely be assumed that the real and imaginary parts of $\mathbf{g}$ do not vanish simultaneously at any point of the curve. When an inversion is present however the real part of $\mathbf{g}$ always vanishes, and since there will in general be points of the curve at which the imaginary part of $\mathbf{g}$ vanishes, we may expect sometimes to find points on the curve where $\delta E(\mathbf{k}+\boldsymbol{\kappa})$ is of the order κ^2 when $\boldsymbol{\kappa}$ is perpendicular to the plane. Whether an inversion is present or not, $\delta E(\mathbf{k}+\boldsymbol{\kappa})$ may be expected to be of the order κ when $\boldsymbol{\kappa}$ is in the plane and perpendicular to the curve.

For contact points on a symmetry axis where m^i and m^j are each one-dimensional we may expect that $\delta E(\mathbf{k}+\boldsymbol{\kappa})$ is always of the order κ when $\boldsymbol{\kappa}$ is not perpendicular to the axis, and when $\boldsymbol{\kappa}$ is perpendicular to the axis is of order κ^2 or κ according to whether the table requires $\boldsymbol{\kappa}\cdot\mathbf{g}$ to vanish or not. It may be noted too from (2), (3), and Table IV that at points near a fourfold axis the energy separation of two bands which stick together everywhere on the axis (representation Δ_5) is always of the order of the square of the distance from the axis; likewise, from Table III, the separation of two bands which stick together everywhere on a threefold axis (representation Λ_3) is of the order of the distance from the axis, except near points of the axis where $\bar{\rho}_{33}$ vanishes.

Consider finally the energy variation near contacts of Λ_3 with one of the other Λ's, or Δ_5 with one of the other Δ's. For a contact of Δ_5 with one of the other Δ's it is easily verified by use of Table IV with (4) and (5), or alternatively by solving the third order secular equation explicitly, that the energy separation of any pair of the three bands may be expected to grow proportionally to κ as we go out from a contact point $\mathbf{k}$ to $(\mathbf{k}+\boldsymbol{\kappa})$ (except when $\boldsymbol{\kappa}$ is in the direction of the axis). In other words, the situation is as in (A) of Fig. 2, for every direction of $\boldsymbol{\kappa}$ except along the axis. For a contact of Λ_3 with one of the other Λ's the secular equation obtained from Table III is more complicated, and since it cannot readily be solved explicitly, (4) and (5) must be used. The result is best described with reference to Fig. 3. The plane of the drawing is a plane through the contact point $\mathbf{k}$ and normal to the axis of C_3, and the three lines are the intersections of this plane with the three symmetry planes JC_2. When the projection of $\boldsymbol{\kappa}$ on the plane of the drawing points in one of the three directions shown by the full lines and the angle between $\boldsymbol{\kappa}$ and the axis of C_3 has a certain value θ, we may expect $\delta E(\mathbf{k}+\boldsymbol{\kappa})$ between one pair of the three bands to be of the order κ^2. We may also expect $\delta E(\mathbf{k}+\boldsymbol{\kappa})$ between a pair of the bands to be of the order κ^2 when the projection of $\boldsymbol{\kappa}$ on the plane of the drawing points in the direction of one of the dotted lines and the angle between the axis of C_3 and $\boldsymbol{\kappa}$ is $(\pi-\theta)$. Thus for these directions of $\boldsymbol{\kappa}$ the situation is as in (B) of Fig. 2; for all other directions of $\boldsymbol{\kappa}$, except along the axis, $\delta E(\mathbf{k}+\boldsymbol{\kappa})$ is on the order κ, and the situation is as in (A) of Fig. 2.

TABLE I.

$Q_{(k)0}$	CASE	$\mathbf{F}_{ii}$ OR $\mathbf{F}_{jj}$	REAL PART $\mathbf{F}_{ij}$	IMAGINARY PART $\mathbf{F}_{ij}$
None (G^k the translation group alone)	(b)	Unrestricted	Unrestricted	Unrestricted
J	(a)	Unrestricted	Unrestricted	0
C_2 or $\bar{C}_2$	(a)	$\perp$	$\perp$	$\parallel$
C_2, J or $\bar{C}_2$, J	(a)	$\perp$	$\perp$, 0	0, $\parallel$
None (G^k the translation group plus S_2 or $\bar{S}_2$)	(b)	$\perp$	$\perp$, $\parallel$	$\perp$, $\parallel$

4. CONTACTS OF EQUIVALENT MANIFOLDS

In this section it will be shown that situations exist in which two energy bands touch at general points in $\mathbf{k}$-space and cannot be separated by any perturbation, and some properties of contacts of this sort will be given. More precisely stated, it will be shown that the existence of wave vectors $\mathbf{k}$ for which the energy of some $M^i(\mathbf{k})$ coincides with the energy of some $M^j(\mathbf{k})$

TABLE II.

ψ^i \ ψ^j	Σ_4	Σ_3	Σ_2	Σ_1
Σ_1	$\rho_{14}\epsilon_a$	$\rho_{13}\epsilon_b$	0	$\rho_{11}\epsilon$
Σ_2	$\rho_{34}\epsilon_b$	$\rho_{23}\epsilon_a$	$\rho_{22}\epsilon$	
Σ_3	0	$\rho_{33}\epsilon$		
Σ_4	$\rho_{44}\epsilon$			

TABLE III.

ψ^i \ ψ^j	Λ_3 +	Λ_3 −	Λ_2	Λ_1
Λ_1	$\rho_{13}\epsilon_a$	$\rho_{13}\epsilon_b$	0	$\rho_{11}\epsilon$
Λ_2	$\rho_{23}\epsilon_b$	$\rho_{23}\epsilon_a$	$\rho_{22}\epsilon$	
Λ_3 −	$\bar{\rho}_{33}\epsilon_b$	$\rho_{33}\epsilon-\bar{\rho}_{33}\epsilon_a$		
Λ_3 +	$\rho_{33}\epsilon+\bar{\rho}_{33}\epsilon_a$	$\bar{\rho}_{33}\epsilon_b$		

TABLE IV.

ψ^i \ ψ^j	Δ_5 +	Δ_5 −	Δ_1'	Δ_2'	Δ_2	Δ_1
Δ_1	$\rho_{15}\epsilon_a$	$\rho_{15}\epsilon_b$	0	0	0	$\rho_{11}\epsilon$
Δ_2	$\rho_{25}\epsilon_b$	$-\rho_{25}\epsilon_a$	0	0	$\rho_{22}\epsilon$	
Δ_2'	$\rho_{2'5}\epsilon_a$	$-\rho_{2'5}\epsilon_b$	0	$\rho_{2'2'}\epsilon$		
Δ_1'	$\rho_{1'5}\epsilon_b$	$\rho_{1'5}\epsilon_a$	$\rho_{1'1'}\epsilon$			
Δ_5 −	0	$\rho_{55}\epsilon$				
Δ_5 +	$\rho_{55}\epsilon$	0				

equivalent to it is not a vanishingly improbable phenomenon in the sense of Section 1.

Consider first the case of a crystal without an inversion center. For simplicity the Hartree case only will be considered, as the reasoning proceeds identically in the Fock case. Suppose the potential $V(\mathbf{r})$ of such a crystal to have a form possessing a twofold axis of symmetry, but no other symmetries except its translational periodicities. Suppose further that at some point $\mathbf{k}$ on the axis the energy of the wave function unchanged by the twofold rotation crosses the energy of the wave function which changes sign on rotation. This is a perfectly possible state of affairs. By the same method as was used in constructing Tables I to IV it can be verified that the only restriction placed on the vectors $\mathbf{f}$ and $\mathbf{g}$ defined

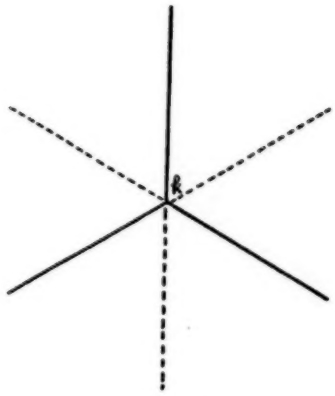

FIG. 3.

in (3) by the symmetry and reality of the Hamiltonian are that $\mathbf{f}$ must lie in the direction of the axis and the real and imaginary parts of $\mathbf{g}$ must be perpendicular to the axis. It will therefore certainly be permissible to assume that the three vectors $\mathbf{f}$, the real part of $\mathbf{g}$, and the imaginary part of $\mathbf{g}$ are not coplanar at the contact point $\mathbf{k}$, i.e., there will certainly exist potential functions $V(\mathbf{r})$ for which a contact occurs at a point on the axis where these vectors are not coplanar. Now let the potential be changed to a form possessing no symmetry at all except the translational periodicity, by addition of a term $vU(\mathbf{r})$. The function $U(\mathbf{r})$ is a fixed unsymmetrical periodic function, and v is an infinitesimal positive number. Treating this term as a perturbation we may calculate its effect on the energies of wave functions whose wave vectors are near to $\mathbf{k}$, by solving a second order secular equation. The result is similar to (2):

$$\delta E=\{[\delta E_0+v(U_{ii}-U_{jj})]^2+4|vU_{ij}|^2\}^{\frac{1}{2}}+R \quad (6)$$

where δE is $(E^i(\mathbf{k}')-E^j(\mathbf{k}'))$ after the perturbation, δE_0 is this quantity before perturbation, and where for sufficiently small v the remainder R satisfies $|R|<2Av^2$ with A independent of $\mathbf{k}'$ in the neighborhood of $\mathbf{k}$. All the quantities on both sides are to be evaluated at the same point $\mathbf{k}'$.

Suppose now that after the potential has been changed to $(V+vU)$ no contact occurs in the neighborhood of the original contact point $\mathbf{k}$. Then the energy separation δE must have a minimum at some point in the neigborhood of $\mathbf{k}$. It can be verified from (6) that the point at

which this minimum occurs must be one at which both the inequalities

$$|\delta E_0+v(U_{ii}-U_{jj})|<4Av^2, \quad |U_{ij}|<2Av \quad (7)$$

were satisfied. At this minimum after the perturbation the gradient of δE must be zero in every direction, i.e., $\mathbf{f}$ must vanish, and so $\mathbf{f}$ must be coplanar with the real and imaginary parts of $\mathbf{g}$. Now a necessary and sufficient condition that these three vectors be coplanar is that the lower bound of the quadratic form $(\boldsymbol{\kappa}\cdot\mathbf{f})^2+4|\boldsymbol{\kappa}\cdot\mathbf{g}|^2$ for all vectors $\boldsymbol{\kappa}$ of unit length and varying direction be zero. This lower bound depends only on the subspace $[u^i, u^j]$ and is independent of the choice of basis functions u^i, u^j within it. Before the perturbation this lower bound was not zero at $\mathbf{k}$, and since the subspace $[u_{k'}{}^i, u_{k'}{}^j]$ must vary in a continuous manner with $\mathbf{k}'$, there must be a finite neighborhood of $\mathbf{k}$ in which this lower bound was $>\epsilon>0$. It will therefore be possible, whatever the form of the function $U(\mathbf{r})$, to find a v small enough to insure that the lower bound of the quadratic form remains >0 after the perturbation at every point at which the inequalities (7) were satisfied. For such a small value of v the supposition that no contact occurs after the perturbation is therefore untenable: after the potential has been changed to the form $(V+vU)$ there is still a contact at some point near $\mathbf{k}$, and since the Hamiltonian no longer possesses any but translational symmetry, this contact is a contact of *equivalent* manifolds $M^i(\mathbf{k})$ and $M^j(\mathbf{k})$.

For a crystal with an inversion center a similar argument can be constructed, which need only be given in outline. Let a potential function possessing an inversion center and a symmetry plane be made into a potential function possessing an inversion center but no symmetry plane by addition of a small unsymmetrical perturbation vU. If a closed curve of contact of the even with the odd wave function in the symmetry plane exists before the perturbation, a closed curve of contact must persist after the perturbation, if the perturbation is sufficiently small. This is because if any portion of the curve disappeared there would have to have to be a whole line of points after the perturbation at which $\mathbf{f}$ practically vanished. It can be seen from the second line of Table I that this means that $\mathbf{f}$ and $\mathbf{g}$ must be practically collinear at these points, and this is impossible if these vectors were not collinear at the corresponding points of the curve of contact before the perturbation.

The preceding paragraphs, although they are not intended as complete proofs and leave unanswered numbers of questions which may come to mind, will, I hope, suffice to make plausible most of the theorems which will now be stated. The proofs of these are too lengthy to be given here;[8] they are based upon the type of perturbation considerations which have been used in this section and in the preceding one. The theorems are:

For crystals without an inversion center, contacts of equivalent manifolds $M^i(\mathbf{k})$, $M^j(\mathbf{k})$ may occur for isolated points $\mathbf{k}$, and such contacts cannot be destroyed by an infinitesimal change in the potential function V. Such contact points $\mathbf{k}$ may lie in a symmetry plane in the B-Z or in a plane perpendicular to a twofold axis, provided the representation of the space group in each of the manifolds $M^i(\mathbf{k})$, $M^j(\mathbf{k})$ is irreducible, i.e., provided case (*a*) occurs; in such case no infinitesimal change in V preserving the symmetry of the crystal can cause the contact point to move out of the plane. Except for this possibility, it is vanishingly improbable for a contact point to lie in a plane or line of symmetry in the B-Z.

For a crystal whose space group consists only of its translation group the total number of distinct points $\mathbf{k}$ of the B-Z at which the energies of two given bands i and j come into contact must be a multiple of four, i.e., any other number is vanishingly improbable. (Time-reversal symmetry requires that $-\mathbf{k}$ be a contact point if $\mathbf{k}$ is a contact point, hence merely that the number of contacts be a multiple of two; the restriction to multiples of four is therefore rather noteworthy.) Since any crystal of higher symmetry can be made into one of such low symmetry by an infinitesimal change in the form of the potential V, this implies a restriction on the number of contact points for any crystal without an inversion center.

[8] They are contained in a dissertation submitted to the faculty of the department of physics at Princeton University, 1937. The proofs are there given for the Hartree case, but may easily be generalized to the Fock case or to the frequency spectrum of normal modes of vibration.

For crystals with an inversion center, contacts of equivalent manifolds $M^i(\mathbf{k})$, $M^j(\mathbf{k})$ may occur at all points $\mathbf{k}$ of an endless curve, or of a number of such curves, in $\mathbf{k}$-space. These contact curves cannot be destroyed or broken by any infinitesimal change in the potential V which preserves the inversional symmetry. It is vanishingly improbable for such curves to lie in planes of symmetry in the B-Z; however a contact curve may pass through a symmetry axis at a point where necessary degeneracy or contact of inequivalent manifolds occurs.

Suppose that for a crystal with an inversion center a contact of inequivalent manifolds $M^i(\mathbf{k})$, $M^j(\mathbf{k})$ occurs at a point $\mathbf{k}$ on a symmetry axis, and suppose that $m^i(\mathbf{k})$ and $m^j(\mathbf{k})$ are each one-dimensional. Then if the vector $\mathbf{g}$ (proportional in the Hartree case to $(\psi_k{}^i, i\nabla\psi_k{}^j)$) does not vanish, a curve of contact must pass through $\mathbf{k}$. This curve may be a curve of contact of equivalent manifolds of the type just described, or it may be a curve of contact of inequivalent manifolds in a plane of symmetry. Naturally if there is no such symmetry plane in the space group, the former alternative must hold.

For a crystal whose space group consists only of its translation group plus an inversion, three types of contact curves may occur, which are most easily described when energy is considered as a trebly periodic function of wave vector in the infinite reciprocal lattice space. The first type is a simple closed circuit which is distinct from the circuit obtained from it by the inversion $\mathbf{k}\rightarrow-\mathbf{k}$. The second type is a simple closed circuit which either coincides with the inverse circuit or can be brought into coincidence with it by 2π times a translation of the reciprocal lattice. The third type is a curve extending periodically to infinity. Now consider any energy band i, and the band j next above it. For each of the eight distinct points $\mathbf{k}_r$ ($r=1$ to 8) of the B-Z whose G^{k_r} contain the inversion let the numbers $N^+(\mathbf{k}_r, i)$, $N^-(\mathbf{k}_r, i)$, of odd and of even eigenfunctions $\psi_{k_r}{}^l$ be counted which have energies $E^l(\mathbf{k}_r) \leqslant E^i(\mathbf{k}_r)$. Now the quantity

$$\tfrac{1}{2}\sum_{r=1}^{8}\left[N^+(\mathbf{k}_r, i)-N^-(\mathbf{k}_r, i)\right]$$

is an integer, and according to whether this integer is odd or even the number of circuits of the second type along which contact between the bands i and j occurs must be odd or even. Since any crystal with an inversion center can be made by an infinitesimal change in the form of V into one whose space group is merely its translation group plus the inversion, this implies certain restrictions on the numbers of contact curves which may occur for crystals of higher symmetry. Prediction of the existence of curves of contact of equivalent manifolds may therefore be possible from a knowledge merely of the energies of the different $M^l(\mathbf{k}_r)$ at the eight points $\mathbf{k}_r$.

For a crystal without an inversion center, the energy separation $\delta E(\mathbf{k}+\boldsymbol{\kappa})$ in the neigborhood of a point $\mathbf{k}$ where contact of equivalent manifolds occurs may be expected to be of the order of κ as $\kappa\rightarrow 0$, for all directions of $\boldsymbol{\kappa}$.

For a crystal with an inversion center, the energy separation $\delta E(\mathbf{k}')$ at a point $\mathbf{k}'$ near a curve of contact of equivalent manifolds may be expected to be of the order of the distance of $\mathbf{k}'$ from the curve.

All kinds of contacts of equivalent manifolds except the ones described above are vanishingly improbable. In particular, the occurrence of isolated points of contact of equivalent manifolds for crystals with an inversion center is vanishingly improbable.

I should like to express my gratitude to Professor E. Wigner for his interest in this work, and to Dr. L. P. Bouckaert and Dr. R. Smoluchowski for some interesting discussions.

The Second Virial Coefficient of Argon

KARL F. HERZFELD
Catholic University of America, Washington, D. C.
(Received June 4, 1937)

The second virial coefficient of argon is calculated from the energy expression obtained for frozen argon.

SOME time ago, K. F. Herzfeld and M. Goeppert-Mayer investigated[1] the equation of state of frozen argon. The potential energy between two argon atoms at the distance was assumed to have the form

$$U=-ar^{-6}+b\exp(-r/\rho) \qquad (1)$$

with a van der Waals attraction according to London and a repulsion of the form introduced by Born and Mayer.[2] For ρ, two values were used: $\rho=0.345$A, which is the value found to fit the alkalihalides,[2] and $\rho=0.2091$, calculated[3] from quantum theory for the interaction between neon atoms. This latter is in close agreement with that obtained theoretically for helium atoms.[4] a and b were then calculated from the experimental data for the lattice constant and heat of sublimation.

The resultant formulae are

$$U=-1.11\times10^{-10}r^{-6}+1.34\times10^{-9}\exp(-r/\rho)\text{ erg for }\rho=0.345\text{A}, \qquad (2)$$

$$U=-0.78\times10^{-10}r^{-6}+0.74\times10^{-6}\exp(-r/\rho)\text{ erg for }\rho=0.2091\text{A}, \qquad (3)$$

r in A.

At the suggestion of Professor R. H. Fowler, the second virial coefficient B for argon gas, defined by

$$pV=RT(1+BV^{-1}\cdots)$$

was calculated according to the well-known expression

$$B=2\pi N\int[1-(\exp-U/kT)]r^2dr.$$

The results are found in the following table.

TABLE I. *Second virial coefficient of argon B in cc.*

T	B exp	$B(2)$	$B(2)-B$ exp	$B(3)$	$B(3)-B$ exp
173.1	−64.35	−66.37	−2.02	−44.80	19.55
223.1	−37.83	−37.69	0.14	−21.75	16.08
273.1	−22.09	−20.75	1.34	−7.47	14.62
323.1	−11.04	−9.69	1.35	0.63	11.67
373.1	−4.29	−1.93	2.36	6.75	11.04
423.1	1.16	3.82	2.66	11.28	10.12
473.1	5.28	8.07	2.79	14.60	9.32
573.1	11.22	14.17	2.95	19.41	8.19
673.1	15.30	18.24	2.94	23.11	7.81

The column headed "exp" embodies the measurements of Holborn and Otto,[5] $B(2)$ and $B(3)$ are the theoretical values calculated with (2) and (3). As can be seen, the fit of $B(2)$ is rather good. A slight modification of ρ (which has been taken over from the alkalihalides) could probably improve it further, if one took the trouble to recalculate the new values of a and b for the crystal.

If argon atoms were rigid spheres without attraction of diameter 3.78A (the distance of the minimum of the potential curve), B would be 69.2 cc.

[1] Karl F. Herzfeld and M. Goeppert-Mayer, Phys. Rev. **46**, 995 (1934).
[2] M. Born and Joseph E. Mayer, Zeits. f. Physik **75**, 1 (1932).
[3] W. E. Bleick and J. E. Mayer, J. Chem. Phys. **2**, 252 (1934).
[4] J. C. Slater and J. G. Kirkwood, Phys. Rev. **37**, 682 (1931).
[5] L. Holborn and J. Otto, Zeits. f. Physik **30**, 320 (1924); **33**, 1 (1925). The values are cited according to K. F. Herzfeld, *Handbuch der Physik*, Vol. 24, second edition (1933), p. 205.

Neutron-Induced Radioactivity of the Noble Metals

EDWIN MCMILLAN, MARTIN KAMEN
Radiation Laboratory, Department of Physics, University of California, Berkeley, California

AND

SAMUEL RUBEN*
Department of Chemistry, University of California, Berkeley, California

(Received July 19, 1937)

WE have started a study of the effects produced by neutrons on the elements in the neighborhood of platinum, and some of the results, although admittedly incomplete, seem sufficiently striking to merit publication at this time. Strong activities are induced in Ir, Pt and Au by slow neutrons, and in these metals and Hg by fast ($Li+H^2$) neutrons. Os, Tl, Pb and Bi give only comparatively weak activities with either type of neutrons. Our results so far on the strong activities, in order of increasing complexity, are given below.

MERCURY

This element has been reported to give a weak activity of 40 hr. half-life with slow neutrons,[1] and a strong activity of 43-min. half-life with fast neutrons.[2] We find the fast neutron 43-min. period to be indeed very strong, corresponding to an intensity with 10 μA of 5.5 Mev deuterons striking the Li target, after exposure to saturation, of 18 divisions per second on the electroscope.[3] Also a new period of 25 hrs., with a saturation intensity of 2 div./sec., was found. This was only weakly activated by the exposures used, and its properties have not been studied. The particles emitted by the 43-min. activity are negative (determined by a Thibaud trochoid apparatus, for the use of which we are indebted to Mr. Ernest Lyman). A chemical separation showed that this (as well as the 25-hr. period) is a mercury isotope. From this information we can place the 43-min. period in the system of isotopes, as being most probably Hg^{203}.

The 43-min. beta-particles are very soft; the absorption curve in aluminum shows a well-defined end point at 0.130 ± 0.005 g/cm², giving an upper limit of 0.42 Mev by Feather's formula. This low energy for such a short life does not fit at all on the usual Sargent curves. There is also a strong gamma-ray, with an absorption in Pb indicating a possible complex structure with energies in the range 70–250 Kev.

GOLD

With slow neutrons, the well-known 2.7-day period[4] is produced with a saturation intensity of 860 div./sec. The absorption curve of the beta-rays has an end point at 0.31 ± 0.01 g/cm² of Al, corresponding to an upper limit of 0.78 Mev. The strong gamma-ray has an absorption in Pb indicating an energy of about 460 Kev. The beta-particles are all negative.

Fast neutrons on Au produce a much more complex activity. There is a 13-hr. period of saturation intensity 1 div./sec., and what appears at first to be a 3.3-day period of saturation intensity 6 div./sec. On following the decay of this, however, the logarithmic plot deviates from a straight line after about 10 days, and seems to be going into a slope of 4–5 days. This shows that the apparent 3.3-day period is a mixture, presumably of the 2.7-day period and a longer one in about equal amounts. We have shown that neither resonance nor thermal neutrons are responsible for producing the 2.7-day period here, since a sample surrounded by a thick sheet of

* Abraham Rosenberg Fellow.

[1] Anderson, Nature **137**, 457 (1936).

[2] Heyn, Nature **139**, 842 (1937).

[3] One division per second corresponds to about 10^4 beta-particles per second emitted from the target. All intensities given are calculated for an exposure to saturation with a 10 μA deuteron beam, although of course different intensities and times were actually used. For the Li neutron exposures, the samples were about 2 cm from the target, surrounded by a layer of B_2O_3 containing about 1/2 g/cm² of B. For the slow neutron exposures, they were about 5 cm from a Be target, enclosed in a large block of paraffin. The samples were all of about the same size (~0.1 g) but in some cases the beta-particles are so soft that even the thin sheets used do not allow them all to escape. No attempt has been made to correct for this.

[4] Fermi, Amaldi, D'Agostino, Rasetti, and Segrè, Proc. Roy. Soc. **146A**, 483 (1934).

gold is activated as strongly as one without this, and the boron layer is sufficient to stop all thermal neutrons.

Chemical separation shows that all these periods belong to gold isotopes, and they are also found to emit only negative electrons. This leads to some difficulty in placing the 13-hr. and 4–5-day periods in the system of isotopes, since only one space (Au^{196}) satisfies the necessary conditions for both of them. Au^{195} would be expected to emit positive electrons, unless a new stable Hg isotope (Hg^{195}) should exist. It seems possible that we have here another case of nuclear isomerism.[5]

Iridium

With slow neutrons, we find the known 19-hr.[4] and 2-month[6] periods, with saturation intensities 120 and 280 div./sec., respectively. We find also a 1.5-min. period with intensity 28 div./sec. This is easily missed if the longer periods are activated strongly, and the observations delayed until several minutes after activation, but by using short exposures it is brought out prominently. It was observed in three different iridium samples, one of which is known to be of very high purity, and we feel that it cannot be due to a contamination. We have done no chemistry on iridium, but by analogy with other slow neutron processes all three of these periods should be attributed to the two isotopes Ir^{192} and Ir^{194}, so that we may have another case of isomerism here.

The 19-hr. beta-rays have an end point in Al of 0.99 ± 0.02 g/cm^2, corresponding to an energy of 2.1 Mev. The 2-month beta-particles are much softer.

With fast neutrons, a very long period (presumably 2 months) is produced with saturation intensity 10 div./sec., as well as a complex array of shorter periods that we have not succeeded in analyzing, using the present data. The 1.5-min. period is present with a saturation intensity of 0.2 div./sec., and the 19-hr. period is buried in the midst of a continuously curving logarithmic plot, so that we cannot be sure of its presence. It is certainly less intense relative to the 2-month period than with slow neutron activation, just as is the 1.5-min. period, so that we can provisionally assign the 2-month period to Ir^{192} and the other two to Ir^{194}. The other unresolved periods again offer difficulties, since all the emitted electrons are negative. No chemical separation has been made.

Platinum

Platinum with slow neutrons gives three periods, 31 min., 18 hrs., and 3.3 days, the saturation intensities being, respectively, 1.2, 0.8, and

[5] Snell, Phys. Rev. **51**, 1011 (1937), and Bothe and Gentner, Naturwiss. **25**, 284 (1937), find such a case in bromine.

[6] Fomin and Houtermans, Physik. Zeits. Sowjetunion **9**, 273 (1936).

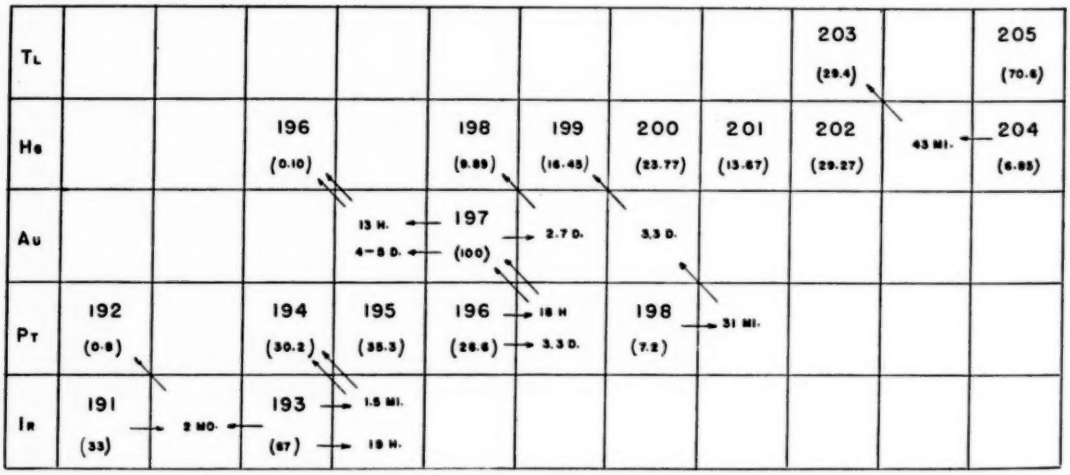

FIG. 1. Isotope chart, showing provisional assignment of identified activities. Figures in parentheses are percentage abundances of stable isotopes. Horizontal arrows indicate neutron capture or ejection, and diagonal arrows indicate β-particle emission.

1.2 div./sec. These might be assigned to the isotopes Pt^{193}, Pt^{197}, and Pt^{199}, but the observation that they all give negative beta-particles makes this unlikely, since Pt^{193} cannot form a known stable isotope by emitting a negative electron. A chemical separation helped to clear up this situation—the gold precipitate showed a 3.3-day activity. Reference to the isotope chart shows that one would expect Pt^{199} to form unstable Au^{199}. We made successive separations of gold from activated platinum to find which platinum period is its parent, and found that it does not come from the 18-hr. period, but most probably does come from the 31-min. period. When two separations $1\frac{1}{4}$ hr. apart were made, the second gold fraction showed about the right ratio of activity to the first to agree with this interpretation. The platinum fraction carries the 18-hr. activity (this incidentally shows that it is not due to Ir contamination), and also, even after repeated separations of gold, still has a period of about 3.3 days. Thus there seem to be two active bodies with the same period (within our present accuracy), one of which fits into the scheme very nicely, while the other (the Pt isotope) again causes trouble. The best that we can think of doing is to make the 18-hr. and 3.3-day platinum periods another pair of isomers. Au^{199} accounts for about 1/3 of the total 3.3-day activity; the agreement between the cross sections for the 31-min. and 3.3-day periods is spurious, since the latter has an extremely soft beta-radiation which can get out of only a fraction of the thickness of the sample.

Pt with fast neutrons gives, like Ir, what appears to be a very complex set of periods, ranging from about 30 min. to more than 5 days. One chemical separation made two days after activation showed that all the long period activity is isotopic with Pt, except for a trace of Au activity, which was much weaker relative to Pt than after slow neutron activation. (We should mention that any active Os would be lost in this and the other separations during the solution in aqua regia, so that we cannot exclude the possibility of its presence. With this exception, all the separations were made to distinguish an element from its two lower neighbors, and in some cases its upper neighbor.) The beta-particles from Pt activated with fast neutrons were found to be nearly all negative, but there was some evidence of a weak long period positron activity.

The results of this work so far do not seem to be capable of any simple explanation without the introduction of a fantastic number of isomeric nuclei, but other explanations may be suggested. Some of the arguments based on the nonexistence of certain stable nuclei may be wrong, or one might assume that some of the active bodies found are excited states of stable nuclei. A search was made using a linear amplifier for α-particles from Au, Ir, and Pt activated with both slow and fast neutrons, and none were found, so no explanation involving α-particle emission can be valid. It also seems strange that so little evidence for the formation of positron emitters is found, although there would appear to be ample chance for their production. We are continuing the work, and expect to publish a fuller account later.

In conclusion, we wish to express our gratitude to Professor Ernest O. Lawrence for his particular interest in this investigation. The financial support of the Research Corporation, the Chemical Foundation, and the Josiah Macy, Jr. Foundation is greatly appreciated.

LETTERS TO THE EDITOR

Prompt publication of brief reports of important discoveries in physics may be secured by addressing them to this department. Closing dates for this department are, for the first issue of the month, the eighteenth of the preceding month, for the second issue, the third of the month. Because of the late closing dates for the section no proof can be shown to authors. The Board of Editors does not hold itself responsible for the opinions expressed by the correspondents.

Communications should not in general exceed 600 words in length.

Visible Radiation Produced by Electrons Moving in a Medium with Velocities Exceeding that of Light

In a note published in 1934[1] as well as in the subsequent publications[2–4] the present author reported his discovery of feeble visible radiation emitted by pure liquids under the action of fast electrons (β-particles of radioactive elements or Compton electrons liberated in liquids in the process of scattering of γ-rays). This radiation was a novel phenomenon, which could not be identified with any of the kinds of luminescence then known as the theory of luminescence failed to account for a number of unusual properties (insensitiveness to the action of quenching agents, anomalous polarization, marked spacial asymmetry, etc.) exhibited by the radiation in question. In 1934 the earliest results obtained in the experiments with γ-rays led S. I. Wawilow[5] to interpret the radiation observed as a result of the retardation of the Compton electrons liberated in liquids by γ-rays. A comprehensive quantitative theory subsequently advanced by I. M. Frank and I. E. Tamm[6] afforded an exhaustive interpretation of all the peculiarities of the new phenomenon, including its most remarkable characteristic —the asymmetry.

According to their theory, an electron moving in a medium of refractive index n with a velocity exceeding that of light in the same medium ($\beta > 1/n$) is liable to emit light which must be propagated in a direction forming an angle θ with the path of the electron, this angle being determined by the equation:

$$\cos\theta = 1/\beta n, \qquad (1)$$

where β is the ratio of the electron velocity to that of light in vacuum.

A successful experimental verification of formula (1) was only performed with water[4] for which, at the moment

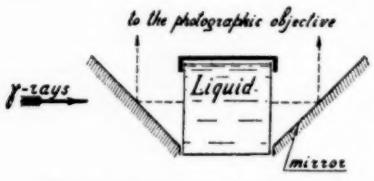

FIG. 1. Arrangement of apparatus.

of publication of the above theory, data were already available which had been obtained by visual observations by the method of quenching.[7, 8]

We recently performed additional experiments in which the intensity of radiation was recorded photographically, the records being taken simultaneously for all the angles θ lying in a plane passing through the primary electron beam. The liquid was placed in a cylindrical glass vessel with very thin walls, and the light emitted by the liquid was reflected by a conical mirror in an upward direction to the object glass of a photographic camera as indicated in Fig. 1. An approximately parallel beam of γ-rays, filtered through a 3-mm lead plate, fell on the liquid horizontally. The γ-radiation used was equivalent to that of 794 mg of radium. The considerable thickness of the lead screen, the large aperture of the object glass (f : 1.4) and the long exposure (72 hours) ensured sufficient distinctness of the photographs.

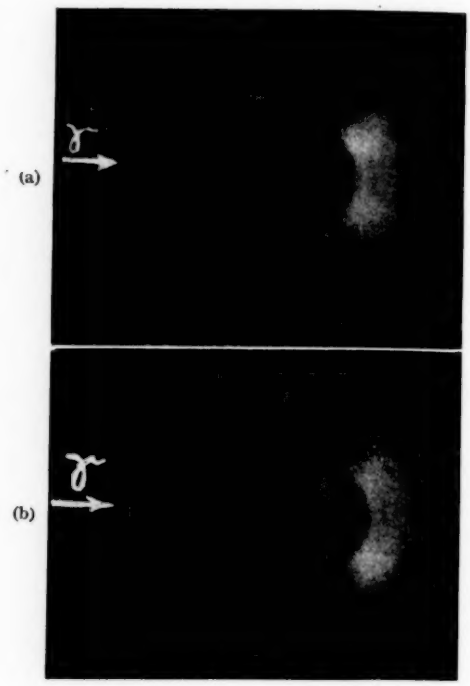

FIG. 2. Photographs showing asymmetry of luminescence. (a) water. $n = 1.337$; (b) benzene, $n = 1.513$.

The latter were obtained for ten different liquids. Two of the photographs taken (positive) are represented in Fig. 2. An examination of these photographs leads to the following conclusions:

(1) In all the pure liquids investigated the radiation propagates mainly in the onward direction of the primary beam, the blackening of the negatives being only visible on part of the annular circle.

(2) The area of the blackened sector increases with the

refractive index of the liquids (see Fig. 2: (a) $n=1.337$ for water and (b) $n=1.513$ for benzene).

(3) Each photograph exhibits two diffuse but clearly visible maxima of blackening, which are symmetrical with respect to the primary beam. Their angular spacing increases with the refractive index of the liquids, and, to a first approximation, agrees with the values which might be expected according to Eq. (1). The absence of distinct maxima of blackening is undoubtedly associated with the difference in energy of the Compton electrons liberated from the molecules of the liquids by γ-rays, with the nonparallelism of these electrons and with the fact that the energy of each electron, moving in a liquid, gradually changes from the initial energy to zero.

All the results obtained are in good agreement with I. M. Frank and I. E. Tamm's theory of the coherent radiation of electrons moving in a medium.[6]

P. A. ČERENKOV

The Physical Institute of the Academy of Sciences of U.S.S.R.,
Moscow,
June 15, 1937.

[1] Čerenkov, C. R. Ac. Sci. U.S.S.R. **8**, 451 (1934).
[2] Čerenkov, C. R. Ac. Sci. U.S.S.R. **12** (3), 413 (1936).
[3] Čerenkov, C. R. Ac. Sci. U.S.S.R. **14**, 102 (1937).
[4] Čerenkov, C. R. Ac. Sci. U.S.S.R. **14**, 105 (1937).
[5] Wawilow, C. R. Ac. Sci. U.S.S.R. **8**, 457 (1934).
[6] Frank and Tamm, C. R. Ac. Sci. U.S.S.R. **14**, 109 (1937).
[7] Bull. Ac. Sci. U.S.S.R. No. 7, 919 (1933).
[8] E. Brumberg and S. Wawilow, C. R. Ac. Sci. U.S.S.R. **3**, 405 (1934)

Maximum Voltage of Wisconsin Electrostatic Generator as a Function of Air Pressure

The large electrostatic generator developed at this laboratory[1] has been in use for more than a year and during regular operation some information was obtained regarding the maximum generator voltage as a function of air pressure in the enclosing tank. This information was very limited, however, since during regular operation the pressure is generally kept at 115 lb. (100-lb. gauge pressure) and when making tests on apparatus atmospheric pressure was used.

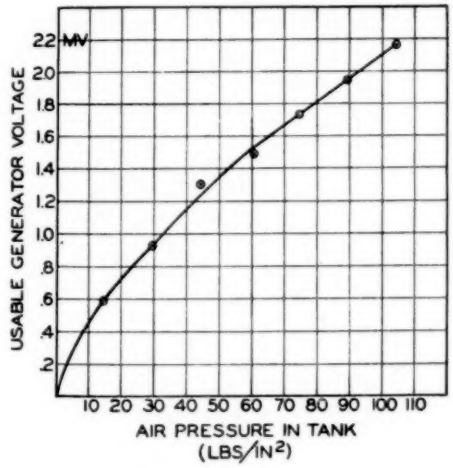

FIG. 1. Curve showing maximum usable generator voltage as a function of air pressure in the enclosing tank. Air pressure is given in lb./in², absolute (not above atmospheric).

To determine the maximum usable voltage over the entire pressure range, a test run was recently made giving the data shown in Fig. 1. The maximum voltage was found to be somewhat indefinite at all air pressures, since a region of voltage instability exists in which the generator will run steadily except for an occasional spark, the average interval between sparks decreasing as the voltage is increased. During the first 15 minutes of running the maximum voltage generally shows a very appreciable increase with time. This increase may, however, depend more on the number of sparks that pass than on the length of running time. To determine the maximum usable generator voltage corresponding to each of the air pressures indicated in Fig. 1, the performance of the generator was studied at each value of the pressure chosen. The voltage values plotted are voltages for which the time interval between sparks was approximately 3 minutes after the generator had been run 15 minutes. A time interval of 3 minutes between sparks is too short for good running conditions, but this criterion was adopted during the test run in order to get consistent data in a reasonable length of time.

The sparks pass radially from the high potential electrode to the tank wall. They do no damage and after a spark has passed the voltage rises to its former steady value in approximately 10 seconds. At air pressures up to about 95 lb. (80-lb. gauge pressure) the generator voltage is always limited by this radial sparking, but at higher pressures the limit is sometimes determined by sparking down the charging belts. This is caused by excessive charging current on the belts, and can only be eliminated by decreasing current drain from the generator and hence allowing a decrease in the charging current. Generally, when the belts fail, an increase in tank pressure gives a decrease in usable voltage. When the data shown in Fig. 1 were taken the corona gaps along the accelerating tube were set too close for voltages above 2200 kv. Their high current drain necessitated high charging currents, and when the tank pressure was increased to 115 lb. sparking along the belts limited the usable voltage to approximately 2100 kv. This value was not plotted in Fig. 1, since a voltage limitation due to sparking along the belts is not characteristic of the generator operating under good conditions.

No explanation has been found for the nonlinearity of the curve of Fig. 1 in the region of low air pressures. At pressures above 45 lb. the curve is very nearly linear with a slope somewhat greater than had been expected.

From a consideration of these results it seems that higher air pressure may be of value for a generator of this type providing that the limitations due to sparking along charging belts and insulating supports can be avoided.

R. G. HERB
E. J. BERNET

University of Wisconsin,
Madison, Wisconsin,
July 23, 1937.

[1] R. G. Herb, D. B. Parkinson, D. W. Kerst, Phys. Rev. **51**, 75 (1937).

On the Preparation of Polonium Sources

Erbacher[1] has described a technique for preparing polonium sources, wherein polonium deposits on platinum from a 0.1 *N* HCl solution saturated with hydrogen. However, some difficulty has been experienced in this laboratory in getting sources as strong as his by his method. Being guided by the assumption that the hydrogen adsorbed on the surface of the backing is involved in the process, palladium was substituted for the platinum with gratifying results. Whenever polonium was deposited first on platinum and then on palladium from the same solution, the palladium took up many times more radioactive material than did the platinum. Sources may be prepared on palladium as easily as on silver,[2] are about of the same strength, yet have far more uniform range distributions.

Since Ra E is also deposited by this method, it must be removed by repeated depositings of the polonium on silver. The palladium foil needs no preparation other than heating in a flame to clean the surface. It is attached to a glass rod with Picein and is immersed in the radioactive solution, through which hydrogen is bubbled and which is rotated at 100 to 200 r.p.m.

The strengths and range distributions of these sources have been tested by counting the emitted particles with a linear amplifier. Sources of 3 or 4 mC per sq. cm showed no evidence of tarnish whatsoever, and the variation in range, which was between one and two millimeters, was possibly inherent in the counting system. Stronger sources, up to 17 mC per sq. cm, have been prepared, but these become covered with a thin layer of black material. In the case of the strongest source, 82 percent of the particles had ranges greater than 3.5 cm, and 60 percent of the particles came to the ends of their ranges within a region of 2 mm. On platinum, Erbacher has obtained 10 mC per sq. cm on sources of similar area.

I wish to thank Mr. C. M. Herget for his assistance in the preparation of these sources.

W. R. KANNE[3]

Johns Hopkins University,
Baltimore, Maryland,
July 24, 1937.

[1] Erbacher, Zeits. f. physik. Chemie **A156**, 142 (1931); **A163**, 196 (1932).
[2] I. Curie, J. chim. phys. **22**, 471 (1925); L. R. Hafstad, J. Frank. Inst. **221**, 191 (1936).
[3] Now at the University of Wisconsin.

Positron-Electron Emitting Isomer in Radiosilver

When silver is bombarded with very high energy neutrons, ranging up to 20 Mev, a 25.5-min.[1] and an 8-day radioactive period are produced, the former emits positrons and the latter electrons. For slow neutron bombardment only the well-known 20-sec. and 2-min. periods are obtained, both emitting electrons. Table I shows the positions of the two stable isotopes of silver, Ag^{107} and Ag^{109}, in relation to other neighboring known stable nuclei. The assignment of the two long radioactive periods is also shown, and is based upon the following observations.

Neutron bombardment: When Be is bombarded by deuterons of 6 Mev, neutrons of about 8 Mev are emitted; however, these neutrons, when used to bombard silver, do not seem to have sufficient energy to produce the two long periods. Neutrons of nearly 20 Mev, obtained from deuteron bombardment of boron or lithium, do produce these periods. Neutrons of about 11 Mev from a Ra-Be source produce the 25.5-min. period.[2] High energy neutron bombardment of cadmium produces in the silver separation both the positron and electron emitting periods.

TABLE I. *Positions of the two stable isotopes of silver in relation to other known isotopes. The assignment of the two long radioactive periods is also shown.*

	103	104	105	106	107	108	109	110
$_{45}$Rh	99.9%							
$_{46}$Pd		9.3%	23%	27%		27%		14%
$_{47}$Ag				25.5 m ↑ 8 d ↓	52%	2 m ↓	48%	20 s ↓
$_{48}$Cd				1.5%		1%		15%

Deuteron bombardment: Palladium, when bombarded by 6.3 Mev deuterons gives in the silver separation both the 25.5-min. and 8-day periods.[3]

Helium bombardment: Helium was admitted into the cyclotron so that rhodium could be bombarded by about 12 Mev alpha-particles. A weak activity was observed which had about the correct periods. The signs of the particles were not observed. A chemical check was made on only the 25.5-min. period which initially is much the stronger of the two.

These observations can be made consistent among themselves if Ag^{106} is assigned the double duty of emitting positrons with a period of 25.5 min. and electrons with a period of 8 days. The positron period cannot be assigned to Ag^{105} because this period could then not be obtained from cadmium by high energy neutron bombardment. Also confirmatory evidence by alpha-bombardment of rhodium would be lacking. If the 8-day and 25.5-min. periods were assigned to Ag^{108} or Ag^{110}, they should be obtained by slow neutron bombardment of silver, which however is not observed.

The reaction equations which give the radioactive isomeric Ag^{106} may be written as follows:

$$n' + Ag^{107} \rightarrow Ag^{106} + 2n'$$
$$n' + Cd^{106} \rightarrow Ag^{106} + p'$$
$$D^2 + Pd^{105} \rightarrow Ag^{106} + n'$$
$$He^4 + Rh^{103} \rightarrow Ag^{106} + n'$$
$$_{47}Ag^{106} \rightarrow {}_{46}Pd^{106} + {}_{+1}e^{\circ}$$
$$_{47}Ag^{106} \rightarrow {}_{48}Cd^{106} + {}_{-1}e^{\circ}$$

So far only one other artificial radioactive isomeric nucleus has been reported, namely Br^{80} with an 18-min. and a 4.2-hour period.[4] However, in this case both members of the isomer emit electrons. This work was made possible by a grant from the Horace H. Rackham fund.

M. L. POOL*
J. M. CORK
R. L. THORNTON

Department of Physics,
University of Michigan,
Ann Arbor, Michigan,
July 16, 1937.

[1] Heyn, Nature **138**, 842 (1937).
[2] Rotblat, Nature **139**, 1110 (1937).
[3] Kraus and Cork, Phys. Rev. **51**, 383 (1937).
[4] Snell, Phys. Rev. **51**, 1011 (1937).
* Elizabeth Clay Howald Scholar.

Note on the Absolute Determination of Magnetic Field Strength

For determinations of the energies of charged particles by means of a focusing magnetic spectrograph it is becoming increasingly desirable to know not the average value of the strength of the magnetic field of the spectrograph over a sizable area, but the strength of the field at the source of the particles. This is especially true for absolute determinations of energies with high precision involving precise absolute determinations of the strength of the given magnetic field, because the necessary corrections for the small nonuniformities which may occur in even the most nearly uniform magnetic fields found in practice require a knowledge of the field strength at the source of particles.[1] Since these corrections also require a knowledge (obtained by small exploring coils, e.g.) of the variations of the magnetic field from perfect uniformity in the region traversed by the particles, it is but a little more trouble to determine absolutely the field strength at the source of the particles, utilizing a knowledge of these variations from uniformity. The following derivations are for the inductometric, "flip-coil" method of measuring magnetic field strengths.[2]

Let the given magnetic field (everywhere parallel to some fixed direction) be H, and let it be required to determine the value H_0 of H at some point O in H. If a flat circular coil having N turns of wire, having an average effective area A, and having its center at O is rotated 180° about an axis in its plane and through O, and if the breaking of a current I produces (through a mutual inductance M) an equal effect, then the average value of H over the area of radius $(A/\pi)^{\frac{1}{2}}$ about O is

$$\bar{H}=MI/2AN. \tag{1}$$

However, let H' defined by $H=H_0+H'$ be determined by moving in suitable jumps a coil of a much smaller area a than A but having a much greater number n of turns of wire than N; it would be convenient to construct a set of coordinate x and y axes perpendicularly to H and with origin at O and then to determine H' as a function of the two variables x and y. Then we can use instead of Eq. (1),

$$H_0=(MI-2N\int\int_A H'ds)/2AN, \tag{2}$$

where ds is an element of area in the xy plane. Here M, I, A and N are quantities which can be measured with high precision; the term in $(\int\int H'ds)/A$ is just a small correction term which of course grows smaller as H becomes more nearly uniform over A. Eq. (2) is the chief equation to be used in getting H_0 instead of $\bar{H}$ experimentally. Note in passing that

$$\bar{H}-H_0=(\int\int_A H'ds)/A. \tag{3}$$

It will of course be of interest to know the conditions under which Eq. (2) should be used instead of the simpler Eq. (1). We see directly by Eq. (3) that the relative error introduced into H_0 by taking $H_0=\bar{H}$ is

$$E_1=(\int\int_A H'ds)/H_0A, \tag{4}$$

which would exist in addition to the effects of the experimental errors in M, I, A and N. Also, a glance at Eq. (2) will show that the relative error introduced into H_0 by the use of Eq. (2) is equal to the product of $1/H_0$ into the absolute error in $(\int\int H'ds)/A$, which would also exist in addition to the effects of the experimental errors in $MI/2AN$; letting e_1 and e_2 be the relative errors possibly present in $(\int\int H'ds)$ and in A respectively, this additional relative error caused by Eq. (2) is thus

$$E_2=(e_1+e_2)(\int\int_A H'ds)/H_0A,$$

whence by Eq. (4)

$$E_2/E_1=e_1+e_2. \tag{5}$$

Now the computation of the volume-like $\int\int H'ds$ may be considered to involve the product of the average value H_{Av}' of H' into A; so if e' is the possible relative error present in H', we have that

$$e_1=e'+e_2. \tag{6}$$

But e' will be composed of first, the experimental uncertainties in the determinations of H', and second, the effects of taking as the value of H at a point the average value of H over the area a placed with its center at that point. Thus if ϵ is the absolute, purely experimental error considered possible in H', we see by Eq. (3) that

$$e'\leqq[\epsilon+2(\int\int_a h'ds)_{Av}/a]/H_{Av}' \tag{7}$$

the factor of two being used to account for the fact that the experimental determination of an H' involves the difference of exploring coils effects for two points in H; here h' is the difference between the actual value of H and the value of H at the center of the small coil, and "Av" refers to the average value for many locations well scattered over A. Defining h_{Av} by

$$(\int\int_a h'ds)_{Av}=h_{Av}a \tag{8}$$

and substituting Eqs. (6), (7) and (8) into Eq. (5), we get

$$E_2/E_1=2e_2+(\epsilon+2h_{Av})/H_{Av}'.$$

Thus, *especially if*

$$2e_2+(\epsilon+2h_{Av})/H_{Av}'<1, \tag{9}$$

it would be an advantage to use Eq. (2) instead of Eq. (1). A little consideration will show that in many cases it would be easy to satisfy Eq. (9).

In conclusion, two facts should be noted. First, Eq. (7) is not entirely rigorous, for its second term is only an approximation, so Eq. (9) is not entirely rigorous; to be more nearly consistent until Eq. (7) is improved, we should consider Eq. (9) as requiring only that the left member be of the order of magnitude of unity. And second, although Eq. (9) requires h_{Av} and H_{Av}', it is not necessary to obtain very many values of H' in order to obtain reliable estimates of them; a few values for points well scattered over A should suffice.

F. T. Rogers, Jr.

The Rice Institute,
Houston, Texas,
July 20, 1937.

[1] E.g., for the method of Hartree, Proc. Camb. Phil. Soc. **21**, 746 (1923).

[2] An analogous method has already been presented for the Cotton balance; see Phys. Rev. **50**, 515 (1936).

Cosmic-Ray Shower Production Curves on Mt. Evans

The position of the maximum and the general shape of the shower-production curves obtained by Woodward[1] at Denver and Mt. Evans agree with those obtained by the authors[2] at the same stations within experimental error. However, for thin lead Woodward's curve is concave upward; ours concave downward. The arrangement of counters used by Woodward was set off less frequently than ours by two-particle showers. The theory of cumulative pair production as pointed out by Y. Watase[3] predicts the number of two-particle showers, N_2, produced in a thin sheet of lead should be proportional to the thickness, t, while the number of four-particle showers, N_4, should be proportional to t^2. For thin sheets N_2 should greatly exceed N_4; also the effect of absorption will be small. For a counting system which would detect two or more particles, N_2 would predominate and one would expect a curve concave downward near the origin; whereas for a system which would detect three or more particles, we would expect a curve in this region which would vary as some power of t greater than unity, i.e., concave upward.

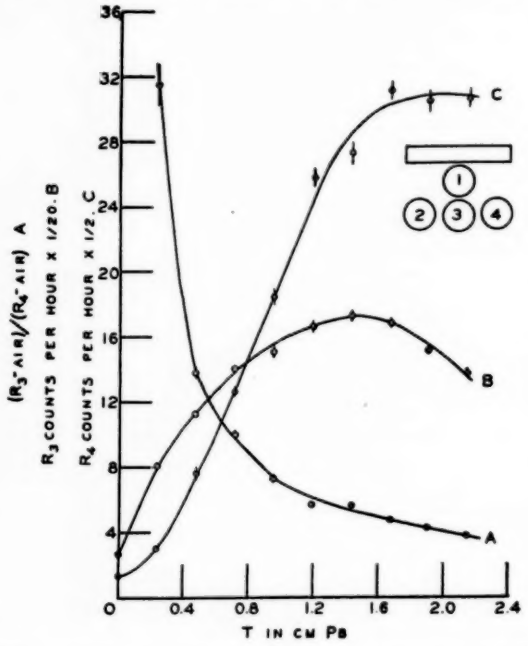

FIG. 1. Shower production curves for three and four counters and their ratios.

To test this, the following experiment was performed at Mt. Evans Laboratory, University of Denver, and Massachusetts Institute of Technology. The altitude is 14,160 feet. The apparatus was housed in a room with thin wooden walls and roof. The temperature fluctuations were not great enough to influence materially the results.

Four Geiger counters were placed below shower-producing sheets of lead, A. The arrangement is shown in Fig. 1. Two or more particle showers were registered when triple coincidence counting rates, R_3, were taken with counters 1, 2, and 3. When counters 1, 2, 3, and 4 were used to determine quadruple counting rates R_4, three or more ionizing particles were required to actuate the counting mechanism. The values obtained are shown in Table I.

TABLE I. *Triple and quadruple counting rates.*

t cm Pb Block A	R_3	R_4	$\frac{R_3\text{—Air Rate}}{R_4\text{—Air Rate}}$
0 (air)	52.7±2.3	2.7 ±0.4	
0.238	161.6±2.6	6.15±0.3	31.5 ±1.3
0.476	226 ±3.0	15.20±0.7	13.8 ± .38
0.714	280 ±4.1	25.3 ±0.75	10.04± .24
0.952	301 ±6.1	36.8 ±1.1	7.27± .21
1.19	332 ±6.5	51.6 ±1.1	5.71± .15
1.43	345 ±5.7	54.6 ±1.5	5.63± .14
1.67	336 ±6.0	62.1 ±1.1	4.77± .12
1.90	301 ±5.3	60.9 ±1.2	4.26± .11
2.14	274 ±5.5	61.2 ±1.2	3.78± .11

In Fig. 1, the data in Table I are represented graphically. It is noticed that there is a difference in concavity of the curves for R_3 and R_4 near the origin as predicted. It also appears that the maximum for R_4 occurs at about 2 cm of lead whereas the maximum for R_3 occurs at about 1.5 cm lead. We have previously reported[2] a shower production curve obtained with a counting system which required only a single shower particle to operate the mechanism. This curve has a maximum at 1.0 cm of lead. Fig. 2 shows this curve in comparison with R_3 and R_4. The absolute values of the counting rates for R_3 and R_4 are comparable with each other, but the values for R_1 were taken

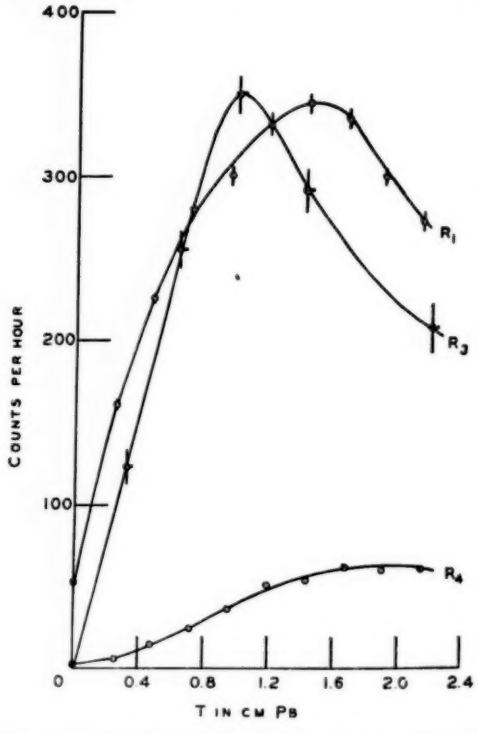

FIG. 2. One, two, and three particle shower production curves for lead.

with a different set of counters. It appears from Fig. 2 that the optimum thickness for shower production increases with the minimum of particles required for registration, at least up to 3 particles. Since the relative probabilities of recording showers of different numbers of particles will vary with the geometrical arrangement of the counters, agreement as to the position of maximum of this production curve is not to be expected among observers using different arrangement of counters.

This work is being continued at lower altitudes and will be extended to thicknesses of lead including the second maximum of the shower producing curve.

We are indebted to the American Association for the Advancement of Science, the Rumford Committee, the National Research Council of the United States, and the National Research Council of Canada, for grants-in-aid which made this work possible.

DAROL K. FROMAN

McDonald College,
McGill University,

J. C. STEARNS

University of Denver,
Denver, Colorado,
July 28, 1937.

[1] R. H. Woodward, Phys. Rev. **49**, 711 (1936).
[2] J. C. Stearns and D. K. Froman, Phys. Rev. **49**, 473 (1936).
[3] Y. Watase, Nature **139**, 671 (1937).

Temperature Variation of the Magnetic Anisotropy of Ammonium Nitrate

The variation of the crystal structure of ammonium nitrate with temperature has been studied by S. B. Hendricks and others[1] (1932) by x-ray analysis. From intensity measurements they have deduced the orientations of the nitrate ions in the several crystalline modifications. They also postulate a free rotation of the NO_3 group in the cubic form which is stable above 125° C. Now the orientation of the nitrate ions in the crystal can also be determined from measurements of the magnetic anisotropy of the crystal, as has been shown by Krishnan[2] in his well-known investigations on magnecrystallic action. Besides, it should be possible to follow the temperature variation of the crystal structure from the study of the magnetic anisotropy at various temperatures, and the results may be expected to provide a check on the findings of x-ray analysis. I have carried out measurements employing the torsional method of Krishnan,[3] with suitable modifications in technique. Particular care was taken to select only flawless crystals prepared by slow crystallization from aqueous solution, since imperfect ones showed a tendency to become opaque, and crumble at high temperatures. The space surrounding the crystal was also kept perfectly dry since moisture affects the crystal adversely. A serious obstacle in making accurate determinations at the higher temperatures was the sublimation of the crystal. The error introduced thereby was however corrected for by taking into account the loss in weight at different stages of heating, and by rapid manipulation. Determinations of the magnetic anisotropy at room temperature (27°C) gave values: $\chi_b-\chi_a=5.92\times10^{-6}$, $\chi_b-\chi_c=6.42\times10^{-6}$, $\chi_a-\chi_c=0.58\times10^{-6}$, in e.m.u., the symbols having the usual meaning. The variation of magnetic anisotropy with temperature when the crystal is suspended with the c axis vertical is shown in Fig. 1. No significant change of orientation of the crystal in the magnetic field could be noticed in the course of heating the crystal. The character of the curve affords convincing evidence of the change of structure of the crystal with varying temperature. It is seen that at 130°C the anisotropy is zero, as should be expected if the crystal structure is cubic. Moreover, it has been found by x-ray analysis that there is only one molecule NH_4NO_3 in the unit of structure, and therefore magnetic isotropy is possible only on the postulate of a freely rotating NO_3 ion with spherical symmetry. The magnecrystallic data also definitely indicate that in the orthorhombic room temperature modification the planes of the nitrate ions are perpendicular to the b axis of the crystal in conformity with the results of Hendricks. The lower value of the magnetic anisotropy in the temperature range (32°–84°C) may also be explained in the light of the structure proposed on the basis of x-ray analysis, according to which the planes of the nitrate ions are inclined to each other, if we make the assumption that the c axis of the new modification remains vertical. In this case the angle of inclination of the planes of the ions to each other in the (001) projection, on calculation from the magnetic measurements, comes out to be about 51° when the temperature of the crystal is 59°C, which seems to agree with the value 52° found by Hendricks. A similar argument in the case of the tetragonal modification would imply that it is probably only pseudo-tetragonal, in view of the observed anisotropy which is definite though small. These inferences regarding the orthorhombic (32°–84°C) and tetragonal (84°–125°C) forms are, however, purely tentative. Owing to experimental difficulties the variation of anisotropy when the crystal is cooled down from a high temperature to room temperature could not be studied quantitatively, although the reappearance of anisotropy on cooling was noticed. However, the effect of cooling the crystal from 60°C down was investigated. It was observed that at 27°C the anisotropy did not reach the original value but remained more or less the same as at 60°C. On cooling further to 20°C the original room temperature value was attained. This seems to indicate a lag in the transition, a fact which has been noticed previously by microscopic examination[1] also. Further details of the investigation will be published elsewhere.

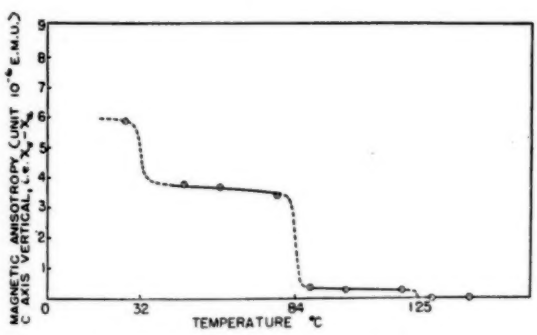

FIG. 1. (In the abscissa χ_c should be χ_b.)

My sincere thanks are due to Professor C. V. Raman for many helpful suggestions and kind encouragement in the course of the work.

P. NILAKANTAN

Department of Physics,
Indian Institute of Science,
Bangalore, India,
July 15, 1937.

[1] S. B. Hendricks, E. Posnjak, and E. C. Kracek, J. Am Chem. Soc. **54**, 2766 (1932).
[2] K. S. Krishnan, B. C. Guha, and S. Banerjee, Phil. Trans. **231**, 235 (1933).
[3] K. S. Krishnan and S. Banerjee, Phil. Trans. **234**, 265 (1935).

Magnetic Scattering of Neutrons

Halpern and Johnson[1] have recently pointed out that it should be possible to detect the magnetic scattering of slow neutrons by comparing the scattering by selected metals and their respective ions. Experiments of this kind have been undertaken with manganese and iron together with certain of their compounds as scattering materials. Preliminary results of these experiments are given here.

The slow neutrons were obtained from a 200 mg Ra-Be source surrounded by paraffin and were detected by the radioactivity they produced in silver. The source was sometimes in a paraffin cylinder and sometimes in a curved block of paraffin just outside a large Pyrex Dewar vessel (15 cm inside diameter). This vessel contained perforated blocks of paraffin which could be cooled by liquid air. The detectors were placed on the paraffin with the scattering substances immediately above them so that large angle scattering was observed.

In the first experiments the relative scattering by equal numbers of atoms of Mn, MnO, MnO_2, was determined. There is no evidence in these data that the Mn in MnO scatters more than the Mn atom. The accuracy of the experiment is such that a magnetic scattering cross section of as much as 10 percent of the theoretical value (23×10^{-24} cm^2) for Mn^{++} should easily have been detected. Trivalent iron has the same magnetic moment as bivalent manganese and hence should have the same large magnetic scattering cross section for neutrons in the energy range covered by the theory. Measurements on Fe and Fe_2O_3 failed to indicate any increase in the Fe cross section when so combined with oxygen. These experiments are less conclusive than those on Mn because of fewer observations made and because of the larger nuclear cross section of iron.

The magnetic scattering cross sections are calculated on the assumption that $\lambda/2\pi$ for the neutron is larger than the linear dimension of the section of the atomic system responsible for the magnetic moment. In order to increase the number of the incident neutrons satisfying this condition the scattering from Mn, MnO, and MnO_2 was repeated at approximately liquid-air temperature. Again there was no evidence of a larger than nuclear cross section for Mn in MnO.

Finally, a physical mixture of Mn and S (containing the same number of atoms of each) was prepared. Equal amounts of this physical mixture and of chemically pure MnS were used as scattering materials. The silver detector was found to be about 3 percent more active when the MnS was used as scatterer. This difference is several times the probable error due to statistical fluctuation. If attributed to magnetic scattering this difference corresponds to a magnetic scattering cross section for Mn^{++} about 5 percent as great as the theoretical value. But since this same ratio of activities was maintained after the slow neutrons were removed by a sheet of cadmium introduced between source and detector, it does not seem possible to attribute any of this increased scattering to the magnetic cross section of Mn^{++} for neutrons satisfying the energy conditions of the theory. The greater scattering of the MnS is now thought to be due to the presence of water in the compound in spite of assurances to the contrary from the manufacturer. The presence of water should not invalidate the test since the introduction of the cadmium filter should eliminate the magnetic scattering and increase the ratio of neutrons scattered by the physically mixed Mn and S to those scattered by the MnS. It is believed that any magnetic scattering by Mn^{++} as large as 5 percent of the theoretical value (predicted on the basis of a sufficiently slow neutron beam) would have been detectable in these preliminary experiments unless masked by some unsuspected anomaly in the capture of neutrons by Mn. The work is being continued with emphasis on low temperature and small angle scattering. A detailed report will be made later.

The author wishes to express his gratitude to Professor O. Halpern and Dr. M. H. Johnson for many helpful suggestions and discussions. Financial assistance has been received from the Penrose Fund of the American Philosophical Society through a grant to Professor Allan C. G. Mitchell.

MARTIN D. WHITAKER

Physics Department,
New York University,
University Heights,
August 2, 1937.

[1] O. Halpern and M. H. Johnson, Phys. Rev. **52**, 52 (1937).

Pressure Shifts of Krypton Lines

Very careful interferometer measurements have been made by Jackson[1] of the wave-lengths of a number of krypton lines. These measurements included an accurate determination of their pressure shifts; they indicate, within limits of error, proportionality of shifts with the square of the relative densities.

Recently Kuhn[2] has given an interpretation of Jackson's data, and calculated from them values of a certain parameter which determines the strength of van der Waals forces. In this note we wish to suggest a correction to his manner of calculation, which, though apparently overlooked by Kuhn, changes the results considerably and probably throws doubts upon their meaning.

The interpretation in question involves the assumption that the influence of the atomic motion upon the intensity distribution within the line is small, so that a statistical theory is sufficient to describe the facts. If this is true, the pressure shift of the line maximum is given by the formula

$$\Delta\nu = (\tfrac{2}{3}\pi)^3 C N^2$$

where C is the constant in the van der Waals potential

energy $-C/r^6$, N the number of perturbing atoms per cc. Whether this formula, which was used by Kuhn, is applicable may be seen by inspecting the details of the theory[3] from which it was derived.

The statistical distribution, plotted in a recent article by the authors,[4] has a half-width which is about 3 times the shift. An inspection of Jackson's data shows that his measured lines have widths about a hundred times the observed shifts for the lowest pressures, and that they are several times as wide at the highest pressure. This obviously complicates the interpretation.

The width of the lines is largely due to the Doppler effect. We therefore wish to consider the question: What is the effect of a large Doppler width upon a fairly narrow asymmetrical distribution like the statistical one, or *vice versa?* It is clear that if the statistical distribution were essentially a δ function, displaced, say, a distance s (on a frequency scale) from the origin (undisplaced position of line) the Doppler distribution I_1, which has the form of an error curve, would be displaced bodily the same distance s upon fusing the two. But a much better approximation to the asymmetric distribution is the triangle function

$$I_2(\nu)=\begin{cases}(2/n^2s^2)[(n+1)s-\nu] & \text{if } s<\nu<(n+1)s\\ 0 \text{ otherwise}\end{cases}$$

in which s represents the shift and ns the width of the triangle at the base. If I_2 is united with $I_1=\text{const.}\ e^{-\nu^2/\Delta^2}$ according to

$$I=\int I_1(\nu-x)I_2(x)dx,$$

then, for the conditions prevailing in Jackson's experiments ($s<\Delta$), the maximum of I is found to be very nearly at $\nu_{\max}=(1+n/3)s$. Now n may reasonably be taken to be about 5 or 6, which makes the apparent shift something like three times the purely statistical shift. Hence, if the other assumptions implied by Kuhn are accepted, the values of C calculated by him are several times too large.

We feel, however, that there may be difficulties whose effect can not so easily be estimated. Pressure shifts proportional to N^2 do not necessarily justify the assumption of pure van der Waals forces of the London type. Jackson's measurements were made on *emission* lines from a discharge tube, so that the possibility of Stark effects cannot be excluded. The Stark effect of some of the lines in question is known.[5] The data indicate that shifts of the order of magnitude found by Jackson can be produced by electric fields of about 600 volts/cm. Such fields are easily set up in even a mild discharge. The use of emission lines for the calculation of van der Waals constants is usually uncertain. The degree to which ordinary velocity broadening, aside from Doppler effect, influences the line is difficult to estimate. The Doppler width of Jackson's lines corresponds to a temperature slightly above room temperature for which, with a gas of half the atomic weight of krypton, the kinetic effect is considerable.[6]

HENRY MARGENAU
WILLIAM W. WATSON

Sloane Physics Laboratory,
Yale University,
New Haven, Connecticut,
July 29, 1937.

[1] C. V. Jackson, Phil. Trans. Roy. Soc. **A236**, 1 (1936).
[2] H. Kuhn, Phys. Rev. **52**, 133 (1937).
[3] H. Margenau, Phys. Rev. **48**, 755 (1935).
[4] H. Margenau and W. W. Watson, Rev. Mod. Phys. **8**, 22 (1936).
[5] N. Ryde, Zeits. f. Physik **83**, 354 (1933).
[6] G. F. Hull, Jr., Phys. Rev. **50**, 1148 (1936); **51**, 572 (1937).

Important Notice

THE American Institute of Physics will pay $2.00 per copy for each of the following issues of the *Physical Review:*

Volume 1, No. 6—June, 1913
Volume 2, No. 2—August, 1913
Volume 2, No. 4—October, 1913
Volume 2, No. 5—November, 1913
Volume 7, No. 1—January, 1916
Volume 7, No. 2—February, 1916
Volume 7, No. 3—March, 1916
Volume 7, No. 4—April, 1916
Volume 7, No. 5—May, 1916
Volume 9, No. 2—February, 1917

Copies should be in good condition. They should be addressed to the Publications Manager, American Institute of Physics, 175 Fifth Avenue, New York, New York, with the name and address of sender and with a covering letter.